TNO innovation for life

HYPO-LIAS

HYDROCARBON POTENTIAL OF THE LIAS

by Sander Houben, Susanne Nelskamp, Tanya Goldberg, Roel Verreussel, Nico Janssen, Susan Kerstholt and Thijs Boxem

TNO Report 2017 R10380

Hydrocarbon Potential of the Lias: HYPO-Lias

Date: 01-03-2017
Authors: Sander Houben, Susanne Nelskamp, Tanya Goldberg, Roel Verreussel, Nico Janssen, Susan Kerstholt and Thijs Boxem
Number of pages: 86
Sponsors: EBN B.V., NAM B.V., Statoil ASA. This project is executed with subsidy from the Ministry of Economic Affairs, National Regulations EA-subsidies, Topsector Energy executed by the Netherlands Enterprise Agency.
Report Number: TNO 2017 R10380

HYPO-Lias is a collaboration between:

Statoil NAM ebn

Ministry of Economic Affairs

TNO innovation for life

Management Summary

The HYPO-Lias-project provides an overview of the depositional and paleoclimatic development of the Early Jurassic in the North Sea area (the UK, Netherlands, Denmark and Norway). This cross-border project was initiated to challenge the assumption that the Lower Jurassic of the North Sea is very homogeneous and predominantly not prospective.For example the Lower Jurassic is known for restricted intervals with excellent source-rock potential such as the Lower Toarcian. In addition, towards the northern fringes of the North Sea, important sandstone reservoirs are of Early Jurassic age. A fundamental understanding of the genesis and distribution of these source- and reservoir units, requires better understanding of the paleogeographic and paleoclimatic context.

As a first step towards cross-border comparisons, a stratigraphic framework is constructed. Outcrop localities in the UK were sampled in high resolution for organic-carbon isotope and palynological analyses. These outcrop localities are important reference sites for ammonite zonations and thus provide a firm ‘chronostratigraphic backbone’. The resultant composite stable isotope curve and palynological marker events form the basis for stratigraphic correlation of cross-border records.

Outcrop and core sections are analyzed in terms of stable isotope composition, quantitative palynology, bottom-water redox indicators and organic petrochemistry. Collectively these analyses provide insight into (1) the paleoclimatic development of the study area and (2) the drivers that affect source-rock potential in various parts of the study area. Through cross-border log correlation we eventually extrapolated trends across the study area.

The results reveal a close correspondence between carbon cycle perturbations as revealed by isotope trends, climate, run-off, anoxia and organic-matter enrichment and preservation. Rapid phases of climate change cause alteration of the hydrological regime, leading to stagnant water-conditions and excessive nutrient supply. As a consequence, marine source-rock genesis is found to be specifically related to elevated anoxygenic primary productivity under anoxic water-column conditions. Areas undergoing enhanced subsidence and having a relatively low supply of clastic material, are best suited for the accumulation of potential source-rocks. We noted that the Toarcian Oceanic Anoxic Event by all means stands out in terms of impact. In the Southern North Sea it represents the only extensive potential source-rock, whereas in other parts of the study area, its environmental fingerprint is noted in a wide array of depositional environments. In addition, the Earliest Jurassic (Hettangian - Early Sinemurian) was a phase of warm and dynamic climatic conditions. Locally, indications for marine organic-rich deposition are recorded. Given that these deposits are more widely distributed than the Toarcian deposits, additional source-rock potential might be invoked in hemipelagic settings.

The results obtained from the combination and integration of the various analytical techniques provide an unprecedented cross-border perspective on the Early Jurassic, bearing relevance to a multitude of geoscientific challenges.

1. INTRODUCTION AND SCOPE

1.1 Rationale and objective 3
1.2 Geographic and temporal scope 4

2. APPROACH AND METHODOLOGY

2.1 Database and samples 7
2.2 Palynology 7
2.3 Stable carbon isotope analysis 8
2.4 Rock Eval Pyrolysis 8
2.5 Bottom Water Redox Conditions 9
2.6 Log Correlation 9

3. GEOLOGICAL SETTING AND REGIONAL STRATIGRAPHY

3.1 Geological setting 13
3.2 Outcrop Reference Sections 14
3.3 Southern North Sea (UK, NL) 20
3.4 Norwegian-Danish and Farsund Basin (DK, N) 20
3.5 Viking Graben Area (N, UK) 21
3.6 Integration of regionally employed lithostratigraphic nomenclature 21

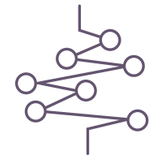

4. STRATIGRAPHIC FRAMEWORK

4.1 Organic carbon isotope records 25
4.2 Palynological marker events 28
4.3 Integrated framework 37

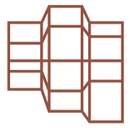

5. REGIONAL LOG CORRELATION

5.1 Input data 41
5.2 Regional correlation 44

6. PALEOCLIMATE

6.1 Hettangian and Early Sinemurian 51
6.2 Late Sinemurian 52
6.3 Early Pliensbachian 52
6.4 Late Pliensbachian 55
6.5 Early Toarcian 55
6.6 Late Toarcian 57
6.6 Summary 57

7. SOURCE ROCKS AND THEIR DRIVERS

7.1 Hettangian - Sinemurian 62
7.2 Pliensbachian 64
7.3 Earliest Toarcian 66
7.4 Toarcian Oceanic Anoxic Event and its aftermath (T-OAE) 68
7.5 Dilution of organic-matter 71
7.6 Summary 72

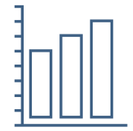

8. PALEOGEOGRAPHY AND CONCLUSIONS

8.1 Hettangian to Early Sinemurian 75
8.2 Late Sinemurian and Early Pliensbachian 76
8.3 Late Pliensbachian 77
8.4 Toarcian 78
8.5 Main observations 80
8.6 Main implications 80

9. REFERENCES 83

10. DATABASES

All data generated and compiled in this study are provided on the USB-drive delivered with the hardcopy of this report. This contains an Excel-Masterfile and several .dex-files for the palynological data .

Runswick Bay Yorkshire

1. INTRODUCTION AND SCOPE

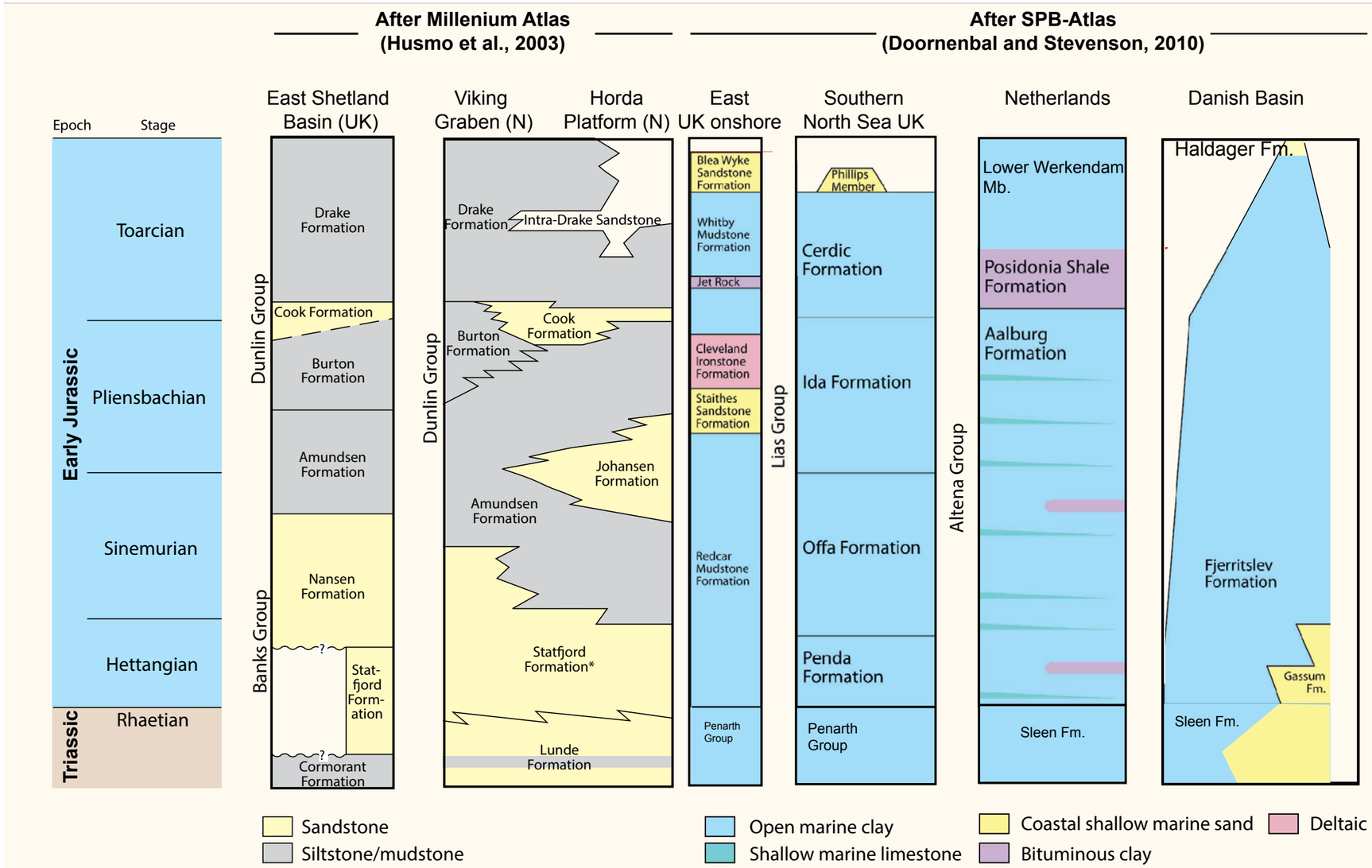

◄ Figure 1.1: Overview of the lithostratigraphic and facies relations across part of the study area as known at the start of the project.
The information from the northern parts of the study area (East Shetland Basin, Viking Graben and Horda Platform) are derived from the Millenium Atlas (Husmo et al., 2003), whereas the information from the UK, Netherlands and Denmark is after the Southern Permian Basin (SPB) Atlas (Doornenbal and Stevenson, 2010). The various colours depict resultant lithologies as used by these atlases. Note that many of the age-relations are very loose and not supported by data. This is for instance illustrated by the long duration of the Posidonia Shale Fm. in the Netherlands.

1.1 Rationale and objective

Early Jurassic deposition in the North Sea Basin is by many considered to have been remarkably homogeneous, leading to the dominance of fine-grained mudstones. Some restricted parts of these Lower Jurassic deposits are enriched in organic-matter and provide source-rocks for hydrocarbons. For instance, in the Netherlands the Lower Jurassic is represented by the Altena Group, which is considered to be dominated by homogeneous shale units. In the Lower Toarcian, these are substantially enriched in organic-matter content, giving rise to source rocks of the Posidonia Shale Fm.

In the UK there is a much more extensive understanding of the Lower Jurassic deposits of the Lias Group, not in the last place because there is a vast number of outcrops allowing detailed investigations (**Figure 1**). In these outcrops, the Lias Group comprises facies types ranging from organic-rich mudstones that were deposited in a hemipelagic setting to restricted oolite shoals and sandstones. Further to the north in Norway, the early Early Jurassic Statfjord Group consists of fluviodeltaic sandstones whereas the Dunlin Group constitutes mudstones intertwined with heterogenously distributed sandstone units (e.g, the Johansen and Cook Formations, **Figure 1.1**).

In spite of the lack of reliable temporal correlations, these phenomena already illustrate that there is signficantly more variability in depositional facies than often assumed, certainly in spatial but likely also in temporal dimensions. It is also becoming increasingly appreciated that the Early Jurassic was repeatedly perturbed by relatively rapid carbon-cycle and related climate change phases. Perhaps the most famous example is the Early Toarcian Oceanic Anoxic Event (T-OAE, Jenkyns, 1988; Hesselbo et al., 2000), which is closely coupled to to the abovementioned Early Toarcian Source Rocks of the Posidonia Shale Fm. in the Netherlands and Germany (**Figure 1.1**). Apart from this specific short-lived period, the paleoclimatic and paleo-environmental evolution of the Early Jurassic in northwest Europe remains relatively poorly known, with most studies skewed towards these short-lived ‘events’ (Riding et al., 2013; Littler et al., 2010).
The current study addresses this issue by providing a stratigraphically sound overview of the climatic, environmental and paleogeographic evolution of northwestern Europe during the Early Jurassic as a whole. Specific attention is paid to the environmental dynamics and paleogeographic context that affect the genesis and distribution of hydrocarbon source rocks.

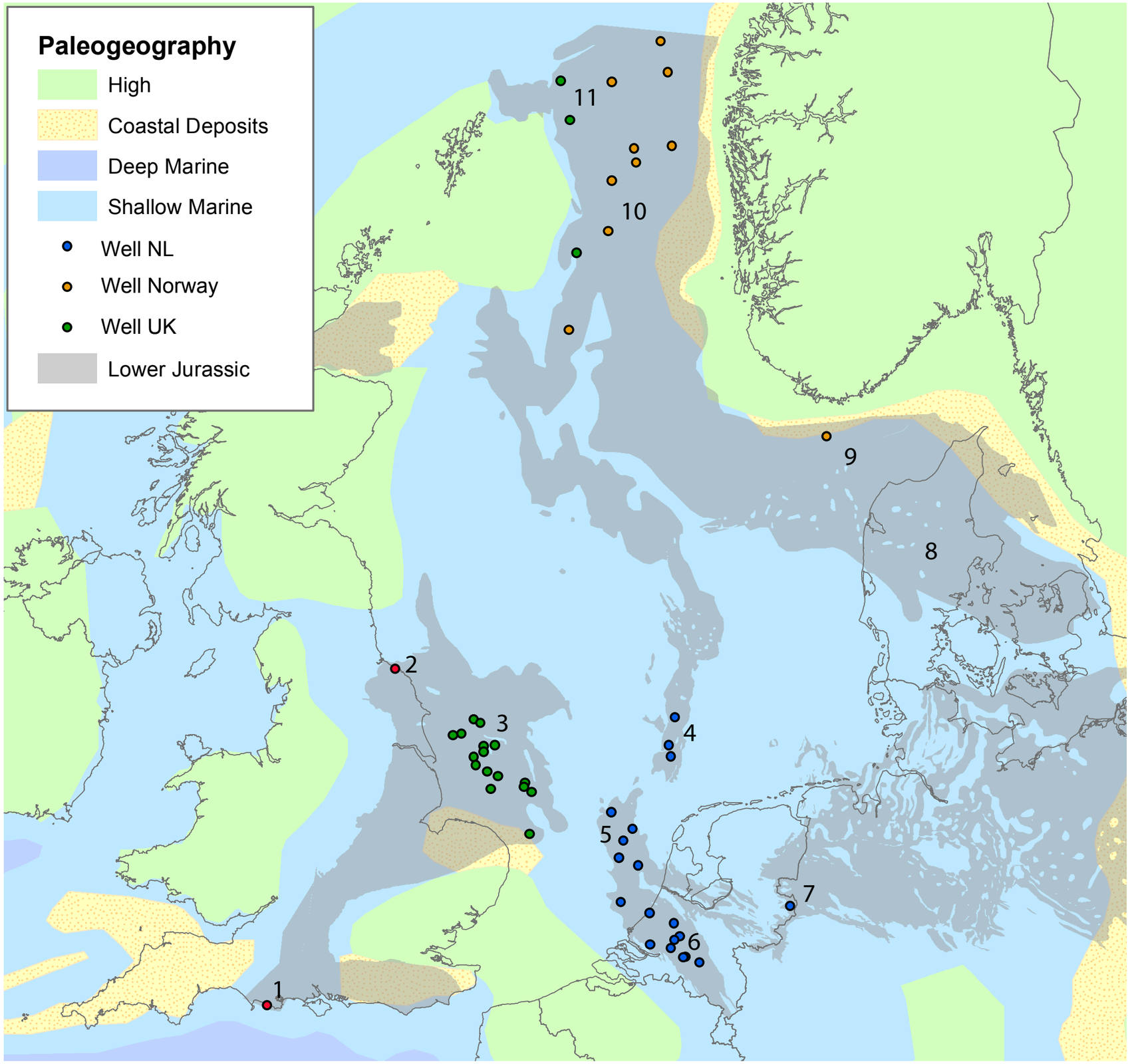

1.2 Geographic and temporal scope

The study area comprises most of the North Sea area and extends into the Southern Norwegian Sea to the north. The onshore exposures of the Cleveland Basin of Yorkshire, UK form the western extremity, whereas the southwestern boundary is the Wessex Basin of Dorset in the UK. The eastern boundary of the study area lies in Denmark and is part of the Norwegian-Danish Basin. The northern part of the Viking Graben Area of Norway forms the northern boundary of the study area. The presence of Lower Jurassic strata is limited due to uplift and inversion and confined to basinal areas (see grey shading **Figure 1.2**). The geographical nomenclature throughout this report follows that indicated in **Figure 1.2**.

The two outcrop reference sections in the Wessex Basin (1 in **Figure 1.2**) and the Cleveland Basin (2 in **Figure 1.2**) form the stratigraphic backbone of this study. We have sampled cores from the Netherlands (6 and 7 in **Figure 1.2**) and Norway (10 and 9 in **Figure 1.2**). Information from Denmark is derived from the publication of Petersen et al. (2008).

The temporal scope is the entire Early Jurassic (e.g., the Hettangian, Sinemurian, Pliensbachian and Toarcian Stages) but also addresses the changes taking place during the Triassic-Jurassic boundary interval (**Figure 1.1**).

◄ Figure 1.2: Paleogeographic map of the study area.
This map is based on information from the Millenium (Husmo et al., 2003) and SPBA-atlases (Doornenbal and Stevenson, 2010). The grey shading indicates the distribution of Lower Jurassic deposits. The coloured dots represent well-data used in this study. The numbers refer to geographic areas and basins used throughout this report: 1= Wessex Basin/Dorset Coast, 2= Cleveland Basin/Yorkshire Coast, 3= UK Southern North Sea (East Midlands Shelf and Sole Pit Basin), 4= Dutch Central Graben, 5= Broad Fourteens Basin, 6= West Netherlands Basin, 7= Lower Saxony Basin, 8= Norwegian-Danish Basin, 9= Farsund Basin, 10= Viking Graben area, 11= East Shetland area. Note that the yellow coloration represents coastal marine deposits and not necessarily sand.

Whalestone Level from Jet Rock in Yorkshire

2. Approach and Methodology

2. APPROACH AND METHODOLOGY

2.1 Database and samples

Samples
Rock samples are collected from outcrops and from cored intervals and side-wall cores of exploration wells. Most of the samples are analysed for both palynology and stable isotope analyses. For details reference is made to the digital Masterfile in Excel format. Next to that, all palynological data is provided in Stratabugs-format (.dex).

Outcrop samples
The stratigraphic framework (Chapter 4) is based on outcrop samples from England, UK. In the coastal successions from the Wessex Basin in Dorset, 145 samples were collected. These samples cover the uppermost Triassic to Lower Pliensbachian, with a varying resolution achieving multiple samples per Ammonite Subzone. In the coastal successions from the Cleveland Basin in Yorkshire, 260 samples are collected for analysis. These samples cover the uppermost Sinemurian to uppermost Toarcian, also with resolution of multiple samples for each Ammonite Subzone. Each outcrop sample is assigned a composite depth on the stratigraphic column. The composite thickness of the Wessex Basin sequence (Uppermost Triassic - Lower Pliensbachian) is 125 m and 350 m for the Cleveland Basin sequence (Upper Sinemurian - Uppermost Toarcian).

Well samples
More than 330 core and side-wall core samples from seven wells are collected in core repositories from Norway and the Netherlands (see **Table 2.1**).

2.2 Palynology

Introduction
Palynologists study acid-resistant organic matter from sedimentary rocks. Organic matter is classified into palynomorphs, organic microfossils within a certain size range, and palynodebris (e.g., all other organic material such as plant-tissue, wood fragments, amorphous organic matter). The combination of palynomorphs and palynodebris is called palynofacies. Within the palynomorph category, two groups are considered the most important: the dinoflagellate cysts, or dinocysts, and the pollen and spores, or sporomorphs. Because palynology straddles both the marine and the terrestrial realm, it is ideally suited for the study of shallow to non-marine sedimentary rocks (see **Figure 2.1**).

Processing and workflow
The organic matter is extracted from the rock by a standard laboratory processing procedure. During the first step, the sedimentary rock is crushed and treated with hydrochloric acid to digest the carbonate. After that, the mineral bonds of the silicates are destroyed by using hydrofluoric acid, thus releasing the acid-resistant organic matter. The organic residue is then concentrated by sieving over a 10 μm mesh. The organic matter particles larger than 10 μm are brought on a glass slide, fixed by a mounting medium (glycerine jelly), and covered by a thin glass cover slip. The result is called a palynological preparation or slide. Its content is studied using a transmitted light microscope with magnifications varying between 100 and 1000 microns. The microfossils such as dinoflagellate cysts and pollen and spores are identified on species level and counted. In principle, three rows are counted using the 40x objective. Illumination with ultra violet light is applied for the identification of small acritarchs and other palynomorphs (**Figure 2.1**). The counts of the organic matter assemblages and of the palynomorph assemblages are displayed in “closed SUM” diagrams, while the occurrences of the different species are displayed in distribution charts.

Area	Well	Stratigraphic focus
Netherlands	Boeikop-01 (BKP-01)	Upper Pliensbachian – Lower Toarcian
Netherlands	Oldenzaal-04 (OLZ-04)	Rhaetian – Upper Pliensbachian
Farsund Basin (Norway)	IKU 13/1-U1	Sinemurian – Toarcian
Viking Graben area (Norway)	34/7-5	Sinemurian – Toarcian
Viking Graben area (Norway)	34/10-35	Pliensbachian – Toarcian
Viking Graben area (Norway)	30/6-16	Pliensbachian – Toarcian
Viking Graben area (Norway)	34/8-10s	Hettangian - Sinemurian

▲ Table 2.1: Overview of wells selected for biostratigraphic and paleo-environmental analysis.

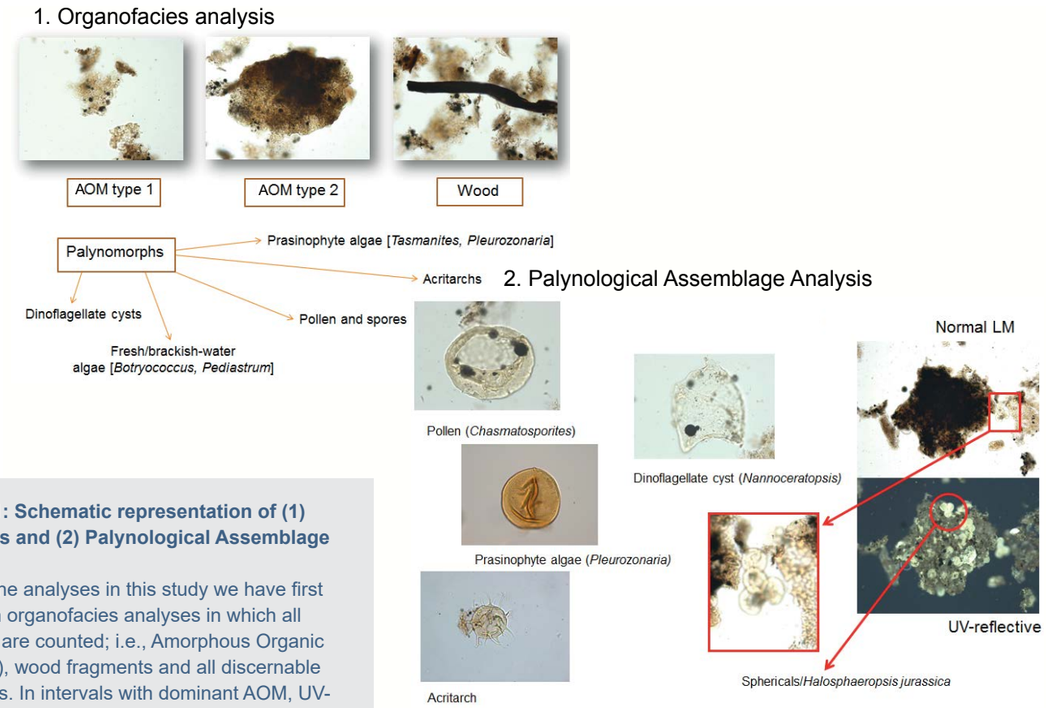

▲ Figure 2.1: Schematic representation of (1) Organofacies and (2) Palynological Assemblage analyses.
For parts of the analyses in this study we have first performed an organofacies analyses in which all organoclasts are counted; i.e., Amorphous Organic Matter (AOM), wood fragments and all discernable palynomorphs. In intervals with dominant AOM, UV-fluorescence microscopy was employed in order not to underestimate palynomorphs enclosed in AOM. Subsequently, all palynomorphs were counted and grouped in-line with their biological affinity.

Age interpretations
The outcrop sections in the UK are calibrated to the global standard via detailed ammonite stratigraphy. Therefore, the palynological marker events derived from the palynological analyses in this study can be tied to this ammonite zonation as well. The marker events are compiled in the stratigraphic framework and compared with literature data in Chapter 4. Also the chronostratigraphically calibrated carbon isotope shifts established in this study will be addressed to this end.

Palaeoenvironmental interpretations
Palaeoenvironmental information is deduced from the organofacies, or organic matter assemblages, and from the quantitative palynomorph assemblages. For the organofacies interpretation, four groups are important:

1. Amorphous Organic Matter (AOM), also called Structureless Organic Matter (SOM): This type of organic matter consists of mid-size to large (50 to 300μ) particles with no obvious structure, i.e. no cell walls, vessels etc. Two types are distinguished:
Type 1 is more or less translucent and is in general less massive than Type 2.
Type 2 is not translucent, darker and more massive than Type 1. Type 2 may reach 300μ, which is in the same range size as medium sand.

In most cases, AOM-particles reveal small “hidden” palynomorphs when studied under ultra-violet light (instead of “normal” transmitted light). Apparently, this type represents aggregates of organic-matter, likely related to bacterial polymeric substances (Pacton et al., 2011), resulting from high biological productivity and burial.

2. Wood: These are organic matter particles that can be attributed to wood remains. Three types are distinguished, based on their coloration, opacity and the appearance of vascular structures.

3. Palynomorphs These are organic matter particles that constitute individual biological entities. This group is further subdivided and is displayed in “closed sum” diagrams.

For the interpretation of the quantitative palynomorph assemblages, the following categories are important:

1. Sphaeromorph algal cysts Albeit these may be attributed to numerous taxonomic entities we noted two; *Leiosphaera* and *Halosphaeropsis liassicus*. These are relatively small spherical particles with no obvious ultra-structure such as spines, granules or openings. Their biological origin is not fully clear, but it is generally thought that they are attributed to the cysts (or phycomae), representing part of the life-cycle of photosynthetic prasinophyte algae (see also section below).

2. Acritarchs: These are small algal cysts that cannot be attributed to either dinoflagellate cysts or resting cysts of known algae. In this study particularly the genus *Michrystridium* was found abundantly. In marine palynological assemblages, acritarchs are always present but usually quite rare. They are restricted to marine environments.

3. Prasinophyte algae are a class of unicellular algae, containing green-pigment chlorophyll. They belong to the Division of Chlorophyta. High abundances of prasinophytes occurs when reactive nitrogen and phosphorous become freely available in the photic zone (Prauss, 2007; Van de Schootbrugge et al., 2013). This typically happens when surface-water stratification (de)stabilizes and the chemocline moves into or out of the photic zone. As a result, mass-occurrences often mark ecological tipping points.

4. Organic-walled dinoflagellate cysts (dinocysts) represent the resting cysts of a type of marine plankton. The fossil group appears in the Triassic and is known to have undergone rapid diversification from the Toarcian onward (Fensome et al., 1993). Dinocysts are commonly used in biostratigraphy. They are essentially restricted to marine environments.

5. Sporomorphs: This is a general term for all occurring pollen and spores. In Jurassic times, the pollen record was only represented by gymnospermous pollen (e.g. from conifers). Angiosperm pollen only appear later, in the Cretaceous. The quantitative sporomorph record is very useful in the paleoclimatic interpretation (see Chapter 6).

6. Some **other** groups also reach abundances in the studied record: *Botryococcus* represents a type of fresh-water-tolerant algae, that proliferates under brackish conditions, whereas *Pediastrum* is affiliated with fresh-water conditions.

2.3 Stable carbon isotope analysis

Introduction

Isotopes are variants of a chemical element that differ in the number of neutrons, but not in the number of protons (see Figure 2.2). Therefore, two isotopes of the same element display similar chemical behaviour, but differ in the molecular weight. Isotopes can be radioactive, like for instance ^{14}C, or stable like ^{12}C and ^{13}C. For this project the stable carbon isotopic composition of bulk organic material was analyzed ($\delta^{13}C_{org}$). In this type of stable isotope analysis, these two stable carbon isotopes, ^{12}C and ^{13}C are measured and expressed as a ratio against a standard (the Vienna Pee Dee Belemnite, VPDB). Note that it is also possible to assess $\delta^{13}C$ on the calcite of fossils (e.g. belemnites) or on the bulk carbonate fraction of the sediment ($\delta^{13}C_{carbonate}$).

Processing

The technique used for isotope analysis is the Elemental Analyser - Isotope Ratio Mass Spectrometry (EA-IRMS). For this technique, samples and reference materials are weighed into tin capsules, sealed and then loaded into an automatic sampler on a Europa Scientific Roboprep-CN sample preparation module. From there, they are dropped into a furnace held at 1000 °C and combusted in the presence of oxygen. The tin capsules flash combust, raising their temperature in the region of the sample to ~1700 °C. The combusted gases are swept in a helium stream over a combustion catalyst (Cr_2O_3), copper oxide wires (to oxidize hydrocarbons) and silver wool to remove sulphur and halides. The resultant gases (N_2, NO_x, H_2O, O_2, and CO_2) are swept through a reduction stage of pure copper wires held at 600 °C. This removes any oxygen and converts NO_x species to N_2. A magnesium perchlorate chemical trap removes water. Carbon dioxide is separated from nitrogen by a packed column gas chromatograph held at an isothermal temperature of 100 °C. The resultant CO_2 chromatographic peak enters the ion source of the Europa Scientific 20-20 IRMS where it is ionised and accelerated. Gas species of different mass are separated in a magnetic field then simultaneously measured using a Faraday cup collector array to measure the isotopomers of CO_2 at m/z 44, 45, and 46. Both references and samples are converted and analysed in this manner. The analysis proceeds in a batch process, whereby a reference is analysed followed by a number of samples and then another reference.
The output voltages of the IRMS, combined with careful weighing of the sample, also provide the means to reconstruct weight percent total organic carbon (TOC).

Application

The application of stable isotope analysis is based on the assumption that the measured ratio between ^{12}C and ^{13}C in a sediment sample reflects the atmospheric ratio at the time of deposition. Variations in the stable carbon isotope composition reflect changes in the isotopic composition of the global carbon pool (i.e., the exchange between the oceanic, terrestrial and atmospheric reservoirs, see Figure 2.2). Most organisms exhibit preferential uptake of light carbon (^{12}C), due to chemical interactions at molecule level. As a consequence, during geological times when excessive burial of organic matter occurs, the oceanic background ratio will become enriched in heavy carbon (^{13}C). During times of excessive oxidation of organic matter, like with today's anthropogenic activity, ^{12}C is brought back into the atmosphere, leading to enrichment in light carbon, a negative excursion in $\delta^{13}C$. These shifts can be correlated for stratigraphic purposes.

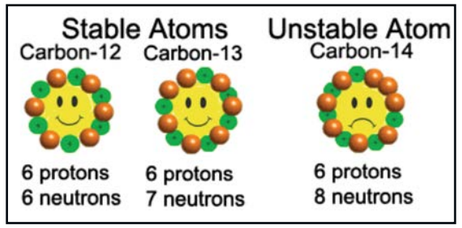

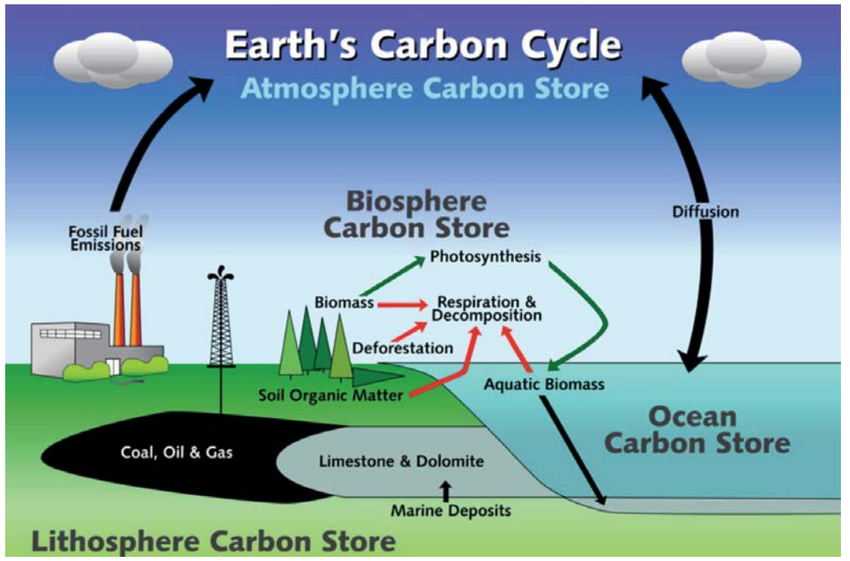

▲ Figure 2.2: The carbon pools of the earth.
Carbon may be stored in the lithosphere as rock, e.g. in limestone, or as fossil fuel, e.g. coal, oil or gas. Carbon is also stored in the oceans and atmosphere, as (dissolved) CO_2. When exchange of carbon occurs between these pools fractionation occurs thus affecting ratio between 12C and ^{13}C.

2.4 Rock Eval Pyrolysis

Rock Eval Pyrolysis analyses were performed at Lausanne University in collaboration with Dr. Thierry Adatte.

During Rock-Eval pyrolysis ca. 100 mg of ground and ho-mogenised sample is subject to a pyrolysis step followed by the complete oxidation of the residual sample. A FID detector measures the hydrocarbon released during pyrolysis, while CO_2 and CO are detected by infrared absorbance during both steps. In the here applied standard cycle for "whole rock" (IFP 2001), pyrolysis starts isothermally at 300°C for 3 minutes, after which the sample is heated to 650°C. The oxidation step starts isothermally at 400°C (3 min) and then heats up to 850°C. Organic carbon decomposition results in 4 main peaks: the S 1 peak (hydrocarbons released during the isothermal phase), the S2 peak (hydrocarbons produced between 300 and 650°C), the S3 peak (CO_2 from pyrolysis of OM up to 400°C), and the S4 peak (CO_2 released from residual OM below ca. 550°C during the oxidation step). Mineral carbon decomposition is recorded by the S3' peak (pyrolysis-CO_2 released above 400°C), and the S5 peak (oxidation-CO_2 released above ca. 550°C).

These peaks are used to calculate the amount of total organic carbon (TOC) and the amount of mineral carbon (MINC). In addition, the so-called hydrogen index (HI = S2/TOC) and oxygen index (OI = S3/TOC) are calculated. The HI and OI indices are proportional to the H/C and OIC ratios of the organic matter, respectively, and can be used for OM classification in Van-Krevelen-like diagrams (Espitalie et al. 1977). The calibration standard used was the IFP-55000 (Institut Francais du Petrole; IFP 2001), a

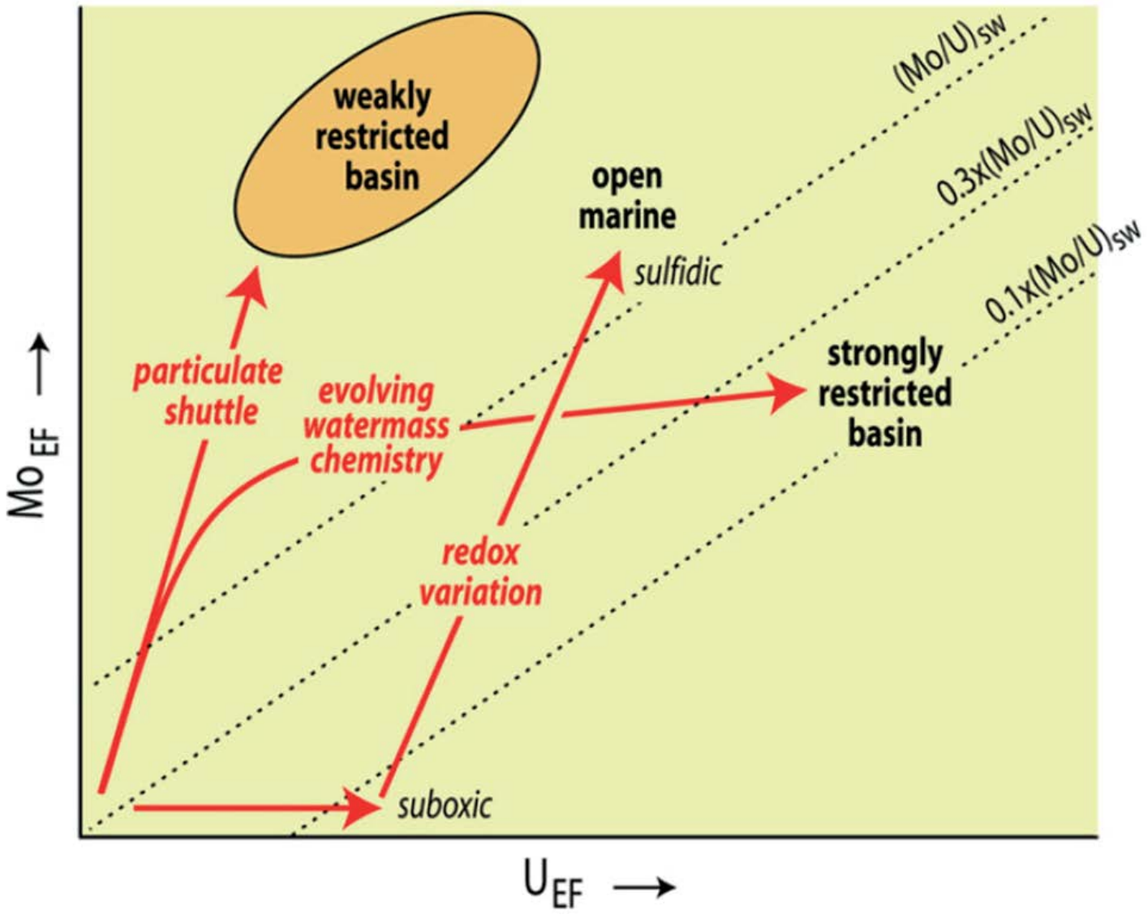

▲ Figure 2.3: Model of enrichment patterns and changes in Mo and U enrichment factors in response to redox conditions and hydrology, from Algeo & Tribovillard (2009).

Jurassic marine sediment.

2.5 Bottom-water redox conditions

Major and trace element compositions as well as TOC were utilised to undertake a palaeo-redox evaluation. The evaluation was performed on the Wessex Basin, Cleveland Basin, Boeikop-01 and Oldenzaal-04 successions.

Redox sensitive trace elements (RSTE) are elements that change in the charge and/or speciation with varying redox conditions (Brumsack and Gieskers, 1983; Algeo, 2004; Tribovillard et al., 2006). This change determines the solubility of the RSTEs, with preferential authigenic enrichment under anoxic to sulphidic conditions. In oxic marine conditions uranium has a valence of $^{6+}$ that prevents it from being scavenged to the sediment (Anderson et al., 1989). The main form of U in anoxic conditions is U^{4+}, which is preferentially taken up by organic matter, accelerated through the formation of organometallic ligands in humic acids (Klinkhammer & Palmer, 1991; Algeo & Mynard, 2004; Tribovillard et al., 2006). Similarly, the change in the oxidation state of vanadium from $^{5+}$ to $^{4+}$ governs its sequestration into sediment under anoxic conditions, which is also promoted by presence of organometallic ligands (Morford and Emmerson, 1999). However, further sedimentary enrichment may occur in the presence of H_2S as V^{4+} is reduced to V^{3+} and precipitated as a (hydr)oxide or taken up by geoporphyrins (Breit and Wanty, 1991; März et al., 2008). Molybdenum undergoes a species as well as oxidation state change with reducing conditions and is particularly sensitive to the H_2S concentration (Zheng et al., 2000, Helz et al., 2004). Unlike U it can be scavenged directly from the anoxic water column. In anoxic conditions Mo tends to be affiliated to sulphides (mainly pyrite) as well as organic matter (Helz et al., 2004; Goldberg et al., 2009). Although trace elements are an indication of redox conditions, they cannot distinguish whether the chemocline is below or above the sediment–water interface. Nevertheless at least the bottom water would have been anoxic to achieve high concentrations of RSTEs.

The Total organic carbon over phosphorous ratio has also been proposed as a local seawater redox indicator, where TOC/P ≥ 50 (mol organic carbon/mol P) is thought to reflect anoxic conditions (Algeo & Ignall, 2007). Phosphorous is delivered to the ocean via riverine input. It is the main nutrient for marine organisms and is therefore largely present in biomass. When organic biomass passes an oxic water column it is mostly oxidised, releasing organic carbon (as CO_2) and P. While carbon dioxide escapes, the greater portion of P is trapped as fourapatite or sorbed and fixed to Fe-(oxyhydr)oxides. Under anoxic conditions the majority of organic matter is not remineralised and both TOC and P remain in the sediment. In conclusion, TOC/P ratios are higher in anoxic conditions and lower in oxic conditions. This relationship is however not straightforward, as the carbon/phosphorous ratio is also governed by the type of organism and burial diagenesis results in a differential loss of C to P.

High S content is also indicative of euxinic conditions. However, it is possible that these conditions were achieved beneath the sediment-water interface and not in the water column.

When considering trace elements it is important to use element ratios to deduct the effect of background sedimentation (e.g. V/Al). Enrichment factors (EF) represent the enrichment of the RSTE relative to the Post-Archean Average Shale. High Mo and U EFs are indicative of euxinic conditions and progressively greater enrichment of Mo over U is considered to reflect unrestricted anoxic conditions (Algeo and Tribovillard, 2009;Tribovillard et al., 2012). In semi-closed sulfidic water bodies, Mo burial overwhelms Mo resupply faster than U, resulting in Mo/U ratios that are smaller compared to seawater as EFs increase. A third process describes an enhanced export of aqueous Mo to the sediment via a metal oxyhydroxide particulate shuttle with little effect on U. This process is characterised by high Mo EFs and low U EFs.

2.6 Well log correlations

In the UK sector, 16 wells from the Silver Pit Basin, Offshore East Midland Shelf and Sole Pit High are correlated (see Chapter 5). In the Dutch sector, 18 wells from the Dutch Central Graben, Broad Fourteens and Roer Valley Graben are correlated. Mainly the Gamma Ray (GR) and Sonic (DT) logs are used for the correlations. The GR is scaled from 0 – 200 gAPI, the DT is scaled from 40 – 240 µS/ft. ■

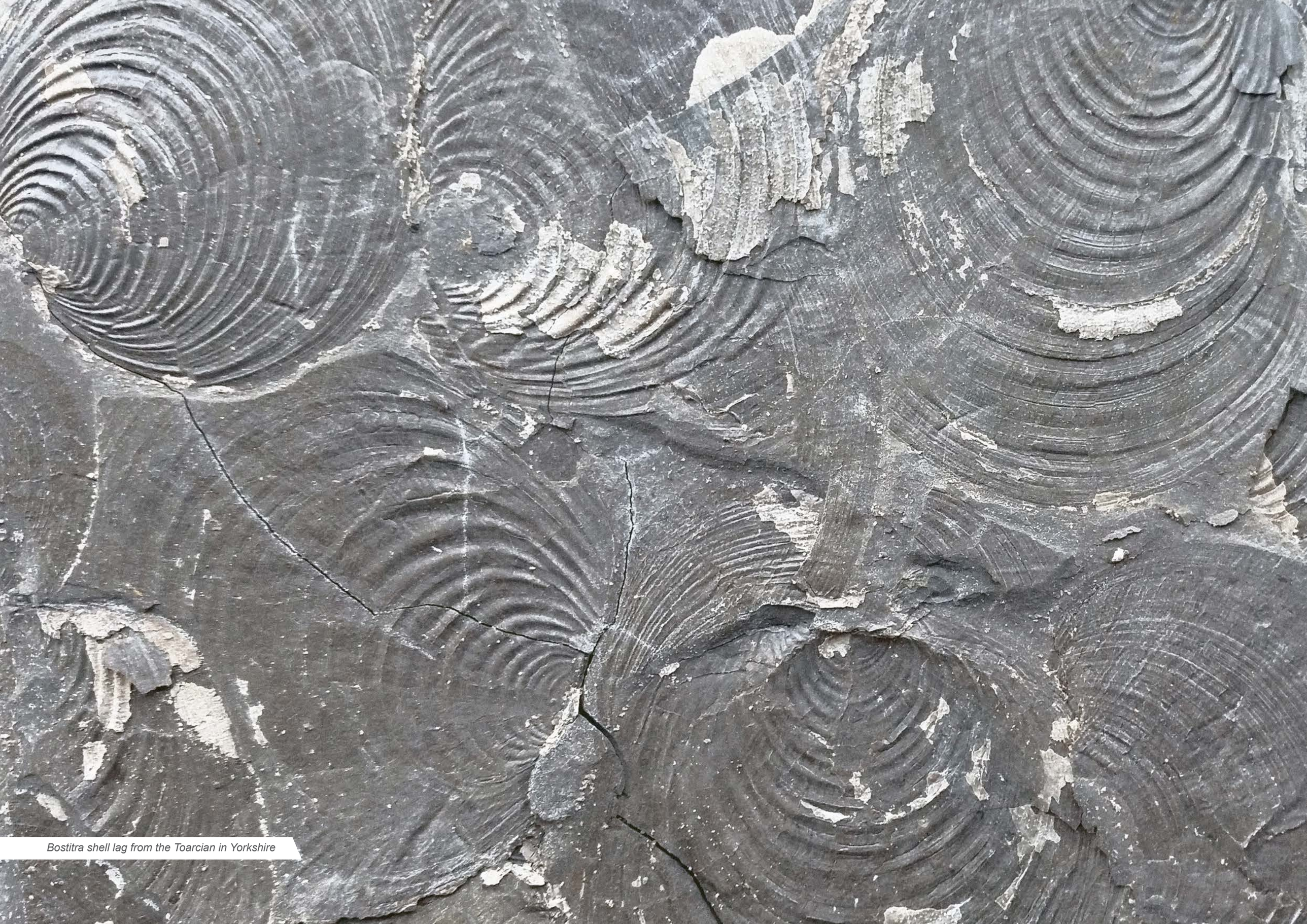

Bostitra shell lag from the Toarcian in Yorkshire

3. Geological setting and regional stratigraphy

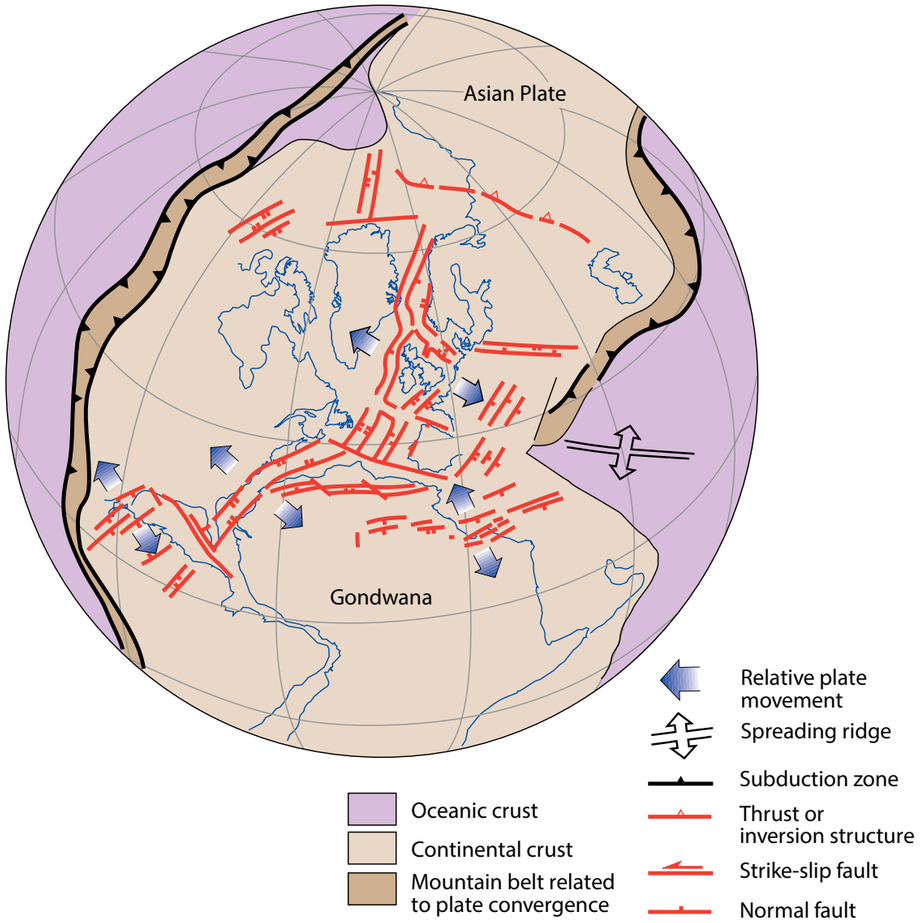

▲ **Figure 3.1: Simplified overview of tectonic processes active during the Early Jurassic.** Modified after Coward et al. (2003).

▲ **Figure 3.2: Map for the Early Jurassic showing the distribution of active structures and sediment facies.** The location of the Mid-Jurassic thermal dome in the central North Sea is also shown. Modified after Coward et al. (2003).

3.1 Geological setting

During Early Jurassic times, rift phases related to incipient sea-floor spreading in the Tethys and Central Atlantic oceans to the south began to affect tectonic structures in northwest Europe (**Figure 3.1**). The Central Atlantic rift system spread into the basins west and south of Ireland, and possibly into the Faeroe–Shetland Basin and offshore Norway. Central Atlantic rifting was transferred along the Azores–Gibraltar and Biscay transform zones into the western Tethys Ocean, opening a deep Early Jurassic basin in south-east France. The west Tethyan basins formed at this time. North-westerly trending Triassic rifts continued to open in the western part of the southern North Sea and along the Biscay margin, and there was some faulting along the Polish Trough; these orthogonal structures may represent the influence of Tethyan opening (Coward et al., 2003).

During most of the Triassic, sedimentation in the study area was predominantly terrestrial. By the end of the Triassic, rising sea levels started to flood parts of the study area. In combination with the abovementioned local tectonic subsidence and more humid climate, a shallow open epicontinental sea developed in the uppermost Triassic to lowermost Jurassic, essentially extending from the present-day UK into the Netherlands, western Germany and parts of Denmark. In contrast, there seems to have been very little Early Jurassic rifting in the northern North Sea (except for the Central and Viking Graben systems). This is mainly because the main areas of extension were in the Central Atlantic and rifting was extended into the Western Tethys, opening a very deep basin in Southeast France. As a consequence, Lower Jurassic deposits are generally thin or absent in the northern North Sea (**Figure 1.2**). Elsewhere, the present limits of Lower and Middle Jurassic strata commonly coincide with the hanging walls of Late Jurassic faults, although the thickness pattern of the Lower and Middle Jurassic successions suggests that they formerly extended across the faults and that their present-day absence is likely to have been caused by erosion during Late Jurassic footwall uplift. Hence, the distribution of Lower Jurassic strata was formerly much more extensive.

The occurrence of widespread Middle Jurassic volcanic rocks in the Central North Sea suggests the presence of a major mantle hot spot (Partington et al., 1993) and associated uplift caused erosion down to Lower Jurassic or older strata. Evidence for regional uplift affecting the North Sea during the Toarcian to early Aalenian comes from stratigraphic data, giving rise to the Mid-Jurassic (Mid-Cimmerian) unconformity. It is erosion of the uplifted dome that yields the Bajocian to Bathonian sands of the important Brent Group reservoirs in the northern part of the North Sea. Further to the south, these sediments are absent due to local uplift.

Hence, the present-day distribution of Lower Jurassic strata is complex due to effects of three factors:

(I) Pre-existing Triassic rift topography
(II) Middle Jurassic thermal doming and
(III) Late Jurassic rifting and subsequent inversion.

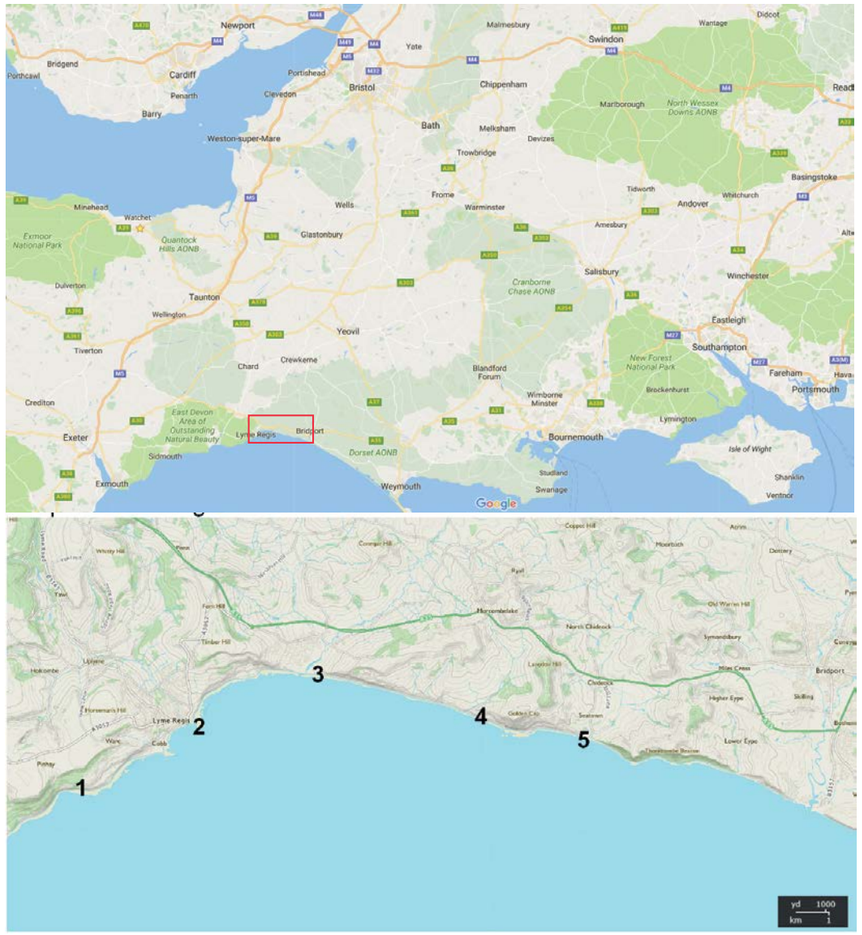

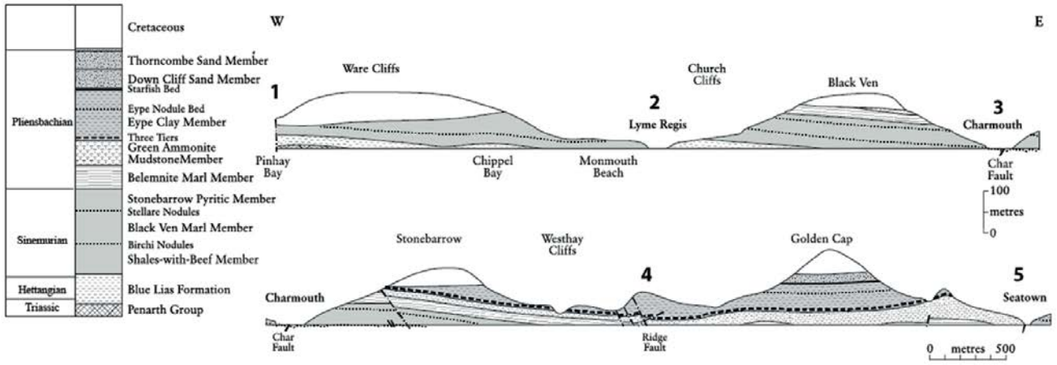

▲ **Figure 3.3:**
Upper panel: Location of the Dorset Coast succession (red square).
Middle Panel: Sampling localities along the Dorset Coast.
The numbers refer to the locations of the cross-section depicted in the Lower Panel.
Lower Panel: Overview of the exposure of the different stratigraphic units along the coastal stretch between Pinhay Bay and Seatown.
1=Pinhay Bay, 2= Lyme Regis, 3= Charmouth, 4= Ridge Fault and 5= Seatown.

3.2 Outcrop reference sections

Wessex Basin - Dorset Coast
The Wessex Basin consists of a system of post-Variscan sedimentary depocentres and intra-basinal highs that developed across central southern England and adjacent offshore areas. Given its limits in age and area, the Wessex Basin may be considered to represent a series of extensional subbasins that are part of a more extensive network of Mesozoic intracratonic basins that covered much of NW Europe (Ziegler 1990). Like many of the other basins around the British Isles (e.g. the Weald, Southern North Sea, Cleveland Basin etc.), the Wessex Basin also records the effects of Cretaceous-Cenozoic intraplate contraction and structural inversion of basin-bounding and intra-basinal faults. The lowest division consists of Permian and Triassic continental (red bed) sediments. The Penarth Group at the top of the Triassic succession heralds the effects of widespread Liassic marine transgression that led to the re-establishment of marine waters in the area for the first time since the Carboniferous.

The Dorset Coast (Pinhay Bay to Seatown, **Figure 3.3**) exposes the most important marine stratigraphic reference succession for the lowermost part of the Lower Jurassic (Hettangian-Sinemurian) in northwest Europe. In addition, the succession beautifully provides non-mature outcrop analogues for extensive source-rock intervals (Blue Lias Fm., Charmouth Mudstone Fm.) that have sourced oil fields in the vicinity, such as the giant Wytch Farm Oil Field (Buchanan, 1998). For the purpose of this study we sampled the Hettangian to Lower Pliensbachian of these sections.

A few metres beneath the base of the Jurassic (already within the Blue Lias Fm.), remarkable and widely recognized slumped beds of the Langport Mb. or “White Lias” are found (**Figure 3.4 and 3.5**). These are interpreted to represent a series of seismites (Wignall, 2001) related to extensive volcanism of the Central Atlantic Magmatic Province (CAMP, Lindstrom et al., 2015, **Figure 3.7**). It has been inferred that this magmatic phase contributed to elevating atmospheric greenhouse gas concentrations and sustaining warm climates during the Jurassic. The overlying Blue Lias Fm. thus encompasses the highest part of the Triassic Rhaetian Stage, the Hettangian Stage and the lowest part of the Sinemurian Stage.

The Blue Lias Fm comprises interbedded organic-rich millimetre-laminated shales, light and dark marls and massive limestones in tabular beds and concretions (Hesselbo and Jenkyns, 1995), reflecting both primary carbonate production as well as diagenetic cementation (Bottrell & Raiswell 1989, **Figure 3.6**). Illite is the predominant clay mineral with minor kaolinite also occurring, indicating an overall chemical weathering regime (DeConinck et al, 2003). It has been suggested that the

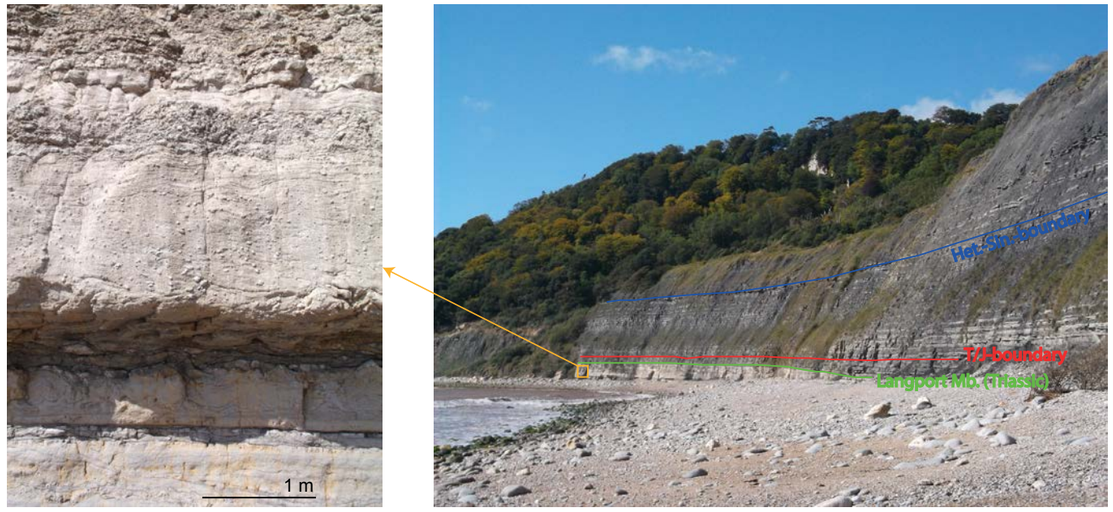

▲ **Figure 3.4: Field photographs of the Triassic-Jurassic boundary section in Pinhay Bay (right).**
Note that the actual T/J-boundary lies above the transition between the so-called White Lias (Langport Mb.) and Blue Lias Fm. The Hettangian Sinemurian boundary is also marked. The upper part of the Langport Mb. constitutes a series of slumped beds, containing imbricated coral clasts and fluid-escape structures. These beds are interpreted as a series of ‘seismites’ associated with CAMP-volcanism (left photograph, see also Figures 3.5 and 3.7). The Blue Lias Fm. is composed of very rhythmic variations of shale, marl and limestones (see also Figure 3.6).

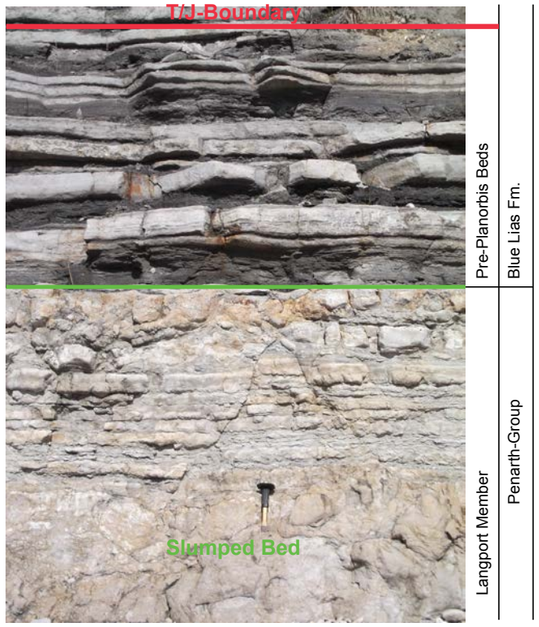

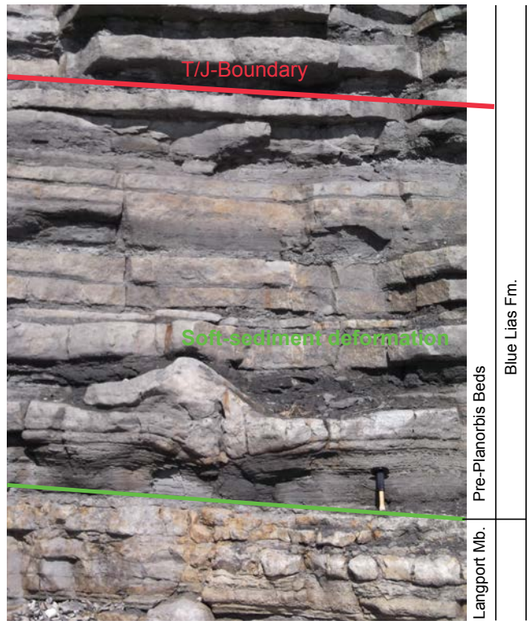

▲ Figure 3.5: Field photographs of the Uppermost Triassic in Pinhay Bay.
The left photograph depicts the major slumped bed, still belonging to the Langport Mb. Above that the first black shales of the Blue Lias Fm. are deposited in a sharp transgressive manner. Also in the basal (still Triassic) Blue Lias Fm. soft-sediment deformation is recorded (right photograph).

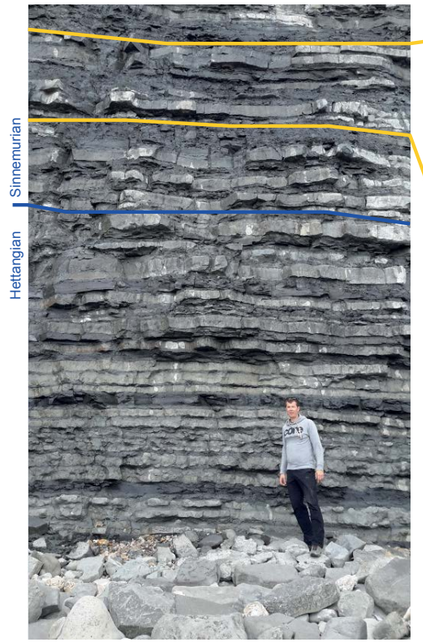

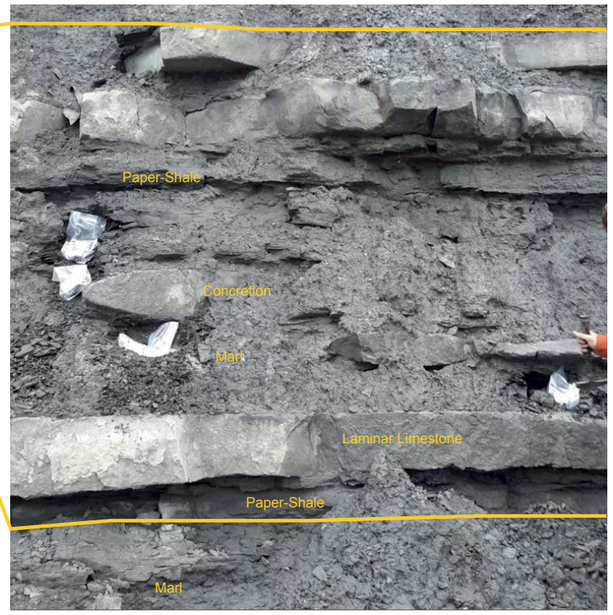

▲ Figure 3.6: Field photographs of the Blue Lias Fm. between Pinhay Bay and Lyme Regis.
This photograph illustrates the cyclic nature of the succession. The right graph is a close-up illustrating the composition of these alterations.

interbedding of limestones and mudstones so apparent in the Blue Lias was produced by orbitally forced climatic oscillations (Weedon 1986), with the proximal mechanism possibly being variation in runoff affecting surface productivity. Work on the macrofossils recovered from the section (Wignall & Hallam 1991) has defined oxygen-controlled biofacies, which are indicative of bottom-water oxygenation that varied from strongly anaerobic to weakly dysaerobic conditions and which correlate well with the lithofacies (**Figure 3.8**).
Throughout the Wessex Basin, the Blue Lias Fm. is developed in a typical facies of alternating limestones, mudstones and paper shales.

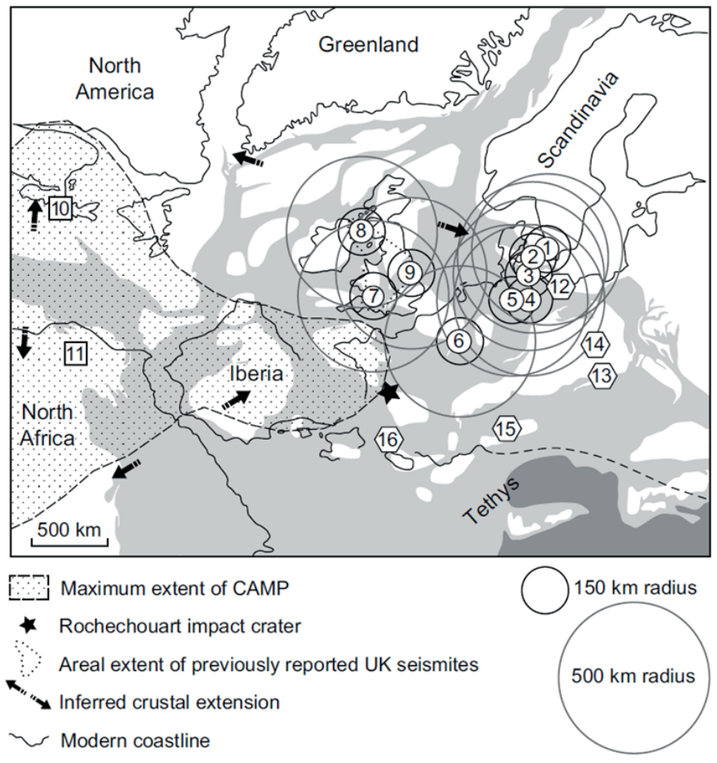

► Figure 3.7: Paleogeographic map of western Europe showing seismite localities investigated by Lindstrom et al. (2015) and their spatial radius.
The extent of the Central Atlantic magmatic province (CAMP) is also shown. The star shows the location of Rochechouart crater, which is not deemed fully synchronous to the T/J-boundary. The arrows show inferred crustal extension. This Figure is after Lindstrom et al. (2015).

▲ Figure 3.8: Field Photograph of the so-called Top-Tape bed from the middle of the Blue Lias Fm.
This picture is taken between Pinhay Bay and Lyme Regis. The age is Early Sinemurian. This limstone bed is packed with large specimens of **Metophioceras conybeari,** illustrating that the depositional environment at times was certainly more oxygenated.

▲ **Figure 3.9: Field Photograph of Shales with Beef Mb. (left) and the contact between the Stonebarrow Pyritic Mb. and the Belemnite Marl Mb. (right).**
All these units belong to the Charmouth Mudstone Fm. The left photographs illustrate the occurrence of fibrous calcite ('beef'). The upper photograph shows beef encroaching an early diagenetic carbonate concretion, whereas beef is also found in thin streaks thoughout the organic-rich mudstones (left). The right photograph shows the boundary between the Sinemurian and Pliensbachian.

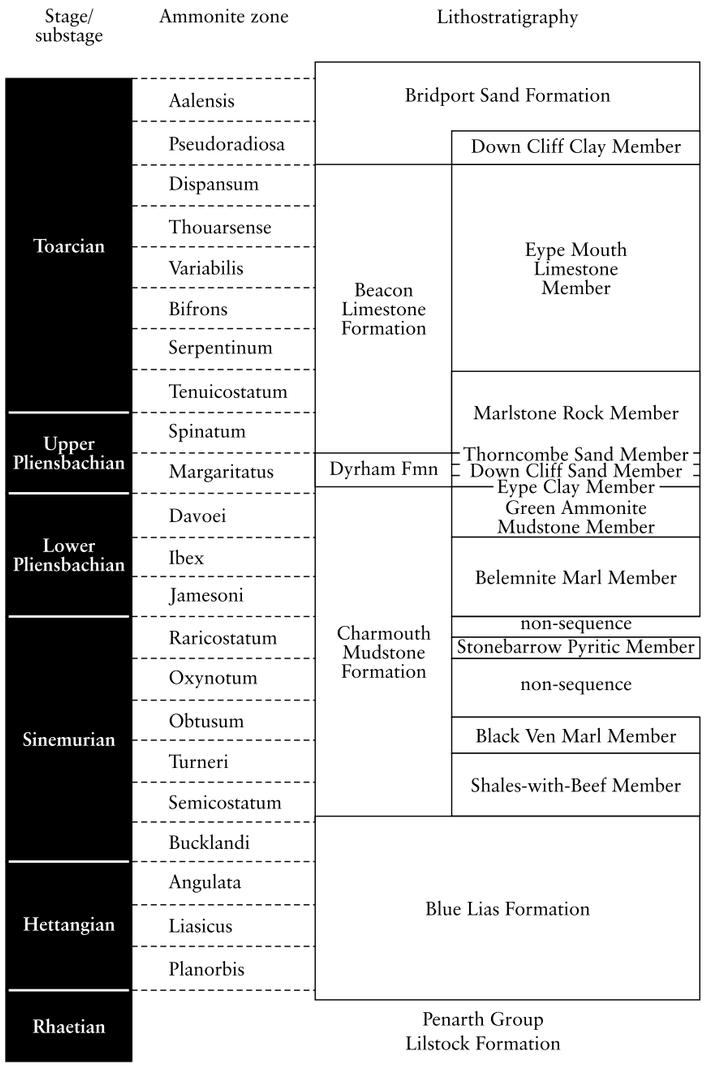

▲ **Figure 3.10: Overview of the lithostratigraphic nomenclature used for the Wessex Basin.**
We have sampled the Hettangian and Sinemurian and the Lowermost Pliensbachian for the purpose of this study. This figure is modified after Simms (2004).

The succeeding Charmouth Mudstone Formation, which encompasses much of the Sinemurian Stage and the lower part of the Pliensbachian Stage, is divided into five members (**Figure 3.9**). The Shales-with-Beef Member consists of finely laminated and bituminous dark-grey mudstones with a few bands of limestone nodules or septaria and thin beds of fibrous calcite, or 'beef ', which give the member its name. The succeeding Black Ven Marl Member is very similar lithologically, although 'beef' lenses are less well-developed. The boundary between the two members is essentially arbitrary but was drawn below a conspicuous limestone band, the Birchi Tabular. The succeeding Stonebarrow Pyritic Member for the upper part of the Sinemurian Stage, comprises blue-grey shaly to blocky mudstones with often abundant pyritic ammonites (**Figure 3.9**). Along the Dorset coast it is represented by some 14 m of sediment in the lower part of the Raricostatum Zone, bounded above and below by significant non-sequences. The Belemnite Marl Member comprises rhythmic alternations of light and dark calcareous or pyritic mudstones often rich in belemnites.

The succeeding part of the Lower Jurassic succession is not sampled for the purpose of this study but the general lithology is briefly described to facilitate comparison in terms of facies trends (**Figure 3.10**). The Green Ammonite Mudstone Member consists of bluegrey mudstones with a few thin beds of nodules. The considerably more condensed Dyrham Formation is divided into three, increasingly sandy members. The Beacon Limestone Formation comprises two units and is highly condensed and shows marked lateral thickness changes associated with synsedimentary faults (Jenkyns and Senior, 1991). It spans the highest part of the Pliensbachian Stage and most of the Toarcian Stage. On the Dorset coast it is succeeded by several tens of metres of siltstones and sandstones of the Bridport Sand Formation, which encompasses the highest part of the Toarcian Stage and the lowest part of the Aalenian Stage.

Cleveland Basin (Yorkshire Coast)

Along the Yorkshire Coast between the town of Staithes in the north down to the hamlet of Ravenscar in the south, the Lower Jurassic sequence of the Cleveland Basin is exposed in the coastal cliffs, in several repetitive outcrops (Figure 3.11).

Likewise the Wessex Basin, subsidence in the Cleveland Basin started in the Permian. However, a distinct basin only developed in the Late Triassic (Kent, 1980). The basin is bounded to the west and northeast by uplifted blocks like the Pennine and Mid-North Sea High. To the southeast, the basin extends into the Sole Pit Basin (Kent, 1980). The southern limit is formed by the Market Weighton High. Through much of the Mesozoic Era the North Sea Basin experienced considerable tectonic activity that led to the development of a complex system of extensional rifts and basins, though these have only a limited manifestation onshore. The Cleveland Basin forms part of the North Sea Basin complex, and is associated particularly closely with the Sole Pit Trough. It appears to have been asymmetrical, with maximum sediment thicknesses towards the south close to the E–W-trending Howardian–Flamborough Fault Belt, which lies between the basin and the Market Weighton High (Figure 3.11).

Although the coastal exposures are relatively undisturbed, a number of N–S-trending faults are present. The most significant of these is the Peak Fault, well exposed near Ravenscar. These define a narrow graben, the Peak Trough, about 5 km wide. This can be traced on seismic profiles for some 20–30 km offshore to the north (Milsom and Rawson, 1989). The most complete Toarcian succession in the region is preserved in the Peak Trough, west of Ravenscar. Outside the graben erosion prior to deposition of the Dogger Formation (Middle Jurassic) has cut down to the level of the Alum Shale Member. Inversion of the Cleveland Basin occurred in late Cretaceous or early Tertiary times (Kent, 1980), transforming it into a gentle E–W-orientated pericline. The small dome exposed in the cliffs and foreshore of Robin Hood's Bay is a subsidiary structure within this dome.

The Lower Jurassic succession of the Cleveland Basin is dominated by mudrocks, with subordinate sandstones and only a relatively minor, though remarkable, development of ironstones. Limestones are only poorly developed, although diagenetic carbonate nodules form a conspicuous feature at some levels. Despite this predominance of mudrocks, various units within the succession were sufficiently distinctive, or were economically important enough in the past, to have been given lithostratigraphical names since at least the early 19th century (Young and Bird, 1822). These include the 'Staithes Beds', 'Ironstone Series', 'Jet Rock' and 'Alum Shales'. These lithostratigraphical names have been formalized by Cox et al. (1999), who recognize five distinct formations (Redcar Mudstone, Staithes Sandstone, Cleveland Ironstone, Whitby Mudstone and Blea Wyke Sandstone) in the Lower Jurassic succession (Figure 3.19). All but the Staithes Sandstone Formation are subdivided into two or more members, or smaller informal divisions, with all of these divisions well exposed along the coast between Staithes and Ravenscar. An abundance of ammonites has long enabled this lithostratigraphical framework to be tied in precisely to the ammonite biostratigraphy for the Lower Jurassic sequence.

The Redcar Mudstone Formation is by far the thickest, at about 250 m, of the five formations and has been subdivided into four members. The lowest of these, the Calcareous Shale Member, is composed predominantly of mudstones with thin, laterally persistent, shell beds. It rests on the Penarth Group (Upper Triassic) and extends up into the Obtusum Zone. The overlying Siliceous Shale Member (Figure 3.12) comprises shales or silty shales with numerous siltstone or fine sandstone bands, thin silt–sand laminae, and storm-related scour fills. It extends up to the Raricostatum Zone (Aplanatum Subzone), and the base of the member was placed by Ivimey-Cook and Powell (1991) and by Hesselbo and Jenkyns (1995) at the base of the lowest significant sandstone.

The base of the Pyritous Shale Member is marked by a rapid transition to dark pyritous mudstones. This member spans the Raricostatum–Jamesoni zonal boundary. Within the lower part of the Pyritous Shale Mb. in Robin Hood's Bay, the formal Geomagnetic Stratigraphic Section and Point (GSSP) for the base of the Pliensbachian is placed (Meister et al., 2006, Figure 3.13).

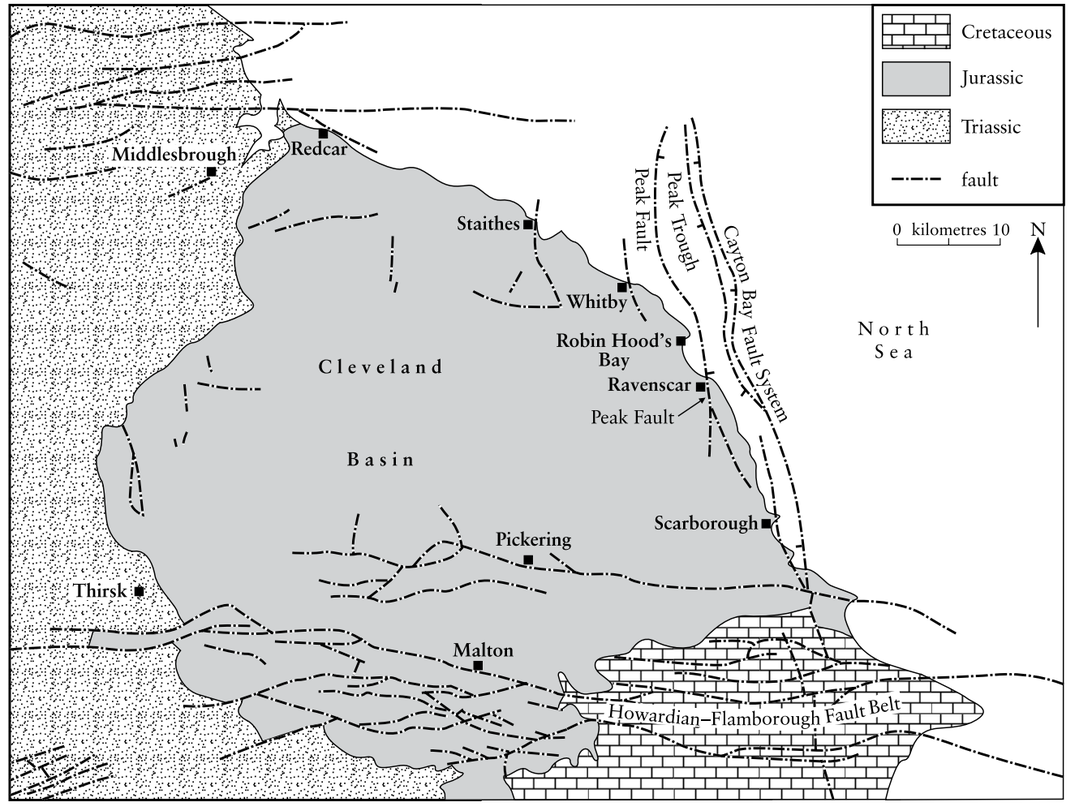

▲ **Figure 3.11: Simplified geological map of the onshore Cleveland Basin in northeast Yorkshire, UK.** The main structural elements, including the north-south trending Peak Fault are also indicated. Only in the narrow graben east of Peak Fault is the Upper Toarcian preserved, whereas it is eroded elsewhere. This map is modified after Simms (2004).

◄ **Figure 3.12: Field Photographs of the Upper Sinemurian Siliceous Shale Mb. in Robin Hood's Bay.** The left photographs are scoured sandy beds, reflecting deposition during storms. These are deposited in an overall grey silty mudstone facies. In the foreground the Gryphaea Scar is visible, a hard calcareous bed rich in Gryphaea (oysters) and Asteroceras (ammonites). These limestones are also thought to be the result of redeposition during storm surges.

The succeeding Ironstone Shale Member comprises mudstones, with fine silty streaks becoming increasingly abundant upwards, and bands and nodules of sideritic ironstone. The base of the member is placed at the lowest of these ironstone bands and the top is taken immediately below the Oyster Bed, a distinctive shell bed in the Davoei Zone (Maculatum Subzone) which can be traced across the Cleveland Basin.

The overlying Staithes Sandstone Formation is approximately 25 m thick and is dominated by sandstones and siltstones, often of tempestitic facies (Figure 3.14). It extends up into the Margaritatus Zone and encompasses the Capricornus, Figulinum and Stokesi subzones.
The Cleveland Ironstone Formation, encompassing the remainder of the Margaritatus Zone and the entire Spinatum Zone, is characterized by silty mudstone coarsening-upward cycles capped by oolitic ironstones (Figure 3.15). Subdivided into two distinct units, the Penny Nab and Kettleness members, the formation shows greater lateral variation than any other in the Lower Jurassic succession of the Cleveland Basin (Young et al.,1990). The Penny Nab Member comprises up to five ironstone-capped cycles. An erosion surface separates it from the overlying Kettleness Member.

◄ **Figure 3.14: Field Photograph of the upper part of the Staithes Sandstone Fm**, showing hummocky cross-stratification, waveripple lamination and gutter casts. This is indicative of a storm-influenced lower shoreface depositional environment.

► **Figure 3.13 Field Photograph of the level corresponding to the GSSP of the Sinemurian-Pliensbachian boundary in Robin Hood's Bay.** This level occurs in the lower part of the Pyritous Shale Mb.

◄ **Figure 3.15: Field Photograph of the upper part of the Cleveland Ironstone Fm. and the base of the Whitby Mudstone Fm. (Grey Shale Mb).** This transition marks the base of the Toarcian Stage. The main ironstone seams are indicated. In between these oolitic grainstones, fine silty mudstones are found. This picture is taken near Kettleness.

The base of the overlying Whitby Mudstone Formation is taken at a rapid upward change to mudstone and is coincident with the Pliensbachian–Toarcian boundary. The formation is characterized by a dark, mudstone-dominated sequence, more than 100 m thick. The formation has been divided into five members, commencing with the silty mudstones and calcareous or sideritic nodule bands of the Grey Shale Member, passing through the predominantly bituminous shales of the Mulgrave Shale and Alum Shale members, before passing back into silty mudstones of the Peak Mudstone Member and finally the still more silty Fox Cliff Siltstone Member (**Figure 3.19**).

The Mulgrave Shale and Alum Shale members have been further subdivided into several informal units, namely the Jet Rock and Bituminous Shales, and the Hard Shale Beds, Main Alum Shale Beds and Cement Shale Beds respectively. The Jet Rock corresponds to the Toarcian Oceanic Anoxic Event and has substantially elevated organic-carbon content. The unit is characterized by a series of early diagenetic limestone beds that formed in relation to sulphate reduction and methane oxidation under anoxic conditions (**Figure 3.16 and 3.17**). The Bituminous Shales unit remains characterized by laminations, however relatively diversified macrofossil assemblages as well as calcareous nannofossil fauna re-appear, suggesting diminishing anoxia.

Above the Whitby Mudstone Formation, the overlying Blea Wyke Sandstone Formation, at the top of the Toarcian Stage, encompasses much of the Dispansum and Pseudoradiosa zones. It is divided into the Grey Sandstone Member, of muddy micaceous siltstone or fine sandstone, and the overlying and somewhat coarser Yellow Sandstone Member. However, across much of the Cleveland Basin the upper part of the Toarcian succession is absent, with the base of the Dogger Formation (Middle Jurassic) resting unconformably upon various levels in the Alum Shale Member. Only to the south-east of the Peak Fault, as at Blea Wyke in the Peak Trough, are these higher Toarcian units preserved.

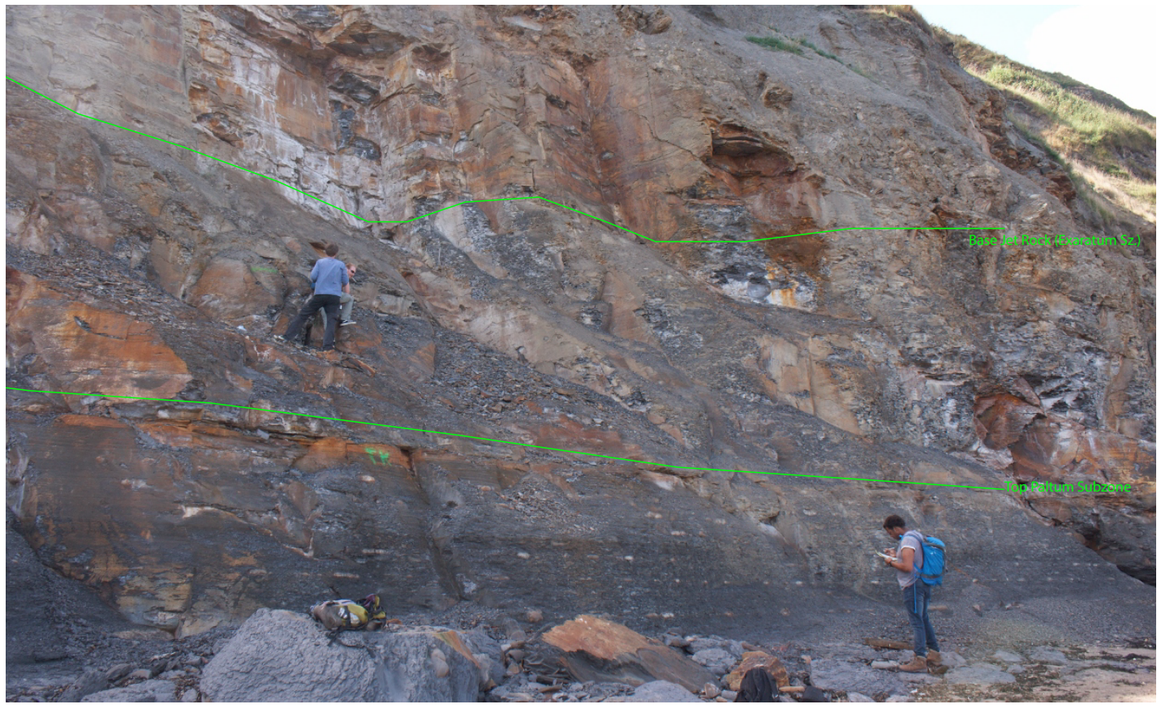

▲ Figure 3.16: Field Photograph of the Lower Toarcian Grey Shale Mb. and the Jet Rock (part of the Mulgrave Shale Mb.)
The carbonate nodules at the base are of an early diagenetic origin and sulphur-rich laminated shales occur throughout the Grey Shale Mb.

▲ Figure 3.17: Field Photograph of the upper half of the Jet Rock.
This level corresponds to the maximum excursion and recovery of the CIE associated with the T-OAE. The top of the recovery is at the Top Jet Dogger level. Note the conspicuous large carbonate concretions. These relate to anoxic methane oxidation in relation to sulphate reduction.

◄ Figure 3.18: Field Photograph of the upper Lower Toarcian Alum Shale Mb.
Alum (white streak in middle), or Potash is double salt of Aluminum and Potassium and was extensively mined along the Cleveland Coast.

Stage	Ammonite zone	Lithostratigraphy	
Toarcian	Aalensis		
	Pseudoradiosa	Blea Wyke Sandstone Formation	Yellow Sandstone Member (9 m)
	Dispansum		Grey Sandstone Member (9 m)
	Thouarsense	Whitby Mudstone Formation	Fox Cliff Siltstone Member (11 m)
	Variabilis		Peak Mudstone Member (13 m)
	Bifrons		Alum Shale Member (37 m)
	Serpentinum		Mulgrave Shale Member (32 m)
	Tenuicostatum		Grey Shale Member (14 m)
Upper Pliensbachian	Spinatum	Cleveland Ironstone Formation	Kettleness Member (10 m)
	Margaritatus		Penny Nab Member (19 m)
Lower Pliensbachian	Davoei	Staithes Sandstone Formation (25 m)	
	Ibex	Redcar Mudstone Formation	Ironstone Shale Member (57 m)
	Jamesoni		Pyritous Shale Member (26 m)
Sinemurian	Raricostatum		Siliceous Shale Member (40 m)
	Oxynotum		
	Obtusum		Calcareous Shale Member (127 m)
	Turneri		
	Semicostatum		
	Bucklandi		
Hettangian	Angulata		
	Liasicus		
	Planorbis		

Figure 3.19: Overview of the lithostratigraphic nomenclature used for the Cleveland Basin.
We have sampled the Upper Sinemurian to Uppermost Toarcian for the purpose of this study. This figure is modified after Simms (2004).

3.3 Southern North Sea (UK, NL)

A transgression from the south and west occurred during the Rhaetian to Hettangian. Coupled with local tectonic subsidence this led to the establishment of an open, shallow epicontinental sea extending from the present-day UK into the Netherlands, Germany and west and central Poland. Sedimentation was more terrestrial farther to the north and east in the Danish, German and Polish regions. In these areas, the sediments are commonly coarser-grained, particularly along the eastern boundary with the Fennoscandian–East European Platform area and adjacent to the London-Brabant, Rhenish and Bohemian massifs to the south. This development of shallow, open-marine, fine-grained mudstone sedimentation is seen in the UK (Lias Group), the Netherlands (Altena Group), Southern Norway and Denmark (Fjerritslev Formation) and Germany (Lias Group). This variably calcareous mudstone and sandstone facies is gradually replaced to the north and east of Denmark by coarse-grained, clastic-dominated, fluviodeltaic and nonmarine sedimentation (Gassum Formation, **Figure 3.20**).

In the Netherlands, the Altena Group is divided into three units; the Lower Werkendam Mb. of the Werkendam Fm. (which extends into the Middle Jurassic), the Toarcian Posidonia Shale Fm. and the Aalburg Fm. This nomenclature is applied in the on- and offshore.

Albeit the overall lithological descriptions for the Lias Group in the offshore of the UK Southern North Sea Basin seem quite comparable to that recorded in the outcrops of the Cleveland Basin, a differential lithostratigraphic nomenclature currently exists. The oldest (Hettangian – Early Sinemurian) formation in the Lias Group is the Penda Fm., which on the basis of log-responses is considered to represent relatively shallow limestone development, much akin to the Calcareous Shale Mb. of the Redcar Mudstone Fm. Successively, the Offa Fm. (Late Sinemurian to Early Pliensbachian) corresponds to the Siliceous Shale, Ironstone Shale and Pyritous Shale Mb. The Ida Fm. is considered a condensed winnowing phase and corresponds to the Late Pliensbachian Staithes Sandstone Fm. and Cleveland Ironstone Fm. The uppermost Cedric Formation is often truncated by erosion related to Aalenian thermal doming. This unit comprises the Toarcian Oceanic Anoxic-event as expressed by the Jet Rock Unit of the Whitby Mudstone Fm. in the onshore. Whenever complete, like in the Peak Through of the Cleveland Basin a sand-rich member of Late Toarcian age is recorded, the Philips Mb. This thus corresponds to the Blea Wyke Sandstone Mb. of the onshore (**Figure 3.20**, Lott and Knox, 1994; Van Adrichem Boogaert and Kouwe, 1993).

3.4 Norwegian-Danish and Farsund Basin

In order to document changes in the Norwegian-Danish Basin we use the published information of Petersen et al. (2008). Structurally we confine our compilation to the sedimentary infill of the NW-SE trending Norwegian-Danish Basin, including the deep Fjerritslev through and the Skagerrak-Kattegat Platform, forming the northeastern boundary of this feature. In the Norwegian-Danish Basin the Lower Jurassic is characterized by the Fjerritslev Formation, which is subdivided into four members (F-I to F-IV). These members reflect four main sea-level cycles (see also Section 6). In the Lowermost Jurassic, the Gassum Fm. is used to characterize shallow marine to paralic silt- and sandstones, found in the eastern extremity of Denmark. Above the Fjerritslev Formation, in the Middle Jurassic subsidence in the Norwegian-Basin diminished leading to erosion at many places, but also deposition of shallow marine sandstones of the Haldager Sand Formation, within the Fjerritslev Through (Petersen et al., 2008).

Just to the west, in Norway, the Farsund Basin is an east-west extending 30 km wide and 150 km long through. Structurally, the basin belongs to the Fennoscandian Border Zone, a complex tectonic province between Norwegian-Danish Basin and the Fennoscandian Shield. The basin lies just south of Kristiansand in Southern Norway. For this area the same lithostratigraphic nomenclature is used as in the Norwegian-Danish Basin area. The only exception is the (Middle Jurassic) marginal marine sandstones above the Fjerritslev Fm., which there correspond to the Bryne Fm.

3.5 Viking Graben Area (N, UK)

The Lower Jurassic succession of the northern part of the study area (Viking Graben area) was deposited following Late Permian-Early Triassic rifting (Odinsen et al., 2000). This subsidence led to the northward progradation of the fluvial-dominated Statfjord Formation, constituting alluvial fans, alluvial plains and/or braid plains with occasional coal seams (Ryseth, 2001). The source areas of clastic debris are the Shetland Platform to the west and north-west and south-western Norway to the east (Nystuen et al., 2014).

Although the exact timing remains ambivalent, a sea-way along the Viking Strait was established by Sinemurian times (Steel, 1993). The lower part of the overlying Dunlin Group (Sinemurian–Pliensbachian) encompasses the Amundsen and Burton formations, which consist of shales and siltstones deposited in a shelfal setting (Husmo et al., 2003). The shallow marine Cook Formation built out into this seaway from the Norwegian mainland during Pliensbachian-Toarcian time, in response to basin margin uplift and erosion (Charnock et al., 2001; Folkestad et al., 2012). The Cook Formation can be divided into two distinct units, a lower (regressive) and an upper (transgressive) unit (Steel, 1993). Subsidence continued in the northern North Sea, as the Cook Formation is draped by offshore mudstones of the Drake Formation. However, these shales may be synchronous to the upper Cook Fm., in parts of the area. The sandstone distribution within these sequences is thus primarily controlled by variations in sediment supply, accommodation potential and tectonic subsidence and represents a history of repeated progradation and retrogradation (Charnock et al., 2001).

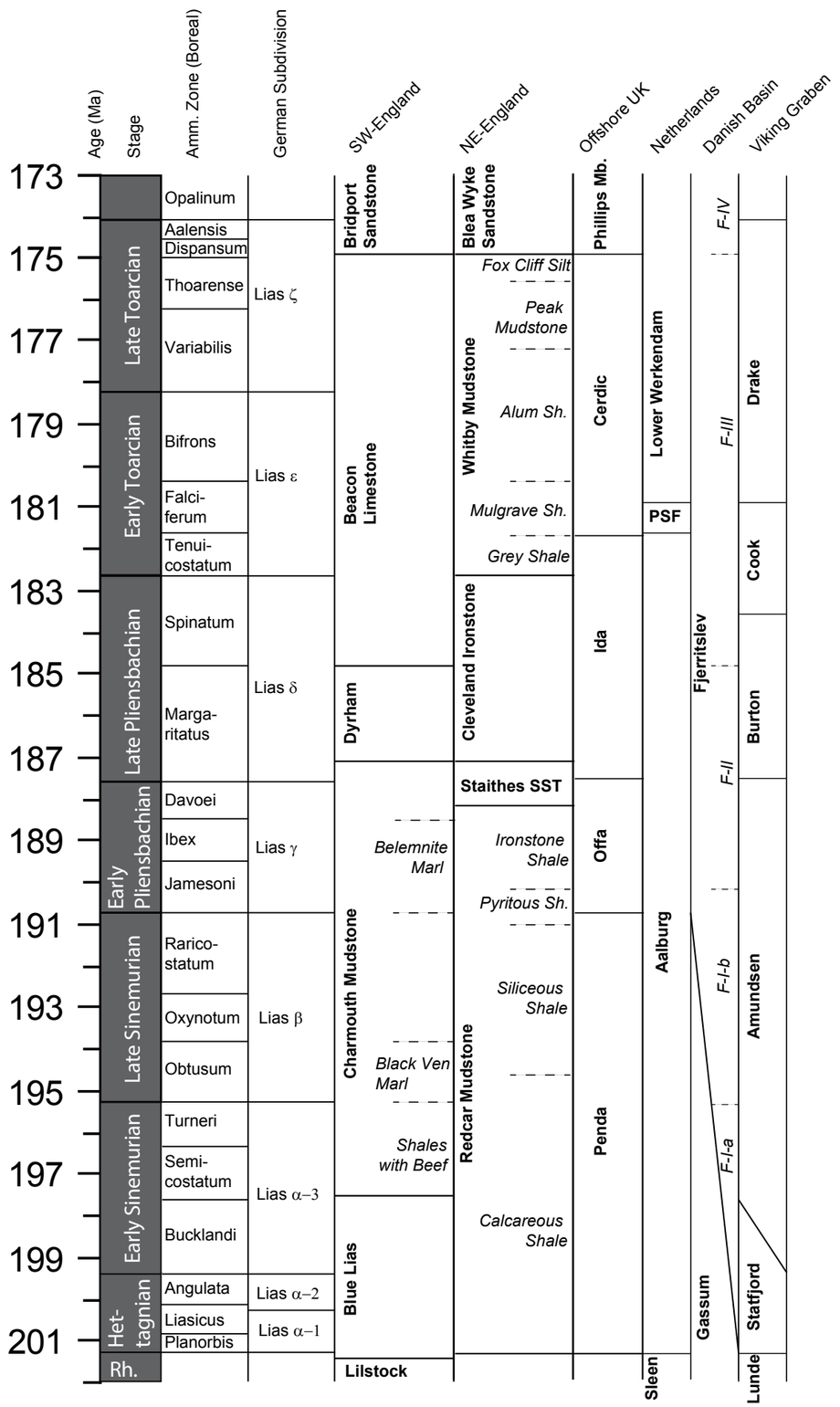

3.6 Integration of regionally employed lithostratigraphic nomenclature

Figure 3.20 shows an overview of the lithostratigraphic nomenclature employed across the study area. The chronostratigraphic assignment of these units is generally after the respective literature references (Charnock et al., 2001; Doornenbal and Stevenson, 2010; Petersen et al., 2008). An exception is the Posidonia Shale Fm. in the Netherlands which has been matched to approximately cover the duration of the Toarcian OAE and its direct aftermath, in consrast to its >2 Million year duration as mentioned in the SPB-Atlas. ■

◄ Figure 3.20: Overview of the regionally used lithostratigraphic nomenclature.
The chronostratigraphic assignments are after Cox et al. (1999) Doornenbal and Stevenson (2010) and Husmo et al. (2003). The duration of the Posidonia Shale Formation (PSF) has been modified to only capture T-OAE.

Blue Lias at Lilstock (Somerset)

4. Stratigraphic Framework

4. STRATIGRAPHIC FRAMEWORK

The following chapter documents the construction of an integrated stratigraphic framework for the Lower Jurassic through combination of organic-carbon isotope analyses and high-resolution quantitative palynology on two outcrop reference sections (Wessex Basin – Dorset and Cleveland Basin – Yorkshire). The major advantage of these records is that they both have detailed ammonite biostratigraphies available, to subzonal level (Dean et al., 1961; Page, 2003, 2004). **Table 4.1** provides an overview of the boreal ammonite zonation schemes and their respective ages used throughout this report.

Stage		Zone	Subzone	Age Base	Age Top
Toarcian	Late	**Levesquei**	Moorei Levesquei Dispansum	174,57 174,71 174,97	174,43 174,57 174,71
		Thouarense	Fallaciosum Fascigerum Thouarense Bingmanni	175,6 175,81 176,02 176,23	174,97 175,6 175,81 176,02
		Variabilis	Vitiosa Illustris Variabilis	176,9 177,57 178,24	176,23 176,9 177,57
	Early	**Bifrons**	Crassum Fibulatum Commune	178,94 179,65 180,36	178,24 178,94 179,65
		Falciferum	Falciferum Exaratum	181,25 181,7	180,36 181,25
		Tenuicostatum	Semicelatum Tenuicostatum Clevelandicum Paltus	181,95 182,2 182,45 182,7	181,7 181,95 182,2 182,45
Pliensbachian	Late	**Spinatum**	Hawskerense Apyrenum	183,14 184,18	182,7 183,14
		Margaritatus	Gibbosus Subnodusus Stokesi	185,31 186,44 187,56	184,18 185,31 186,44
	Early	**Davoei**	Figulinum Capricornus Maculatum	187,89 188,21 188,54	187,56 187,89 188,21
		Ibex	Luridum Valdani Masseanum	188,87 189,19 189,52	188,54 188,87 189,19
		Jamesoni	Jamesoni Brevispina Polymorphus Taylori	189,84 190,17 190,49 190,82	189,52 189,84 190,17 190,49
Sinemurian	Late	**Raricostatum**	Aplanatum Macdonnelli Raricostatum Densinodulum	191,32 191,82 192,31 192,81	190,82 191,32 191,82 192,31
		Oxynotum	Oxynotum Simpsoni	193,31 193,81	192,81 193,31
		Obtusum	Denotatus Stellare Obtusum	194,31 194,81 195,31	193,81 194,31 194,81
	Early	**Turneri**	Birchi Brooki	195,81 196,31	195,31 195,81
		Semicostatum	Sauzeanum Scipionianum Lyra	196,81 197,3 197,8	196,31 196,81 197,3
		Bucklandi	Bucklandi Rotiforme Conybeari	198,3 198,8 199,3	197,8 198,3 198,8
Hettangian	Late	**Angulata**	Complanata Extranodosa	199,7 200,1	199,3 199,7
		Liasicus	Liasicus Laqueus Portlocki	200,35 200,6 200,85	200,1 200,35 200,6
		Planorbis	Johnstoni Planorbis	201,025 201,1	200,85 201,025
	Early	**T/J-boundary**			201,1

▲ **Table 4.1: Boreal Ammonite Zonal scheme after Page (2003). The respective ages are after Gradstein et al. (2012)**

4.1 Organic carbon isotope records

In order to strengthen the potential of bulk organic carbon isotopes as a tool for stratigraphic correlation we have analysed 404 bulk rock samples from the two outcrop analogue sections. The data from the Wessex Basin were analysed in collaboration with Lausanne University in Switzerland.

Hettangian-Lowermost Plienbachian (Wessex Basin / Dorset Coast)

Figure 4.1 depicts the results of the bulk organic carbon isotope analyses from the Hettangian – Lowermost Pliensbachian succession from the Wessex Basin. As can be seen in the leftmost graph the variability is very substantial (between -25‰ to -31‰). Particularly the Hettangian to Lower Sinemurian interval (Blue Lias Fm.) and part of the Upper Sinemurian (Stonebarrow Pyritic Mb.) are susceptible to high-frequency variation. Next to that, a number of transient shifts and trends are identified.
It has been noted by various authors that $\delta^{13}C_{org}$ of sediment samples dominated by Type II kerogen are 2 to 3‰ lighter than those of fossil wood collected from the same horizons (see e.g., Hesselbo et al., 2007). This is primarily because marine organic carbon producers have differential photosynthetic fractionation factors (Popp et al., 1998). Assuming that a similar enrichment in ^{13}C of terrestrial OM compared to marine (Type II) organic matter exists across the interval, the hydrogen index as identified using Rock Eval Pyrolysis, can be used to decouple this mixing effect. In fact, Suan et al. (2015) have recently shown that HI and $\delta^{13}C_{org}$ records are characterized by an inverse relationship across the Late Pliensbachian to Early Toarcian.
Assuming that the $\delta^{13}C$/HI relationship applies across the entire record, it is now possible to calculate changes in $\delta^{13}C_{org}$ that are not explained by HI variations ($\delta^{13}C_{corrected}$, see **Figure 4.1**) using the following equations:

$$\delta^{13}C_{corrected} = \delta^{13}C_{org} - \delta^{13}C_{HI} \qquad (1)$$

$$\delta^{13}C_{HI} = HI * a - b \qquad (2)$$

where $\delta^{13}C_{HI}$ is the $\delta^{13}C$ value expected from changes in HI values and a and b are, respectively, the slope and the intercept in the HI/$\delta^{13}C_{org}$ x-plot (**Figure 4.2**). This allows us to correct the changes in $\delta^{13}C_{org}$ for variations in OM contribution. Via this way we can evaluate whether changes are driven by varying composition of the atmospheric/oceanic $\delta^{13}C$-signature, which would invoke a strong potential for regional correlation or simply by (local) changes in substrate.

This exercise shows that a very relevant and substantial negative carbon isotope excursion is recorded around the Triassic-Jurassic boundary level. This shift is recorded more or less globally and has been assigned to the degassing of organic-rich material in association with incipient Central Atlantic Volcanism (Pálfy et al., 2001; Hesselbo et al., 2002).

The high-frequency shifts recorded in the lower 40 m record have no stratigraphic significance and are caused by changes in marine vs. terrestrial substrate (see also Chapter 7). The ~2‰ shift towards more positive values across the Lower Sinemurian is recorded both in the $\delta^{13}C_{org}$ and in $\delta^{13}C_{corrected}$ records and is consequently considered relevant for stratigraphic correlation. The substantial (~4-5‰) negative shift in $\delta^{13}C_{org}$ across the Lower-Upper Sinemurian boundary (Birchi-Obtusum Zones) is substantially smaller (~1.5‰) but persistently present in the $\delta^{13}C_{corrected}$-record (**Figure 4.1**).

The variability observed in the Upper Sinemurian is smaller once corrected for HI, but remains present, suggesting rather instable climatic conditions. No major shifts are recorded across this interval. In contrast, the values from the Raricostatum Zone, which is truncated at its base, are substantially more positive, in both $\delta^{13}C_{org}$ as well as $\delta^{13}C_{corrected}$. Subsequently, across the hiatus across the Pliensbachian-Sinemurian boundary, a substantial ~5‰ negative shift is recorded. This is certainly not merely the effect of facies change as indicated by a similar magnitude shift in $\delta^{13}C_{corrected}$.

Summary of isotope trends Wessex Basin

- The Triassic /Jurassic-boundary is just preceded by a substantial negative shift
- The Hettangian to Early Sinemurian is character ized by a gradual 1-2‰ positive trend
- The basal Upper Sinemurian is characterized by a gentle negative trend in the Obtusum Zone
- The Pliensbachian-Sinemurian boundary interval is characterized by a substantial negative shift.

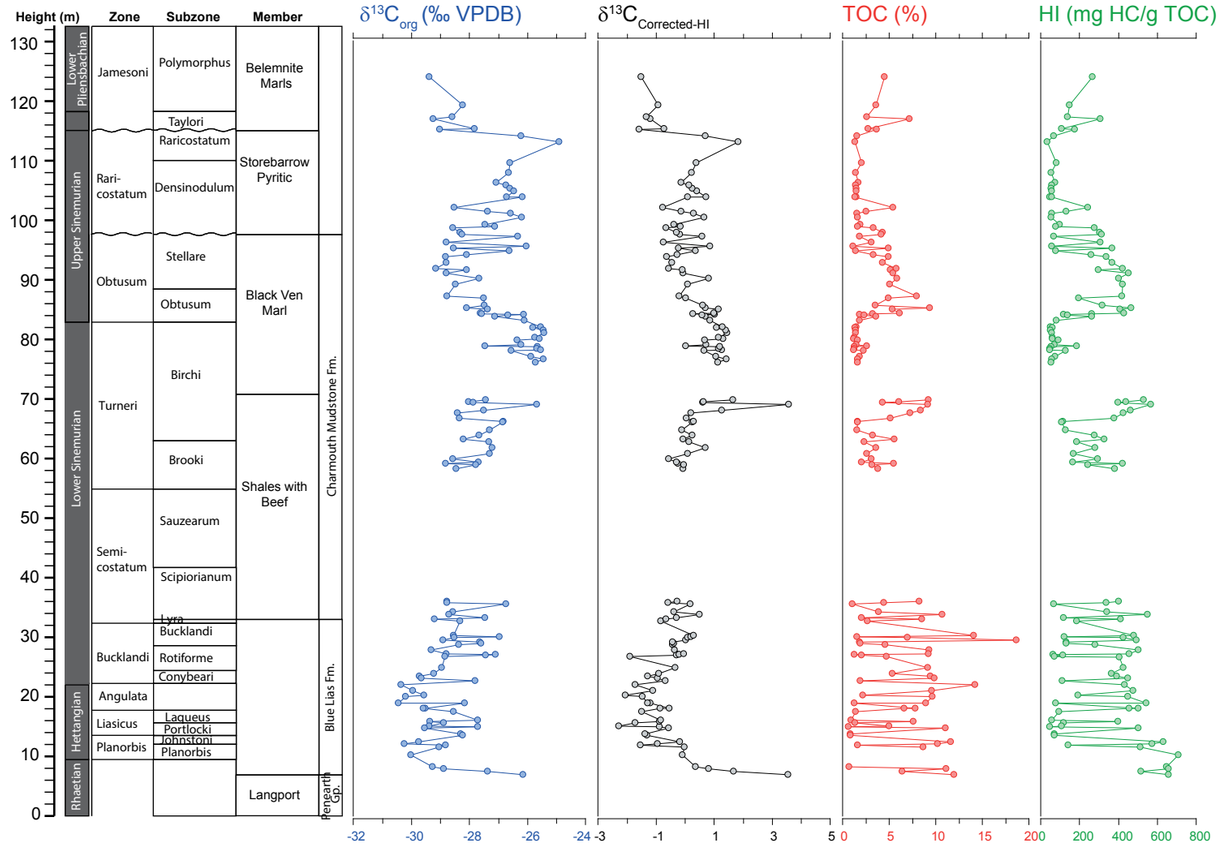

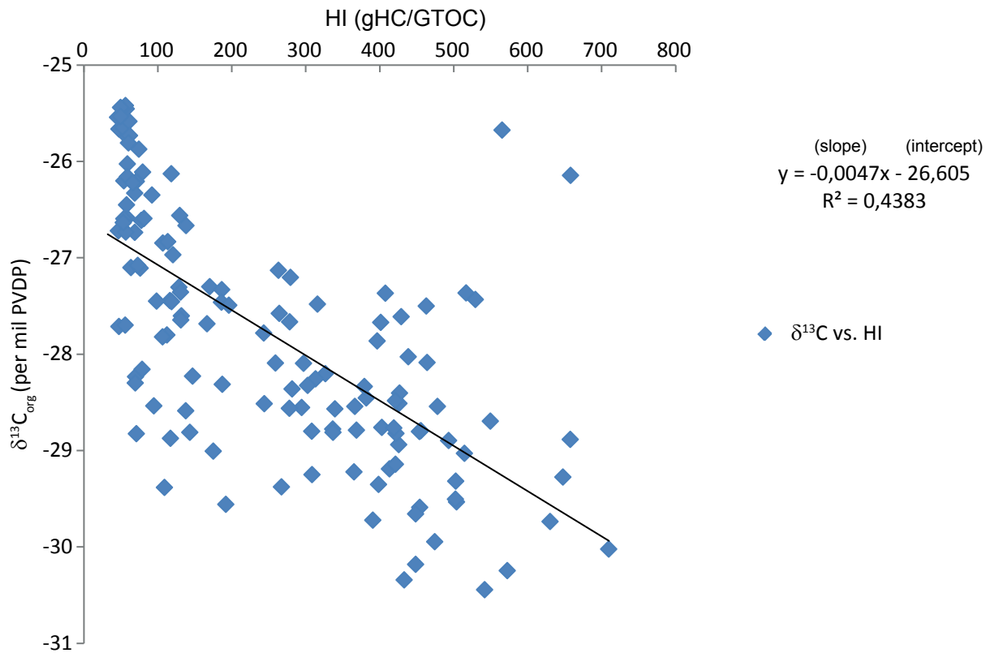

▲ Figure 4.1: Stable carbon isotope results for the Rhaetian to Early Pliensbachian from the Dorset Coast succession in the Wessex Basin.
The bulk organic stable carbon isotope ($\delta^{13}C_{org}$) data are plotted alongside the total organic carbon (TOC) and Hydrogen Index (HI) data, in order to appreciate the relationship between $\delta^{13}C_{org}$ and organic substrate and respiration as indicated by the Hydrogen Index (see also Figure 4.2). In order to be able to evaluate trends in $\delta^{13}C_{org}$ that are attributed to changes in the global carbon pool, thus warranting stratigraphic significance we calculated and plotted $\delta^{13}C_{calculated}$. It then becomes clear that the negative excursions that just pre-date the Triassic-Jurassic (T/J) boundary) and across the Sinemurian-Pliensbachian boundary are clearly not related to changes in substrate. Next to that, we note that the Hettangian to Early Sinemurian is characterized by a gentle 1-2‰ positive trend and that a gentle negative trend is recorded in the Late Sinemurian Obtusum Zone.

◄ Figure 4.2: Cross-plot between $\delta^{13}C_{org}$ and Hydrogen Index data for the Hettangian to Early Pliensbachian from the Dorset succession, showing an apparent correlation between the two. This linear correlation was used to calculate a correction for the $\delta^{13}C_{org}$-values. See Figure 4.1.

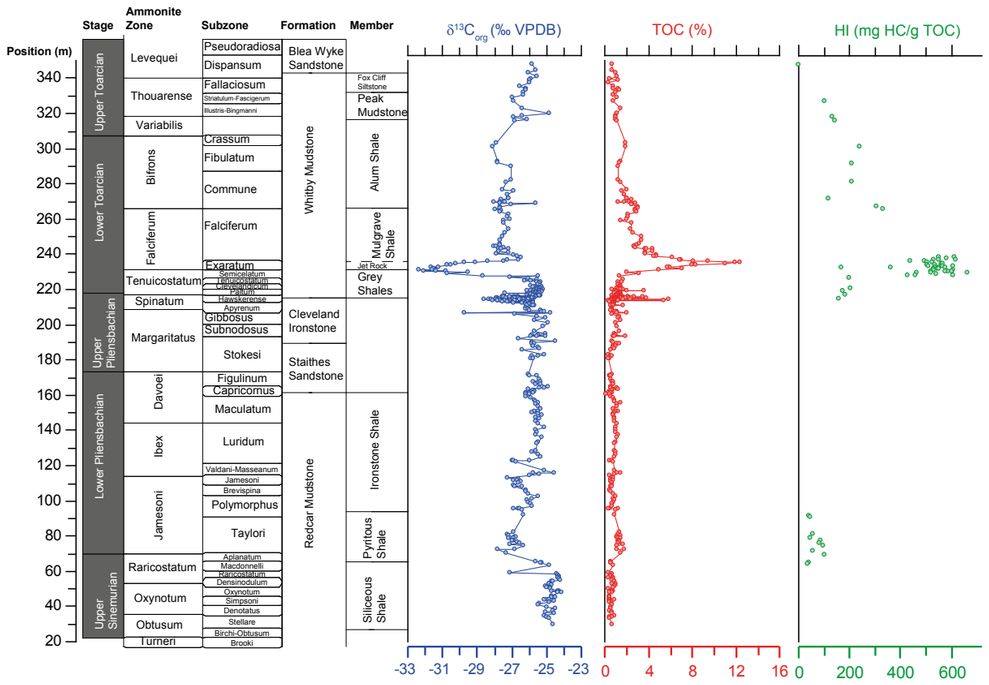

▲ **Figure 4.3: Carbon isotope, TOC and HI-values for the Sinemurian-Toarcian succession from the Cleveland Basin.**
Note that HI-values are only substantially elevated in the Lower Toarcian.

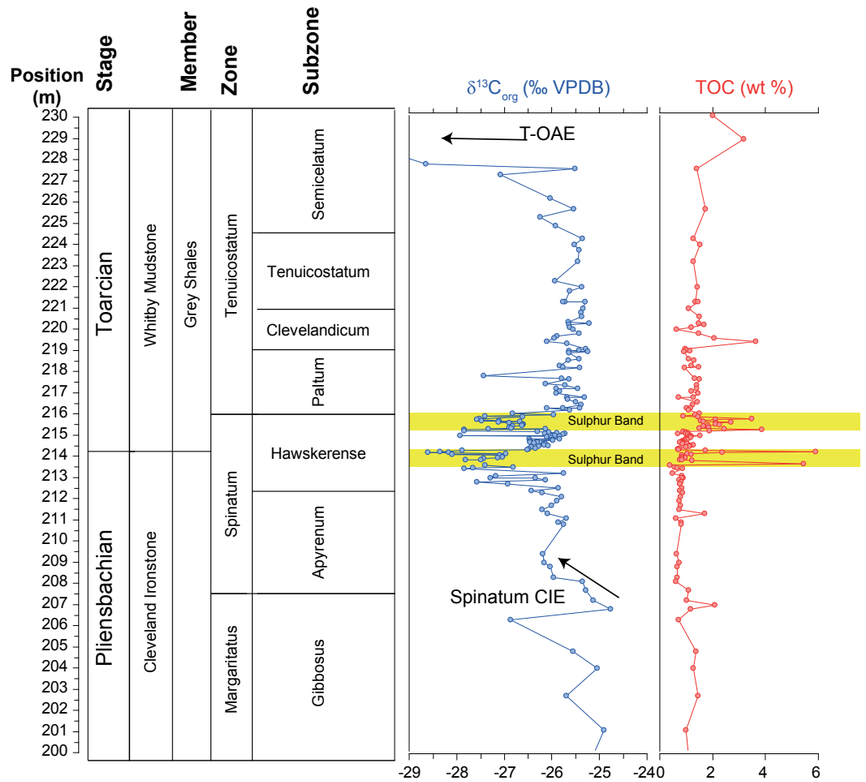

◄ **Figure 4.4: Close-up of the Pliensbachian - Toarcian boundary carbon isotope and TOC record from the Cleveland Basin.**
The negative shifts coincide with the deposition of sulphur bands, with elevated TOCs. Below that, the Spinatum isotope shift is also noted.

Upper Sinemurian to Toarcian (Yorkshire-Cleveland Basin)

The reference section for the latter part of the Early Jurassic is from the Cleveland Basin, sampled along the Yorkshire Coast. Here, Upper Sinemurian to Upper Toarcian deposits were continuously sampled without any major breaks in stratigraphy (**Figure 4.3**). The Upper Pliensbachian Margaritatus and Spinatum Zones comprise phases of condensation but all subzones are present in the record (see e.g., Hesselbo and Jenkyns, 1995). Except for the Toarcian all material is low in TOC (**Figure 4.3**). Therefore, we refrained from fully analysing the succession using Rock Eval Pyrolysis, thus also hampering evaluation of $\delta^{13}C_{corrected}$. This is however not problematic since the observed variation in organofacies is rather limited, with the exception of the Lower Toarcian, which is strongly perturbed by marine influence and the respiration of organic-matter under anoxic water column conditions (see also Chapters 6 and 8).

The lowermost part of the Cleveland Basin succession overlaps with that from the Wessex Basin (Dorset). We also note the characteristic negative carbon isotope shift across the Sinemurian-Pliensbachian boundary. The lowermost Pliensbachian comprises the dysoxic black shales of the Pyritous Shales Mb. Under these circumstances, primary organic-matter may be taken up by microbes (e.g., sulphate reducers) producing light CO_2 which is in turn fixed by primary producers thus recording this light $\delta^{13}C$-value (see Küspert et al., 1982). However, Rock Eval data indicate low Hydrogen Indices thus refuting a major change in organic substrate and/or respired organic matter effect (**Figure 4.3**). Hence, the negative excursion starting at the base of Sinemurian Raricostatum Zone extending into the Pliensbachian Jamesoni Zone is a valuable isotope marker. In the upper part of the Jamesoni Zone we note a ~2‰ negative shift followed by a ~2‰ positive shift in the lower Ibex Zone. The remainder of the Pliensbachian is characterized by remarkably stable values up to the upper Margaritatus Zone.

One sample corresponding to the upper Margaritatus Zone is remarkably lighter. A recent study on the expanded Mochras core in Wales signifies a substantial (~4‰) negative CIE at this correlative level (Storm et al., 2016). However in the Cleveland Basin, this interval is substantially condensed (note the oolitic ironstones). Therefore this one point may be indicative of this same negative CIE across the Margaritatus-Spinatum Zones. Successively, the Pliensbachian-Toarcian boundary interval is a period of high variability. At the base of the Spinatum Zone (**Figure 4.4**), a ~2‰ negative shift is recorded, still within the Cleveland Ironstone Fm. Subsequently, with the deposition of the Sulphur Bed that forms the actual Pliensbachian-Toarcian boundary an additional negative shift is recorded being followed by another transient shift and sulphur bed at the base of the Tenuicostatum Zone. This argues for a strong correlation between relatively negative $\delta^{13}C_{org}$ values and the deposition of the organic-rich sulphur bands, through substrate and C-recycling change. However, coeval shifts are also recorded in the carbonate fraction in Portugal (see also Littler et al., 2010), arguing that these shifts are indeed precursors to the Toarcian CIE and as such provide an indication of drastic climate change prior to the Toarcian OAE.
The Toarcian CIE is clearly recorded across the Jet Rock Unit (Exaratum Subzone, see **Figure 4.3** and top of **Figure 4.4**), including its positive 'hump' after the event. Subsequently, across the remainder of the Toarcian the $\delta^{13}C$-values remain fairly stable. The only exception forms the base of the Alum Shale Mb. (Commune Zone) where a slight ~1‰ shift is accompanied by an increase in TOC (to ~3%), HI (to approximately 400 gHC/gTOC) and an increase in stratification and marine influence, thus arguing for a substrate control (see also Chapter 7). The Upper Toarcian is characterized by a gradual trend towards more positive values.

Summary of isotope trends Cleveland Basin

- The Pliensbachian-Sinemurian boundary interval is characterized by a substantial negative shift at both localities
- The Lower Pliensbachian is characterized by stable values, except for the boundary interval of the Ibex and Jamesoni Zones.
- The Margaritatus and Spinatum are more dynamic with a series of negative shifts, including one across the Toarcian-Pliensbachian boundary. These may be considered precursors to the Early Toarcian CIE.
- The Toarcian CIE is a very good worldwide marker
- The interval above the Toarcian CIE is fairly stable.
- The Upper Toarcian is characterized by a gentle positive shift.

4.2 Palynological marker events

In this section, we discuss relevant extinction and origination events for marine and terrestrial palynomorphs observed in the outcrop reference sections in relation to those published in literature from NW-Europe.

Triassic-Jurassic Boundary

The Triassic-Jurassic boundary interval, spans one of the major 'big five' extinction events. The boundary is characterized by large-scale volcanism, as also manifested by the seismite recorded in NW-Europe (Lindstrőm et al., 2015, see also Chapter 3) and related carbon cycle perturbations (Hesselbo et al., 2002; Ruhl and Kürschner, 2011).

Sporomorphs

For this reason it is not surprising that there is a substantial number of extinctions among terrestrial vegetation components at the top of the Triassic. *Ricciisporites tuberculatus* has a Last Occurrence (LO) within the uppermost Rhaetian, albeit below the base Jurassic. Other widely known Rhaetian markers such as *Rhaetipollis germanicus* and *Ovalipollis ovalis* have a LO in the older part of the Rhaetian (Dybkjær, 1991; Hounslow et al., 2004). In the Wessex Basin, UK the First Occurrence (FO) of *Quadreculina annellaeformis* is recognized in the middle Rhaetian as well. In Denmark and Germany, the base of the Jurassic is also reflected by an increase in the abundance of the non-taeniate bisaccate pollen (e.g., *Pinuspollenites minimus*) and (*Kraeuselisporites reissingerii* = *Heliosporites altmarkensis* = *Heliosporites reisengerii*, see e.g., Lund, 1977; Dybkjær, 1991), implying First Consistent Occurrences (FCOs) of these taxa. At numerous localities, the inception of *Cerebropollenites thiergartii* is also found to approximate the Triassic/Jurassic-boundary (Bonis et al., 2010; Dybkjær, 1991). An abrupt reduction in sporomoroph diversity occurs between the highest Langport Member assemblage and the lowest from the Lias Group, in the Wessex Basin. This occurs biostratigraphically speaking still below the base of the Jurassic as defined by the FO of the ammonite *Psiloceras planorbis*, within the so-called pre-Planorbis Beds. *Classopollis* spp. becomes dominant here at the base of the Lias Group in an assemblage with small numbers of *Chasmatosporites*, *K. reissingerii* and non-taeniate bisaccate pollen.

The lowermost samples included in our study of the outcrops in the Wessex Basin are from the base of the Blue Lias Fm., in the so-called Pre-Planorbis Beds (6.6 – 9.6 m height, **Figure 4.5**). Our results from this interval confirm the inferences mentioned above from literature. *Classopollis* spp. is found dominantly, *Chasmatosporites* spp. and non-taeniate bisaccate pollen are indeed present. *Ricciisporites tuberculatus*, *Rhaetipollis germanicus* and *Ovalipollis ovalis* are absent. *Ricciisporites tuberculatus* is however recorded in the pre-Planorbis beds by Hounslow et al. (2004). *Cerebropollenites thiergartii* is first recorded at 7.5 m height, just predating the T/J-boundary as defined by the FO of *P. planorbis*. Like *C. thiergartii*, the Pre-Planorbis beds capture the FOs of numerous long-ranging Jurassic taxa. Whether these truly represent stratigraphic FOs remains unclear.

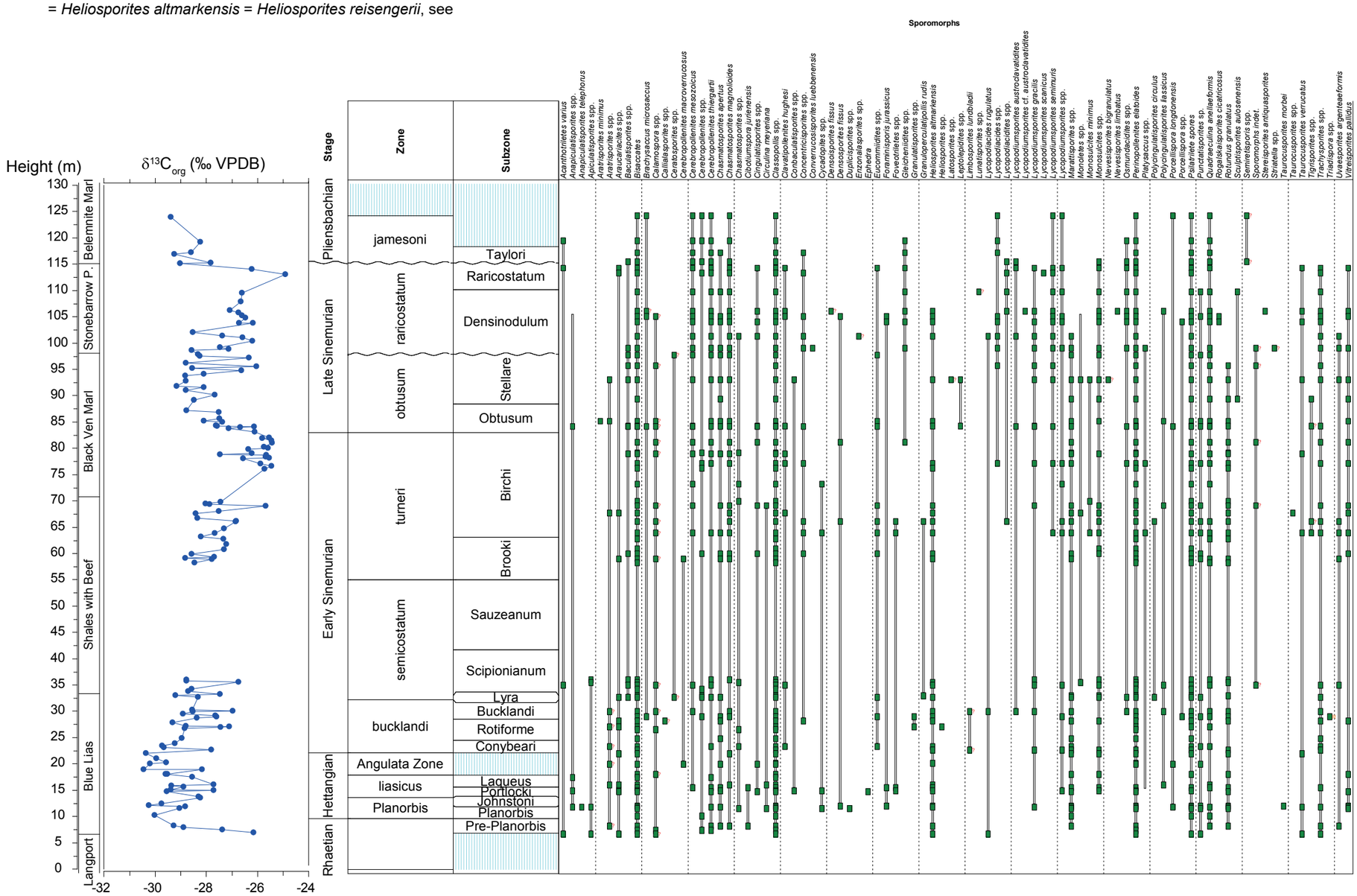

► **Figure 4.5: Distribution-chart of sporomorph (terrestrial palynomorph) taxa from the Rhaetian to Lower Pliensbachian succession in the Wessex Basin along the Dorset Coast.**
The carbon isotope curve and Ammonite Zonations are shown for stratigraphic context.

Marine Palynomorphs

Organic-walled dinoflagellate cysts are first recorded in the Triassic, with the appearance of *Rhaetogonyaulax rhaetica*. The work of Morbey (1975) represents the most detailed examination of Triassic dinoflagellate cysts in Britain carried out so far. He showed that *Rhaetogonyaulax rhaetica*, but also morphologically closely related *Dapcodinium priscum* range from the Blue Anchor Formation through the Westbury Formation and Cotham Member. In the latter two units, also *Beaumontella? caminuspina*, *Comparodinium diacrorhaetium* and *Beaumontella langii* were found to be persistent in their distribution. Morbey (1975) was unable to sample successfully the Preplanorbis Beds in this profile. Later, it was shown that *R. rhaetica* ranges from the Blue Anchor Formation (e.g. Warrington, 1977a, 1983a, 1984) through to the top of the 'White Lias', i.e. Langport Member (Warrington, 1978), just below the base of the Pre-Planorbis beds. Hounslow et al. (2004) however reports (likely reworked) specimens from basal Hettangian samples in the Wessex Basin. In the same account Morbey (1975) also investigated the Rhaetian of Austria, where he in addition recorded *Heibergella kendelbachia* and *Comparodinium koessenium*. There, *R. rhaetica* ranges through the section from the base of the Rhaetian onwards. It is followed successively by appearances of *Suessia swabiana*, *Beaumontella? caminuspina*, *Dapcodinium priscum*, *Beaumontella langii* and *Heibergella kendelbachia*. According to Morbey (1975), all these species range through the Rhaetian section and into the Pre-planorbis Beds. *Suessia swabiana* last appears towards the base of the Pre-planorbis Beds.

Our study of the succession in Wessex Basin starts at the base of the pre-Planorbis beds (6.6 - 9.6 m, **Figure 4.6**). In this interval we note the presence of *Beaumontella? caminuspina*, *Beaumontella langii* and one occurrence of D*apcodinium priscum* (at 6.6 m height). *Rhaetogonyaulax rhaetica, Suessia swabiana* and other Triassic forms are not recorded whatsoever. *D. priscum* only ranges marginally into the Pre-Planorbis beds and is as such not recorded at all in Hettangian or younger strata in the Wessex Basin. According to Riding and Thomas (1992), *D. priscum* ranges all the way up to the early-late Sinemurian boundary, also based on appearances in France and Germany (Morbey and Dunay, 1978; De Vains, 1988), whereas Dybkjaer (1991) provides a top in the earliest Sinemurian. It thus seems that there was a strong environmental control on the proliferation of this Triassic taxon into the Lower Jurassic of England.

Acritarchs are marine palynomorphs that generally resemble dinoflagellates in shape and form, but lack distinctive dinoflagellate characteristics, such as a plate-like pattern on the cyst-wall or a clearly defined excystment opening. Therefore, they are not formally classified as dinoflagellates. The ultrastructure and organic geochemical composition of numerous Neoproterozoic acritarchs have been directly linked to Chlorophyceae, a clade of green algae closely related to Prasinophyte algae (Al-Arouri et al., 1999). Both acritarchs and prasinophyte are known to be abundant in the Lower Jurassic. Hounslow et al. (2004) mention that acritarchs appear to increase in diversity in the basal part of the Blue Lias Fm. The underlying Rhaetian of the Penarth Group in contrast is not marked by any mass-abundances of acritarchs or prasinophyte algae. *Micrhystridium*, *Veryhachium* and a handful of prasinophyte taxa like *Tasmanites*, *Cymatiosphaera*, *Leiosphaera* and *Pleurozonaria* are present throughout the Late Triassic (Courtinat et al., 1998). All these taxa are also recorded by us in the Pre-Planorbis beds and thus do not constitute any last occurrences across the boundary (**Figure 4.6**).

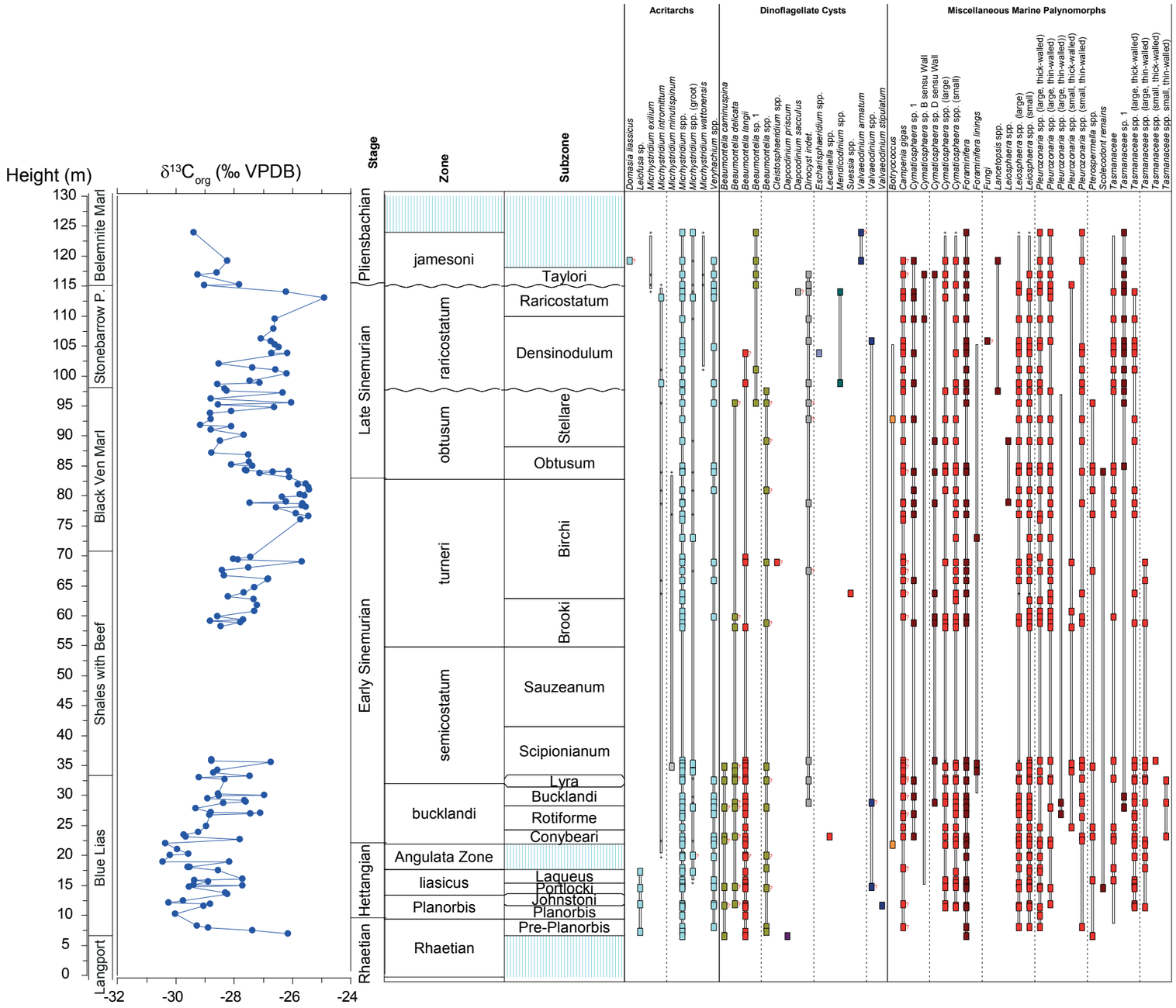

▼ Figure 4.6: Distribution-chart of marine palynomorph taxa from the Rhaetian to Lower Pliensbachian succession in the Wessex Basin along the Dorset Coast.
The carbon isotope curve and Ammonite Zonations are shown for stratigraphic context. The miscellaneous palynomorphs predominantly represent prasinophyte algae.

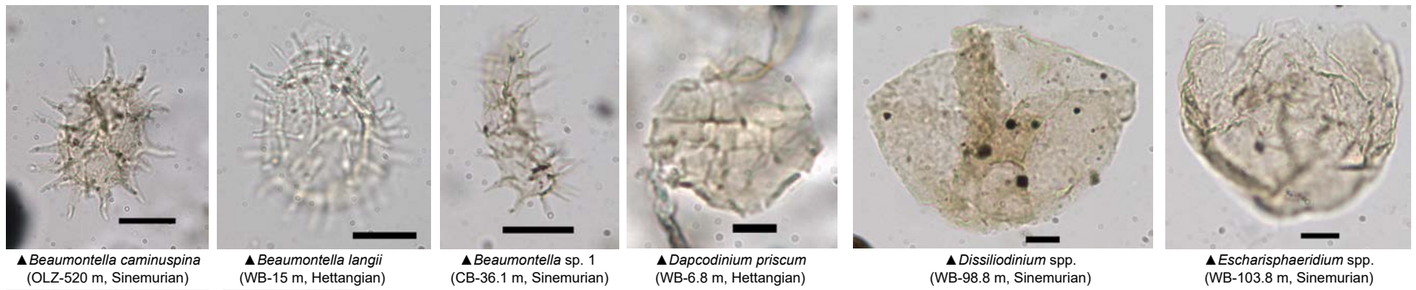

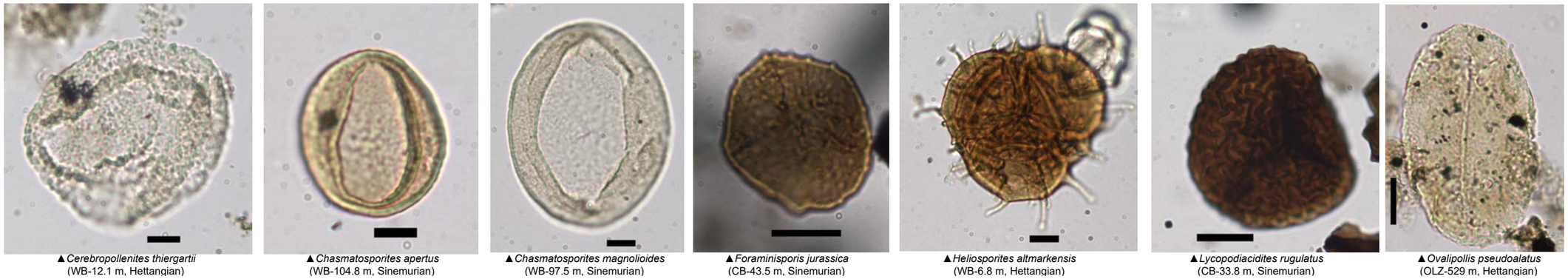

◄ ▼ Figure 4.7: Transmissive Light Microscopy Photographs of selected palynomorphs with biostratigraphic significance.
The scale-bar corresponds to 10 µm. The taxon's name, sampling locality and depth are indicated below the photograph. CB refers to the Cleveland Basin succession, WB to the Wessex Basin succession and OLZ to Well Oldenzaal-4 (Netherlands).

Hettangian

Sporomorphs

As mentioned before the Hettangian succession from Dorset does not yield any species characteristic for the Rhaetian, in contrast to claims in Germany and Denmark (Dybkjær, 1991). We do note that a number of taxa are present just below the base of the Hettangian. In contrast we note no conspicuous appearances or extinctions in the Hettangian. The only exception is the appearance of *Foraminisporis jurassicus* in the Planorbis Subzone. The stratigraphic value of these events is ambiguous. The appearance of *Cerebropollenites macroverrucosus* in contrast is more reliable, in the Wessex basin it is recorded in the Upper Hettangian Angulata Zone, although *Cerebropollenites* is becoming more prominent in terms of abundance further up-section in the Pliensbachian. Many others indicate the FO of *C. macroverrucosus* as Early Sinemurian (see Dybkjaer, 1991). The partitioned, successive appearance of the species *C. thiergarti* and *C. macroverrucosus* therefore has stratigraphic significance. We also reiterate that *Riccisporites tuberculatus* which is by some authors thought to range into the Hettangian was not recorded at all in the Wessex Basin (see also Hounslow et al., 2004, **Figure 4.5**). This may be partly ascribed to the high abundance of *Classopollis* in contrast to the sections in continental NW-Europe that yield abundant spore communities, deposited in a setting with more fluvial input.

Marine Palynomorphs

The range-top of *Dapcodinium priscum* is placed in the upper Hettangian (Morbey, 1978; Wille and Gocht, 1979; Brenner, 1986, i.e., in Germany-Austria) or Lower Sinemurian (Dybkjaer, 1991; Nielsen, 2003, Larsson, 2009) in Denmark and Southern Sweden respectively). Our study in contrast reveals no *Dapcodinium priscum* at all in the Hettangian (**Figure 4.6**, see also Wall, 1965; Van de Schootbrugge et al., 2005; Hounslow et al., 2004). Arguably, the extinction of *D. priscum* is strongly diachronous and delayed further towards the north. Hence, the presence of *D. priscum* is no longer considered a valuable indicator for the Hettangian.
By many authors, dinocysts attributable to *Beaumontella* have been neglected or grouped as an acritarch taxon, thus hampering evaluation of its stratigraphic significance. *Beaumontella langii* is persistently recorded in the Hettangian of Dorset and *Beaumontella? caminuspina* is occasionally present. Acritarchs of genus *Leiofusa* disappear from the record at a level corresponding to the middle Hettangian laqueus Subzone. The distinct acritarch *Michystridium intromittum* has a FO corresponding to the Upper Hettangian Angulata Zone.

► **Figure 4.8: Distribution-chart of sporomorph taxa from the Sinemurian to Toarcian succession in the Cleveland Basin.**

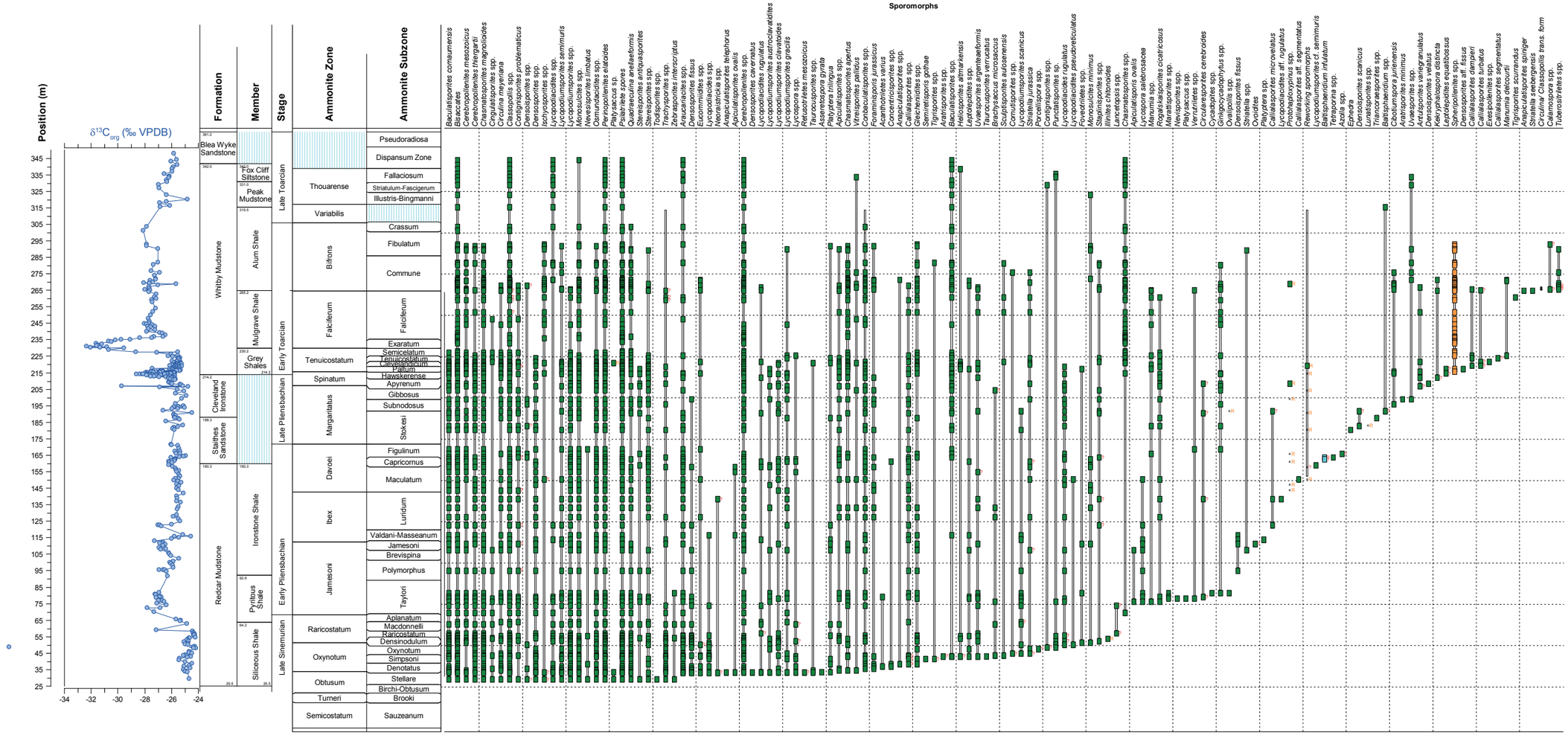

Sinemurian

For the Sinemurian, there is overlap between the two outcrop reference sections. The Wessex Basin record extends into the Lower Pliensbachian, but is characterized by hiatuses and/or non-deposition in the late Sinemurian (Denotatus, Simpsoni and Oxynotum Subzones of the Obtusum and Oxynotum Zones) and the latest Sinemurian (Macdonnelli and Aplanatum Subzone of the Raricostatum Zone). In the Cleveland Basin (Yorkshire), deposition is continuous throughout the Sinemurian. The base of the Cleveland Basin succession is in the Stellare Subzone of the Obtusum Zone (Late Sinemurian).

Sporomorphs

The Hettangian-Sinemurian transition is marked by the FO of *Cerebropollenites macroverrucosus*. In addition we note the FO of *Lycopodiumsporites semimuris* in the Birchi Subzone in Dorset. Although poorly calibrated, this species is repeatedly reported to occur in the lower part of the Sinemurian in Denmark and Germany (Dybkjaer, 1991). Furthermore, we note the extinction of *Rotundus granulatus*, an enigmatic palynomorph of likely terrestrial origin (Koppelhus and Nielsen, 1994) in the Stellare Subzone in Dorset. Furthermore, we record the Last Consistent Occurrence (LCO) of *Kraeuselisporites reisengerii* in the Late Sinemurian Densinodulum Subzone, both in Yorkshire and Dorset. This is in-line with records from Germany (Schulz, 1967) and Denmark (Dybkjaer, 1991), whereas others have recognized (likely reworked specimens as young as Aalenian. The FO of *Leptolepidites major* is recorded in the Oxynotum Zone (Simpsoni Subzone) in Yorkshire and the FO of *Striatella jurassica* is recorded in the lowermost part of the Raricostatum Zone (Densinodulum Subzone) in Yorkshire (**Figure 4.5** and **Figure 4.8**).

Marine palynomorphs

The LO of *Beaumontella? caminuspina* is recorded corresponding to the Early Sinemurian Scipionianum Subzone. In many standard works this species is considered restricted to the Triassic (see e.g., Riding and Thomas, 1992). We suspect that this species is often not recognized as a dinoflagellate and subsequently grouped under acritarchs. The same holds true for *Beaumontella langii*, which has a LO in the Late Sinemurian Densinodulum Subzone of Dorset. This is further confirmed by absence in the younger Cleveland Basin succession. According to Riding and Thomas (1992), *Beaumontella langii* ranges into the Pliensbachian. There is however no underlying citation to a record that supports this claim. We therefore conclude that *B. langii* is confined to the Sinemurian, and as such provides a valuable marker. Furthermore, we note the occurrence of a new species, assignable to *Beaumontella* (here referred to as *Beaumontella* sp. 1, see **Figure 4.7**) approximating the LO of *B. langii*, also in the Densinodulum Subzone. This species is recorded well into the Pliensbachian in the Cleveland Basin (**Figure 4.8**).

We record the appearance of *Mendicodinium reticulatum* in the Cleveland Basin succession in the Denotatus Subzone of the Obtusum Zone. We also find this species appearing in the Densinodulum Subzone, at the base of the Raricostatum Zone. The latter is likely because the Obtusum Zone is missing in Dorset. These Late Sinemurian occurrences are substantially older than the currently known occurrence date of this genus. Morgenroth (1970) described this species and genus from the “Lias Delta”, Germany in assemblages constituting Late Pliensbachian elements (e.g., *Luehndea spinosa*, *Nannoceratopsis gracilis*, see also next section). The taxon was later also recorded from the Pliensbachian in Denmark (Koppelhus and Nielsen, 1994).The presence of this species was deemed anomalous because its range is Bathonian to Callovian according to Riding and Thomas (1992) and Callovian to middle Oxfordian according to Feist-Burkhardt and Wille (1992). Specimens of *Mendicodinium* have been found at other European Lower Jurassic localities, for example Portugal (Davies, 1985), France (De Vains, 1988) and Italy (Palliani and Riding, 1997). In the Cleveland Basin, (Palliani and Riding (2000) report occurrences of *Mendicodinium* (as *M. microscrabatum* and *M. spinosum*) in the Lower

Pliensbachian. However, the resolution in the study of the latter authors in the Upper Sinemurian is limited and non-quantitative. We conclude that the repeated occurrence of *M. reticulatum* in the Late Sinemurian substantially extends the stratigraphic first occurrence of this group. Since this taxon is considered to be constricted to the Tethyan realm, its introduction indicates a connection with the Tethys waters and as such provides insight into the opening of the Hispanic corridor from the earliest Pliensbachian onwards (**Figure 4.9**).

Liasidium variabile is well-known as an excellent marker for the late Sinemurian of northwest Europe (e.g., Riding, 1984; Bujak and Williams, 1985; Woollam and Riding, 1983; Morbey (1978) and Morbey and Dunay (1978). In our study on the Dorset succession, we did not record *Liasidium variabile* at all, which is in-line with the inferred hiatuses in the Obtusum, Oxynotum and Raricostatum Zone. In the Cleveland Basin we record *L. variabile* abundantly in the basal sample (29.6 m height, **Figure 4.9**) and present in low abundance in the overlying sample (33.6 m height), corresponding to Obtusum Subzone. Subsequently, it is absent in the Stellare Subzone of the Obtusum Zone, to return and again to reach abundance in the Denotatus and Simpsoni Subzones. It declines in abundance to remain persistently present up to a level corresponding to the Densinodulum Subzone of the Raricostatum Zone, still within the Late Sinemurian. According to Riding et al. (2013), *L. variabile* is confined to a 2‰ negative excursion recorded in organic carbon isotope data, recorded across the Obtusum and Oxynotum Ammonite Zones. Our combined palynological and isotope data from the Yorkshire outcrops however, display a significantly different picture. *L. variabile* is in fact present in a series of pulses extending into the Raricostatum Zone. These which are likely linked to eustatic sea level fluctuations, themselves exert control on the relatively small carbon isotope variations (**Figure 4.10**). Remarkably, *L. variabile* was also recorded from the late Hettangian of southwest Germany by Brenner (1986). Weiss (1989) reported *L. variabile* from the Turneri and Obtusum Zones (early-late Sinemurian) of Germany. To summarize, *L. variabile* appears to occur abundantly only in the late Sinemurian, but the reports in Brenner (1986) and Weiss (1989) indicate that its FO in continental Europe may be earlier than in England. The LO of L. variabile is clearly confined to the latest Sinemurian. In Yorkshire, the LO predates the base of the negative $\delta^{13}C$-excursion across the Sinemurian-Pliensbachian boundary.

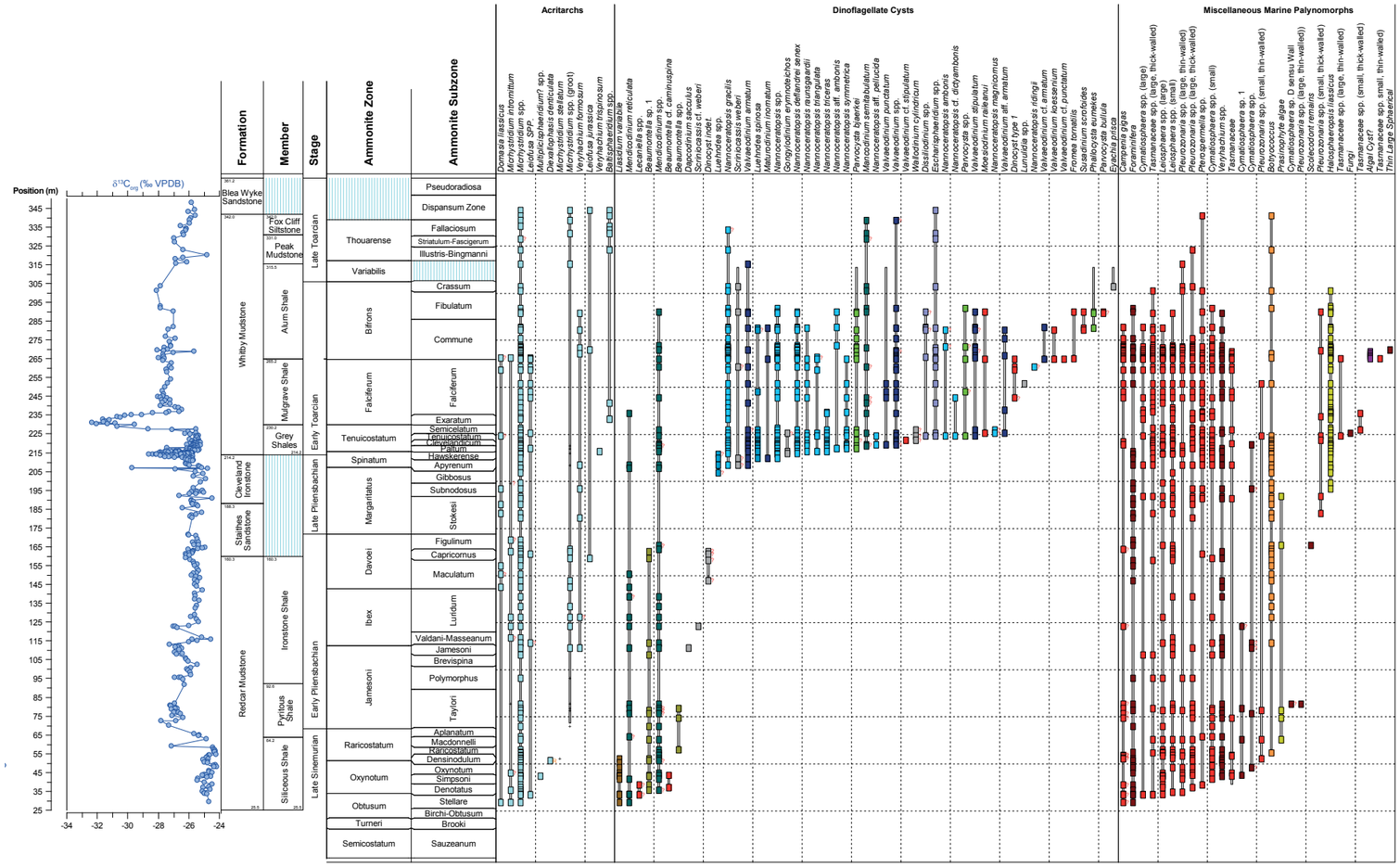

▲ Figure 4.9: Distribution-chart of marine palynomorph taxa from the Sinemurian-Toarcian in the Cleveland Basin.

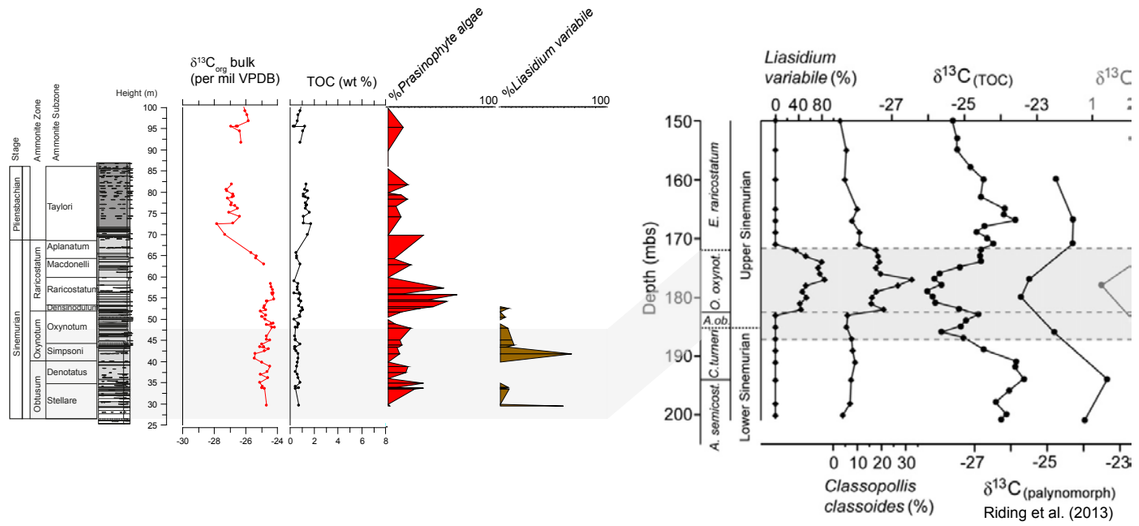

► Figure 4.10: Comparison of palynological and isotope results from the Cleveland Basin and the Winterton Borehole (Riding et al., 2013).
The Cleveland data illustrate that the abundance optima of *L. variabile* are not associated with significant $\delta^{13}C$-shifts. Interestingly, prasinophyte algae are highly abundant after the extinction of *L. variabile*

Early Pliensbachian

Terrestrial palynomorphs

We note the LO of *Zebrasporites interscriptus* in the lowermost Pliensbachian Taylori Subzone. According to various authors, this species has a LO in the Hettangian or Sinemurian. Only Schulz (1967) in Germany describes this species ranging into the Toarcian. Also noteworthy is the consistent presence of *Densosporites fissus*, which by some authors is invoked to be restricted to the Triassic/Jurassic boundary interval (e.g., Schulz, 1967; Lund, 1977 and Dybkjaer, 1991) but ranges more or less consistently into the lowermost Pliensbachian (Taylori Subzone) and then has a number of scattered occurrences up to the Upper Pliensbachian (Subnodosus Subzone of the Margaritatus Zone, **Figure 4.8**).

Marine palynomorphs

In terms of originations and extinctions of marine palynomorphs, the Lower Pliensbachian is known as a period of quiescence (Riding and Hubbard, 1999; Van de Schootbrugge et al., 2005). In fact, the uppermost Sinemurian to lower Pliensbachian is generally considered barren of dinoflagellate cysts, at least in northwestern Europe (see e.g., Van de Schootbrugge et al., 2005). Given that the lowermost Pliensbachian corresponds to a major transgressive phase starting in the Raricostatum Zone and continuing up to the upper Pliensbachian (Hesselbo et al., 2008), it may be argued that sea level rise did not lead to suitable shallow marine habitats for cyst-forming dinoflagellates. One reason for this would have been a decrease in bottom water oxygen levels related to more sluggish circulation on the northwest European shelves. In contrast to previous, often low-resolution studies we now repeatedly record dinoflagellate cysts belonging to *Mendicodinium* and *Beaumontella* (**Figure 4.9**). Only the Upper Pliensbachian (the Staithes Sandstone Fm. and Lower Cleveland Ironstone Fm., Stokesi to Gibbosus Subzone interval) are truly devoid of dinocysts, which we ascribe to the proximal depositional environment. In the Lower Pliensbachian, we have noted a few potentially relevant events. First of all, large (> 30μm diameter) specimens of the acritarch *Michrystridium* are recorded for the first time in basal Pliensbachian strata (Taylori Subzone of the Jamesoni Zone). The genus *Beaumontella* (*Beaumontella* sp. 1) has a LO in the Early Pliensbachian Davoei Zone (Figulinum Subzone). This species is present in Dorset from the Late Sinemurian Densinodulum Subzone onwards. Only in Dorset did we, for the first time find specimens of *Valvaeodinium armatum* in strata corresponding to the Taylori Zone (**Figure 4.6**). This species is not recorded until the Latest Pliensbachian in Yorkshire. Potentially it appeared earlier in the relatively open marine settings, as encountered in Dorset. We also note the short-lived presence of an undescribed number of organic-walled dinoflagellate cysts (see **Figure 4.9**) in the Davoei Zone.

▼ Figure 4.11: Distribution-chart of dinocysts across the Pliensbachian-Toarcian boundary interval.

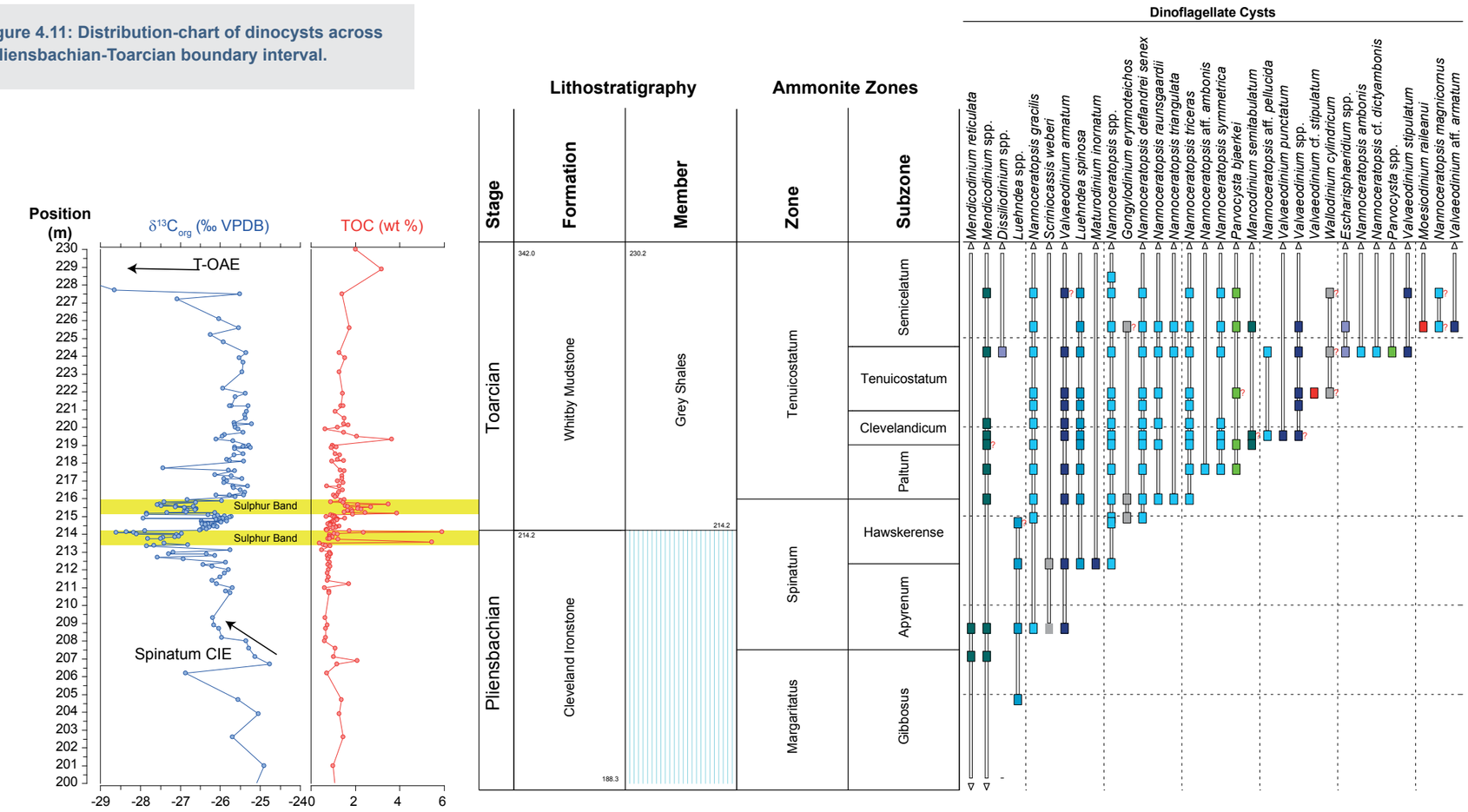

Late Plienbachian

Sporomorphs

There are no noteworthy originations in the Upper Pliensbachian succession from Yorkshire.

The LO of *Densosporites fissus* is recorded in a level corresponding to the Gibbosus Subzone of the Margaritatus Zone. This species is by some authors considered to become extinct in the Hettangian, thus substantially extending its range into the Late Pliensbachian in England. A number of sporomorph taxa become extinct at the Pliensbachian-Toarcian boundary. These include *Stereisporites antiquasporites*, *Lycopodiumsporites austroclavatidites* and L*ycopodiacidites rugulatus*. The range of these taxa is not adequately described in the literature and as a consequence, the biostratigraphic relevance of these LOs remains ambivalent (**Figure 4.8**).

Marine palynomorphs

Most of the Staithes Sandstone Fm. and the lower part of the Cleveland Ironstone Formation (e.g., the upper part of the Davoei Zone and lower half of the Margaritatus Zone) are completely devoid of organic-walled dinoflagellate cysts. This is most likely ascribed to the overall regressive nature of this interval and the consequential reduction of the shelf area in which dinoflagellates thrive. Remarkably however, just below the Pliensbachian – Toarcian boundary, still within the very proximal (lagoonal) facies of the Cleveland Ironstone Fm., we note the occurrences of a series of subsequently long-ranging dinoflagellate cyst taxa (**Figure 4.9**).

The first to appear are specimens closely resembling *Luehndea spinosa* in the Gibbosus Subzone, still within the Margaritatus Zone. Subsequently, *Nannoceratopsis gracilis*, *Scriniocassis weberi* and V*alvaeodinium armatum* appear in the Apyrenum Subzone of the Spinatum Zone. At the base of the Hawskerense Subzone of the Spinatum Zone *Luehndea spinosa* sensu stricto and *Maturodinium inornatum* appear.

Based on paired $\delta^{13}C$ and $\delta^{18}O$-measurements on belemnites, Korte and Hesselbo (2011) reconstruct relatively high amplitude (glacioeustatic) sea-level variability in the Margaritatus-Spinatum interval (see also Chapter 6). According to Palliani and Riding (1999), *Nannoceratopsis gracilis* and *Luehndea spinosa* are both taxa that have substantially older FOs (Early Pliensbachian, Davoei Zone and Jamesoni Zone respectively) in the Tethys. Hence, the introduction of these taxa in the Late Pliensbachian of the North Sea area seems to relate to establishment of a connection with the Tethyan realm, likely via deepening of the Hispanic Corridor, perhaps in response to the high-amplitude relative sea-level change.

According to Riding and Thomas (1992), both *Valvaeodinium armatum* and *Maturodinium inornatum* have a very short stratigraphic range, with a reported LO in the Spinatum Zone. However, we record these taxa well into the Toarcian, with LOs in the variabilis Zone and the Commune Subzone of the Bifrons Zone respectively (**Figure 4.11**).

Toarcian

Sporomorphs

Just above the Pliensbachian-Toarcian boundary, within the Grey Shale Mb. of the Whitby Mudstone Fm. we note the FO of *Callialasporites dampieri* and *C. turbatus*. This is older than generally accepted for this long-ranging Jurassic palynomorph-type. According to Weiss (1989) and Riding et al. (1991) these first occur in the Late Toarcian Levesquei Zone. However, there are also reports of a Latest Pliensbachian to Early Toarcian FO, based on work from boreholes from the eastern Netherlands (Herngreen, 2005) and the closely related species *Callialasporites trilobatus* has a coeval reported FO in the Lowermost Toarcian (Palliani and Riding, 1997). The occurrence of this genus thus forms an excellent marker for the base of the Toarcian (**Figure 4.8**). Also at the base of the Toarcian we note the appearance of several small sphaeromorph forms. Some are clearly fluorescent under UV-fluorescent light. These are considered of prasinophyte affinity and hereafter referred to as *Halosphaeropsis jurassica* (see Chapter 8 for further discussion). Concomitantly we also note similar sized sphaerical bodies that are characterized by the weaker colored fluorescence as also observed in for instance the pollen grains of *Classopollis*. For these forms we retain the name *Spheripollenites*, since a terrestrial origin cannot be excluded. From this perspective this taxon forms a clear indicator for the base of the Toarcian. A bit up-section in a stratum corresponding to the Tenuicostatum Subzone of the Tenuicostatum Zone we note the FO of *Manumia delcourtii*. The species *Staplinisporites telatus*, often also considered a good marker for the Toarcian was not recorded.

Rogalskaisporites cicatricosus has a LO near the top of the Mulgrave Shale Mb. in Falciferum Ammonite Zone, thus post-dating the Toarcian OAE as manifested by the Jet Rock Unit. Perhaps remarkably, although the T-OAE is clearly manifested by a change in abundance patterns of sporomorphs, there are no evident extinctions in sporomorphs associated (see **Figure 4.8**).

Marine palynomorphs

As mentioned above the base of the Toarcian marks the first occurrence of an array of small (10-25 μm diameter) sphaeromorph palynomorphs, including brightly fluorescent specimens which often display openings or slits. These forms referred to *Halosphaeropsis jurassica*, become particularly abundant and dominant during the T-OAE (see also Chapter 8). Next to that, the base of the Toarcian marks a continuation of the radiation of organic-walled dinocysts (**Figure 4.9**). The dinoflagellate cysts *Gongylodinium erymnoteichos*, formerly unknown from the Toarcian and thought to be restricted to the Bajocian (see e.g., Riding and Thomas, 1992), is recorded in the basal Toarcian sample. *Nannoceratopsis deflandrei* ssp. *senex* is also recorded from here onwards. Various other species of *Nannoceratopsis*; e.g., *N. raunsgaardi*, *N. triceras*, *N. triangulata* and *N. symmetrica* occur progressively in the Lowermost Toarcian (Hawskerense – Paltum Subzone). Importantly, *Parvocysta bjaerki* (by some authors referred to as *Limbicysta bjaerki*) a representative of a 'new family' of dinoflagellate cyst taxa (Heterocapsaceae) also first occurs in the Paltum Subzone, whereas other variants of the so-called *Parvocysta*-suite radiate substantially after the Toarcian OAE. *Mancodinium semitabulatum*, an important and relatively long-ranging Jurassic dinoflagellate cyst taxon is first recorded at the base of the Clevelandicum Subzone. Specimens resembling *Wallodinium cylindricum* appear in the Tenuicostatum Subzone (**Figure 4.11**). This species is known to first occur in the Upper Toarcian (Riding and Thomas, 1992). *Valvaeodinium stipulatum* also first occurs in the Tenuicostatum Subzone.

An important observation concerns representatives of a long-ranging Family of dinoflagellates, namely the Gonyaulacales. Cysts attributable to the *Dissiliodinium-Escharisphaeridium* complex first occur in the Tenuicostatum Subzone. These specimens concern a morphologically diverse group characterized by a compound precingular archeopyle in which the apical plates remain adnate (*Dissiliodinium*) or form an apical archeopyle by detachment of the apical plate series (*Escharisphaeridium*). These forms are very thin-walled and pale but are clearly discernible. Most biostratigraphic compilations place the FO of this group of taxa in the Early Aalenian. The observation from the Cleveland Basin substantially extends the occurrence of these to pre-T-OAE strata. An older FO is now also reported for *Moesiodinium raileanui*, e.g., in the Semicelatum Subzone, which was also reported to occur in the Late Toarcian (Riding and Thomas, 1992).

As mentioned extensively in the literature the Toarcian OAE (Exaratum Subzone, Jet Rock Unit of the Mulgrave Shale Mb.), is essentially devoid of organic-walled dinoflagellate cysts. *Halosphaeropsis jurassica* and prasinophyte algae such as *Tasmanites* and *Pleurozonaria* proliferate as a consequence of water column anoxia (see also Chapter 8). Like is the case in sporomorph associations, this temporary 'wipe-out' is associated with only a few true extinctions; those of *Luehndea spinosa* and *Nannoceratopsis triceras*. This suggests that refugia for the adverse conditions characterising the T-OAE persisted.

Above the T-OAE, still within the Early Toarcian we note the FO of *Valvaeodinium koessenium* at the boundary of the Mulgrave Shale Mb. and Alum Shale Mb. of the Whitby Mudstone Fm. (Falciferum-Bifrons Zonal boundary, **Figure 4.9**). The prasinophyte alga *Campenia gigas* last occurs near the top of the Commune Subzone of the Variabilis Zone. At this same level we note the diversification of the *Parvocysta*-suite with the FOs of *Susadinium scrofoides*, *Phallocysta eumekes* and *Parvocysta bullula*. Some species recorded in the Norwegian wells (see Chapter 6) such as *P. nasuta* were recorded in low abundance in a previous study on the Yorkshire section (Riding, 1984) at the same level. Although the *Halosphaeropsis jurassica* demises in abundance after the T-OAE, we note a persistent presence up to the top of the Fibulatum Subzone of Bifrons Zone. In this subzone *Valvaeodinium armatum* is also recorded for the last time. This may be considered remarkable since its reported range (Riding and Thomas, 1992) is restricted to the Late Pliensbachian.

We note the LO of representatives of the *Parvocysta*-suite in the Variabilis Zone, thus still substantially within the Toarcian. It is however generally considered that this group of taxa ranges into the Opalinum Zone of the Early Aalenian. Therefore, this may reflect a local facies-controlled extinction. We note the FO of *Eyachia prisca* in strata equivalent to the base of the Variabilis Zone.

Event	Type	Locality	Stage	Zone	Subzone	Remark
LO *Rhaetipollis germanicus*	SP	W	Rhaetian	-	-	LO in Lilstock Fm. According to Hounslow et al. (2004)
LO *Ovalipollis ovalis*	SP	W	Rhaetian	-	-	LO in Lilstock Fm. According to Hounslow et al. (2004)
LO *Rhaetogonyaulax rhaetica*	DC	W	Rhaetian	-	Pre-Planorbis Beds	Not recorded in our study. Hounslow et al. (2004) displays LO in basal Blue Lias Fm, possibly reworked
LO *Ricciisporites tuberculatus*	SP	W	Rhaetian	-	Pre-Planorbis Beds	Similar pattern in Denmark (Lund, 1977; Dybkjaer, 1991)
FCO Non-taeniate bisaccate pollen	SP	W	Rhaetian	-	Pre-Planorbis Beds	Similar pattern in Denmark (Lund, 1977; Dybkjaer, 1991)
FCO *Heliosporites reisengerii*	SP	W	Rhaetian	-	Pre-Planorbis Beds	Similar pattern in Denmark (Lund, 1977; Dybkjaer, 1991)
FCO *Chasmatosporites* spp.	SP	W	Rhaetian	-	Pre-Planorbis Beds	FO in Rhaetian
FO *Cerebropollenites thiergartii*	SP	W	Rhaetian	-	Pre-Planorbis Beds	In Germany recorded slightly later (Earliest Hettangian, Schulz, 1967)
LO *Dapcodinium priscum*	DC	W	Rhaetian	-	Pre-Planorbis Beds	LO in Early Sinemurian in continental Europe (see. e.g, Lund, 1977; Dybkjaer et al., 1991; Feist-Burkhardt and Wille, 1992)
FO *Foraminisporis jurassica*	SP	W	Hettangian	Planorbis	Planorbis	Might represent a local phenomenon as distribution elsewhere poorly known
FO *Cerebropollenites macroverrucosus*	SP	W	Hettangian	Angulata	-	Generally reported from Early Sinemurian onwards
LO *Leiofusa* spp.	AC	W	Hettangian	Liasicus	Laqueus	Likely a local facies-controlled phenomenon
LO *Beaumontella*? *caminuspina*	DC	W	Early Sinem.	Semicostatum	Scipionianum	Riding and Thomas (1992) report taxon to be restricted Rhaetian.
FO *Lycopodiumsporites semimuris*	SP	W	Early Sinem.	Turneri	Birchi	Considered restricted to Sinemurian by some authors. Dybkjaer (1991) also reports a FO in the Sinemurian.
LO *Rotundus granulatus*	?	W	Late Sinem.	Obtusum	Stellare	Not validly published by Koppelhus and Nielsen (1994). Granulate sphaerical form with dinoflagellate-like aperture
FO *Liasidium variabile*	DC	C	Late Sinem.	Obtusum	Stellare	
FO *Mendicodinium reticulatum*	DC	W/C	Late Sinem.	Obtusum	Denotatus	Reported to occur abundantly in the Tethys before expanding to NW-Europe (Palliani and Riding, 1999).
FO *Leptolepidites major*	SP	C	Late Sinem.	Oxynotum	Simpsoni	
LCO *Liasidium variabile*	DC	C	Late Sinem.	Oxynotum	Oxynotum	
LCO *Heliosporites reisengerii*	SP	W/C	Late Sinem.	Raricostatum	Densinodulum	Consistent in NW-Europe. Younger occurrences likely reworked
FO *Striatella jurassica*	SP	C	Late Sinem.	Raricostatum	Densinodulum	
LO *Beaumontella langii*	DC	W/C	Late Sinem.	Raricostatum	Densinodulum	Early Pliensbachian according to Riding and Thomas (1992).
FO *Beaumontella* sp. 1	DC	W/C	Late Sinem.	Raricostatum	Densinodulum	
LO *Liasidium variabile*	DC	C	Late Sinem.	Raricostatum	Densinodulum	
LO *Zebrasporites interscriptus*	SP	C	Early Pliensb.	Jamesoni	Taylori	LO Hettangian-Sinemurian in Germany (Schulz, 1967)
“FO” *Valveodinium armatum*	DC	W	Early Pliensb.	Jamesoni	Taylori	Specimens are only recorded in Wessex Basin. FO in Cleveland Basin is Late Pliensbachian (see below)
LO *Beaumontella* sp. 1	DC	C	Early Pliensb.	Davoei	Figulinum	LO of *B. langii* at same level according to Riding and Thomas (1992)
FO *Luehndea spinosa* s.l.	DC	C	Late Pliensb.	Margaritatus	Gibbosus	Smaller forms compared to *sensu stricto* (s.s.) type
FO *Scriniocassi weberi*	DC	C	Late Pliensb.	Spinatum	Apyrenum	FO in Margaritatus Zone according to Riding and Thomas (1992)
FO *Valvaeodinium armatum*	DC	C	Late Pliensb.	Spinatum	Apyrenum	Recorded earlier in Wessex Basin.
FO *Nannoceratopsis gracilis*	DC	C	Late Pliensb.	Spinatum	Apyrenum	FO in Margaritatus Zone according to Riding and Thomas (1992). FO is substantially older in the Tethys
FO *Luehndea spinosa* s.s.	DC	C	Late Pliensb.	Spinatum	Hawskerense	Some poorly calibrated FOs are reported earlier in the Tethyan realm as young as Jamesoni Zone.
FO *Maturodinium inornatum*	DC	C	Late Pliensb.	Spinatum	Hawskerense	FO in Margaritatus Zone according to Riding and Thomas (1992)
LO *Stereisporites antiquasporites*	SP	C	Late Pliensb.	Spinatum	Hawskerense	
LO *Lycopodiumsporites austroclavatidites*	SP	C	Late Pliensb.	Spinatum	Hawskerense	
LO *Lycopodiacidites rugulatus*	SP	C	Late Pliensb.	Spinatum	Hawskerense	
Diversification within *Nannoceratopsis*	DC		Late Pliensb.	Spinatum	Hawskerense	
FO *Calialasporites turbatus/trilobatus*	SP	C	Early Toarcian	Tenuicostatum	Paltum	Typically reported from Late Toarcian onwards
FO *Halosphaeropsis liassicus*	PR	C	Early Toarcian	Tenuicostatum	Paltum	
FO *Gongylodinium erymnoteichos*	DC	C	Early Toarcian	Tenuicostatum	Paltum	
FO *Parvocysta bjaerki*	DC	C	Early Toarcian	Tenuicostatum	Paltum	
FO *Mancodinium semitabulatum*	DC	C	Early Toarcian	Tenuicostatum	Clevelandicum	
FO *Manumia delcourtii*	SP	C	Early Toarcian	Tenuicostatum	Tenuicostatum	
FO *Dissiliodinium-Escharisphaeridium* cpx	DC	C	Early Toarcian	Tenuicostatum	Tenuicostatum	Other studies claim FO in the Aalenian
FO *Valvaeodinium stipulatum*	DC	C	Early Toarcian	Tenuicostatum	Tenuicostatum	
FO *Moesiodinium raileanui*	DC	C	Early Toarcian	Tenuicostatum	Semicelatum	Other studies claim FO in Late Toarcian
FAO *Halosphaeropsis liassicus*	PR	C	Early Toarcian	Falciferum	Exaratum	Corresponds to Toarcian OAE.

▲ **Table 4.2: Summary of palynological events recognized in the Wessex Basin (W) and Cleveland Basin (C) outcrop sections and remarks on distribution elsewhere.** AC=acritarch, SP= sporomorph, DC=dinocyst, PR=prasinophyte alga.

Event	Type	Locality	Stage	Zone	Subzone	Remark
LO *Nannoceratopsis triceras*	DC		Early Toarcian	Falciferum	Exaratum	Ranges up to Upper Toarcian elsewhere
LO *Luehndea spinosa*	DC		Early Toarcian	Falciferum	Exaratum	LO reported to correspond to T-OAE
FO *Valvaeodinium koessenium*	DC		Early Toarcian	Bifrons	Commune	
FO *Susadinium scrofoides*	DC		Early Toarcian	Bifrons	Commune	
FO *Phallocysta eumekes*	DC		Early Toarcian	Bifrons	Commune	
FO *Parvocysta bulula*	DC		Early Toarcian	Bifrons	Commune	
FO *Susadinium scrofoides*	DC		Early Toarcian	Bifrons	Commune	
FO *Parvocysta nasuta*	DC		Early Toarcian	Bifrons	Commune	
FO *Parvocysta nasuta*	DC		Early Toarcian	Bifrons	Commune	
FO *Phallocysta eumekes*	DC		Early Toarcian	Bifrons	Commune	According to Riding (1984) LO in Thouarsense Zone
FO *Parvocysta bulula*	DC		Early Toarcian	Bifrons	Commune	
LO *Valvaeodinium armatum*	DC		Early Toarcian	Bifrons	Fibulatum	Considered restricted to Pliensbachian according to Riding and Thomas (1992)
LO *Halosphaeropsis liassicus*	PR		Early Toarcian	Bifrons	Fibulatum	Likely related to end of anoxic conditions
FO *Eyachia prisca*	DC		Late Toarcian	Variabilis	-	Recorded in Bifrons Zone by Riding (1984). FCO in Levesquei Zone
LO *Maturodinium inornatum*	DC		Late Toarcian	Variabilis	-	Considered restricted to Pliensbachian according to Riding and Thomas (1992)

▲ Table 4.2: Continued

4.3 Integrated framework

All analyses from the Wessex Basin and Cleveland Basin were assigned an absolute age, based on the relative position within Ammonite Subzones (**Figure 4.12**). We follow the ages of the Boreal Ammonite Zones after Gradstein et al. (2012). Via this way, a composite $\delta^{13}C$-curve is constructed. As can be seen, the Dorset-record is offset from the Yorkshire-record in the overlapping part of the Late Sinemurian. This is ascribed to the C-recycling under anoxic conditions in Dorset. We therefore reemphasize that this curve can not be used in terms of absolute values but for detecting of directional shifts. The most important bio-events and isotope shifts are plotted alongside this graph. This framework forms the backbone for ensuing correlations in this study. ■

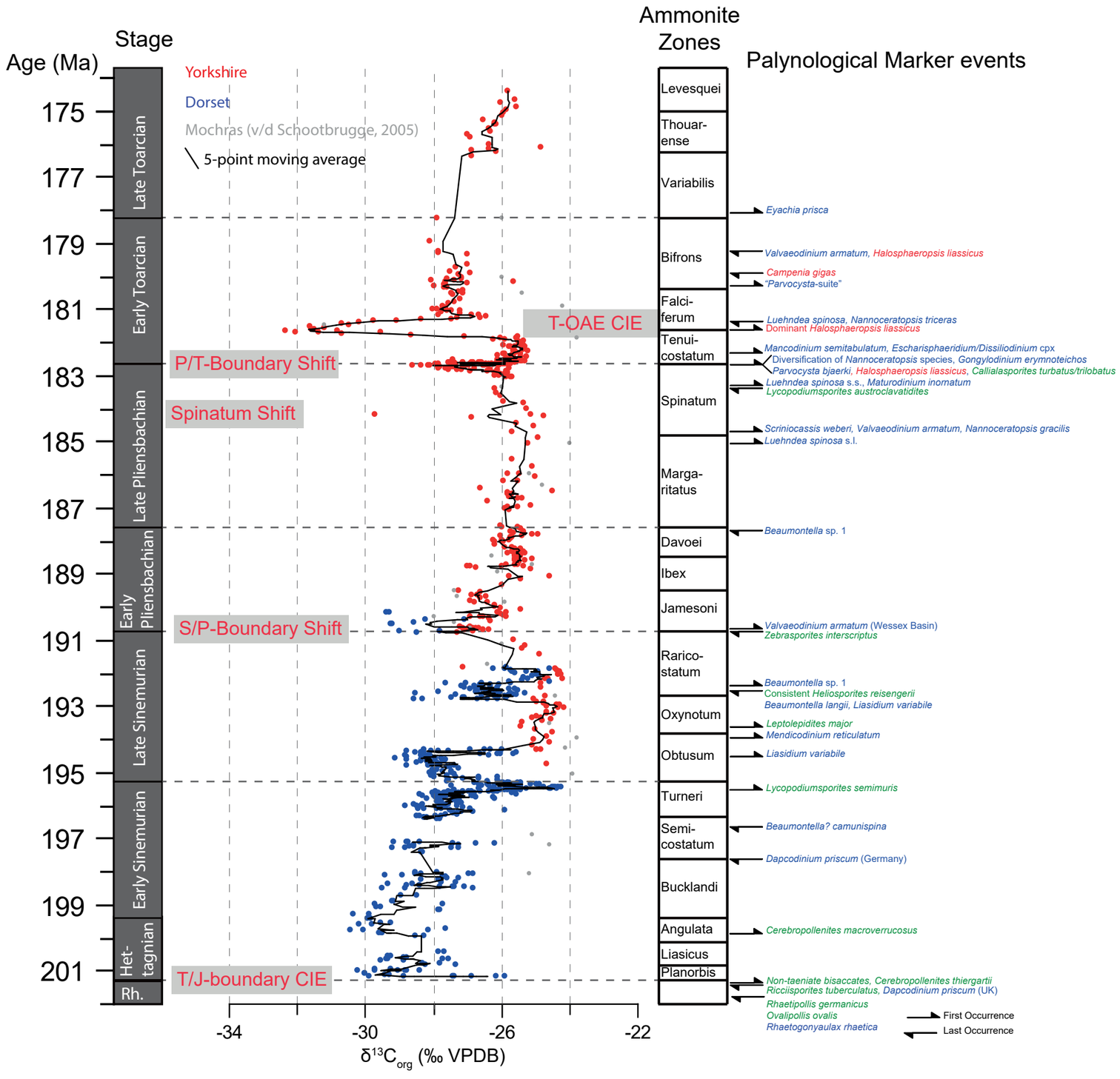

► Figure 4.12: Summary of the stratigraphic framework.
This figure shows the stable carbon isotope results from the Wessex Basin (blue dots) and the Cleveland Basin (red dots) scaled against age (Gradstein et al., 2012, following the Ammonite Zones of Page, 2003). The main "isotope events" are indicated. At the right the most important palynological marker events as recognized in the outcrop reference sections are indicated. Names written in green are sporomorphs, in blue dinocysts and in red prasinophyte algae.

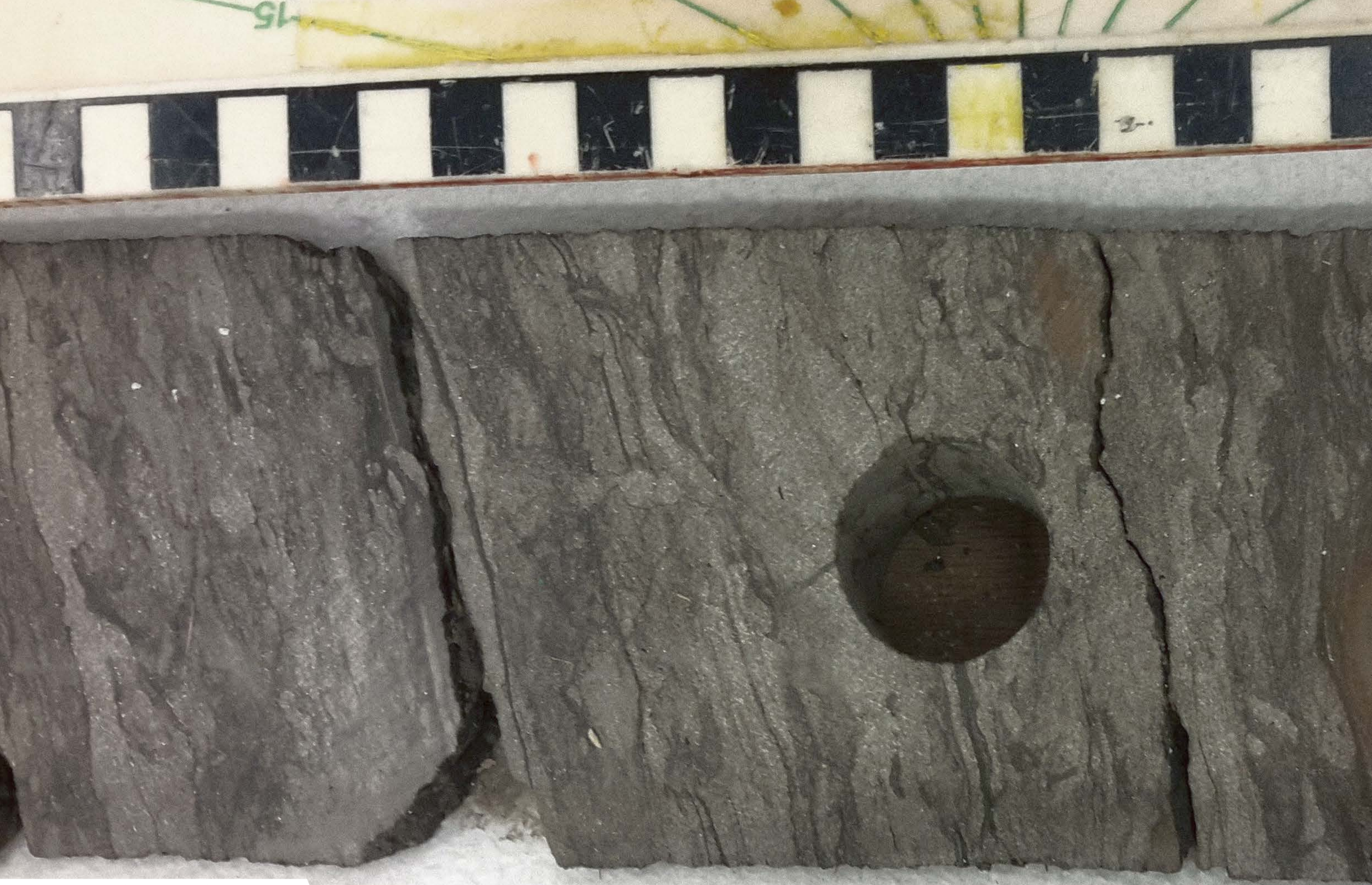

Core from the Cook Fm. (Well 34-10-35)

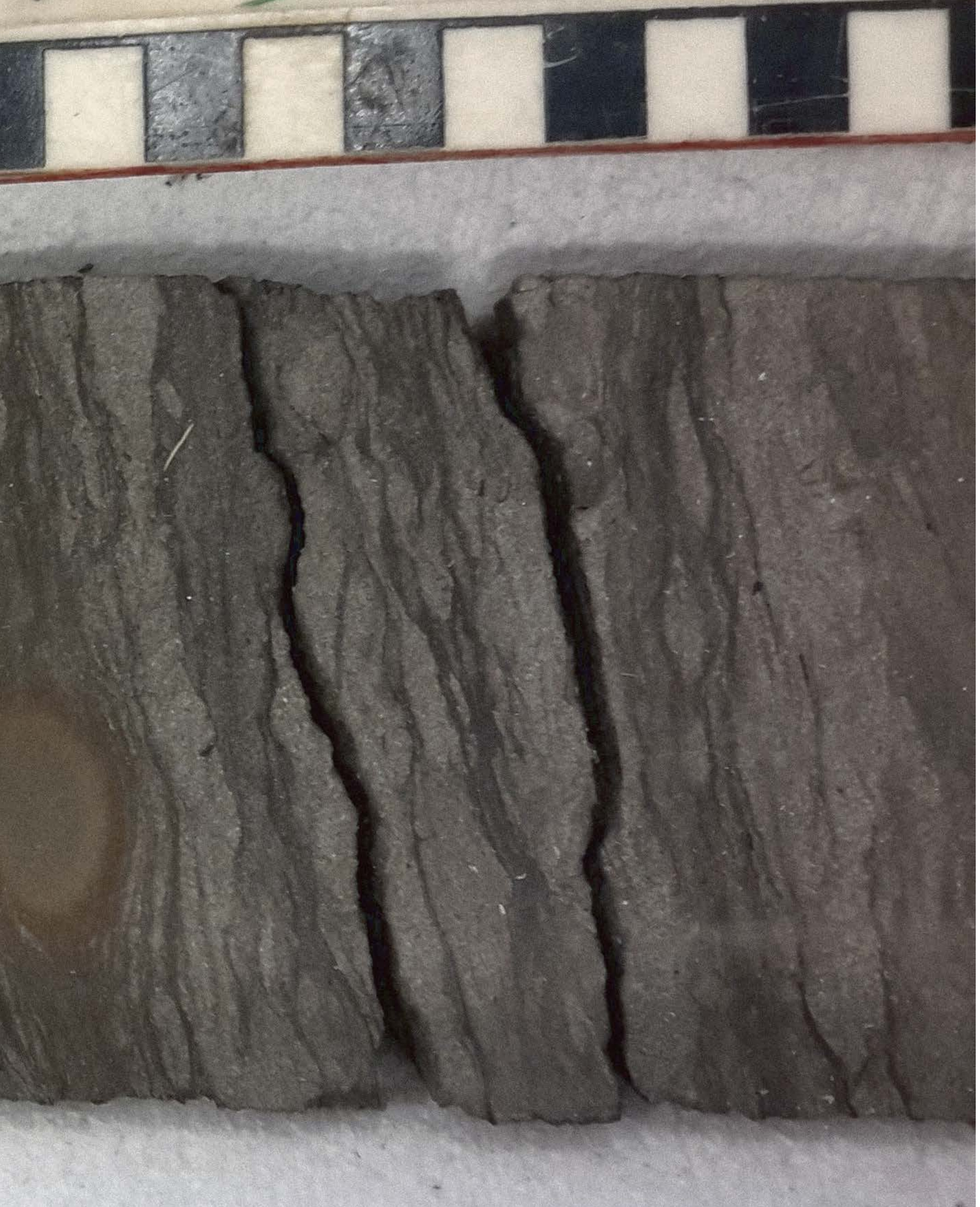

5. Regional Log Correlation

5. REGIONAL LOG CORRELATION

In order to upscale the results from the detailed core and outcrop campaigns a well log correlation exercise was included in the study. The main aim of this log correlation is to identify log markers that can be traced through the study area and link the log responses to the outcrop and core results. This way large scale lateral changes can be identified and regional trends explained.

5.1 Input data

For well correlations, data from the Netherlands, UK northern and southern North Sea and Norway were collected. The logs from the UK were made available by NAM for the use in this study and consist mainly of gamma ray (GR), sonic (DT) and density (RHOB) logs. The logs from Norway were made available by Statoil. All of the Norwegian logs have GR log information. For several of the Norwegian wells DT, caliper (CAL), neutron (NEU) and RHOB logs were available. However, for the wells from which cored sections were studied in detail for stratigraphy (Chapters 6, 8) only GR logs were available. The Dutch wells were selected for the presence of the Posidonia Shale Formation in the wells and the quality of the available logs. Only wells with at least GR and DT logs were included in the correlation.

The log correlation was performed using mainly GR and DT logs (scaled to 0 to 200 gAPI and 40 to 240 µs/ft respectively) in a viewing template that visualizes differences in composition using a grey-orange-yellow colour coding, relating to very fine grained sediments (grey – high GR, high DT), coarser grained to silt (orange

Chronostratigraphy	NL	UK_south	southern_NS inter-preted	Lithostratigraphy
Top Lias	Top ATPO/PO8	Top LI/JL/JT	Top_Lias	Top Cerdic Fm
	PO4		Red	
Top Pliensbachian	Top ATAL/PO0	Top JE	Yellow	Top Ida Fm
			JE_Int	Top Offa Fm
Top Sinemurian		Top JS	Orange	Top Penda Fm
Top Sinemurian*		Top JS*	JS_Int	Top Penda Fm*
			Green	
Top Hettangian		Top JH	JH_Int	
Base Lias	Top ATRT	Base LI/JL	Pink	Base Penda Fm

* If Orange marker was not identifiable “JS_Int marker” can be considered as Top Sinemurian

Table 5.1: Well marker/tops used in the correlation study of the southern North Sea area in the UK and Dutch on- and offshore regions

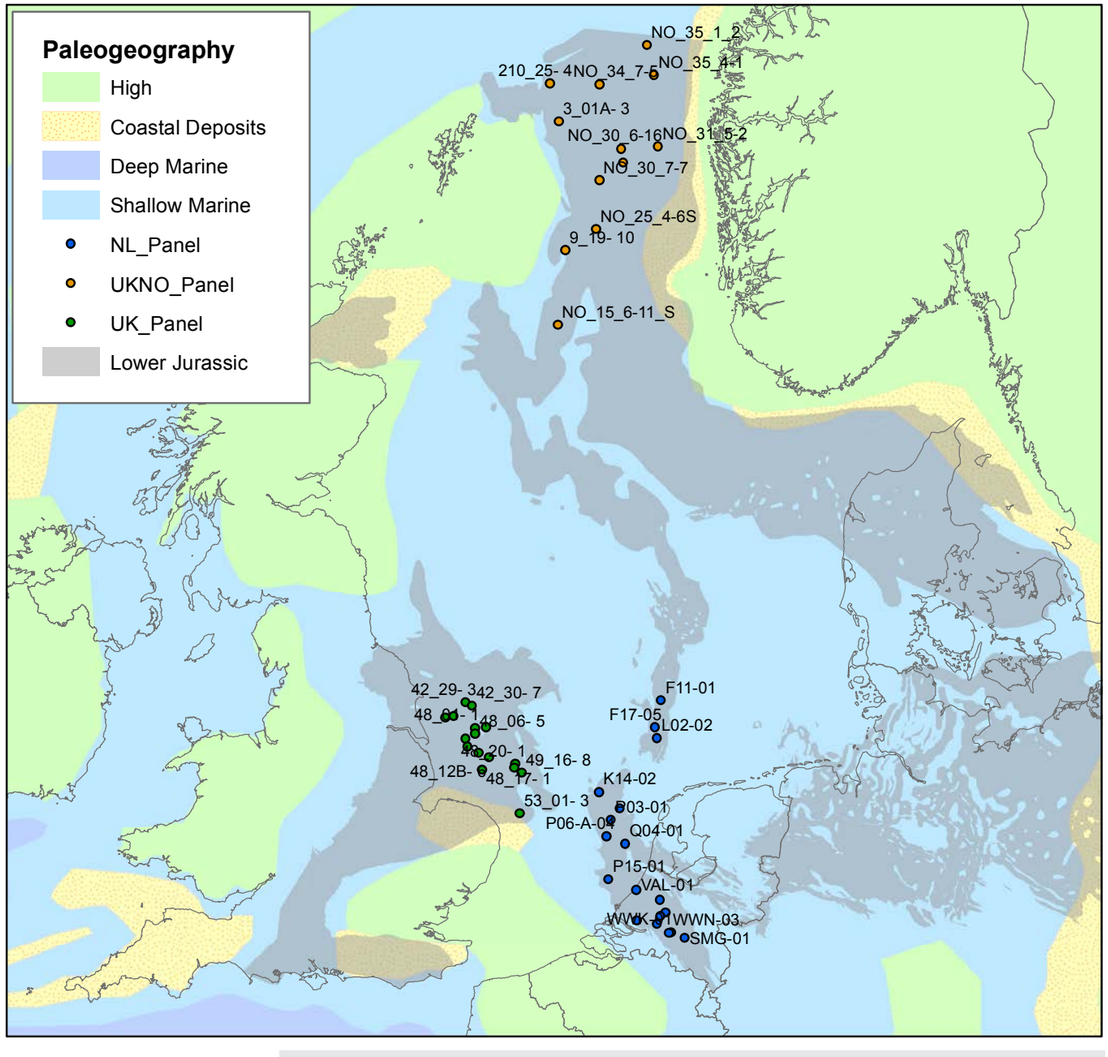

▲ Figure 5.1 Paleogeographical overview of the Lower Jurassic.
Grey: present-day extent of the Lower Jurassic sediments (compiled from Evans et al. 2003 and Doornenbal & Stevenson, 2010), Dots: wells included in the log study.

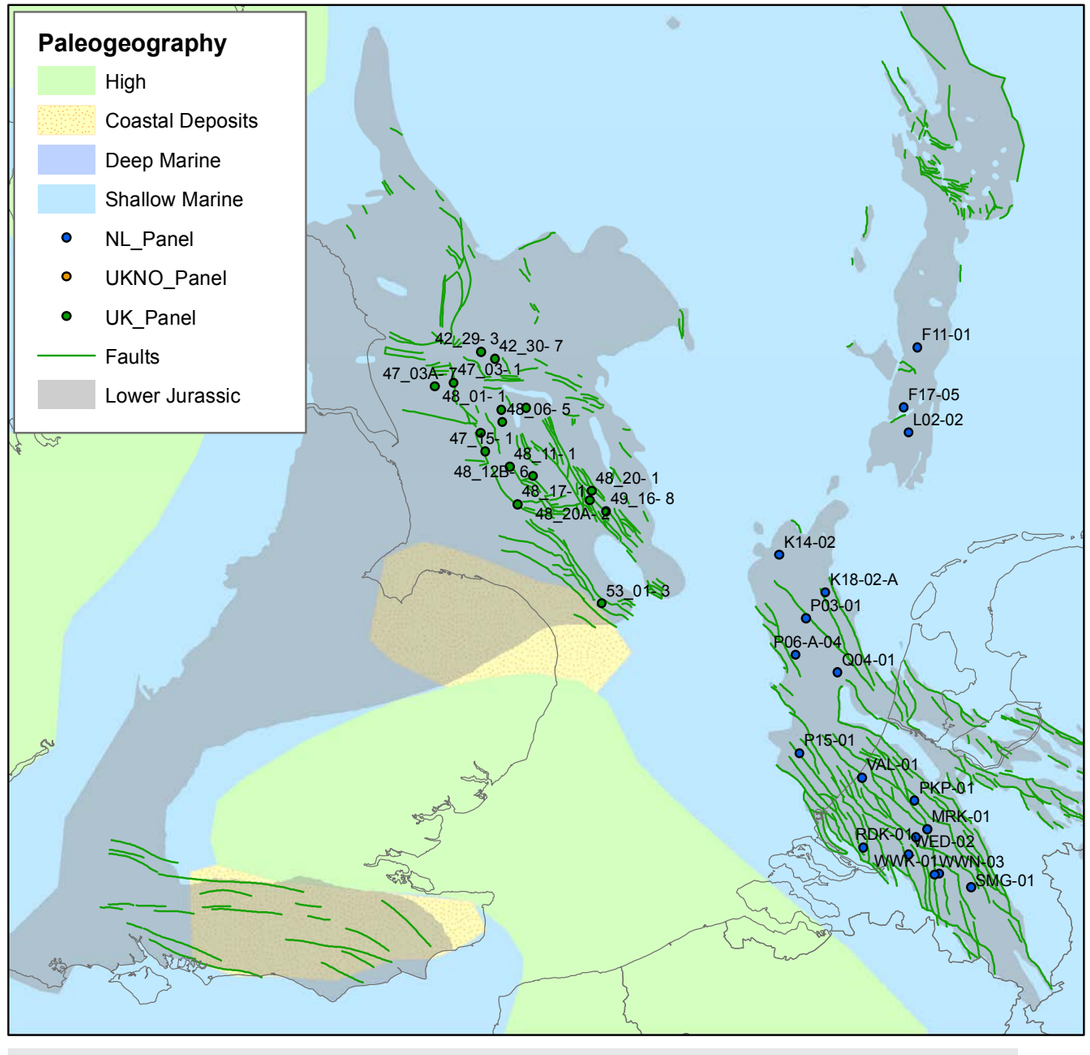

▲ Figure 5.2 Detailed view of the paleogeography of the Lower Jurassic in the Southern North Sea area.
Grey: present-day extent of the Lower Jurassic sediments, Green: Major faults of the Jurassic (compiled from Doornenbal & Stevenson, 2010), Dots: wells included in the log study.

– intermediate GR and DT) and sand or carbonate streaks (yellow – low GR and DT). In general, organic rich intervals can be related to a very high GR response related to a high uranium content in the organic matter.
For the correlation existing stratigraphic well markers were used as much as possible. For the UK part of the southern North Sea these stratigraphic markers were retrieved from the website of the UK Oil and Gas Authority (OGA)[1]. On this website, the stratigraphic information as reported by the operators is collected for all offshore wells. The level of detail of these stratigraphic markers differed significantly.

For some wells only the base and the top of the Jurassic succession was available while in other cases a more detailed chronostratigraphic subdivision into Hettangian, Sinemurian, Pliensbachian and Toarcian (JH, JS, JE and JT respectively) was given. In addition to this, the offshore lithostratigraphic subdivision (Penda, Offa, Ida and Cerdic Formation) as published by Lott & Knox (1994) was used for the correlations (see **Figure 5.3** for an example).
For the Netherlands on- and offshore wells (see **Figure 5.4** for an example), the stratigraphic well markers as published on the Dutch Oil and Gas Portal (NLOG)[2], supplemented with detailed log correlation markers for the Posidonia Shale Formation from previous TNO-projects (e.g., Nelskamp et al., 2015) were used.

The stratigraphic well markers for the UK-sector in the the correlation were supplied by Statoil together with the logs or taken from the website of the Norwegian Petroleum Directorate[3]. northern North Sea are also taken from the website of the OGA. In this case however the lithostratigraphic subdivision (Drake, Cook, Burton, Amundsen, Nansen and Statfjord Formation) was used for the correlations as these are more readily correlatable to the Norwegian lithostratigraphic markers. The Norwegian lithostratigraphic markers used for the correlation were supplied by Statoil together with the logs or taken from the website of the Norwegian Petroleum Directorate[3].

1 https://itportal.decc.gov.uk/information/well_data/bgs_tops/geological_tops/geological_tops.htm

2 http://www.nlog.nl

3 http://factpages.npd.no/

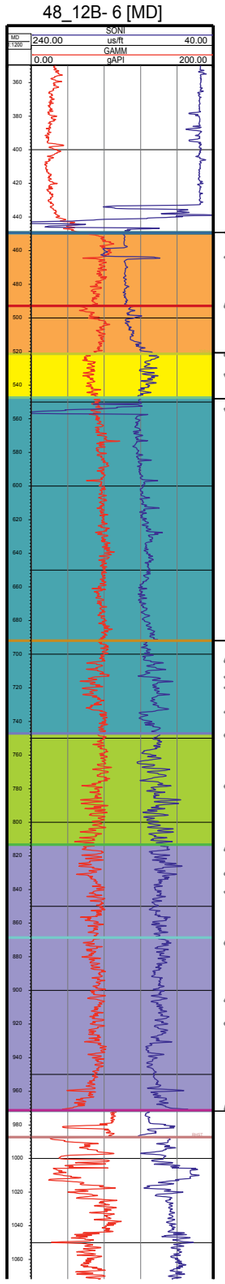

Log cyclicity	Liassic stratigraphy (Lott & Knox, 1994)	Log description and regional distribution
	Cerdic Formation	The log characteristics of the Cerdic Formation show a mudstone dominated sequence with clear limestone beds inbetween. The first limestone bed was interpreted as the Top Jet Dogger as seen in the onshore. Compared to the log expression of the Dutch equivalent, the Posidonia Shale Formation, the GR shows lower values.
	Ida Formation	The Ida Formation can be recognized on logs by its lower GR and lower Sonic expression. It can be traced throughout the whole southern NS.
	Offa Formation	The Offa Formation on logs is characterized by a very homogeneous GR and Sonic expression. It is described as a thinly bedded mudstone with interbedded argillaceous limestone. The Offa Formation can be identified throughout the whole southern North Sea study area.
	Penda Formation	The uppermost part of the Penda Formation is characterized by overall finer grained sediments with some calcareous or silicious intercalations. It is less cyclic and difficult to trace over longer distances.
		The middle part of the Penda Formation is characterized by very cyclic GR and Sonic log peaks that can be very well traced over a large part of the study area. This interval shows several longer fining and coarsening upwards cycles.
		The lowermost part of the Penda Formation is characterized by a very distinct transition from the high GR and high Sonic Rhaetian interval to low GR and Sonic values. Towards the northwest a clear cyclicity between high GR and high Sonic intervals related to mudstone dominated layers and low GR and low Sonic limestone beds can be seen. Towards the southeast the high GR mudstone intervals are less clearly visible.

▲ Figure 5.3 Example of a log interpretation from the southern UK North Sea area. Interpreted log marker (Pink – Pink, light blue – JH_Int, Green – Green, Purple – JS_Int, Orange – Orange, Light green – JE_Int, Yellow – Yellow, Red – Red, Blue – Top Lias), visible log cycles, lithostratigraphic interpretation and detailed log description.

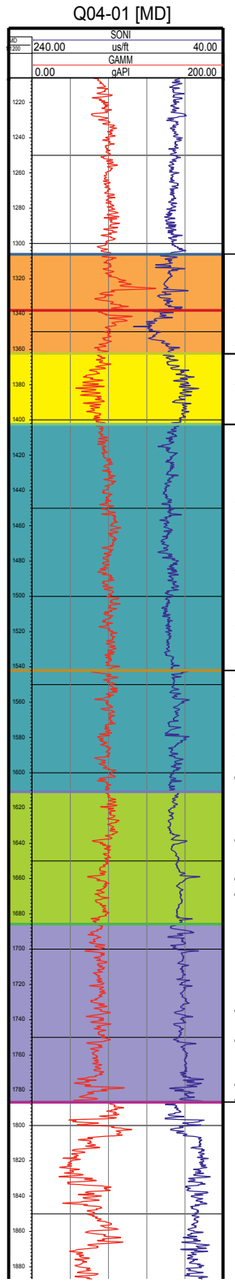

Log cyclicity	Liassic stratigraphy (Lott & Knox, 1994)	Dutch Nomenclator	Log description and regional distribution
	Cerdic Fm.	ATPO	The Posidonia Shale Formation has a very distinct log expression that can be traced throughout the Dutch on- and offshore. It shows very high GR values cyclically interbedded with carbonate rich layers. The red line marks the end of the CIE as based on isotope measurements.
	Ida Fm.		The upper Aalburg Fm. can be recognized on logs by its lower GR and Sonic expression. It can be traced throughout the whole southern NS. In the southern onshore area the characteristic coarsening is less visible.
	Offa Fm.	ATAL	The middle Aalburg Formation is the lateral equivalent of the UK Offa Formation. On logs it is characterized by a very homogeneous GR and Sonic expression. It is described as a thinly bedded mudstone with interbedded argillaceous limestone. The Offa Formation can be identified throughout the whole southern North Sea study area.
	Penda Fm.		The uppermost part of the lower Aalburg Formation is less cyclic and can only be identified in some wells in the Dutch part of the study area. It is characterized by mudstones with irregular silicious or calcareous layers.
			The middle section of the lower Aalburg Formation in the offshore is very similar to the UK while the onshore region shows clearer and longer cycles between mudstone dominated intervals and intervals with alternating mudstone and limestone layers.
			The very distinct transition from the Rhaetian interval into the lowermost Aalburg Formation can also be identified thoughout the Netherlands. The log signature is very similar to the UK, showing a clear cyclicity between mudstone and limestone beds. Some wells show a high GR and high Sonic signal in the mudstone intervals which could indicate a higher OM content.

▲ Figure 5.4 Example of a log interpretation from the Dutch North Sea area. Interpreted log marker (Pink – Pink, Green – Green, Purple – JS_Int, Orange – Orange, Light green – JE_Int, Yellow – Yellow, Red – Red, Blue – Top Lias), visible log cycles, lithostratigraphic interpretation and detailed log description.

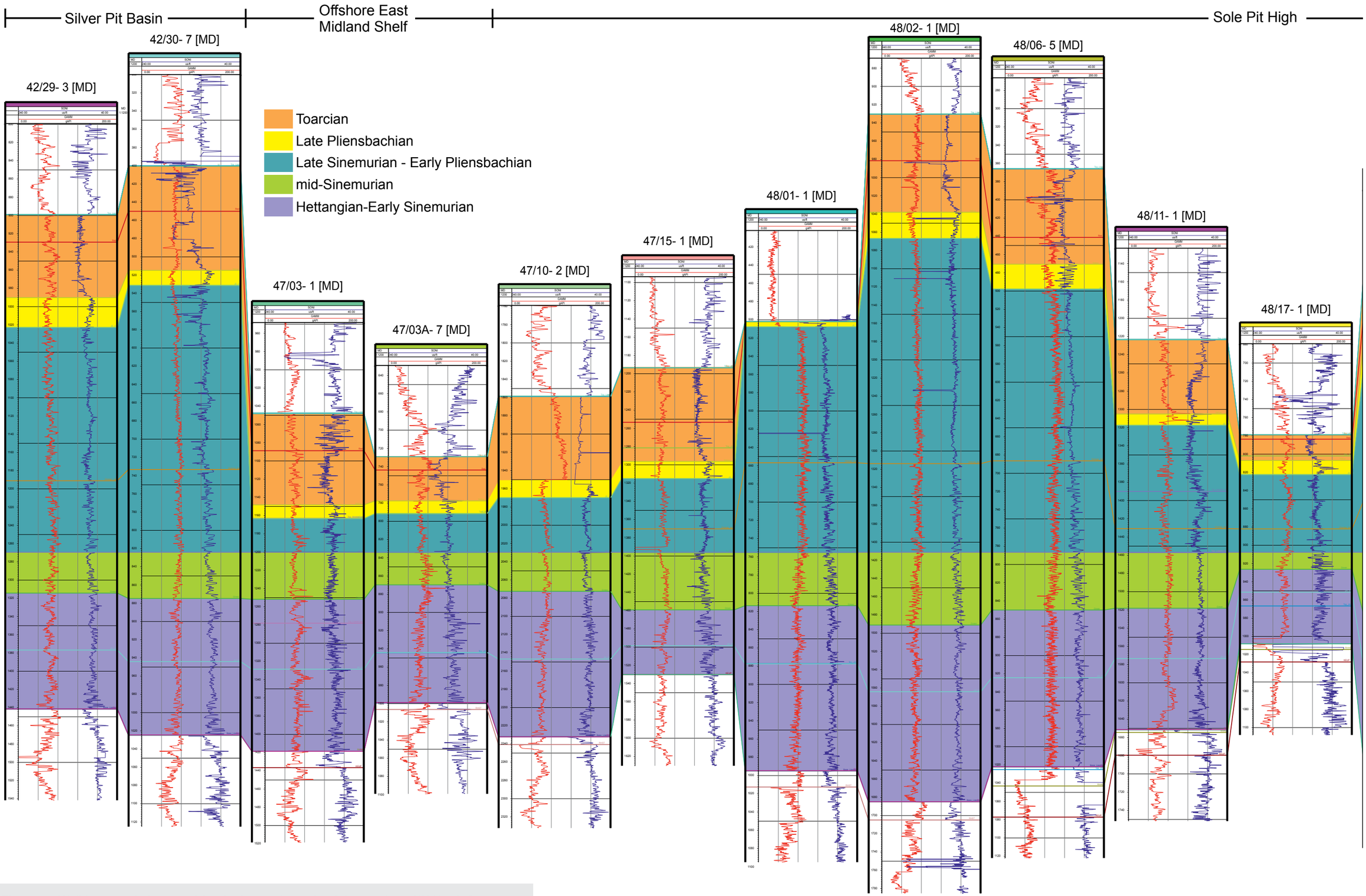

▲ Figure 5.5 Well log correlation panel for the Lower Jurassic of the southern UK North Sea area.
The location of the wells can be seen in Figure 5.2.

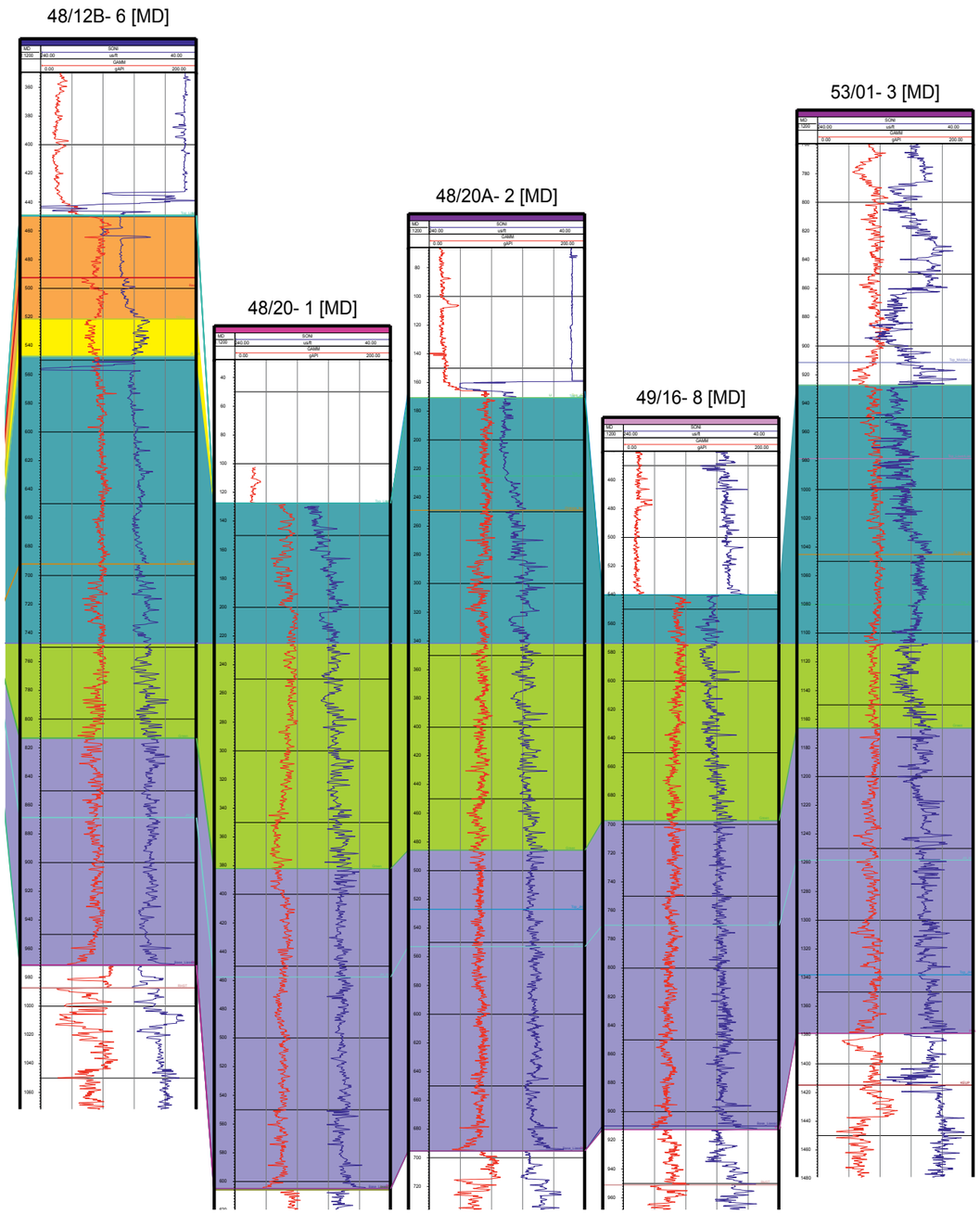

5.2 Regional correlation

Southern North Sea

The main focus of the regional correlation was put on the southern North Sea region. Here, we aimed to identify traceable markers in the Lower Jurassic and to identify regional differences in the log responses of the identified units. For this exercise the scheme depicted in **Table 5.1** was developed.

Especially in the lower part of the Lower Jurassic, the very cyclic nature of the logs and sedimentation resulted in well traceable log wiggles. The “green” marker as well as the “JS_Int” marker were identified in most logs. The reported marker JH showed significant variation whilst tracing the marker in the logs. It was attempted to include this marker in the correlation (JH_Int), but a successful and consistent correlation could not be achieved for all wells.

The log signature of the lowermost part of the Lower Jurassic shows the most regional variation. Closer to the UK onshore area, in UK blocks 42 and 47 (**Figure 5.1**) several clear cycles of (probably) carbonate banks interlayered with mudstones can be identified (see also **Figure 5.5**). Further offshore, in blocks 48 and 49 these cycles are replaced by an overall increase in sonic velocity and GR. A similar log response could be identified in the Dutch P blocks (**Figure 5.6**). In the Dutch onshore the log response was much more variable, showing highly cyclic GR and sonic intervals alternating with high GR, probably mudstone intervals.
According to the lithostratigraphic description of the offshore wells (Lott & Knox, 1994) the transition from the Penda Formation to the Offa Formation is marked by a change in GR log signature from a rather cyclic, wiggly response to a very homogeneous signature. This could be identified in several wells and was marked by the “orange” marker, situated between markers “JS_Int” and “JE_Int”. However in several wells this coincided with the interpreted Top Sinemurian (Top_JS, JS_Int) marker. According to Lott & Knox (1994) the Offa Formation is of Late Sinemurian to Early Pliensbachian age, suggesting that the Offa Formation should start below “Top_JS”. The log signature did not support that.

The lithostratigraphic formation that was best identifiable throughout the study area is the Middle to Late Pliensbachian Ida Formation. The Ida Formation can be recognized by first a gradual decrease in GR and an increase in sonic velocity and then a reversal of the pattern resulting in a sort of ball shaped log characteristic. In several wells up to three distinct cycles could be identified within the formation. The Ida Formation can be linked to the Staithes Sandstone and Cleveland Ironstone Formations, that were described in the Cleveland Basin onshore. It is described as thinly interbedded, brown to grey siltstones to fine sandstones and argillaceous limestone which are occasionally oolitic and carbonaceous (Lott & Knox, 1994). From a regional point of view, this formation could be traced throughout the study area. It is thickest in the Dutch Central Graben area and shows thinning on the Offshore East Midland Shelf and the more distal parts of the onshore West Netherlands Basin. In the southern part of the West Netherlands Basin and Roer Valley Graben the distinct log signature is less evident, suggesting an overall finer grained character compared to the offshore regions.

Above the Ida Formation lies the Cerdic Formation, which is the UK offshore analogue to the Dutch Posidonia Shale Formation. In the Dutch on- and offshore area the Posidonia Shale Formation has a very distinct log signature. It is characterized by several cycles of very high GR peaks and low sonic velocity and very low GR peaks with high sonic velocity. The low GR peaks also have low neutron porosities and high bulk densities and are interpreted as carbonate streaks or concretion layers. The high GR peaks coincide with high neutron porosities and low bulk density values together with high resistivity values. This is interpreted as high porosity and high TOC streaks. One very distinct low GR, high sonic velocity peak was correlated using stable organic carbon isotopes to the Top Jet Dogger carbonate layer of the UK onshore outcrops (PO4, **Figure 5.2**). In the UK offshore area this very distinct pattern of the Dutch Posidonia Shale Formation is less clear. The logs show an overall increase in GR values but do not reach as high values as in the Netherlands and the sonic velocity decreases as well compared to the underlying formations **Figure 5.1** and **5.5**). Locally a similar log pattern to the Dutch Posidonia Shale Formation could be observed (e.g., 47/03A-7) but the log signature is very variable. Most logs show one or more distinct low GR and high sonic velocity peaks (“red” marker). This was interpreted as the lateral equivalent of the PO4 horizon of the Dutch Posidonia Shale, making this the Top Jet Dogger.

The upper boundary of the Cerdic Formation is quite heterogeneous throughout the study area. This is partly related to an erosional unconformity, located between the early and middle Jurassic in the UK part of the study area and partly due to the deposition of the Late Toarcian Phillips Member. The Phillips Member is a silty to fine sandy unit that can only be found in rim synclinal structures and along fault zones and is lying conformably above the mudstones of the Cerdic Formation. In the Netherlands the Posidonia Shale Formation is either conformably overlain by the silty claystones of the Lower Werkendam Member or its upper boundary is formed by the Mid to Late Kimmerian Unconformity.

The log correlation showed an overall very homogeneous, layer-cake type of deposition during the whole of the Lower Jurassic. This was especially evident in the lower part of the Liassic (Hettangian to Lower Sinemurian) as well as during the Upper Pliensbachian to Toarcian. Differences in thickness can be related to either differential subsidence, intraformational hiatuses or availability of sediment.

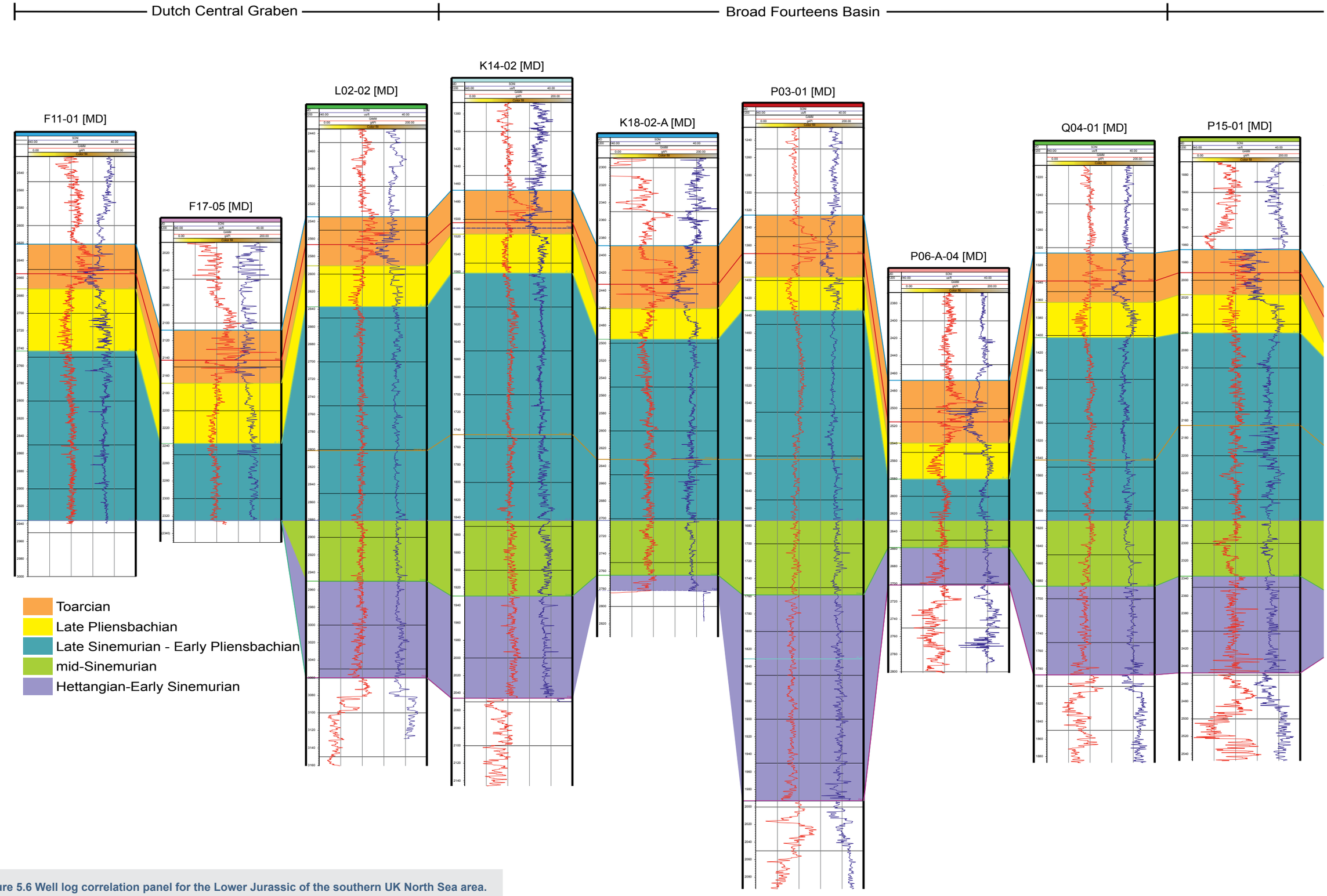

▲ Figure 5.6 Well log correlation panel for the Lower Jurassic of the southern UK North Sea area.
The location of the wells can be seen in Figure 5.2.

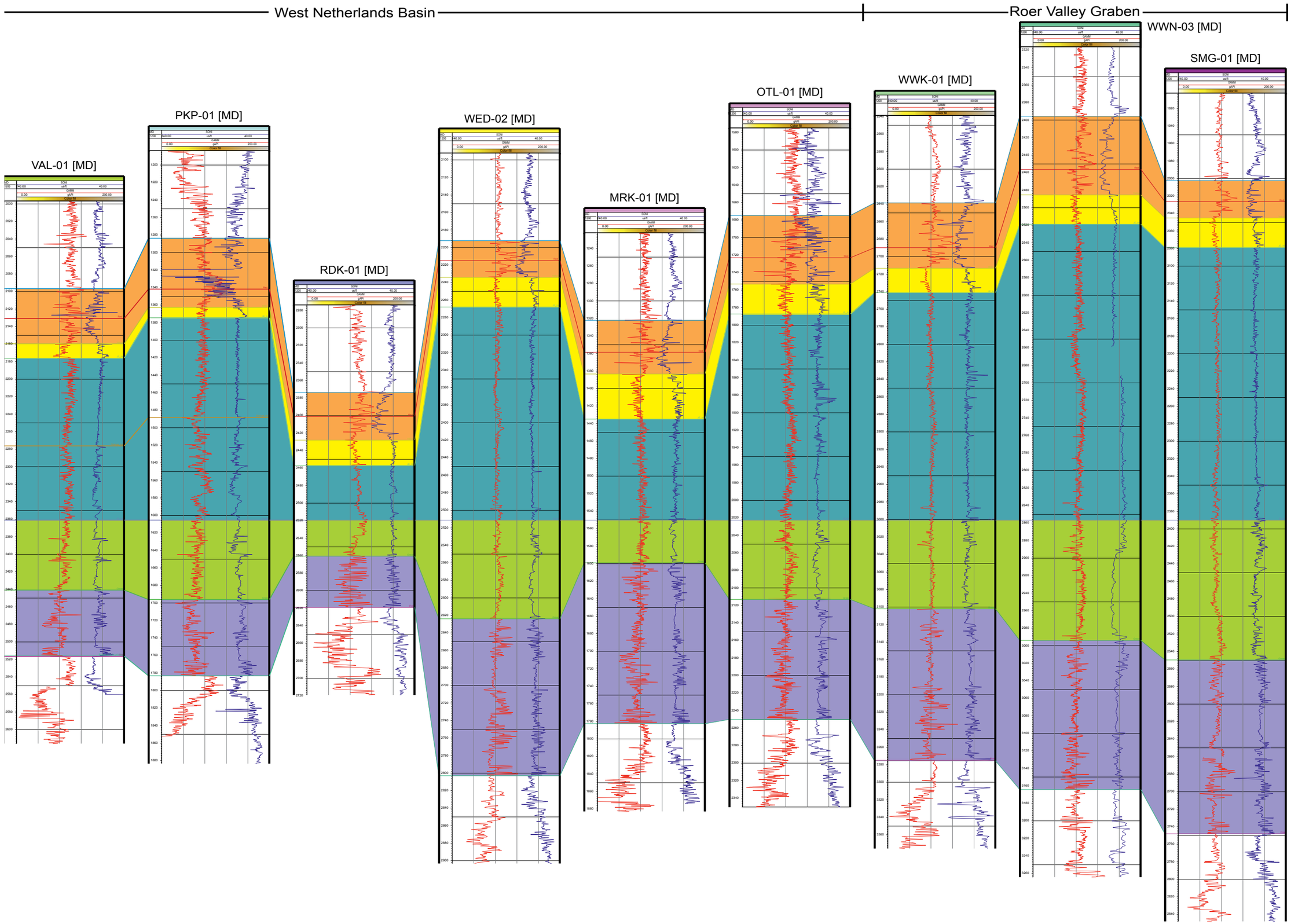
West Netherlands Basin
Roer Valley Graben
VAL-01 [MD]
PKP-01 [MD]
RDK-01 [MD]
WED-02 [MD]
MRK-01 [MD]
OTL-01 [MD]
WWK-01 [MD]
WWN-03 [MD]
SMG-01 [MD]

Northern North Sea and Viking Graben

Due to the already very detailed lithostratigraphic interpretation of the Lower Jurassic in the Northern North Sea region, no additional log correlation was performed. The main question in the northern North Sea and Viking Graben area was the regional expression of the Toarcian CIE event. The results of the isotope (chrono-)stratigraphy were compared with previous stratigraphic models for the studied wells and the general log characteristics were compared with the previously identified patterns from the southern North Sea.

The main focus of the study was on the Upper Pliensbachian to Lower Toarcian Cook Formation and the Middle to Upper Toarcian Drake Formation. In the Norwegian part the Cook Formation is described as a succession of relatively shallow marine deposits sourced from the eastern basin margin (Ager, 1975; Gage and Doré, 1986; Dreyer and Wiig, 1995; Marjanac and Steel, 1997, Folkestad et al. 2012). It can be subdivided into two units, a lower regressive and an upper transgressive unit. The lower unit is described as a tidal-fluvial delta situated on top of the marine mudstones of the underlying Burton Formation. It shows gradual shallowing upwards, coinciding with the gradual marine regression until it is capped by a maximum regression surface (Folkestad et al. 2012). The upper unit is described as a drowned delta top, transformed into a wave-dominated estuary.

In the UK area the Cook Formation is described as consisting of grey siltstones to silty mudstones with streaks of very fine grained well sorted sands that can constitute up to 20% of the formation (Richards et al., 1993). These deposits are interpreted to have been deposited under offshore marine conditions with prograding shelf sands, marine shoal sands or redeposited (turbidite) sands. No further subdivision into an upper and a lower unit was made.

The Middle to Upper Toarcian Drake Formation is a medium to dark grey silty marine mudstone which gets more sandy towards the top (Richards et al., 1993). In the Norwegian part it is described as interlayered with the Cook Sandstones.

The results of the stable carbon isotopes of two studied wells in the Viking Graben area (34/7-5 and 30/6-16) show that in both cases the CIE is located in the uppermost part of the Cook Formation (**Figure 5.7**). This is equivalent with the transgressive estuary unit that was described in block 34 (Folkestad et al. 2012). The log response for the CIE event in well 34/7-5 shows a gradual increase in GR towards the Drake Formation while in most other wells the boundary between the Cook and the Drake Formations is marked by a sharp increase in GR log response, marking the transition from more sandy/silty deposits to marine mudstones. The Cook Formation in the UK wells of blocks 3, 210 and 211 shows a much higher GR response, which is in agreement with the more mudstone dominated facies in this area. According to our interpretation we assume that the CIE event is also located in the upper part of the Cook Formation. Even though the logs in the UK show a mudstone dominated facies during the CIE event, the log response does not suggest high organic content. The log character of the overlying Drake Formation, on the other hand, shows high GR which could be interpreted to be related to high organic matter content. Additional isotope and TOC measurements on core material from these wells would be needed to confirm this. ■

▼ Figure 5.7 Log characteristics and locations of selected wells from the Northern UK North Sea and Norwegian Viking Graben.
The grey intervals mark the location of the T-OAE in the wells. Detailed view of the palaeogeographic map of the Lower Jurassic in the Northern North Sea area. Grey: Present-day extent of the Lower Jurassic sediments, Green: Major faults of the Jurassic (compiled from Evans et al., 2003).

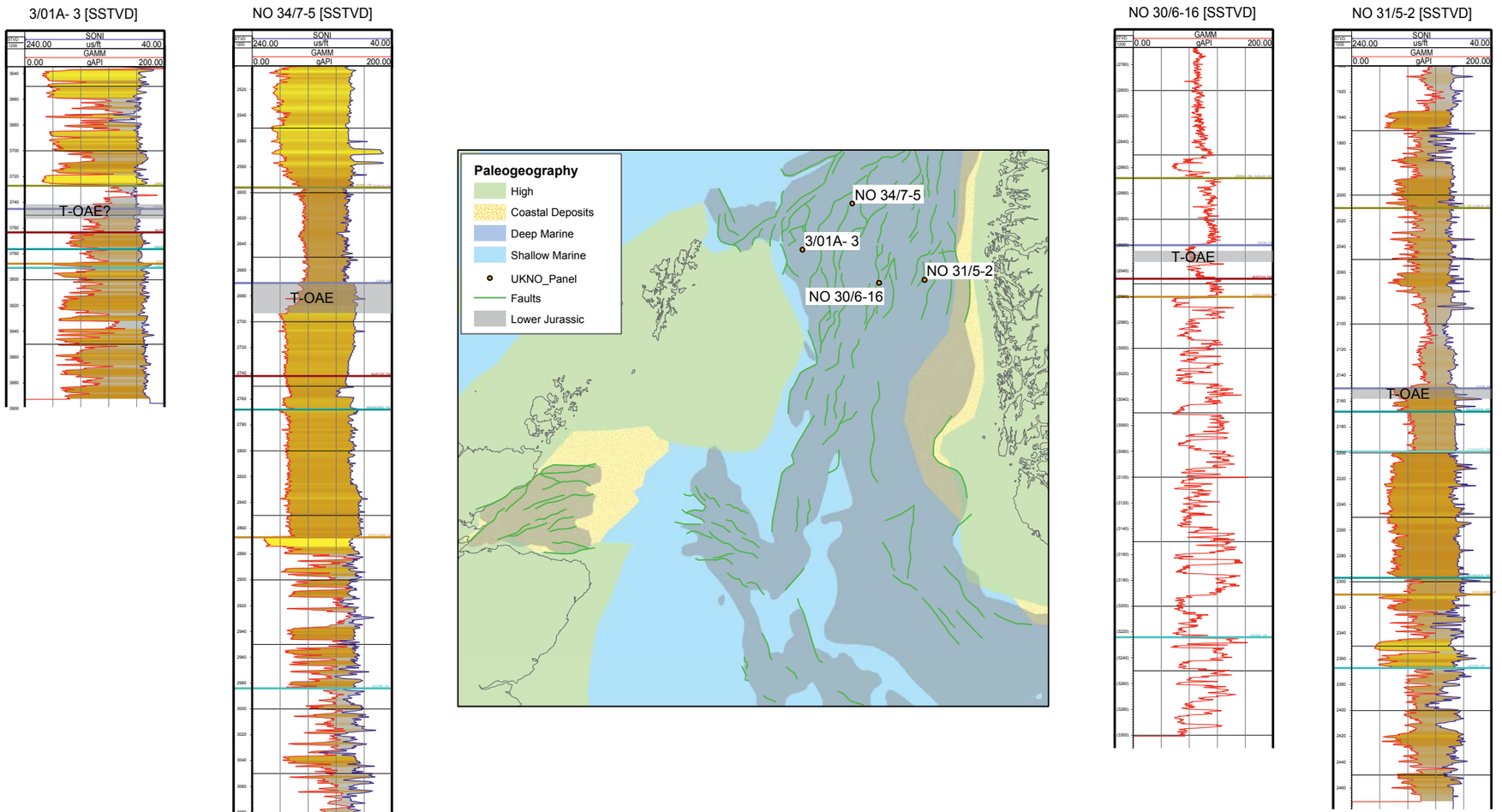

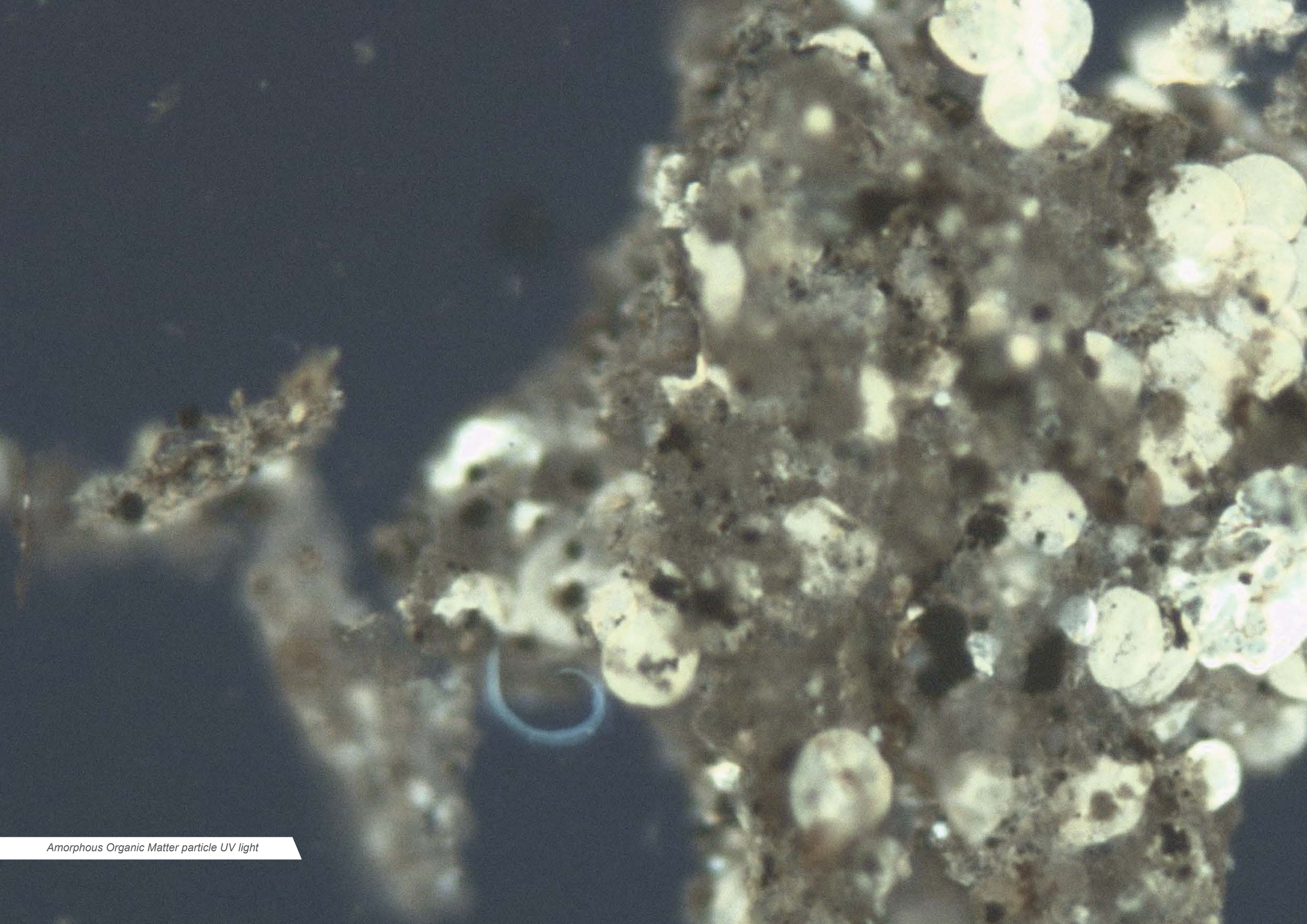

Amorphous Organic Matter particle UV light

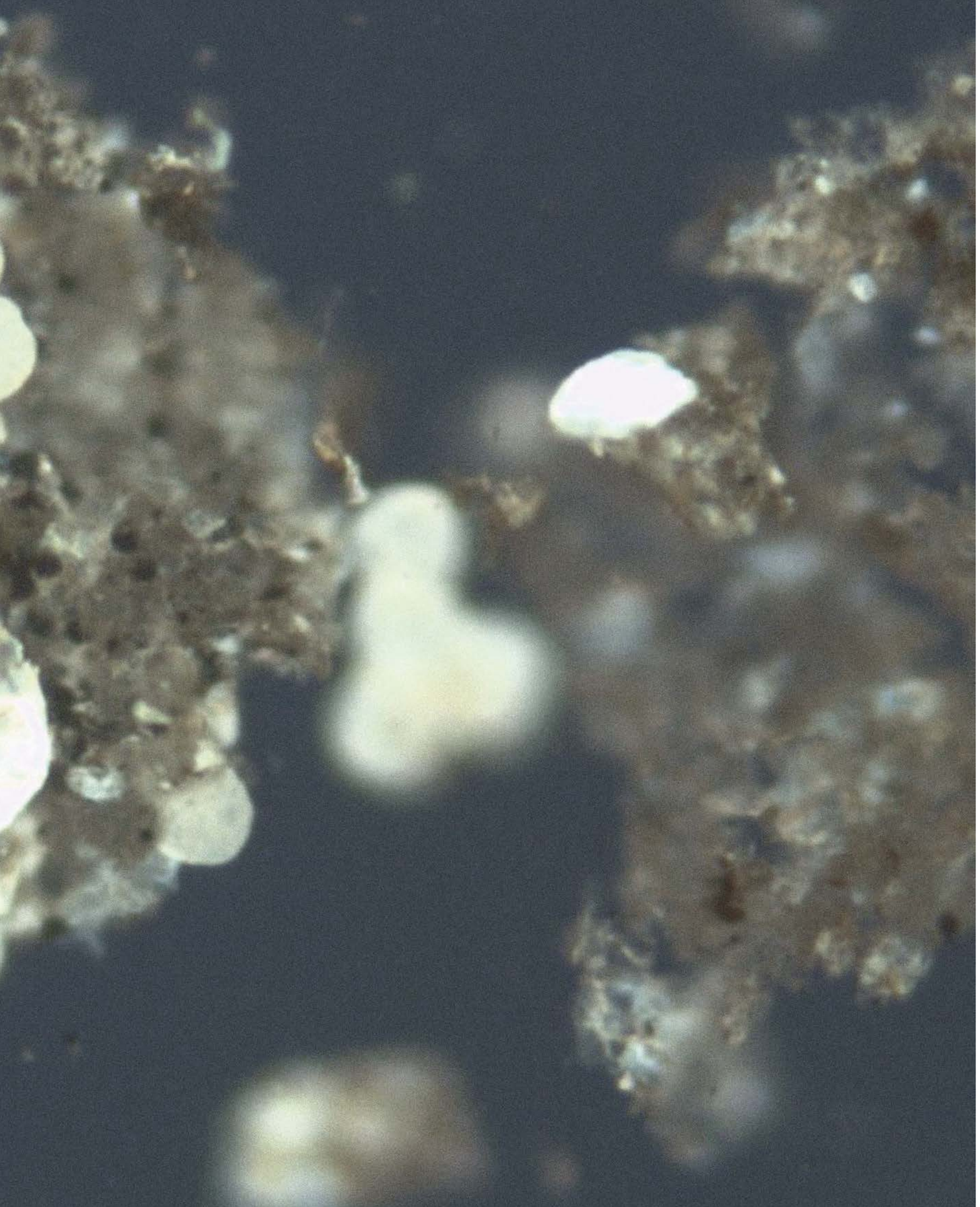

6. Paleoclimate

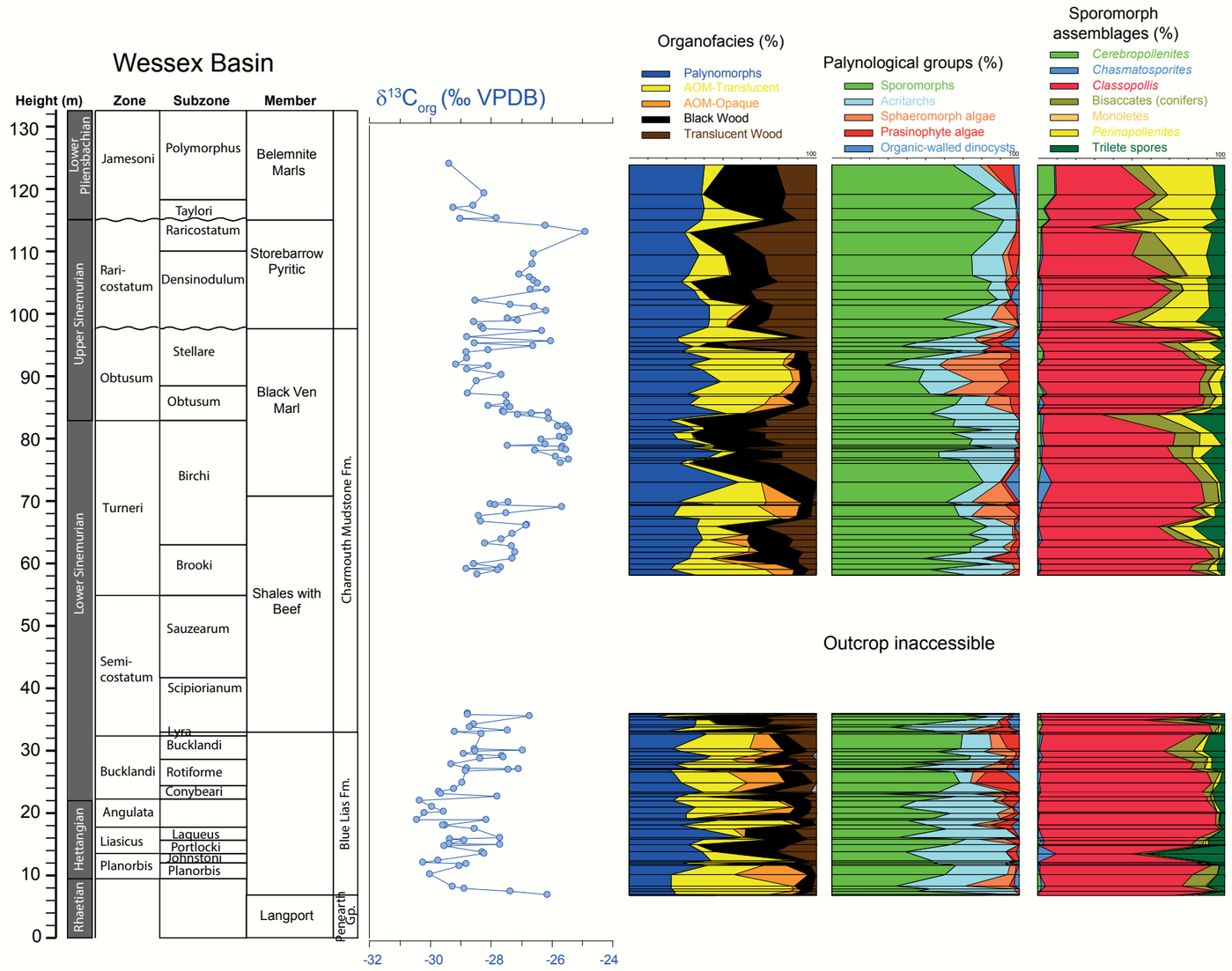

◄ Figure 6.1: Results of the organofacies and palynological study from the Dorset Coast succession.
The data are plotted alongside ammonite stratigraphy and carbon isotope data. The **left graph** reflects the composition of the organofacies assemblages and was constructed based on counts using UV-fluorescence. Clearly, from the base of the Blue Lias Fm. through the Hettangian and Lowermost Sinemurian (Pre-Planorbis beds to Scipionianum Ammonite Zone) there are relatively high frequency alterations between associations that are dominated by wood remains and Amorphous Organic Matter (AOM). The same holds true for the overlying Lower-Upper Sinemurian (Brooki Subzone to Raricostatum Subzone) interval, but these "cycles" become clearly more expanded.

The **middle graph** shows the closed-sum composition of the palynological assemblages (also identified using UV-fluorescence microscopy in order to prevent underestimating palynomorphs entrapped in AOM-clusters). Like the organofacies associations, the assemblages are also very cyclic in the lower part, with sporomorphs alternating with marine palynomorphs (predominantly acritarchs). In the intervals dominated by AOM, we note elevated abundances of prasinophyte algae. With dinoflagellate cysts being very scarce throughout the record, we assume the photic zone to have been predominantly anoxic. The relative abundance of terrestrial vs. marine palynomorphs is the result of the combined effects of changes in run-off and elevated marine productivity (see Chapter 8). However, the relative abundance of wood is considered to be indicative of the general relative sea-level baseline, because under relatively low-sea-level conditions wood is more easily transported to the site of deposition. We thus infer relative sea-level lowstands in the upper Birchi Subzone and in the Raricostatum Zone. The **right graph** shows the relative abundance of important sporomorph taxa. *Classopollis*, pollen of the gymnosperm plants of the Cheirolepidiaceaen Family are clearly dominant throughout. In intervals that are dominated by wood and higher loading of sporomorphs, trilete spores are more abundant. This is ascribed to increased fluvial influence (run-off). It takes up to the Upper Sinemurian Raricostatum Zone for *Perinopollenites* to become prominent as well. We interpret this to reflect a relative demise in monsoon intensity, possibly linked to climatic cooling in the Late Sinemurian.

In this chapter, the paleoclimatic and paleo-environmental evolution of the study area are discussed. To do so, we integrate palynological data generated from outcrops and cores with other proxies derived from literature. The stratigraphic and environmental interpretation of each record are discussed in their respective figure captions. The regional climatological and environmental trends are then discussed in chronological order.

6.1 Hettangian and Early Sinemurian

The section along the Dorset Coast (**Figure 6.1**) provides insight in the climate- and environmental evolution following directly upon the Triassic-Jurassic boundary (T/J-boundary). The boundary itself is known to have been accompanied by profound changes in both marine and terrestrial biota, leading to the recognition of the end-Triassic mass extinction event. The associated carbon cycle and $\delta^{13}C$ perturbation are attributed to volcanic emissions from the Central Atlantic Magmatic Province (CAMP, Lindstrom et al., 2015).

As also recognized in Denmark, Austria and Germany (Dybkjaer et al., 1991; Van de Schootbrugge et al., 2009; Bonis et al., 2010; Lindstrom et al., 2012), the T/J-boundary interval witnesses an increased influx of *Classopollis* pollen. These are related to the conifer plants of the Family of the Cheirolepidiaceae, which are predominantly occupying relatively arid and warm upland biomes (see e.g., Batten, 1974; Van Konijnburg-Van Cittert and Van den Burgh, 1996). This thus suggests the proliferation of a warm climate mode with a strong seasonal humidity contrast, specific for a strong monsoonal climate mode in the subtropical paleolatitudes of the study area.

We studied Hettangian - Early Sinemurian deposits from core Oldenzaal-4 in the Netherlands (see **Figure 6.2**). Here *Classopollis* is also dominant in the Hettangian part of the succession, with the exception of the fern spore dominated sample just above the T/J-boundary and its characteristic $\delta^{13}C$-excursion. The few samples we have investigated from the Hettangian - Early Sinemurian Statfjord Fm. from the Viking Graben area are also dominated by *Classopollis* (see also Hubbard and Boulter, 2000; Nystuen et al., 2014).

The dominance of *Classopollis* in the lowermost part of the Lower Jurassic in the entire study area is ascribed to the prevalence of a warm and arid continental climate mode. Warming across the T/J-boundary (McElwain et al., 1999; Korte et al., 2009) was likely partly induced and subsequently sustained by CO_2-input in assocation with CAMP-volcanism (see also Bonis et al., 2010; Ruhl et al., 2011). Under these warm climatic conditions, the degree of run-off into the basin was likely (seasonally) high and variable on Milankovitch scales.

In the Dorset Coast succession, the dominance of *Classopollis* persists up to the top of the Obtusum Ammonite Zone (earliest Late Sinemurian). The records from the Netherlands and the Viking Graben area support this persistence throughout the Early Sinemurian.

In theory, the oxygen isotopic composition ($\delta^{18}O$) of biogenic calcite (e.g., oysters or belemnites) may provide a means to assess temperature change in the Mesozoic. In reality, data-coverage is often sparse and the effects of diagenetic alterations and local salinity change profound. Nevertheless, there are the data compilations of Jenkyns et al. (2002) and Dera et al. (2011) that we can use to infer general trends in temperature development. These records reveal a predominance of light (warm) values in the

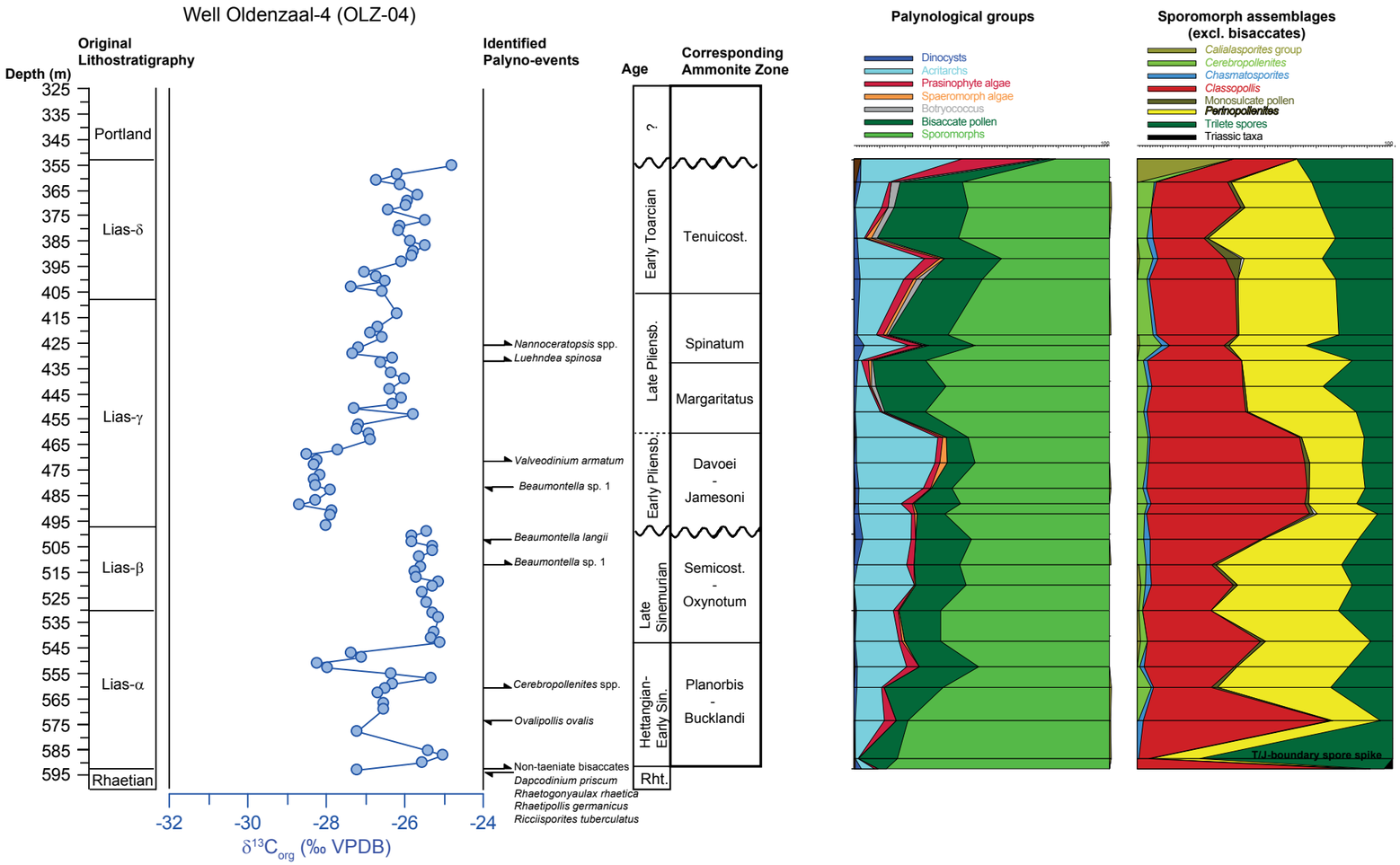

◄ Figure 6.2: Palynological and $\delta^{13}C_{org}$-data from the cored section from well Oldenzaal-4 (OLZ-4) in the eastern Netherlands.
This well was drilled by the Bataafse Petroleum Maatschappij in the 1940s. The original German subdivision of the Lias is shown based on the original well report. By integrating the $\delta^{13}C_{org}$-data with palynological events an updated stratigraphic interpretation was achieved. The basal sample is clearly of Rhaetian age. The cyclical nature of the $\delta^{13}C_{org}$-curve together with the first occurrence of *Cerebropollenites* and the extinction of *Ovalipollis ovalis* suggest an Hettangian age for the lower 40 m of succession. The shift towards more positive $\delta^{13}C_{org}$-values and subsequent extinction of *Beaumontella langii* at ~500 m depth suggest a Upper Sinnemurian sequence between 500 and 540 m depth. The abrupt shift to negative $\delta^{13}C_{org}$-values suggests the presence of a fault or hiatus at 498 m depth. Above this, the $\delta^{13}C_{org}$-values are substantially lighter. We therefore intepret the Sinemurian-Pliensbachian boundary to be within this missing part of section. The extinction of *Beaumontella* sp.1 and the appearance of *Valvaeodinium armatum* suggest a Lower Pliensbachian succession up to ~460 m depth. The positive shift in $\delta^{13}C_{org}$-values recorded at this level is characteristic for the shift into the Late Pliensbachian. The appearance of the dinocyst *Luehndea spinosa* at ~430 m depth indicates a late(st) Pliensbachian age, corresponding to the Spinatum Zone. This is in-line with the successive appearance of *Nannoceratopsis*. A lowermost Toarcian succession is inferred above, however the T-OAE is not recovered in the core. The palynological analyses are shown in the **right graph** and reveal a depositional setting that remains shallow marine throughout. Note that organofacies associations are persistently dominated by wood an palynomorphs and therefore not separately quantitatively analyzed. Acritarchs are persistently present. Organic-walled dinoflagellates and prasinophyte algae are only marginally present. In the Hettangian-Early Sinemurian, prasinophytes are somewhat more abundant, possibly reflecting a higher degree of stratification. Relatively high marine influence is recorded in the Early Pliensbachian, followed by a transition to more continental influence in the Late Pliensbachian. *Botryococcus*, indicative of brackish water conditions is also present n the Upper Pliensbachian. A two-fold increase in marine influence in the Earliest Toarcian reflect two widely recognized transgressions. Apart from bisaccate pollen, which are not taken into consideration due to long-distance transport, the terrestrial palynological assemblages comprise varying proportions of *Classopollis, Perinopollenites* and psilatrilete spores. The increase in spores just above the T/J-boundary is the regionally recognized fern spike accompanying the T/J-extinction (Van de Schootbrugge et al., 2009). *Classopollis* is particularly dominant in the Hettangian and Early Pliensbachian. *Perinopollenites* is more prominent in the remainder of the succession.

Hettangian and Early Sinemurian compared to the Upper Sinemurian.

6.2 Late Sinemurian

The Late Sinemurian climate appears to have been relatively cool. This is examplified by decreasing proportions of *Classopollis* in favour of *Perinopollenites*. The few datapoints available from this interval, indeed indicate heavier $\delta^{18}O$-values, particularly in the Raricostatum Ammonite Zone, just before the S/P-boundary carbon isotope shift (see Korte and Hesselbo, 2011). By some authors it has been suggested that these relatively cooler climate conditions relate to a deminishment of the rate of CO_2-outgassing associated with CAMP-volcanism (Knight et al., 2004). This is also in-line with the general trend to heavier $\delta^{13}C_{org}$-values (see Chapter 5). The Late Sinemurian was a period of relatively lower sea-level compared to the underlying and overlying intervals. This is manifested by the high degree of terrugineous organic-matter and hiatuses in the Wessex Basin succession and the relatively shallow depositional setting of the Siliceous Shale Mb. in Cleveland Basin.

6.3 Early Pliensbachian

The negative carbon isotope shift across the Sinemurian - Pliensbachian boundary is accompanied by a change to warmer climate conditions than in the Late Pliensbachian. The boundary is also manifested by a rise in relative sea-level, as indicated by the transition to the finer-grained and dysoxic Pyritous Shale Mb. in the Cleveland Basin and the deeper marine Belemnite Marls in the Wessex Basin. Terrestrial palynomorph associations comprise abundant *Classopollis*, particularly in the upper Jamesoni and Ibex Ammonite Zones. Also, seawater strontium isotope ($^{87}Sr/^{86}Sr$) data show relatively stable values in the Jamesoni and Ibex Zones (Ruhl et al., 2016). It is possibly linked to a late phase of CAMP-volcanism that induced enhanced global weathering of continental crustal materials, leading to an elevated radiogenic strontium flux to the global ocean (Ruhl et al., 2016). The Lower Pliensbachian has relatively high coverage of belemnite-based $\delta^{18}O$-analyses; these indicate relatively light (warm) for the Jamesoni and Ibex Zones (see e.g., Korte and Hesselbo, 2011). The younger Ammonite Zone of the Early Pliensbachian, the Davoei Zone in contrast marks the onset of a gradual cooling. In the Cleveland Basin, it marks the onset of the Staithes Sandstone Fm. It however seems unlikely that this coarsening is purely related to eustatic sea-level fall, as very proximal deposits lacking coarse clastics like Cleveland Ironstone Fm. overly the Staithes Sandstone. In contrast, the regional extent of this coarsening in basins fringing the Mid North Sea High, suggests a possible link with a phase of local uplift (see also Chapter 5).

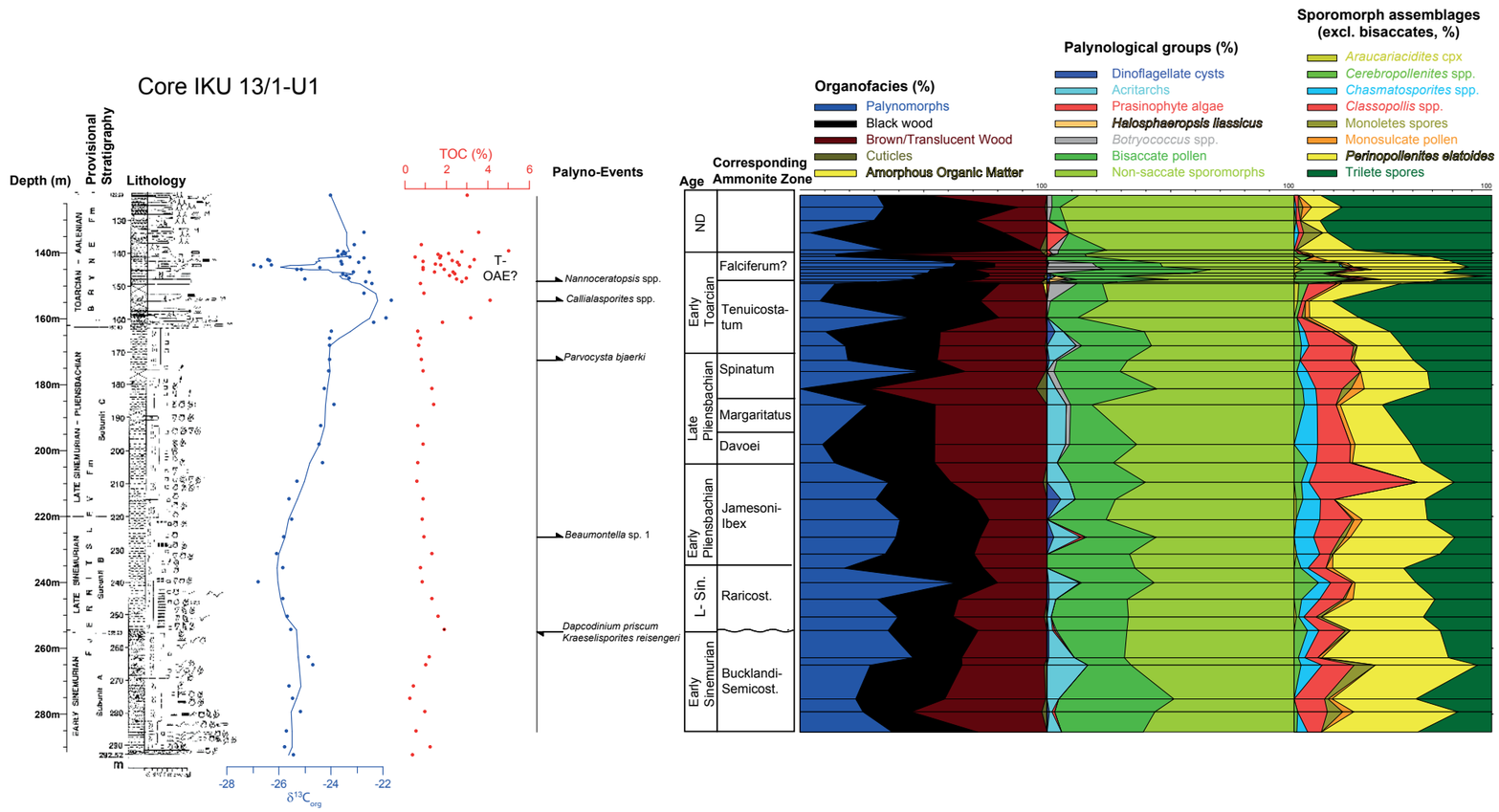

▲ Figure 6.3: Organofacies, palynological and $\delta^{13}C_{org}$- and TOC-data from the 13/1-U1 drillcore in the Farsund Basin (Norway). This well was drilled by the IKU-Sintef Gruppen in 1988. The lithostratigraphy, lithology and original age-assignments after the initial report (Smelror et al., 1989) are shown on the left. By integrating the $\delta^{13}C_{org}$-data with palynological events, an updated stratigraphic interpretation was achieved. Note that organic-walled dinoflagellates are only rarely recorded, hampering more detailed age-assessments. However, Smelror et al. (1989) have identified numerous macrofossils, allowing them to link to the ammonite zonations. The basal part of the succession below 255 m comprises a typical Sinemurian association, without any Hettangian or Rhaetian markers. *Dapcodinium priscum* is occasionally recorded, which ties this interval to the Early Sinemurian, based on the distribution of this taxon in Denmark (see Chapter 4). Based on lithological evidence for an erosive surface we infer a (minor) hiatus at this level (Smelror et al., 1989). From the LO of *Beaumontella* sp. 1 and a gentle negative shift in the $\delta^{13}C_{org}$-record we infer a Lower Pliensbachian succession up to ~205 m depth, where we note the inception of a positive trend in $\delta^{13}C_{org}$, characteristic for the Upper Pliensbachian. At ~172 m depth *Parvocysta bjaerki* first occurs, signalling the base of the Toarcian. Successively the FO of *Callialasporites* and *Nannoceratopsis gracilis* suggest an overlying Lower Toarcian succession. This would mean that the negative $\delta^{13}C_{org}$ may relate to the T-OAE in the Falciferum Zone. However, all these taxa are long-ranging and as a consequence the interval may also be as young as Aalenian as was inferred by the initial report (see Chapter 8 for more discussion).

The organofacies as shown in the **left graph** is dominated by wood and palynomorphs, AOM was virtually not recorded. The palynomorph assemblages (**middle graph**) are dominated sporomorphs with bisaccates being subordinate to non-saccates. Marine influence is very minor and comprising acritarchs and occasionally dinoflagellate cysts. The virtual absence of prasinophyte algae indicates oxygenated conditions throughout. Except for one sample at 147 m depth, the interval above 162 m depth is lacking indications for marine influence. Between 147 and 141 m we record abundant *Botryococcus*, indicating brackish-water conditions in a deltaic environment. This interval potentially corresponds to the T-OAE (see Chapter 8 for more discussion).

The hinterland vegetation (**right graph**) stands in marked contrast to the observations from the UK and the Netherlands, with *Perinopollenites* and trilete spores being dominant constituents. *Classopollis* is present throughout but only reaches abundant to dominant values in the Early Pliensbachian and Latest Pliensbachian. Combined with the overall lithological development, we infer a very shallow upper shoreface environment in the Early Sinemurian part (with scarce but persistent marine input), then a gentle deepening is reconstructed for the Late Sinemurian, based on an increase of palynomorphs at the expense of wood fragments and more frequent occurrences of dinoflagellate cysts. The overlying Upper Pliensbachian to Early Toarcian reflects progessively a more proximal environment, becoming deltaic in the Early Toarcian as manifested by the dominance of trilete spores. The interval with the negative $\delta^{13}C_{org}$-values stands out, with dominant *Perinopollenites* at the expense of trilete spores. Remarkably *Cerebropollenites* becomes abundant, we interpret this turnover to reflect a substantial intensification of the hydrological cycle.

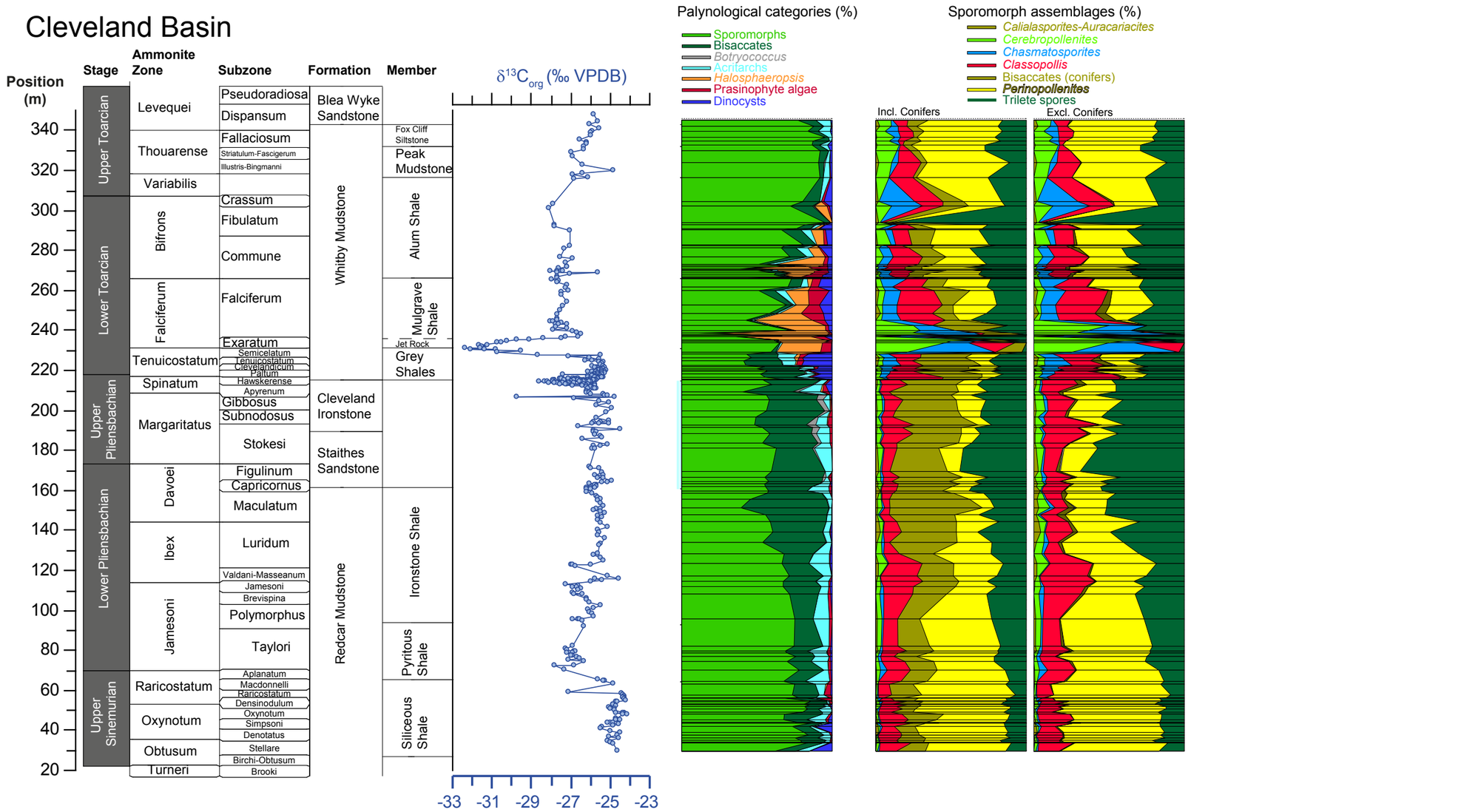

▲ Figure 6.4: Palynological and $\delta^{13}C_{org}$-data from the Cleveland Basin succession sampled in Yorkshire. The data are plotted alongside the local lithostratigraphic and ammonite zonations (after Hesselbo and Jenkyns, 1995 and Simms, 2004). We refrained from performing detailed oganofacies analyses because amorphous organic matter was only recorded abundantly in the Toarcian. The palynological assemblages are presented in the **left graph.** The oldest part of the record dates back to the Upper Sinemurian Obtusum and Oxynotum Zones corresponding to the Siliceous Shale Mb, where like the vast majority of the remaining record terrestrial elements are dominant. This implies that the depositional environment is substantially more proximal than that of the time-equivalent strata exposed along the Dorset Coast. Distinctive for the Late Sinemurian here is that organic-walled dinoflagellate cysts, primarily *Liasidium variabile* are abundantly found. Across the Sinemurian-Pliensbachian boundary, within the Pyritous Shale Mb., terrestrial elements remain dominant, however prasinophyte algae are now abundantly found as well, suggesting water-column stratification (see also Chapter 8). The negative carbon isotope shift, so characteristic for the S/P-boundary is marked by a minor increase in marine material (acritarchs and prasinophytes). The remainder of the Early Pliensbachian remains very stable in terms of palynological assemblages. Prasinophytes are absent in the Ironstone Shale Mb. (Upper Jamesoni to Davoei Zones). At the base of the Staithes Sandstone Fm. we note the appearance of *Botryococcus* signifying the incursion of brackish water conditions, these remain abundant through the Staithes Sandstone and Cleveland Ironstone Formations. With demising numbers of marine palynomorphs and considering first an increase in grain size (Staithes Sandstone Fm.) and subsequently a lagoonal depositional environment (Cleveland Ironstone Fm.), the early Late Pliensbachian is the most proximal depositional environment encountered in the record. This suggests a sustained minimum in terms of relative sea-level. Corresponding to the first isotope shift (the Spinatum-shift) we record the re-appearance of dinoflagellate cysts, these proliferate dramatically (both in terms of diversity, see Chapter 5) and in abudance throughout the Earliest Toarcian Tenuicostatum Zone. The Jet Rock unit of the Exaratum Subzone clearly marks a major deviation in palynological assemblage composition; *Halosphaeropsis jurassica* becomes overwhelmingly dominant thereby "wiping out" dinocysts and overwriting the background deposition of terrestrial elements. This phenomenon is ascribed to a combination of relative sea-level rise as well as run-off driven water mass stagnation during the T-OAE (Van de Schootbrugge et al., 2005; Houben et al., 2015) Albeit dinoflagellate cysts recover shortly after the T-OAE (in the Falciferum Subzone), *Halosphaeropsis* remains abundant, particularly in the Commune Subzone, indicating prevalence of seasonal water column stagnation (see Chapter 8). In the Late Toarcian (Variabilis to Levesquei Zones), the marine influence substantially deminishes again, signifying a relative sea-level drop.
The **two right graphs** indicate the terrestrial palynomorph assemblages, with- and without (transported) bisaccates respectively. Apart from trilete spores, *Perinopollenites* is generally dominant. *Classopollis* is more prominent in the Early Pliensbachian (Jamesoni Zone), in the Pliensbachian-Toarcian boundary interval, and after the T-OAE. These abundance optima are interpreted to reflect phases of warmer climate. Remarkably however, during the T-OAE and its immediate aftermath, dominant alterations between *Cerebropollenites* and *Chasmatosporites* are recorded. This somehow suggests a major perturbation of terrestrial climate during this events, likely related to enhanced precipitation.

6.4 Late Pliensbachian

The oldest part of the Late Pliensbachian (the Margaritatus Ammonite Zone) was the coolest phase of the Early Jurassic. Terrestrial palynomorph assemblages are dominated by *Perinopollenites*, suggesting diminished seasonal monsoon activity around the study area.
The depositional environments are consistently the shallowest and most proximal recorded as evidenced by the deposition of lagoonal oolitic ironstones in the Cleveland Basin, the overall dominance of sporomorphs over marine palynomorphs and consistent presence of *Botryococcus*. The most proximal setting is reached in the Gibbosus Ammonite Subzone. A belemnite $\delta^{18}O$-study from the Cleveland Basin (Korte and Hesselbo, 2011) indicates maximum values in the Gibbosus Subzone of the Margaritatus Zone, leading these authors to distinguish a so-called “Late Pliensbachian Cold Event”. Heavy carbon isotope values were reported for this interval by Jenkyns and Clayton (1986) based on bulk carbonate samples in Tethyan sections, and by Rosales et al. (2006) from belemnites from northern Spain. A late Pliensbachian influx of cooler water on the northwest European shelf can also be inferred from the migration of other Boreal faunal elements. Important ammonite families of Boreal descent, penetrated as far south as Morocco (Smith and Tipper 1986). Cooler and more saline surface water, a regressive trend, and the southward push of typical Boreal faunal elements all suggest glacio-eustatic control on sea level fall during the late Pliensbachian (Van de Schootbrugge et al., 2005).
The Latest Pliensbachian (Spinatum Zone) however stands in considerable contrast to the Margaritatus cold phase. The $\delta^{13}C_{org}$-data are characterized by a substantial negative shift leading up to an even more prominant negative excursion at the Pliensbachian-Toarcian-boundary (Littler et al., 2010; see also Chapter 5). $\delta^{18}O$-data also indicate climatic warming across the Spinatum Zone. Yet, the depositional environment in the Cleveland Basin remains very shallow as indicated by the fact that the main ironstone seams of the Cleveland Ironstone Fm. are occurring in this interval. This interval also witnesses the abrupt occurrence of dinoflagellate cysts, that were already widely abundant in the Tethys before that time (Bucefalo-Palliani and Riding 1999). This possibly suggests that part of this warming is ascribed to deepening of the Hispanic Corridor connecting the Southern North Sea Basin, bringing in warmer low-latitude derived water masses, locally. The absence of a clear vegetational response to warming is in-line with this hypothesis, as elevated abundances of *Classopollis* are not recorded in the Spinatum Zone.

6.5 Early Toarcian

The Cleveland Basin record (**Figure 6.4**) clearly exemplifies that the Early Toarcian was a period of major paleo-climatic and -environmental reorganisation. Initially, the basal Lower Toarcian (Paltum Subzone), marks a substantial

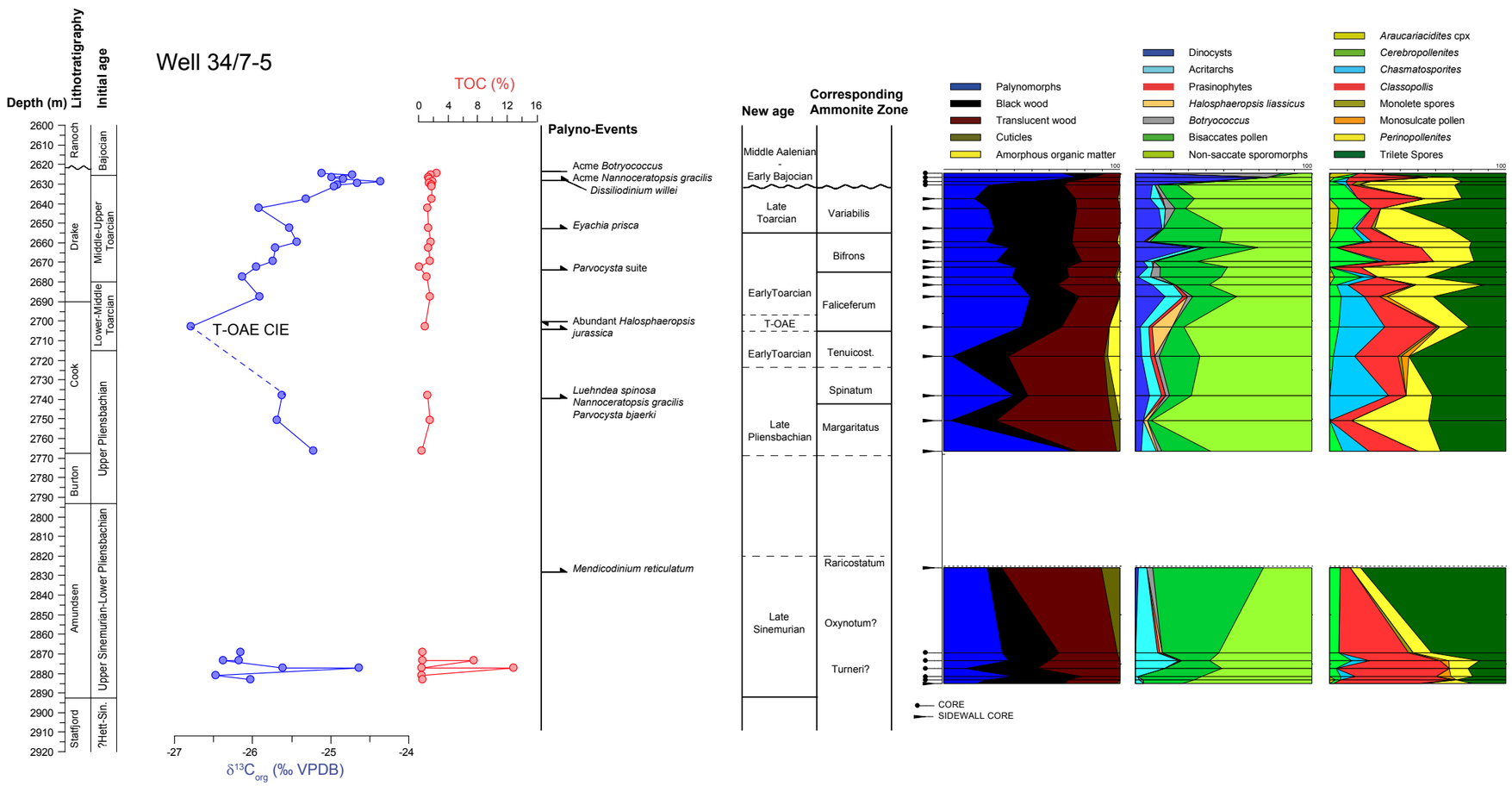

▲ Figure 6.5: Palynological and $\delta^{13}C_{org}$ and TOC-data from the well 34/7-5 in the Viking Graben area (N). The data shown in this graph are based on a combination of core and sidewall core samples. The initial litho- and chronostratigraphic interpretations are depicted at the left of the Figure. A basal cored section recovered material from the Amundsen Fm. sidewall core samples cover the Burton, Cook and Drake Formations. The top of the record, covering the transition from the Drake Fm. to Brent Group sediments are also covered in cores. The new palynological and carbon isotope results provide a refined chronostratigraphic interpretation. The samples from the Amundsen Fm. are difficult to gauge in age. The FO of *Mendicodinium reticulatum* at 2825 m depth indicates a Late Sinemurian age, with the absence of Liasidium variabile, likely corresponding to the Raricostatum Zone. At 2738 m depth we note the appearance of a relatively diversified dinocyst assemblage including *Parvocysta bjaerki, Nannoceratopsis gracilis* and *Luehndea spinosa*, specific for the Pliensbachian-Toarcian boundary interval. The overlying sidewall core sample is characterized by substantially more negative $\delta^{13}C_{org}$-values and abundant occurrences of *Halosphaeropsis jurassica***.** Hence, this level in the upper part of the Cook Fm. likely captures the T-OAE. Successively, we note a recovery towards higher $\delta^{13}C_{org}$-values. The FOs of a diversified *Parvocysta*-suite and *Eyachia prisca* are characteristic for a rather complete Upper Toarcian succession in the Drake Fm. Above the inferred top of the Drake Formation we note the characteristic euryhaline association with dominant *Botryococcus* and monotypic assemblages of *Nannoceratospis gracilis* characteristic for the Aalenian to Early Bajocian (Verreussel et al., 2008).

The organofacies (**left graph**) is dominated by wood and palynomorphs, the only exception being the Early Toarcian corresponding to the T-OAE, which also contains AOM. The palynological assemblages are depicted in the **middle graph**. The basal samples from the Amundsen Fm. core are dominated by sporomorphs with the marine fraction solely comprising acritarchs. Successively, the Late Pliensbachian and Toarcian remain marine throughout with abundant dinocysts. The supposed T-OAE equivalent sample comprises abundant *Halosphaeropsis liassicus*. The terrestrial palynomorph assemblages depicted in the **right graph** are dominated by *Classopollis* in the Late Sinemurian. By Pliensbachian-Toarcian times, a relatively diverse association comprising *Cerebropollenites*, *Chasmatosporites*, *Perinopollenites*, *Classopollis* and trilete spores was established. *Classopollis* and trilete spores are dominant. Above the T-OAE *Cerebropollenites* becomes more prominent.

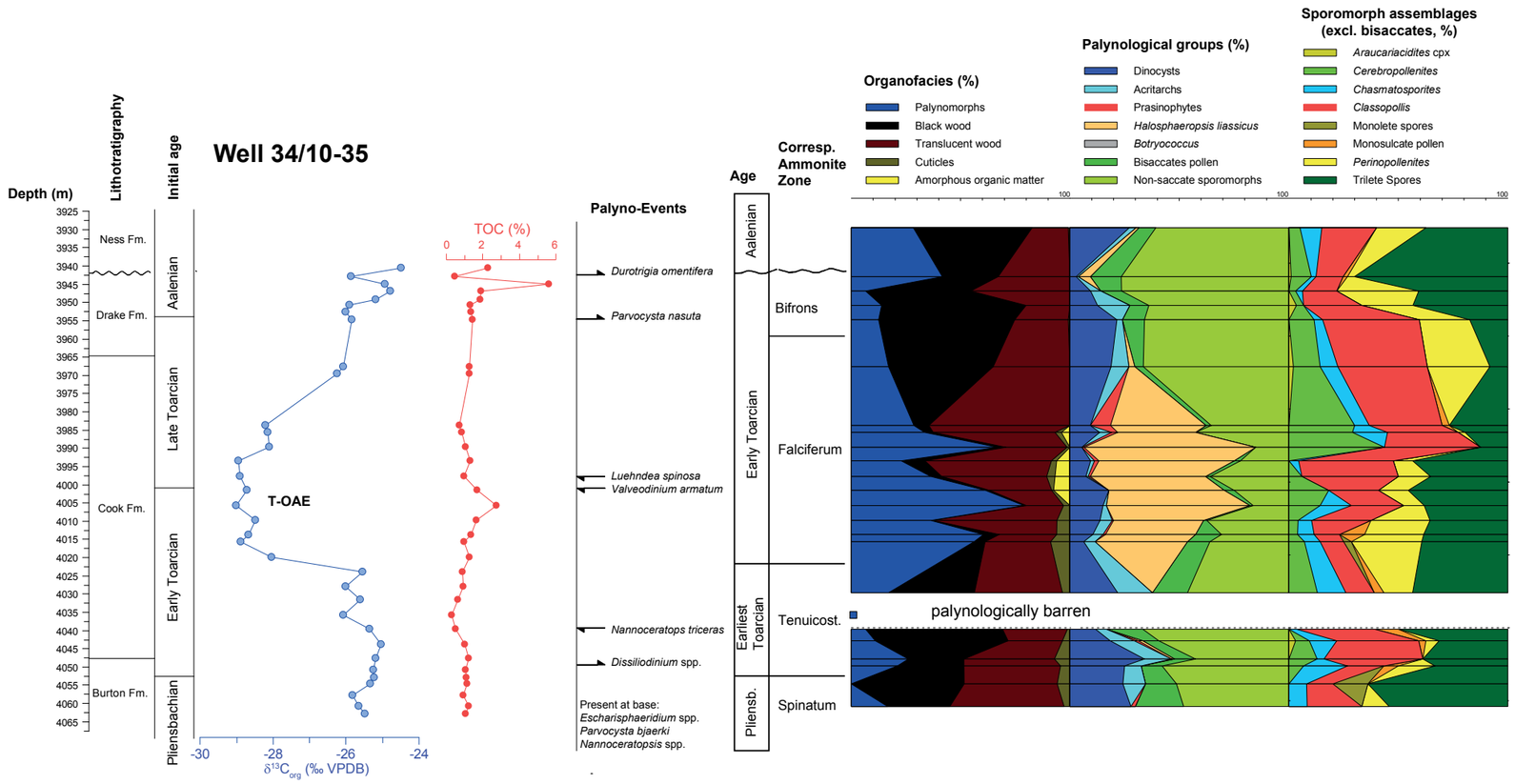

▲ Figure 6.6: Palynological and $\delta^{13}C_{org}$ and TOC-data from the core in well 34/10-35 in the Viking Graben area (N).
The new palynological and carbon isotope results provide a refined chronostratigraphic interpretation. The $\delta^{13}C_{org}$-record displays a conspicuous negative shift between 4015 and 3980 m depth, to be followed by a recovery to more positive values. At the base of the investigated interval we record *Parvocysta bjaerki* and *Nannoceratopsis gracilis*, signifying an approximating the Pliensbachian-Toarcian boundary interval (Spinatum Ammonite Zone). Remarkably, specimens resembling *Dissiliodinium* and *Escharisphaeridia* are also recorded in this lower part. In the Yorkshire section these appear somewhat later, well within the Tenuicostatum Zone. These taxa are precursors to the successively long-ranging gonyaulacean dinoflagellate lineage. Based on these patterns, their origination biome seems to be in the Arctic realm. This suggests that substantial water mass exchange across the Viking Corridor was established by latest Pliensbachian-earliest Toarcian times. In the interval capturing the T-OAE, dinoflagellate cysts remain abundant, so that the LO of *Luehndea spinosa* can indeed by tied to the actual Carbon Isotope Excursion (CIE). Even in this sandy facies of the Cook Formation the stratification indicator *Halosphaeropsis liassicus* becomes very abundant during the T-OAE. Above the inferred T-OAE interval we furthermore note the appearance of representatives of The *Parvocysta*-suite like *Parvocysta nasuta*, signifying a late Early Toarcian age for the basal Drake Fm. at this locality.
The organofacies results are dominated by wood and palynomorphs. Only in the T-OAE interval we note the presence of AOM. In terms of palynological assemblages, sporomorphs are dominant except during the T-OAE, when H*alosphaeropsis liassicus* is dominant. Dinocysts are consistently abundant, indicating consistent open marine conditions. Prior to the CIE, the sporomorph associations are generally dominated by trilete spores. *Classopollis* becomes more abundant just before the T-OAE in levels corresponding to the Tenuicostatum Zone. In association with the CIE, *Cerebropollenites* becomes transiently abundant. In strata corresponding to the Bifrons Zone, a mixed assemblage also consituting *Perinopollenites* is recovered.

transgression, leading to the deposition of open marine mudstones (Grey Shales Mb.) that boast well-diversified dinoflagellate cyst assemblages of predominant Tethyan origin. Concomitantly, increased abundance of *Classopollis* indicates climatic warming and intensified seasonal run-off patterns. Note that this phase corresponds to the transient P/T-boundary CIE.

Successively, up-section in the Tenuicostatum Subzone an additional origination phase pertains to the occurrence of 'young forms' like *Escharisphaeridia* and *Dissiliodinium.* These forms are also recorded in time-equivalent strata in the Viking Graben area (**Figure 6.5** and **6.6**). This new observation indicates increased connectivity with the Arctic realm, as similar forms are found in Arctic Siberia in the Late Pliensbachian (Zakharov et al., 2006).
In the entire Grey Shale Mb., we note the occasional occurence of sulphur bands; cm-thick pyritic shale horizons with elevated TOCs. These likely represent localized stratification events that lead to organic-matter enrichment. The T-OAE and its characteristic CIE corresponds to the Exaratum Subzone of the Falciferum Zone. In association with this event, we note an increase in the abundance of *Halosphaeropsis liassicus* along with acmes of other prasinophyte algae completely eliminating dinoflagellate cysts from the record. This is interpreted the consequence of the installation of strongly stratified, anoxic surface water conditions (see also Chapter 8). In the meantime the terrestrial palynomorphs become remarkably dominated by *Cerebropollenites* spp. and *Chasmatosporites* spp. replacing otherwise prevalent *Classopollis* or *Perinopollenites*-dominated floras. This indicates a major alteration of the terrestrial ecosystem, likely as a consequence of rapid CO_2-induced warming, increased seasonal run-off and subsequent hydro-ecological change. This perturbation of terrestrial climate and consequent marine stratification, is noted across the entire study area, e.g., in the Viking Graben area (**Figure 6.5** and **6.6**) and the Netherlands (Dutch Central Graben and West Netherlands Basin, Houben et al., 2015). These observations support the hypothesis that the T-OAE primarily represents a change in surface-water salinity, through increased run-off in response to rapid CO_2-induced warming, consequently leading to water column-stratification and increased productivity (see Chapter 8). In addition, it now seems that the Toarcian was paleogeographically preconditioned to stratify, because the influx of boreal low-salinity waters just predated the event. Also in the deltaic setting of the Farsund Basin, we find indications for a perturbation of the hydrological cycle during the T-OAE, leading to the deposition of *Botryococcus*-bearing overbank deposits (**Figure 6.3**).

It has been argued that the CO_2 of the T-OAE-perturbation stems from the volcanic degassing of organic-rich deposits in the Karoo Farrar Large Igneous Province (LIP, Svensen et al., 2007). In this light it is noteworthy that Early Toarcian warming lasted substantially beyond the CIE, as exemplified by the regional proliferation of *Classopollis* after the event until the Bifrons Zone. It seems likely that the emplacement of this LIP caused the overall and prolonged Early Toarcian warmth. However, it fails to explain the transient character of the CIEs associated with the T-OAE and the Pliensbachian-Sinemurian boundary. To explain these, additional mechanisms like the thermodynamic release of methane hydrates (Hesselbo et al, 2000; Kemp et al., (2005) need to be invoked.
Immediately after the T-OAE CIE, organic-walled dinoflagellate cysts return in abundance in the Cleveland Basin and in the Netherlands. Prasinophyte algae and *Halosphaeropsis liassicus* however remain abundant until the base of the Upper Toarcian. This indicates that dynamic oxic-anoxic environments persisted, likely varying on a seasonal scale. Note however that in the Viking Graben area, this stratification only affected the immediate CIE-interval (F**igure 6.5** and **6.6**). Overall, the results illustrate that the Early Toarcian marks both the effects of a longer term climatic warming that is interrupted by two so-called 'transients' at its base.

Possibly an additional event occurs in the lower part of the Bifrons Zone, where we note higher loadings of *Halosphaeropsis liassicus* and prasinophyte algae in the Cleveland. This level marks also the incursion of a diverse group of boreal dinoflagellate cyst taxa, the so-called *Parvocysta*-suite (see Chapter 5). This interval is not accompanied by a substantial negative CIE, but seems to also herald a response in the Viking Graben area (**Figure 6.3**).

6.6 Late Toarcian

The Late Toarcian marks a return to cooler climate conditions, *Perinopollenites* returns dominantly in the Cleveland Basin. Also the carbon isotope signature is characterized by a gradual shift towards more positive values. Progressively, the depositional environment also becomes shallower, culminating in the Blea Wyke Sandstone Fm. In many other areas the Upper Toarcian is absent and/or eroded as a combined consequence of Aalenian cooling and associated sea-level fall (Price, 2010) and progressive uplift of the Mid North Sea Dome (Korte et al., 2015).

6.7 Summary

Figure 6.8 shows a synthesis of the climatic evolution of the study area. To this end, we combined the δ^{13}C-curve and constructed an idealized relative sea-level curve based on the lithology and palynological trends recorded in the outcrop sections. The climatic information itself is inferred based on the trends in δ^{18}O-data as outlined in this chapter. The vegetation patterns from the studied successions are outlined by plotting the dominant sporomorph components. From this picture emerges the conclusion that there was a close correspondence between temperature and relative sea-level.

The Triassic-Jurassic boundary marks a phase of warming, likely driven by the inception of CAMP-volcanism and consequent rise in atmospheric CO_2-concentrations. This leads to widespread proliferation of *Classopollis*-dominated vegetation. Relative sea-level change during the Hettangian and Early Sinemurian is of relatively low amplitude. A clear drop in relative sea level is recorded in the late Early Sinemurian in association with a drop in temperature. This is also reflected in vegetation patterns that become dominated by *Perinopollenites*. We ascribe these opposing vegetation patterns to reflect warm conditions with a strong seasonal monsoon and cooler conditions with a weaker seasonal monsoon. The remainder of the Sinemurian is characterized by a relatively cool climate mode.
The Sinemurian-Pliensbachian boundary marks a shift to warmer conditions, and is similar to the T/J-boundary associated with a negative carbon isotope excursion. *Classopollis* proliferates again at many localities and sea-level rose substantially. The remainder of the Early Pliensbachian is relatively stable in terms of climate and sea-level up to the level of the Davoei Subzone. From this time onwards we note the deposition of sandy facies in the Cleveland Basin (Staithes Sandstone Fm.). This shoaling progresses throughout the Late Pliensbachian, leading to the deposition of the clastic-poor but very proximal and shallow Cleveland Ironstone Fm. in the Cleveland Basin. Palynological records from elsewhere in the study area also reflect more proximal depositional settings in the Late Pliensbachian. Based on δ^{18}O-data a Margaritatus

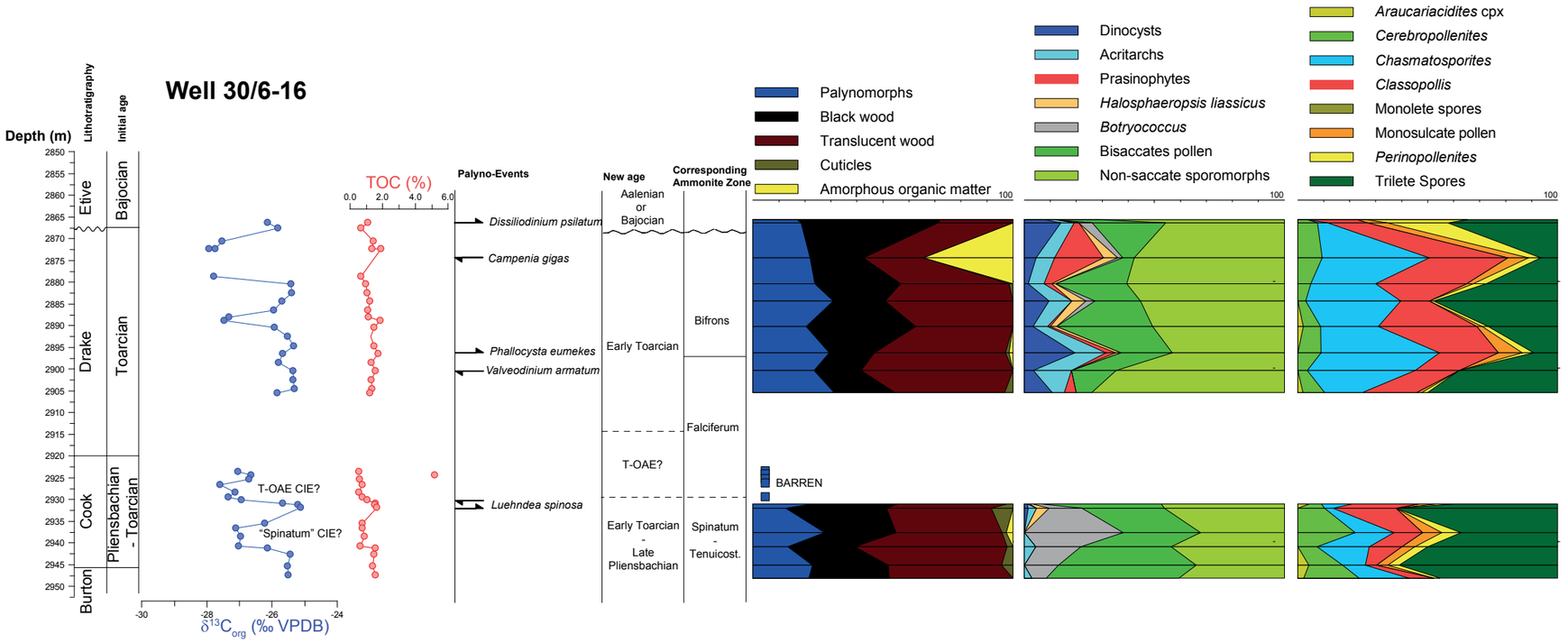

▲ Figure 6.7: Palynological and $\delta^{13}C_{org}$ and TOC-data from the cores in well 30/06-16 in the Viking Graben area (N). The samples corresponding to the upper part of the Cook Fm. are barren of palynomorphs. This is likely related to the fact that the sediments bear oil which consequently dissolved organic microfossils. The carbon isotope stratigraphy reveals a rather spiky pattern in the Cook Fm. These may possibly represent the “Spinatum Shift”, Pliensbachian-Toarcian Shift and/or the T-OAE CIE. . This would be in-line with the biostratigraphic results, especially since the basal samples lack organic-walled dinocysts, explaining the appearance of *Luehndea spinosa* this far up-section. The overlying interval corresponding to the Drake Fm. corresponds to the late Early Toarcian age as manifested by the appearance of the *Parvocysta*-suite.
The lower part of the Cook Fm. yields only few marine palynomorphs and is dominated by Botryococcus, suggesting brackish water deltaic conditions. The Drake Fm. in contrast was deposited in a substantially deeper depositional environment as indicated by the abundant and diverse dinoflagellate cyst assemblages. The carbon isotope shift recorded towards the top of succession is accompanied by a slight increase in TOC and an increase in prasinophyte algae. This does not seem to be a widely recorded “event”, but these observations indicate an increase in water-column stratification. The vegetation patterns stand in some contrast to the other records from the area, in that *Chasmatosporites* is substantially more abundant than elsewhere. The hig abundance of trilete spores in the basal part of the section confirms the deltaic depositional environment and a subsequent deepening through most of the Toarcian.

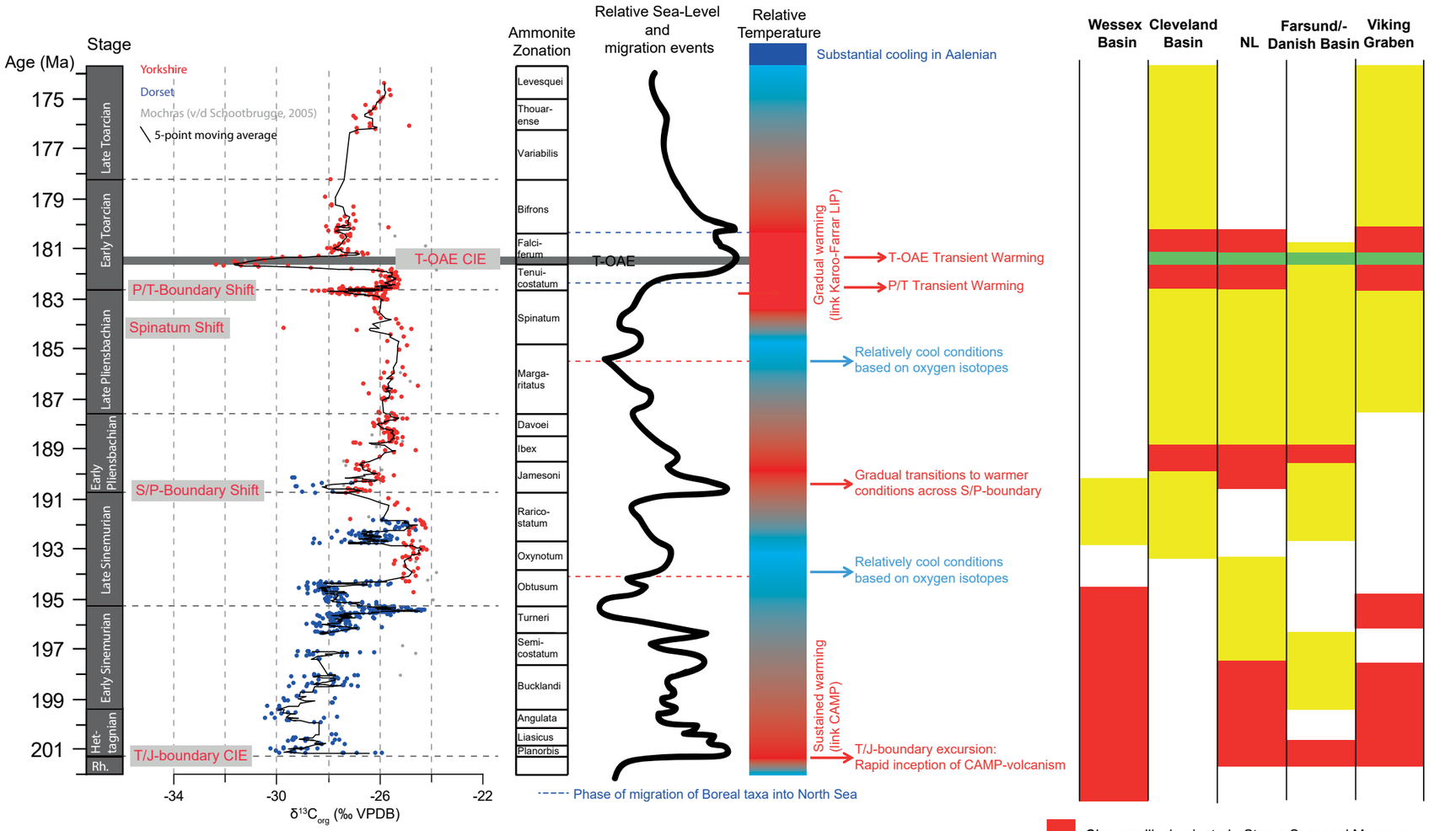

▲ Figure 6.8 Summary of sea-level, climate and schematic regional vegetation composition for the various regions in the study area.
The vegetation patterns are based on quantitative results discussed in this Chapter and references cited in this Chapter.

Cold Event is recognized. The Uppermost Pliensbachian (Spinatum Zone) in contrast marks a phase of local warming in the study area, likely related to the introduction of Tethyan currents. There is no rise in relative sea-level in the Uppermost Pliensbachian.

In contrast, the Pliensbachian-Toarcian boundary marks a significant transgression and a transient negative δ^{13}C-shift. In the Cleveland Basin deposition changes from oolitic ironstones to open marine mudstones with occasional thin organic-rich shales. In association with this transgression, boreal elements are introduced into the North Sea area, thus across the Viking Strait in the north. δ^{18}O-data dictate a substantial warming, also leading to a shift in *Classopollis*-dominated assemblages across most of the study-area. In the Exaratum Subzone, the major negative δ^{13}C-shift associated with the T-OAE is recorded, being accompanied by a transgression in much of the study area and a remarkable shift in vegetation-composition, with *Cerebropollenites* becoming dominant at numerous localities. This illustrates the strong environmental response of this phase of climatic warming. Because the marine ecosystem is also drastically perturbed by salinity-driven stratification, this vegetation change is likely the consequence of excessive (seasonal) precipitation. After the CIE of the T-OAE, climatic conditions remain warm and sea-level remains relatively high. Yet the T-OAE really stands out as an environmental perturbation. The relatively warm climatic mode in the Early Toarcian is likely ascribed to the activity of the Karoo-Farrar Large Igneous Province. The 'transients' across the Pliensbachian-Sinemurian Boundary and the T-OAE however reflect a feedback to this initial warming such as methane hydrate release. The Late Toarcian is overall regressive and cooler. A major sea-level lowering and cooling occurred in the Early Aalenian.

The overall results thus reveal a close coupling between warm climate modes, periods of elevated sea-level and vegetation patterns that indicate high seasonal precipitation. As a consequence these periods (Hettangian-Early Sinemurian, Earliest Pliensbachian, the Early Toarcian) are more susceptible to stagnant water conditions leading to potential organic-matter enrichment. Albeit being superimposed on a longer-term trend, the T-OAE sticks out in this perspective, in being a relatively short-lived transient phenomenon. ■

Ammonite graveyard from Grey Shales

7. Source Rocks and their Drivers

7. SOURCE ROCKS AND THEIR DRIVERS

In this chapter, the driving processes behind the deposition of more prolific source rock intervals in the Lower Jurassic of the study area are discussed. In addition to the detailed climatological and environmental interpretations of the palynological assemblages (Chapter 6), the composition of the visual organic matter can be used to describe the source rock type and quality. Together with the geochemical, and Rock Eval analyses, we use these data to evaluate the effects of changes in surface- and bottom-water redox conditions, detrital input and primary productivity.

Earlier studies on the Toarcian source rock intervals have shown a clear link with runoff, sediment starvation, bottom water conditions and water stratification, while the best source rock intervals could be related to changes in surface water oxygenation and the respective change in biofacies type, causing a dominance of AOM in these intervals (see **Figure 7.4**).

The main focus of this part of the study was put on the detailed outcrop sections from the Wessex and Cleveland Basins as these sections could be studied in most detail and enough sample material was available. To accompany the results from the outcrop sections several cores from Dutch wells were included as well as previously acquired data, partly from cuttings, other studies or literature.

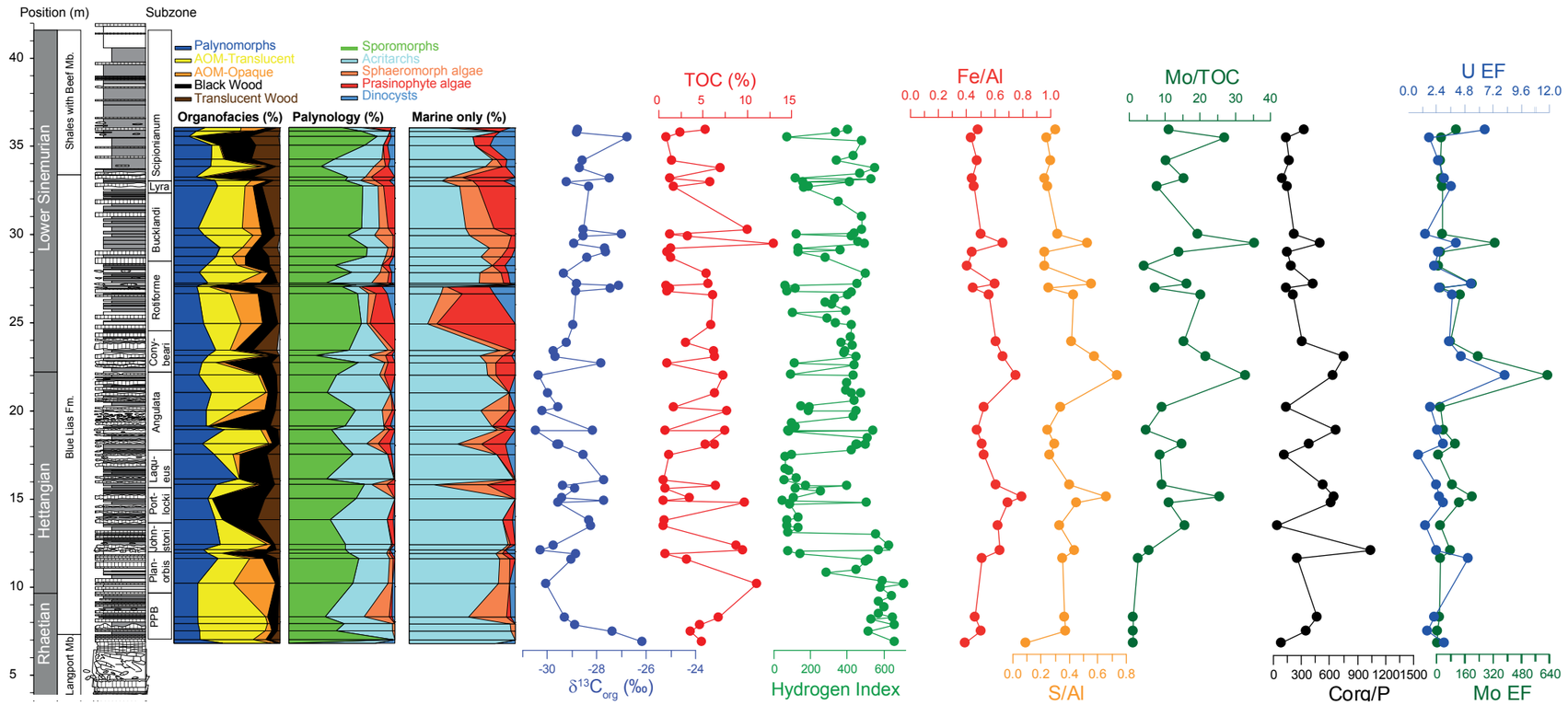

▼ Figure 7.1: Organofacies, TOC, Hydrogen Index (HI) and Redox Geochemical results of the Hettangian-Lower Sinemurian sequence from the Dorset Coast. Note that only shales and marls were sampled for these analsyes. The lowermost part of the Blue Lias Fm. (Uppermost Rhaetian Age, the Pre-Planorbis Beds, PPB) consists of organic-rich shales interbedded by rhythmic marlstones and massive limestone beds. The relatively low TOC-values (~2-5%) are likely due to the relatively high carbonate content. The sediments are dark and laminated without signs of bioturbation. The organofacies analyses show low wood content, high AOM-content, and relatively high abundance of marine algae (acritarchs and sphaeromorph algae like *Leiosphaera*). Dinocysts are virtually absent, but remarkably also prasinophyte algae are scarce. The chemical bottom-water redox proxies (Mo-EF, U-EF, Fe/Al, TOC/P) inidcate anoxic to dysoxic bottom water conditions and the HI-values are consistently very high (> 600 gHC/gTOC). This phase represents a period of water column stagnation and resultant export of HI-rich diazotrophic organic-matter to the an-/dysoxic sea-floor. This is also in-line with biomarkers for purple sulphur bacteria that were recovered from this interval (Jaraula et al., 2013). The absence of prasinophytes is ascribed to prolonged anoxic surface-water conditions, lasting beyond seasonal cyclicity in this interval.

This stands in contrast to the overlying (Jurassic) part of the Blue Lias Fm. which, following the shale-marl cyclicity marks fluctuating TOC-patterns (1-10%), positively correlating with the HI (<100-600 gHC/gTOC). High TOC and HI-values occur together with high abudance of prasinophyte algae in the marine palynomorph fraction, indicating shallow chemocline depths during these intervals. Although less pronounced, this pattern is also followed by the bottom-water redox proxies, with more reducing conditions co-occurring with phases of high TOC-values. Overall bottom-water conditions remain anoxic to dysoxic.

High wood- and sporomorph content correlate to low TOC and HI-values. These results clearly support the cyclic nature of these deposits. The organic and hydrogen-rich source rocks were deposited under stagnant water conditions, likely as a consequence of enhanced seasonal run-off. Under these circumstances, bacterial and algal organic-matter productivity and its net export were sufficient to cause AOM-dominated associations, thus overwriting terrestrial influence in this epeiric setting. The occasional abundance of dinocysts indicates a more or less oxygenated photic zone. These intervals are consistently accompanied by lower TOC and high wood content. This is particularly clear in the lowermost Shales with Beef Mb. (35 m height). This confirms a strong coupling between surface-water productivity and organic matter type.

7.1 Hettangian - Sinemurian

The Wessex Basin succession exposed along the Dorset Coast provides an insight into the dynamics of Lowermost Lower Jurassic organic-rich deposits with source rock potential (**Figure 7.1**). In terms of lithology these represent variations between organic-rich 'paper shales', calcareous marls and tabular and nodular carbonate beds. In the Sinemurian, the most organic-rich intervals bare the effects of diagenetic processes like the formation of fibrous calcite structures. This lithological cyclicity is also recorded in the organofacies, palynology, TOC, Hydrogen Index and bottom-water redox data (**Figure 7.1** and **7.2**) and these parameters closely co-vary (**Figure 7.5**). High TOC values consistently correlate to hydrogen-rich organic matter. Visually, this comprises dominant Amorphous Organic Matter (AOM) and the prevalence of prasinophyte and sphaeromorph algae like *Leiosphaera*. In contrast, low TOC-intervals relate to a high proportion of woody material, sporomorphs and lower hydrogen index-values (**Figure 7.4**).

Given the hemipelagic setting of these deposits, a more or less restricted basin, a scenario in which the variation of solar insolation on Milankovitch timescales modulated land-sea thermal contrasts and consequently run-off in a cyclic way, is plausible. These effects are particularly strong in overall warm (high CO_2) periods, such as the Earliest Jurassic, which was affected by extensive CAMP-volcanism.
These high run-off phases led to freshening of the surface water and eventual stagnation and anoxia. Under these circumstances, anoxygenic photosynthesis by sulphur bacteria provides for high fluxes of hydrogen-rich organic matter, which is in anoxic conditions very efficiently buried in the sediments. During orbitally-induced phases of diminished run-off, this ecosystem was not thriving. As a consequence, 'normal marine hemipelagic sedimentation' proliferated, causing organic-matter assemblages dominated by terrestrial material, that has a lower TOC- and Hydrogen-content.

However, when considered in regional context, the very prolific expression of the system observed in the Wessex Basin, is not clearly widespread. In the Cleveland Basin, the system was too shallow and consequently too well-mixed to become so heavily stratified, as evidenced by the recurrence of shell beds in the Calcareous Shales Mb. of the Redcar Mudstone Fm. When considering the log-expression in the Southern North Sea Basin, the apparent cyclicity with organic rich high gamma shales being so prominent in the Wessex Basin (Bessa and Hesselbo, 1997) is not recorded. This can also be seen in well Oldenzaal-04, **Figure 7.6**). An exception to this rule might be apparent, in the onshore of the West Netherlands Basin, particularly those areas fringing the London Brabant Massif, where high-gamma intercalations are indicative of a potentially similar system. Note that in Norway and Denmark, time-equivalent successions are dominated by coarser grained deposits of the Statfjord Group and Gassum Fm. respectively.

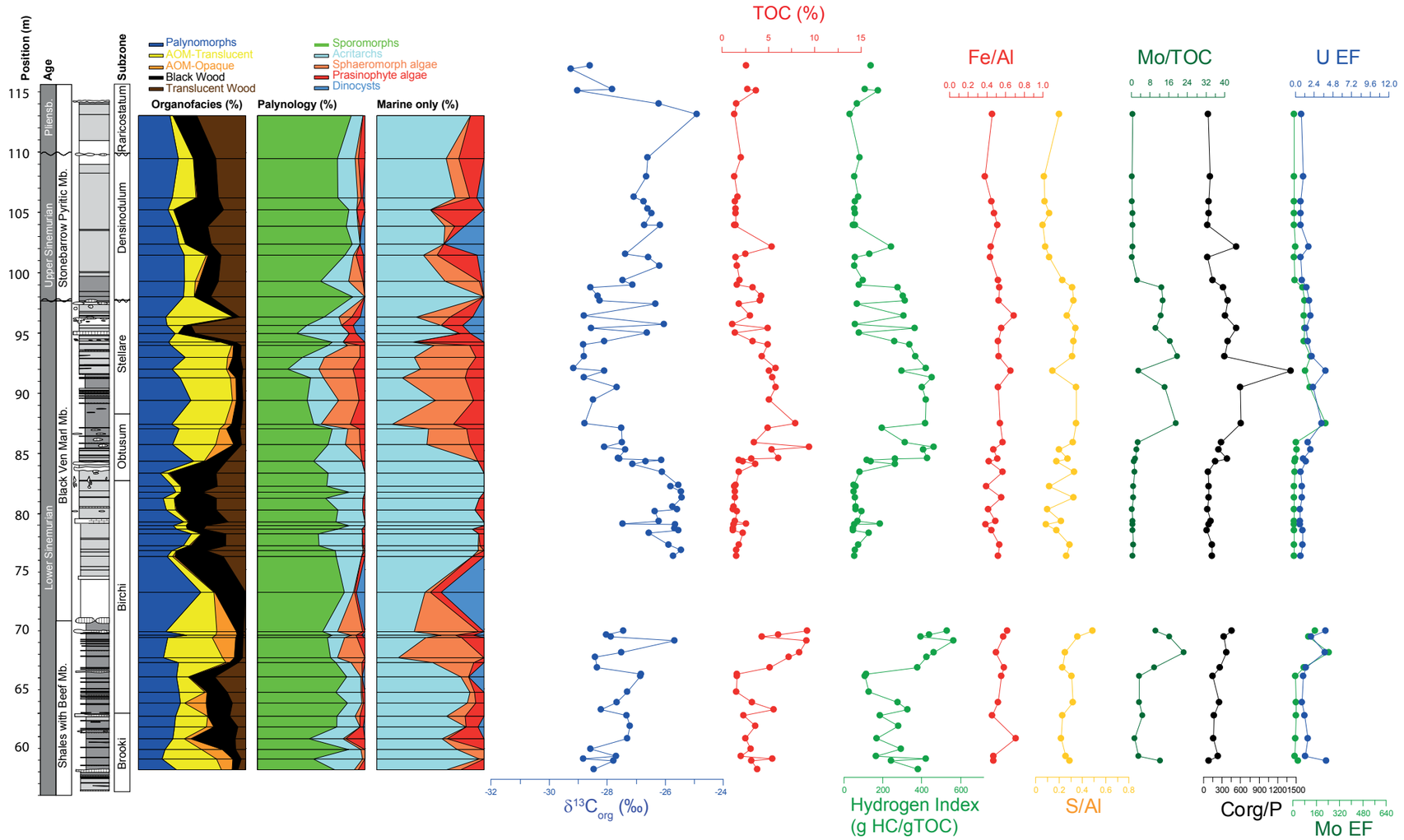

▲ Figure 7.2: Organofacies, TOC, Hydrogen Index (HI) and Redox Geochemical results of the Lower Sinemurian to Lowermost Pliensbachian sequence from the Dorset Coast.
Note that only shales and marls were sampled for these analyses and that there is a sampling gap with the underlying interval as depicted in Figure 7.3.
The first thing that strikes the eye is that the cyclicity in terms of organofacies (wood vs. AOM), marine palynology (prasinophyte algae abundance) and geochemical parameters (TOC and HI) is also present, albeit in 'more expanded' manner. This is considered to be the consequence of the higher average sedimentation rates compared to the underlying interval (Jenkyns and Weedon, 2011; Ruhl et al., 2016). The overall lower maximum TOC-values are possibly caused by elevated detrital dilution associated with higher sedimentation rates. Particularly elevated TOC-values are recorded in the lower part of the Birchi Subzone and in the Obtusum and Stellare Subzones. Consistently, these TOC-optima are accompanied by organofacies associations that are dominated by AOM, relatively high proportions of marine palynomorphs in which prasinophyte algae (including sphaeromorph algae) are abundant and dinocysts generally absent. In contrast to the underlying Blue Lias Fm. interval the geochemical redox indicators more closely follow the TOC-optima, thus indicating a strong coupling between bottom and surface water conditions.
In the TOC-rich intervals the lithology is also characterized by an increased recurrence of early diagenetic carbonate concretions. These likely relate to the anoxygenic oxidation of microbial methane in association with sulphate reduction under periods of prolonged anoxia (see Raiswell, 1971; Lash and Blood, 2004). Also the prevalence of fibrous calcite it bound to these intervals with higher TOC and HI-values. Given that T_{max} values are indicating an early oil-window maturity (μ=419° C), this relates to fluid or gas overpressuring during early-stage expulsion of these hydrogen-rich source rocks (Cobbold et al., 2013). Also note the close correspondence between the organofacies, hydrogen index and the $\delta^{13}C_{org}$-values. This relates to the substrate and the elevated rate of microbial recycling of organic matter under anoxic conditions. We have corrected for this effect whilst interpreting isotope trends for stratigraphic purposes (Chapter 5), justifying the stratigraphic significance of the shift also recorded across the Sinemurian-Pliensbachian boundary.

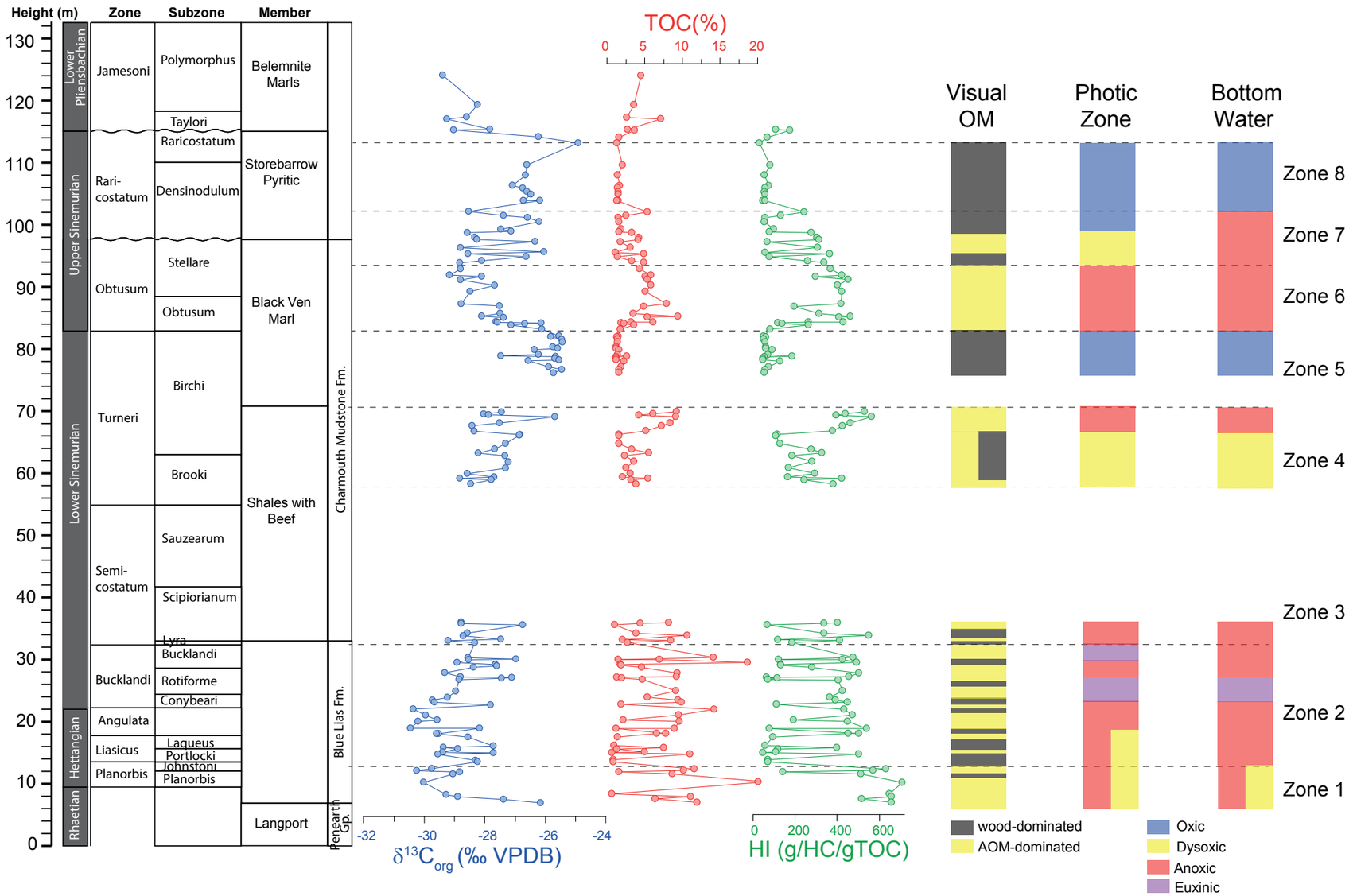

▲ **Figure 7.3: Compilation of organofacies and surface-water- and bottom water environmental change compared to $\delta^{13}C$, TOC- and HI-data for the Hettangian to Lower Pliensbachian sequence from the Dorset Coast.**
The inferred surface-water oxygenation scheme is based on the presence of dinocysts (oxic), presence of prasinophyte algae (anoxic) and dominance of prasinophyte algae (euxinic). The interpretation of euxinic bottom-water redox conditions is based on the Mo and U enrichment factors (see Figure 7.5). This forms the basis for a paleo-environmental chacterisation.

With the exception of the Pre-Planorbis Beds, immediately above the T/J-CIE, the surface-water and bottom signals are strongly coupled to the TOC and HI data. Changes in run-off were brought about by changes in orbital configuration, particularly under the relatively warm 'high CO_2' earliest Jurassic climate state. In the epeiric setting of the Wessex Basin these changes in run-off caused surface-water freshening, stratification and stagnation. This affected the surface water ecology in a way that anoxygenic photosynthesis by green and sulphur bacteria became dominant. This produces a hydrogen-rich prolific organic-matter composition that constitutes excellent source rocks and overprints the steady supply of terrugineous organic matter (wood fragments).
The entire Blue Lias Fm. is characterized by the highly cyclic presence of the source rock intervals. Subsequently, these units get more expanded, likely owing to elevated sedimentation rates. Particularly strong stratification occurred in the earliest Sinemurian Bucklandi Zone, the late early Birchi Zone and in the Obtusum Zone. Also note that the upper Birchi Zone and the Raricostatum Zone are more oxygenated. Based on the terrestrial palynomorph assemblages, these intervals represent 'cooler' climate conditions. Hence, there appears to be a coupling between warm climate modes, enhanced (seasonal) run-off, salinity stratification and the deposition of source rocks.

▼ **Figure 7.4 (top)Ternary diagram showing the results of the palynological analyses**, separated for total wood (wood black and wood brown), total AOM AOM type 1 (translucent) and type 2 (opaque) and palynomorphs for the samples of the Dorset section. The coloring of the symbols is according to the measured hydrogen index of the same samples.
(bottom) Pseudo Van-Krevelen diagram showing the samples of the Dorset section, coloured for the amount of wood identified in the sample.
These figures clearly illustrate how the composition of the visual kerogen composition controls the source rock type, based on the results of the pyrolysis. The samples with predominantly wood have very low hydrogen indices while the samples with mainly SOM have the highest hydrogen indices. The amount of palynomorphs on the other hand is very stable throughout the samples and appears to have no influence on the source rock quality.

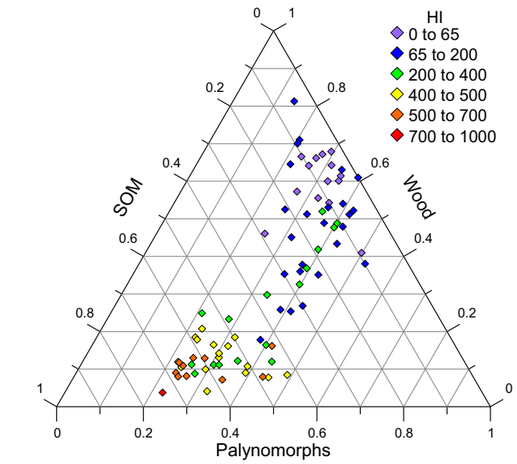

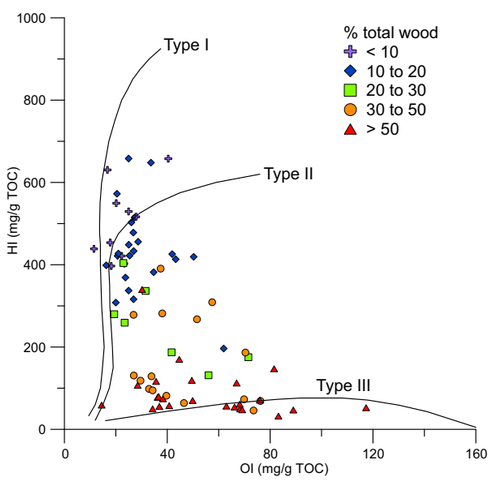

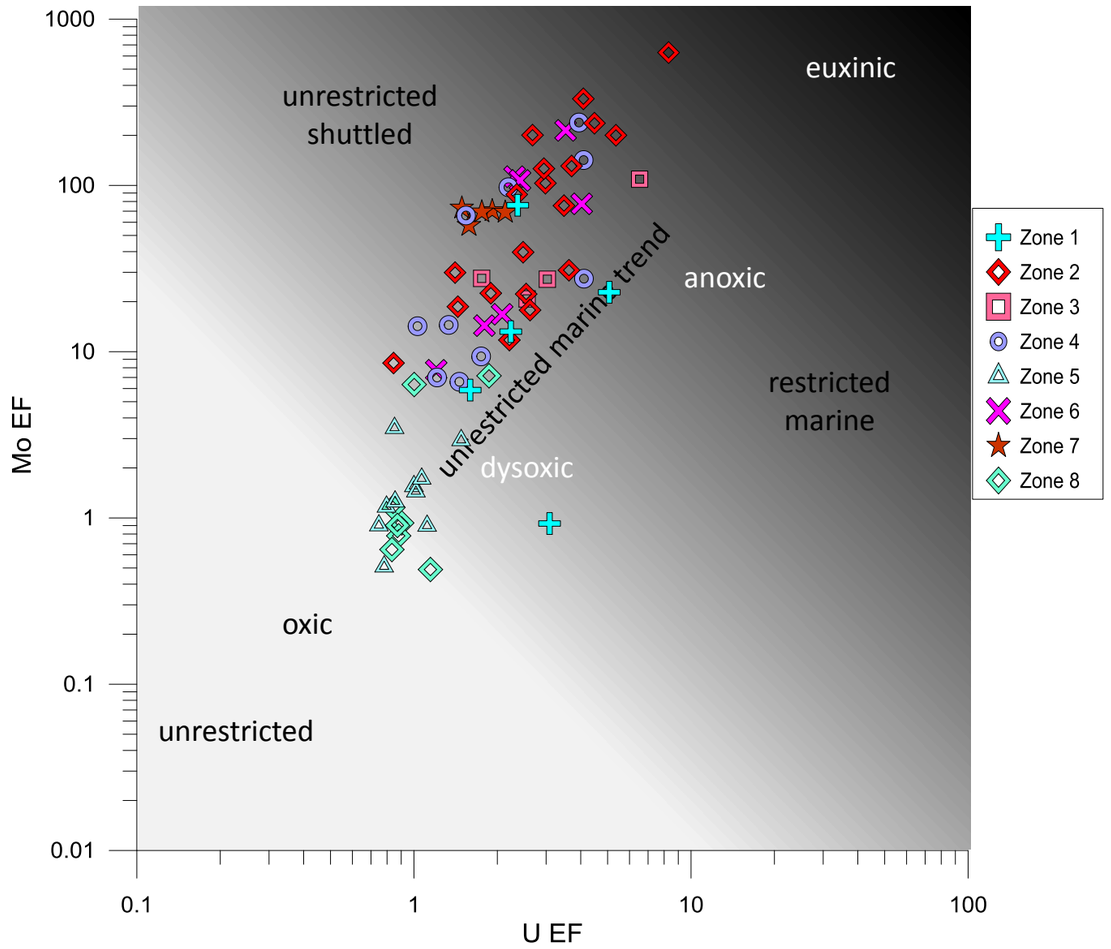

▲ Figure 7.4: Molybdenum (Mo) and Uranium (U) enrichment factors (EFs) for the Dorset Coastal succession.
The symbols correspond to the different zones identified in this Figure 7.3. The shaded area depicts a change from oxic (white) towards euxinic (black) bottom water conditions. This Figure illustrates the spread in terms of bottom water oxygenation ranging from euxinic (free H_2S) to more or less oxygenation. Additionally, Mo and U EFs indicate potential water mass restriction. The data plot in between these two end-members, a phenomenon that may be considered typicaly for the epeiric hemipelagic depositional setting of the Lower Jurassic Wessex Basin.

7.2 Pliensbachian

The Lowermost Pliensbachian is characterized by relatively warm climate, affected by a monsoonal climate mode. This phase follows upon the negative $\delta^{13}C$-shift across the boundary, indicating increased atmospheric CO_2-concentrations compared to the Late Sinemurian. In the Cleveland Basin, this interval corresponds to the Pyritous Shale Mb. Albeit the corresponding sediments are dark, pyrite-bearing and poorly bioturbated, we find no evidence for sustained surface-water nor bottom-water anoxic conditions (**Figure 7.8**), the apparent lithological change is predominantly attributed to a more distal depositional environment. Like in the Cleveland Basin, also the Wessex Basin witnessed a substantial deepening of the depositional environnment, with the calcareous marls of the Belemnite Marls Mb. Thin organic-rich intercalations are found here.

According to Petersen et al. (2008) overall Early Jurassic sea-level rise continued and reached a maximum during Sinemurian-Pliensbachian boundary times. In the centre of the basin, the diversity and abundance of the ostracod fauna decreased and infaunal bivalves and some of the epifaunal bivalves disappeared due to reduced oxygen conditions (Pedersen 1986). In the shallower Farsund Basin core 13/1-U1, we have not identified any indications for anoxia or enhanced productivity (**Figure 7.11**, see also Smelror et al., 1989).

The remainder of the Pliensbachian is characterized by a progressively more regressive nature and a shift to a cooler climate mode (Chapter 6). In the Southern North Sea area an increase in grain-size is recorded in the Davoei Zone. The Margaritatus Zone is considered to represent the coolest interval (see Chapter 6). The latest part of the Early Pliensbachian is also characterized by carbon cycle disturbances, owing to Spinatum CIE and its associated transgression. Although we have not recorded any organic-enrichment in our studied sections (**Figure 7.6, 7.7, 7.8**) or in the literature (see also Petersen et al., 2008), it may be that in the deeper parts of basins in the Southern North Sea area and in Denmark, some organic-enrichment may have occured.

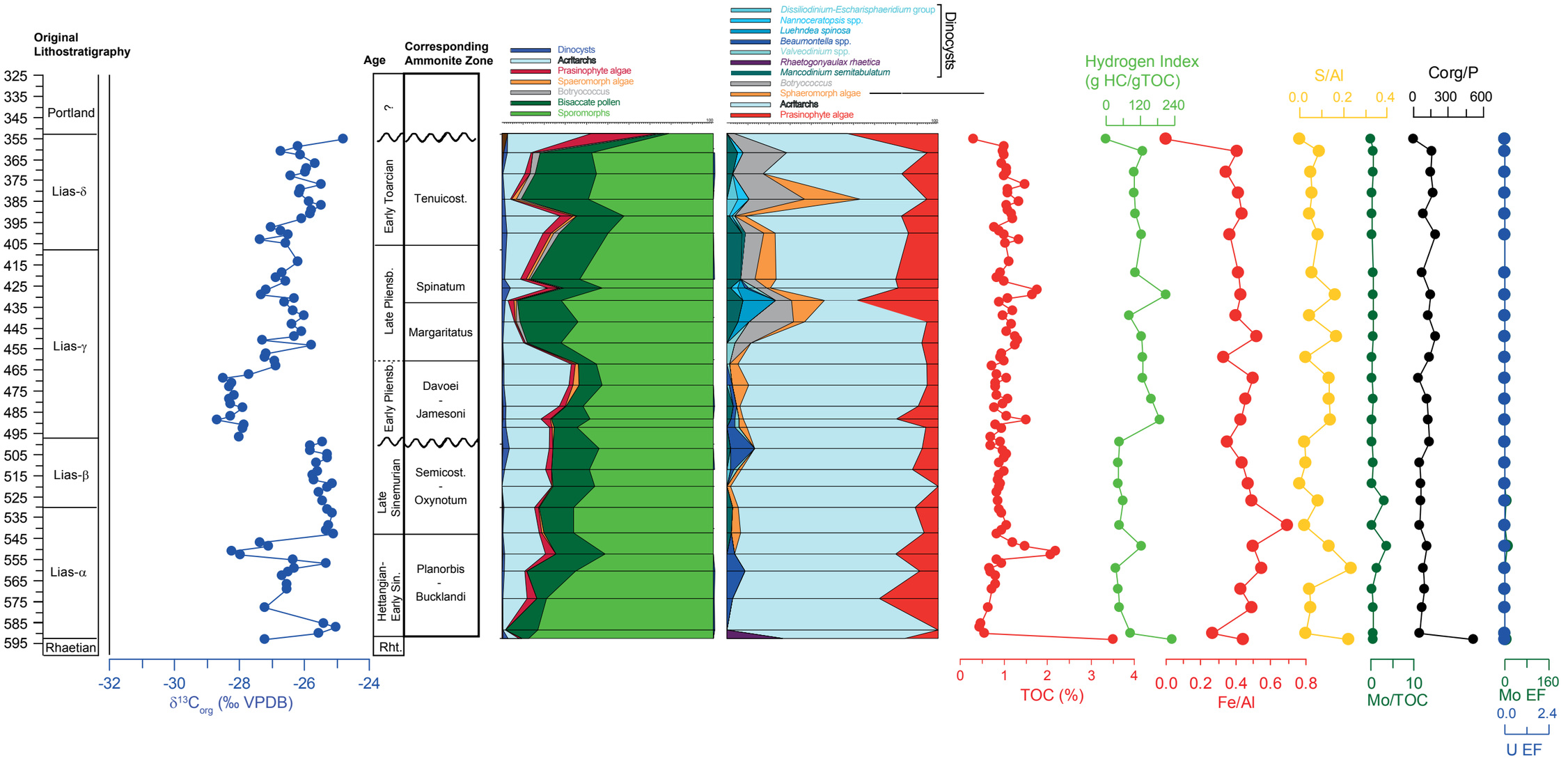

▲ Figure 7.5: Total and marine palynology, TOC, Hydrogen Index (HI) and Redox Geochemical results of the Lower Jurassic sequence in the core from Oldenzaal-4, the Netherlands.
In contrast to the Wessex Basin succession, there is no substantial organic-enrichment in this succession. The highest TOCs are actually recorded in the single Rhaetian sample (Sleen Fm., 6% TOC, HI=~200 gHC/gTOC). The total palynology (left panel) is indicative of shallow but continuously marine conditions, with ample supply of terrestrial material, which is in accordance with the low HIs (<200gHC/gTOC). Also the redox geochemistry is not indicative of any prolonged periods of bottom water anoxia. Only the Hettangian and Early Sinemurian part of the succession capture some fluctuations, particularly in S/Al and Mo/TOC. When looking at the marine palynological record, one can see that the assemblages are fairly stable, with perhaps the most noteworthy feature being the increase of *Botryococcus* in the Upper Pliensbachian and Earliest Toarcian, signifying increased brackish water conditions. Prasinophyte algae are persistenlly present, as are dinocysts. These data do not argue for sustained surface-water stratification nor anoxia. Note that the organofacies is dominated by wood-fragments throughout and therefore not separately plotted.

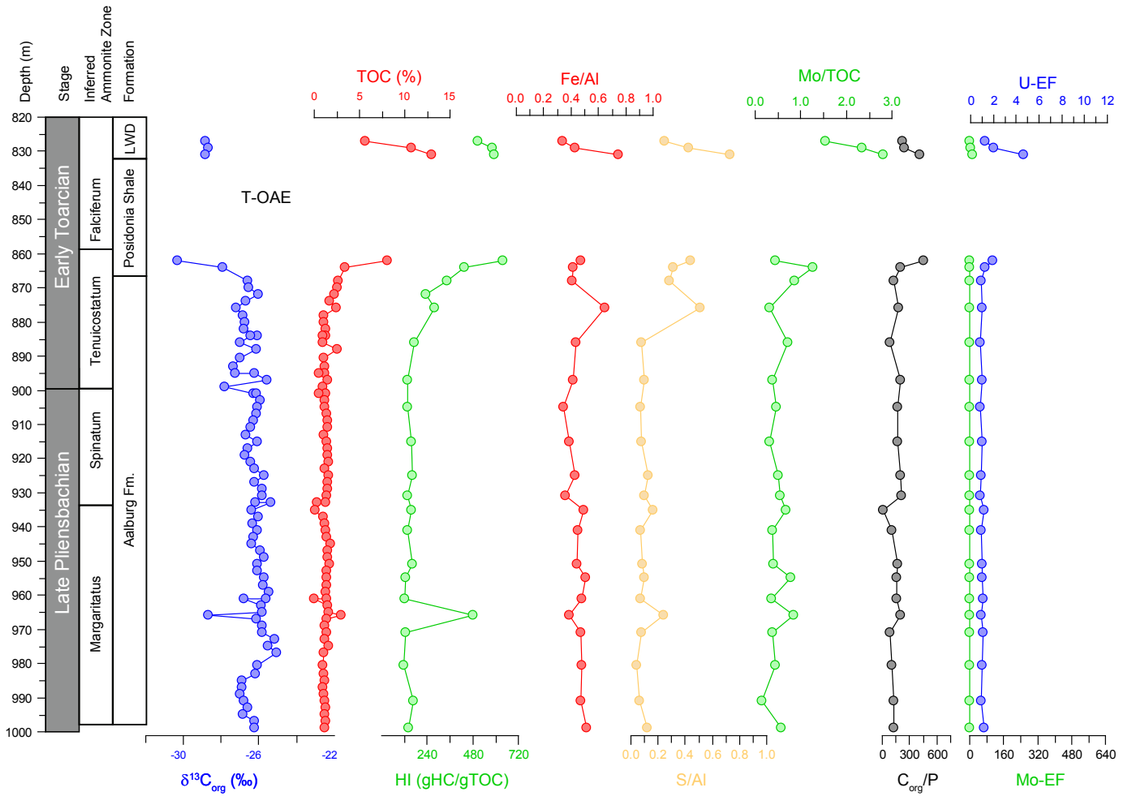

▲ Figure 7.6: $\delta^{13}C_{org}$, TOC, Hydrogen Index (HI) and Redox Geochemical results of the Upper Pliensbachian sequence in the core from Boeikop-1, the Netherlands.
For this well we only generated geochemical data. No detailed palynological investigation was undertaken but six samples were scanned for biostratigraphy. At 912 we note FOs of *Luehndea spinosa* and *Nannoceratopsis gracilis*. This shows that this level corresponds to the Latest Pliensbachian Spinatum Zone. The underlying samples do not yield any organic-walled dinoflagellate cysts, but the terrestrial assemblages are indicative of a Late Pliensbachian age. The remainder of the $\delta^{13}C_{org}$-record is then easy to interpret in terms of stratigraphy since the base of the CIE of the T-OAE is reached at the top of the lower section. The overlying samples between 820 and 830 are placed in the Lower Werkendam Fm. and are based on their 'light' values also of Early Toarcian age.
Only in the initial phase of the T-OAE do we note changes in TOC, HI and bottom water redox conditions. These are similar to what is observed elsewhere in the Netherlands and in Yorkshire (see next section). It is also apparent that the interval corresponding to the Tenuicostatum is more dynamic, both in terms of $\delta^{13}C_{org}$ as well as in the sulphur and molybdenum records. Similar, transiently dysoxic intervals are also found in the time-equivalent strata of the Grey Shales Mb. in Yorkshire.

7.3 Earliest Toarcian

The Pliensbachian-Toarcian boundary also marks a substantial transient carbon isotope excursion (CIE), essentially forming a precursor to the T-OAE and substantial regional transgression. In association, the Grey Shale Mb. is deposited in the Cleveland Basin. This overall mudstone dominated unit spanning the Tenuicostatum Zone, contains isolated, relatively thin (10 cm thick) intervals with elevated TOC-values (up to 8%) and more reducing bottom water conditions (see **Figure 7.8**), often referred to as the Sulphur Bands. By generating trace element concentrations, molecular biomarkers, and bulk carbon and sulphur isotopes Salem (2013) confirms highly variable redox conditions prior to the Toarcian OAE, with repeated anoxia/euxinia during periods of sulphur band deposition. Nevertheless, these perturbations did last sufficiently long to notably alter the marine ecosystem as we find abundant organic-walled dinoflagellate cysts and no elevated abundance of prasinophyte algae. Also the effects seem to have been rather limited as we do not find similar patterns in the time-equivalent Boeikop-01 well from the Netherlands (**Figure 7.7**).

In the Earliest Toarcian we have recorded the incursion of dinoflagellate cysts that were previously only recorded in the Arctic realm in the Southern North Sea Basin. It thus seems that the Early Toarcian transgression coincided with an increase in connectivity with presumably lower salinity waters from the Arctic realm (Dera and Donnadieu, 2012). Although the biogeographic patterns certainly need further investigation, it may be hypothesized that the coincidence of this Arctic connection and the inception of enhanced stratification in the Southern North Sea area are causally related. Hence, it seems that the area was preconditioned to become 'easily' stratified in the Earliest Toarcian, with superimposed phases of Karoo-Farrar LIP volcanism and associated feedbacks (Svensen et al., 2007) that pushed the system into an intensified greenhouse-climate mode.

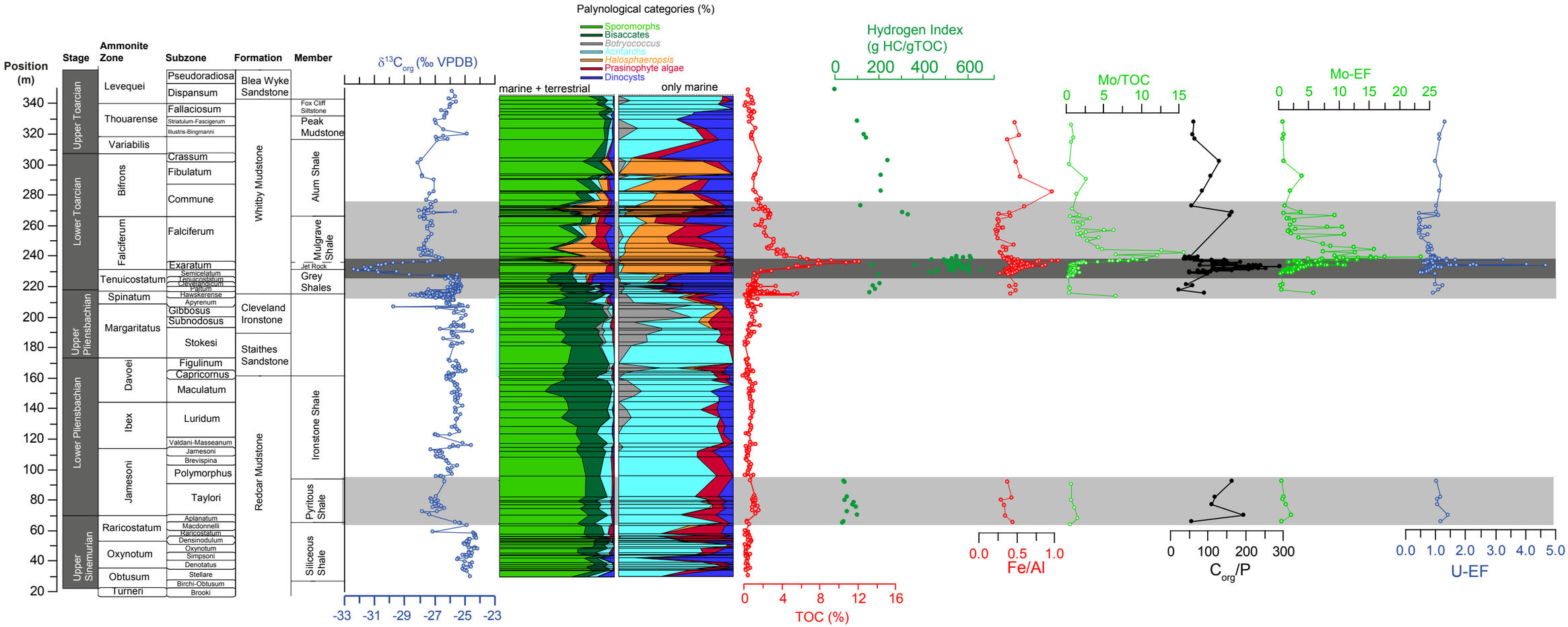

▲ Figure 7.7: Total and marine palynology, $\delta^{13}C_{org}$, TOC, Hydrogen Index (HI) and Redox Geochemical results of the Upper Sinemurian to Toarcian succession from the Cleveland Basin (Yorkshire, UK).
The Sinemurian to Upper Pliensbachian succession is characterized by low TOC-content (<~2 %, see also Chapter 5). Significant organic-enrichment occurs in the Latest Pliensbachian - Earliest Toarcian and through Early Toarcian Falciferum Ammonite Zone, with TOCs gradually declining after the T-OAE in the Exaratum Subzone. The Jet Rock (T-OAE) really stands out in terms of TOC-content, reaching maximum values of 16%.

On the basis of field-observations (presence of pyrite, dark colour, laminations) and the TOC-content we have decided to study the Earliest Pliensbachian Pyritous Shale Mb., and the Toarcian Whitby Mudstone Fm. (Grey Shales Mb., Mulgrave Shale Mb. and the Alum Shale Mb.) in more detail. For these intervals we have generated Rock Eval and bottom-water redox data.

Albeit field observations suggest the Pyritous Shale Mb. to represent a rather organic-rich shale unit, TOC-values are only enriched by 2 % reaching values of 4% TOC (see Chapter 3). The HI is not substantially enriched (<150 gHC/gTOC). The organic-matter in the Jet Rock is characterized by high HI-values (600 gHC/gTOC). Also in terms of palynology, the Lower Toarcian and the Jet Rock in particular stand out by substantially increased marine influence. The bottom-water redox indicators do not unequivocally suggest bottom water anoxia, generally conditions are considered dysoxic. The marine palynology comprises both acritarchs, prasinophyte algae and dinocysts. It thus seems that the earliest Pliensbachian, following the Sinemurian-Pliensbachian CIE was accompanied by a warm climate and high relative sea-level (see also Chapter 6) and that during this highstand phase the sediment pore water became anoxic, without a major effect in the water column.
In correspondence with the negative CIE across the Pliensbachian - Toarcian boundary (base of the Grey Shale Mb.), the TOC content becomes quite variable, increasing up to 6%. This interval also marks a return of more open conditions (Chapter 5). In this interval, following the carbon cycle disturbance manifested by the CIE, bottom water conditions become transiently anoxic as well. There is however no major response in surface water ecology, suggesting that the Grey Shales are subject to diminished bottom-water ventilation only, leading to the episodically organic-enriched sulphur bands.

A major regime shift is noted during the T-OAE represented by the Jet Rock unit of the Exaratum Zone. TOCs rise substantially and the HIs increase to 600 gHC/gTOC. This is also linked with a major change in organofacies, becoming overwhelmingly dominated by AOM which is populated by the stress-affected prasinophyte *Halosphaeropsis liassicus* (Palliani et al., 2002; Van de Schootbrugge et al., 2013), as visible under UV-fluorescence microscopy. Dinocysts are not recorded during the T-OAE. This turnover is linked to the establishment of photic zone euxinia (French et al., 2014) being brought about by surface-water freshening as a consequence of enhanced run-off due to rapid CO_2-induced warming during the T-OAE. Not surprisingly, also the redox indicators show persistent bottom water redox conditions (see also Figure 7.10). Under these circumstances, elevated productivity by sulphur bacteria accounts for the production and export of very prolific (hydrogen-rich) organic matter (Van de Schootbrugge et al., 2013; Houben et al., 2015). After the T-OAE TOC values remain elevated compared to the Late Pliensbachian background, up to the halfway the Bifrons Zone. This is also accompanied by persistent abundance of prasinophyte algae and *Halosphaeropsis liassicus*. Dinocysts however return in the record, suggesting that euxinic to anoxic conditions were not persistent. We arrive at a similar conclusion based on the redox conditions. It takes up to the top of the Alum Shale Mb. (Bifrons Zone) before the *Halosphaeropsis*-dominated assemblage dissappear and fully oxygenated environments re-appear. Hence, the entire Early Toarcian was characterized by anoxic conditions and organic enrichment, but the prolific source rocks are restricted to the T-OAE.

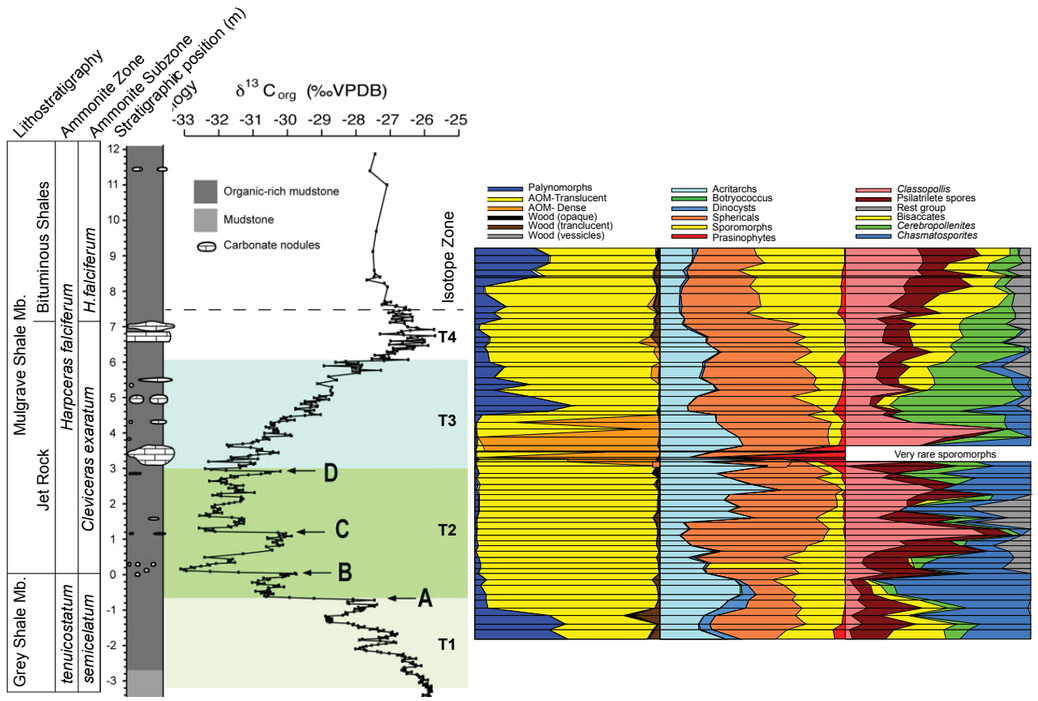

▲ Figure 7.8: Organofacies and palynological analyses across the T-OAE in the Cleveland Basin.
These data are after Houben et al. (2015) and the TNOs Sweet Spot-1 project, scaled against the carbon isotope record of Kemp et al. (2005). The left diagram indicates the composition of the organic material (%), the middle diagram the composition (%) of the palynological associations and at the right the composition of the sporomorph communities.These analyses were performed using UV-fluorescence microscopy in order not to underestimate the presence of palynomorphs found enclosed in AOM-clusters. These analyses show that in correspondence with the CIE, the organofacies becomes overwhelmingly dominated by AOM, overprinting the abundance of wood and palynomorphs. Concomitantly, the dinoflagellate cysts are wiped out, to occur after the T-OAE. Instead Halosphaeropsis liassicus and prasinophyte algae are now by far the dominant palynomorphs. The absence of dinoflagellate cysts and the prevalence of prasinophyte algae is linked to photic zone euxinia. The terrestrial palynomorphs signify associated perturbations of terrestrial vegetation through the dominance of *Chasmatosporites*, *Classopollis* and successively *Cerebropollenites*.

7.4 The Toarcian Oceanic Anoxic Event (T-OAE) and its aftermath

The results of this study show that T-OAE has a pronounced expression in many parts of the study area. In the Southern North Sea Basin, we have noted a major shift in TOC, HI and organofacies. The redox geochemical data and the proliferation of prasinophyte algae and *Halosphaeropsis jurassica* in particular point towards the installation of a sharp chemocline and anoxic to euxinic water column conditions as the main driving factor for TOC enrichment. Intensified monsoonal heat and moisture transport during the Exaratum Subzone led to a surplus of fresh-water in the Southern North Sea Basin, leading to stratification, ample nutrient supply and the installation of an ecosystem fueled by microbial anoxygenic photosynthesis, leading to organic-rich deposits with high HI-values.

The overall temporally homogeneously distributed TOC-trends between the Cleveland Basin outcrops and wells in the Netherlands (**Figure 7.10**) suggests that the Southern North Sea Basin was susceptible to stratification and enhanced preservation of organic matter (**Figure 7.9** and **7.10**). Possibly, the establishment of Arctic connection just prior to the T-OAE (Tenuicostatum Subzone) aided in lowering the salinity budget of the Southern North Sea Basin.

Remarkably, on the basis of well logs, it seems that the characteristic log-response to the organic-rich shales of the T-OAE are absent in the East Midlands Platform and Sole Pit area (see Chapter 5). We hypothesize that this relates to the location with regards to the seaway that spreads across much of modern-day England, which locally supplied well-oxygenated, high salinity water from the Tethys.
Also outside of the fine-grained Southern North Sea area, the effects of the T-OAE are pronounced. In the Gullfaks Area in the Viking Graben, Norway, marine palynological assemblages are also dominated by *Halosphaeropsis liassicus*. Here, surface-water conditions were also anoxic as a consequence of low salinity stratification. However this only happened on a seasonal scale, as marine dinoflagellates were able to proliferate (**Figure 6.5** and **6.6**). In these settings with ample coarse clastic sediment supply, TOCs are not substantially enriched (see also Section 7.5, **Figure 7.14** and **Figure 7.15**). Albeit the exact age of the Bryne Fm. in the Farsund Basin (**Figure 7.11**) remains difficult to constrain we have noted an elevated abundance of the colonial green alga *Botryococcus* in association with isotope anamolies possibly ascribed to the CIE of the T-OAE. In that case, these data point towards a a low-salinity flooding of a fluviodeltaic environment. Hence, it is clear that across the entire study area the T-OAE seems to be marked by a major run-off pulse.

The major phase of environmental change is associated with the actual CIE. However, elevated TOCs are maintained through much of the study area through most of the Early Toarcian (**Figure 7.10**). In the Cleveland Basin, at the base of the Bifrons Zone (Base Alum Shale Mb., **Figure 7.8**) we record an additional 'event' that may bear an expression in the Viking Graben area (in the Drake Fm., **Figure 6.7**). This interval has not been sampled in the Netherlands. Hence,this 'event' may also be picked up in the Lower Werkendam Mb. in the Netherlands. The Late Toarcian marks a regional regression in the Southern North Sea Basin, whereas mudstones of the Drake Fm. characterize the Northern Part of the study area.

▼ Figure 7.9: Schematic representation of surface-water and bottom-water environmental change across the T-OAE in the Cleveland Basin and two localities in the Netherlands.
This figure is after Houben et al. (2015). The three localities are correlated by means of carbon isotopes (Zones T1-T6). The surface water signal is based on the organofacies and palynological data generated for each of these localities. Normal marine conditions are indicated by the abundance of dinoflagellate cysts and well-mixed organofacies. When the chemocline migrates into the photic zone, prasinophyte algae become abundant. Once the chemocline is permanently established in the photic zone and euxinic conditions, *Halosphaeropsis liassicus* becomes dominant and organofacies exclusively consists of AOM. The bottom-water redox conditions are reconstructed using a combination of redox sensitive elements, ratios and iron speciation data. With the latter method, oxic, anoxic and euxinic (free H_2S) conditions can be reconciled.

Iron-speciation and major and trace-element data indicate that euxinic bottom-water conditions were already established at the base of the CIE and persisted throughout the T-OAE at all studied localities. In contrast, the termination of the euxinic conditions is diachronous across the study area and for instance extends way beyond the duration of CIE in the Netherlands . The palynological results reveal that the highest TOCs during maximum $\delta^{13}C$ excursion are just preceded by a major increase in the abundance of prasinophycean vegetative cysts attributable to *Tasmanites*. On the basis of the modern physiology of this group, we assume this to be an indication for chemocline shoaling into the photic zone at all studied localities. During the T-OAE, organic-matter associations almost exclusively consist of dense clusters of Amorphous Organic Matter (AOM) containing abundant *Halosphaeropsis liassicus*. We ascribe the dominant occurrence of these “stress-taxa” to specific conditions, driven by H_2S presence in the photic zone, as also evidenced by recent insights from molecular biomarkers (French et al., 2014).

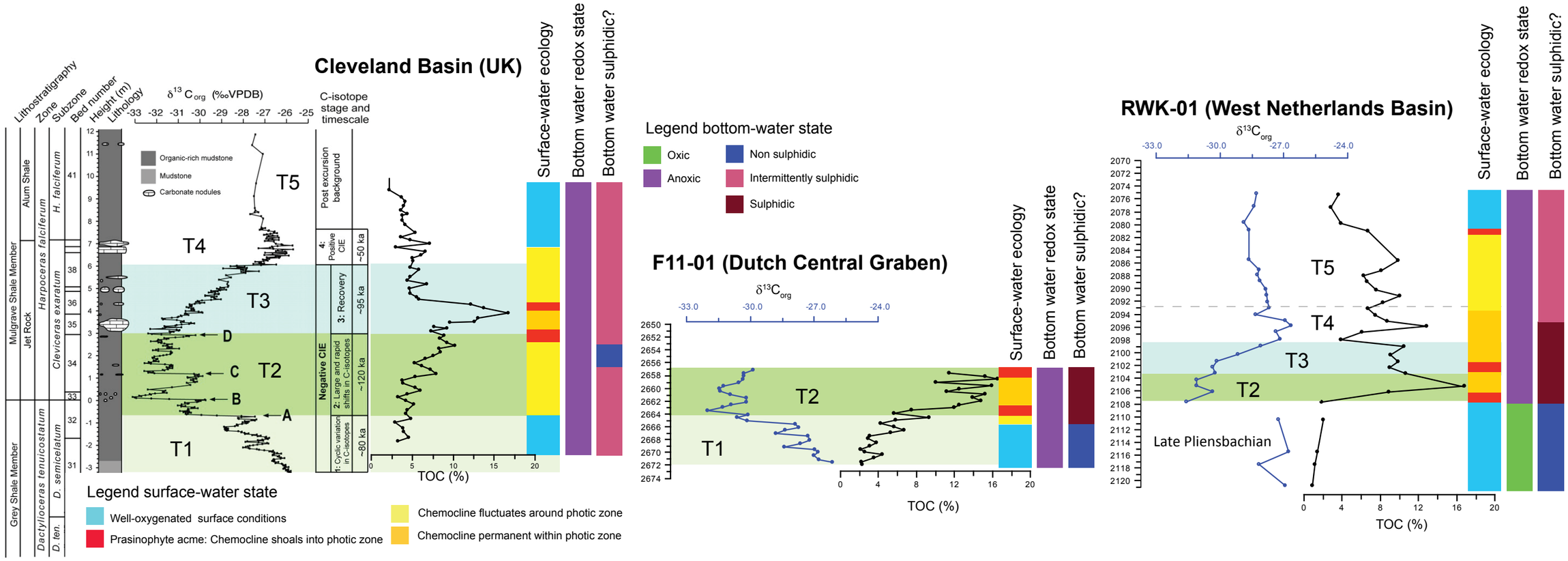

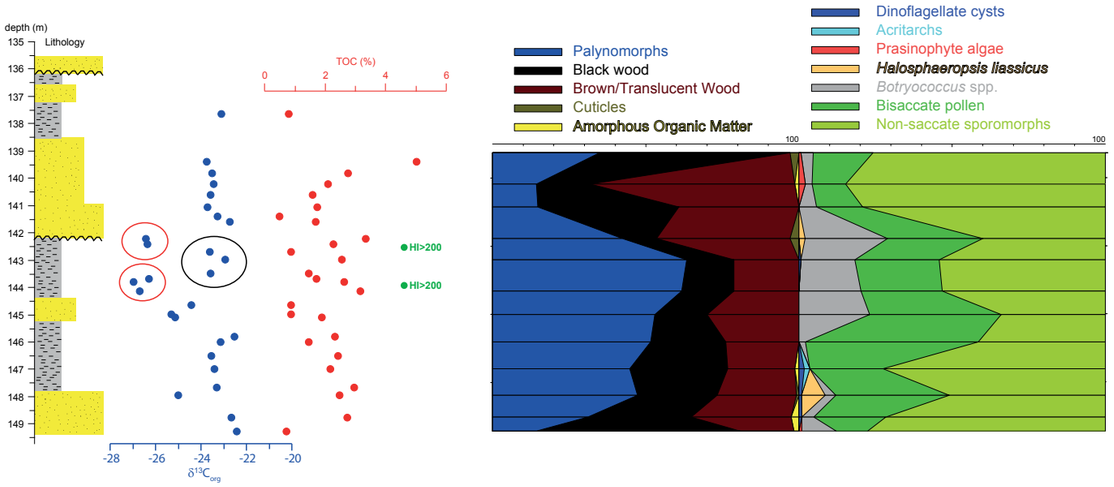

▲ Figure 7.10: Palynological and stable isotope data from the interval ascribed to the Bryne Fm. in core 13/1-U1 from the Farsund Basin.
On the basis of biostratigraphy alone it is difficult to provide an age-dating for this interval (see also Chapter 5 and Smelror and et al.,1989). Consequently it is dated as “Toarcian - Aalenian” by the latter. This is also substantially older than the Bryne Fm. and is elsewhere in the area Bajocian-Bathonian (Vollset and Doré, 1984). The $\delta^{13}C$-data however display a series of substantially depleted values, as negative as -27.5‰. These occur in the more shaly equivalents of sediments characterized as “fluviodeltaic sandstones with interbeddded clayey siltstones and silty shales”. In such truncated and incomplete types of sequences, isotope profiles are unlikely to be complete and thus difficult to compare right away with the reference sections. Hence, it may be possible that these light values (red circles) were deposited during the T-OAE, and that reworked and transported material obscures the signal (black circle).
In the interval with lighter values we note remarkably high abundances of *Botryococcus* spp., the palynological remains of aggregate building green algae that thrive under brackish water conditions. These green algae are even used as a biofuel (Schenk et al., 2008) and consequently it is not suprising that the only substantially elevated HI-values are recorded in these samples (Smelror et al., 1989).
If this interval indeed represents the T-OAE, the record provides an insight into the response to the event in a coarse-clastic dominated fluviodeltaic facies. The effects of enhanced (seasonal) run-off are clearly marked, leading to a major change in terrestrial vegetation (Chapter 6) and the deposition of the colonial green algae in overbank deposits.

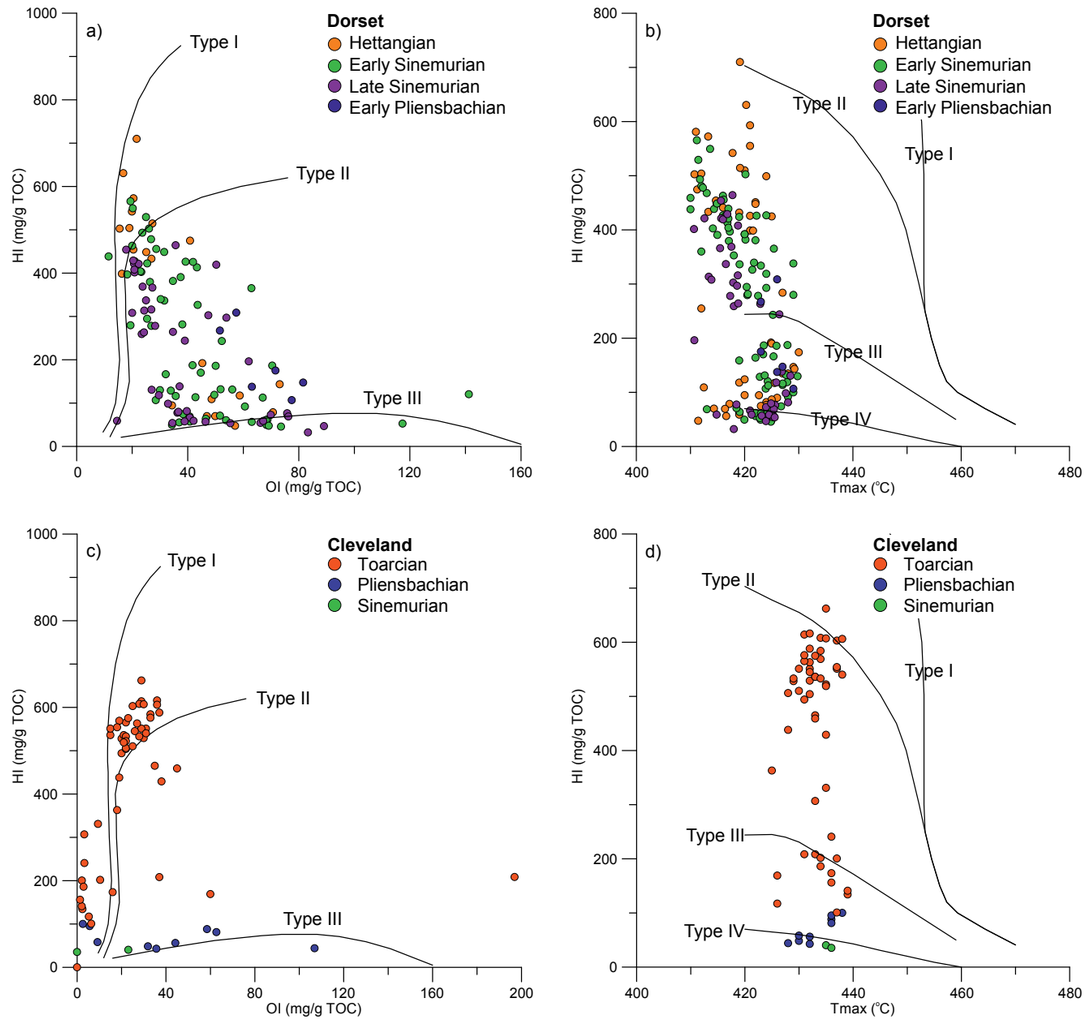

▲ Figure 7.11 Results of the Rock-Eval analyses of the outcrop samples from Dorset (a) Pseudo Van-Krevelen diagram, Tissot & Welte, 1978 and b) HI vs Tmax diagram, Espitalié et al. 1977) and from the Cleveland Basin (c) Pseudo Van-Krevelen diagram and d) HI vs T_{max} diagram).
Both diagrams are used to differentiate between the type and the thermal maturity of the organic matter found in the respective samples. Samples with very low TOC or a Tmax of less than 400 can have a distorted result and should be excluded from these type of plots.
In both outcrop sections the Rock-Eval results support the results from the detailed palynological analyses (Figure 7.1 and 7.2). The Hettangian and Sinemurian samples from the Dorset section show strong variation in organic matter type between terrestrial dominated type III and marine dominated type II organic matter. Highest hydrogen index values (> 600 mg/g TOC) were measured in samples from the Hettangian, indicating excellent source rock quality. The samples from the Early Pliensbachian (Belemnite Marls Mb.) on the other hand show mainly a type III organic matter composition. The maturity of the organic matter, according to the HI vs. Tmax plot (b) is immature to very low maturity.
The samples from the Cleveland Basin tell a different story. In this section only the Pyritous Shale Mb. below the Toarcian was analyzed. Still, the samples from the Sinemurian and Pliensbachian have very little organic matter and show a clear terrestrial type III to type IV signature. The samples from the Toarcian interval on the other hand show mostly excellent type II organic matter, comparable with the best samples from the Dorset section. The maturity of the organic matter in the Cleveland Basin section is slightly higher compared to Dorset and can be generally described as located in the early oil generation window.

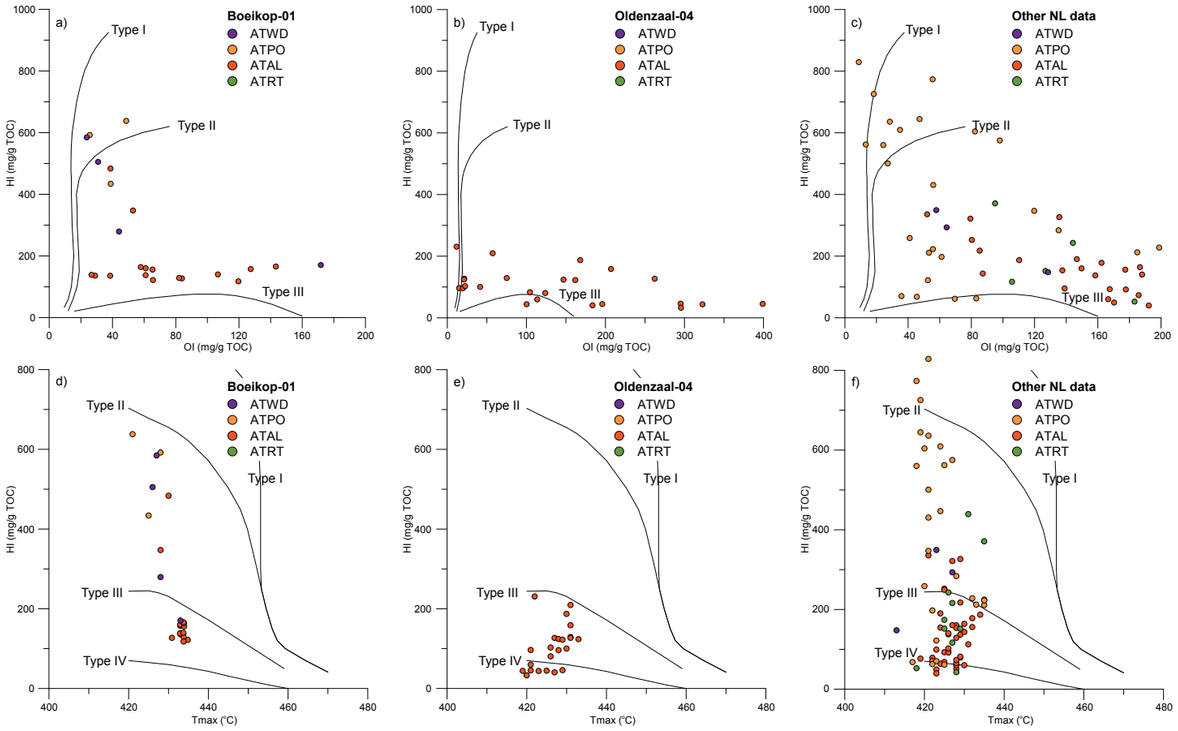

▲ Figure 7.12 Results of the Rock-Eval analyses of the core samples from wells Boeikop-01 (a) Pseudo Van-Krevelen diagram, Tissot & Welte, 1978 and d) HI vs T_{max} diagram, Espitalié et al. 1977) and Oldenzaal-04 (b) Pseudo Van-Krevelen diagram and e) HI vs Tmax diagram) and from earlier analyses of cuttings from several other Dutch on- and offshore wells (c) Pseudo Van-Krevelen diagram and f) HI vs Tmax diagram).
The stratigraphic subdivision of the samples was achieved according to the Dutch stratigraphic subdivision of the Rhaetian and Lower Jurassic Altena Group (van Adrichem Boogaert & Kouwe, 1993-1997). ATRT – Rhaetian Sleen Formation, ATAL – Hettangian to Pliensbachian Aalburg Formation, ATPO – Toarcian Posidonia Shale Formation, ATWD – latest Toarcian to Bajocian Werkendam Formation
The samples from the Dutch wells show very similar results as the outcrop samples from the Cleveland Basin. The samples from the Aalburg Formation in general show very low hydrogen index values and can overall be classified as type III to type IV organic matter. This is particularly the case for the samples from well Oldenzaal-04, that show extremely high oxygen index values, even for samples with reasonable TOC values of around 2%. The best source rock quality can be found in samples from the Toarcian Posidonia Shale Formation. The Rock-Eval results are comparable to the results of the Toarcian samples from the Cleveland Basin with hydrogen index values of > 500 g/mg TOC. Good to reasonable source rock quality can also be attributed to samples from the Werkendam Formation, which was not studied in detail in the context of this study. These results might warrant further research into the hydrocarbon potential of this formation.

7.5 Dilution of organic-matter

In order to evaluate the effect of detritral dilution of organic-matter on the resultant TOC-concentrations we have made use of newly revised cyclostratigraphically-derived ages for the ammonite zones after Ruhl et al. (2016) and Boulila et al. (201), see **Table 7.1**) to calculate relationships between sedimentation rate and TOC-content (**Figure 7.14**). The results indicate that there is a link between sedimentation rate and TOC-content. For instance, during the T-OAE, the TOC-lean record from the Cook Formation is substantially more expanded than the TOC-rich successions from elsewhere. The same holds true for the organic-rich intervals from the Wessex Basin and the T-OAE in an organic-rich facies. The total amount of organic-carbon stored in the respective units is indicated in (**Figure 7.15**) is approximated by multiplying the average TOC-content with the thickness of the Zone/Unit. The results indicate that the T-OAE, even in the organic-lean facies of the Cook Fm. in Well 34/10-35 is a major phase of TOC-accumulation. The production of TOC under anoxygenic marine conditions is an important contributor, however low clastic supply in combination with ample creation of accommodation space is a crucial factor for establishing high TOC, high HI deposits.

Table 7.1 Most recent age-estimates and thicknesses of stratigraphic Zones/Intervals and recorded average and maximum TOC-levels. CB refers to Cleveland Basin, WB to Wessex Basin. The TOC and thickness data from the T-OAE of the Sancerre Core in France are after Hermoso et al. (2012), those from Dotternhausen (Germany after Frimmel et al. (2004), the data from LOZ are after TNO (upubl. data). Other TOC and thickness data are after this study.

Zone/Interval	Duration (Myrs)	Thickness (m)	Average TOC	STDEV TOC	Max TOC in Zone	Reference for Duration
Jamesoni Zone (CB)	2,7	43,2	0,98	0,37	1,75	Ruhl et al. 2016
Margaritatus Zone (CB)	2,4	26	0,98	0,4	2,08	Ruhl et al. 2016
Oxynotum Zone (CB)	1	12,1	0,61	0,17	0,92	Gradstein et al. (2012)
Ibex Zone (CB)	1,8	28	1,14	0,94	0,24	Ruhl et al. 2016
Spinatum Zone(CB)	1,4	6	0,94	0,78	1,19	Ruhl et al. 2016
Raricostatum Zone (CB)	0,8	14,7	0,71	0,21	1,05	Ruhl et al. 2016
Bifrons Zone (CB)	2,15	38	1,97	0,57	3,02	Boulila et al. 2014
Davoei Zone (CB)	0,4	28	0,78	0,28	1,49	Ruhl et al. 2016
Tenuicostatum Zone (CB)	0,6	16	1,42	0,63	3,87	Ruhl et al. 2016
Semicostatum Zone (WB)	1,5	2,75	3,78	3,05	10,68	Gradstein et al. (2012)
T-OAE (Cook Fm., N)	0,5	56	1,29	0,51	2,75	Boulila et al. 2014
Falciferum Zone (CB)	1,2	27	3,32	1,07	6,14	Boulila et al. 2014
Turneri Zone (WB)	1	23,7	3,05	2,25	9,23	Gradstein et al. (2012)
Bucklandi Zone (WB)	1,1	7,6	4,72	4,16	18,69	Ruhl et al. 2016
Obtusum Zone (WB)	1,5	14,4	4,25	2,02	9,39	Gradstein et al. (2012)
Angulata Zone (WB)	0,82	4,6	5,57	3,77	14,22	Ruhl et al. 2016
T-OAE (Sancerre, F)	0,5	4	3,42	2,96	10,80	Boulila et al. 2014
Liasicus Zone (WB)	0,78	2,3	3,67	3,73	11,05	Ruhl et al. 2016
Raricostatum Zone (WB)	0,8	12,4	2,15	1,19	5,41	Ruhl et al. 2016
T-OAE (Dotternhausen, DE)	0,5	3,8	6,5	4,50	14,80	Boulila et al. 2014
T-OAE (Jet Rock (CB)	0,5	7,2	8,08	2,32	12,40	Boulila et al. 2014
T-OAE (LOZ-1, NL)	0,5	15,5	9,46	5,02	17,68	Boulila et al. 2014
Planorbis (WB)	0,31	3,3	7,27	6,15	21,08	Ruhl et al. 2016

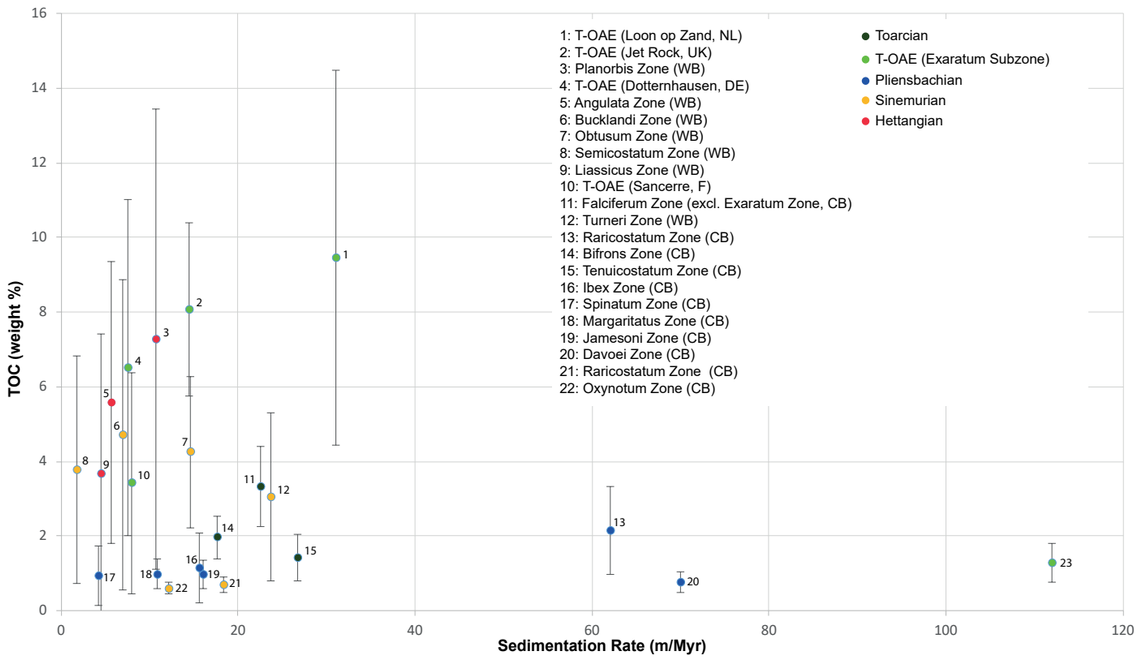

◄ Figure 7.14 Plot between the sedimentation rate and average TOC-content for several 'time-intervals' at several locations. The vertical error bars represent the standard deviation of the mean TOC-value per interval. These time-intervals are Ammonite Zones or the T-OAE. With regards to the latter, the CIE is defined from initiation to recovery for identification in the different locations. The duration is after the information listed in Table 7.1. This plot also includes data from the T-OAE in the Netherlands (Loon-op-Zand core, internal TNO-study), the Sancerre Core in the Paris Basin (Hermoso et al., 2012) and Dotternhausen in Germany (Frimmel et al., 2004).
The results indicate essentially three clusters (A) Intervals with high TOC and low sedimentation rate. These concern the organic-rich intervals from the Wessex Basin and the T-OAE in an organic-rich facies. (B) Intervals with low sedimentation rate and low TOC. These concern the (condensed) siliciclastic Pliensbachian units from the Cleveland Basin. (C) Thirdly there are the intervals with high sedimentation rate and low TOC-values. These concern the Pliensbachian, coarser clastic units from the Cleveland and remarkably, the T-OAE as defined in the Cook Fm. of Well 34/10-35 in Norway.

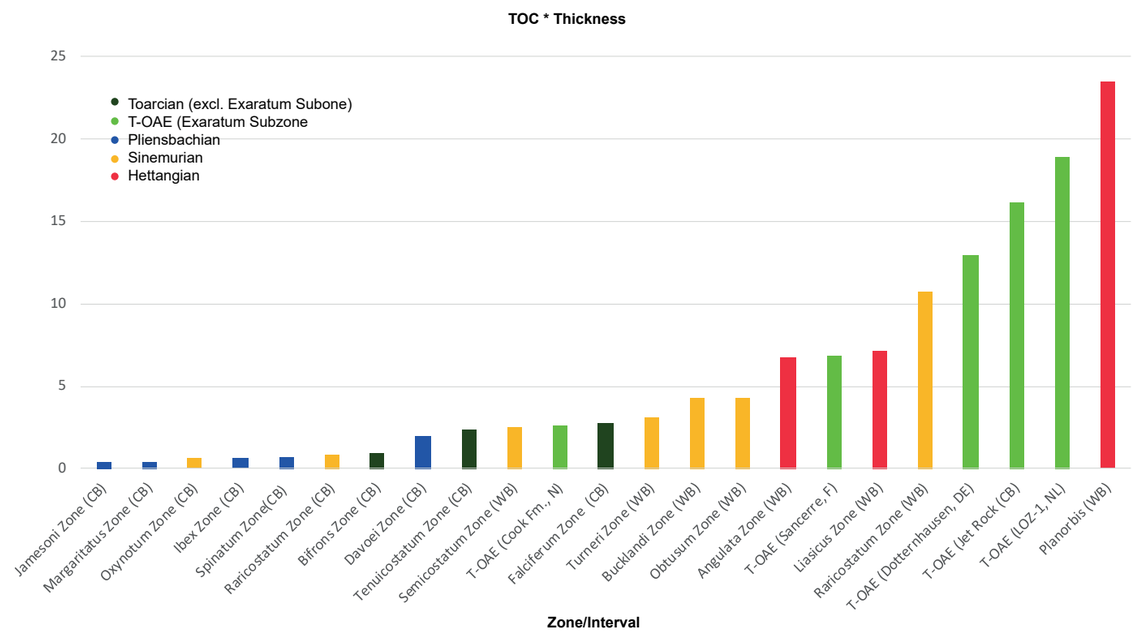

◄ Figure 7.15 Histogram of the TOC * Thickness calculation for the intervals also depicted in Figure 7.14. This graph represents an approximation of the total amount of organic-matter burried in the units. It is clear that the T-OAE represents a major phase of organic-matter accumulation. The same holds true for the basal Hettangian Planorbis Zone from the Wessex Basin.

7.6 Summary

During Triassic-Jurassic boundary times, the emplacement of the Central Atlantic Magmatic Province (CAMP) led to elevated CO_2-concentrations in the atmosphere and installation of a warm climate mode. Due to orbitally-modulated changes in solar insolation, affecting monsoonal run-off patterns, the relatively distal hemipelagic settings with relatively low clastic supply such as the Wessex Basin, were prone to become stratified, leading to the deposition of cycles of excellent hydrogen-rich marine source rocks, marls and limestones through the Hettangian and Early Sinemurian. On the basis of log correlation, a similar system may have been active in parts of the West Netherlands Basin. In many other areas, the clastic supply was too high leading to dilution of organic-matter (**Figure 7.14 and 7.15**).

Through the Late Sinemurian,the climate cooled gradually, possibly as CAMP-volcanism diminished. Across the Sinemurian-Pliensbachian boundary, a substantial transgression and phase of climatic warming is identified. In the outcrop localities we note dysoxic depositional settings and the signs of stagnation, but we do not record any substantial TOC-accumulation (**Figure 7.8**). The remainder of the Pliensbachian is characterized by low relative sea-level and cool conditions.

The Pliensbachian-Toarcian boundary marks a major regime shift in depositional patterns through the study area. The boundary marks a trangression and importantly, a first substantial carbon isotope excursion (CIE). Subsequently a series of high TOC, high HI sulphur bands are recorded in the Cleveland Basin before the system is severely perturbed in association with the CIE of the Toarcian Oceanic Anoxic Event (T-OAE). These CIEs denote perturbations of the carbon cycle and related climatic warming. In turn, this led to an alteration of the hydrological cycle leading to widespread salinity-driven stratification and consequent water-column anoxia. Under these circumstances, areas with relatively low clastic supply are susceptible to the deposition of organic-rich and hydrogen-rich sediments. In areas with higher clastic supply, such as in parts of the Viking Graben area (the Upper Cook Fm.), indicators for water-column anoxia are also recorded. Here however, this has not led to organic enrichment. Hence, in more 'shaly' facies equivalents of the Upper Cook Fm., source-rock presence may be expected.

This 'dysoxic' mode is sustained through parts of the Southern North Sea Basin, and an additional 'stagnation-event' is recorded in the Bifrons Zone. However, perturbations as grave as the T-OAE are not recorded. The early Toarcian carbon cycle perturbations are possibly related to pulses of volcanic outgassing in the Karroo Farrar Large Igneous Province and associated feedbacks. This may explain why the event and its expression is so unique and non-repetitive.

Pecten from Cleveland ironstone

8. Paleogeography and conclusions

8. PALEOGEOGRAPHY AND CONCLUSIONS

In this chapter we discuss the results and insights arising from this study in a regional context. To this end, we have compiled the information for four timeslices and schematically illustrate the depositional development per area (**Figure 8.1 - 8.4**). An overview of the underlying information is depicted in **Figure 8.5**. At the end of this chapter we summarize the main observations and implications from this study.

8.1 Hettangian to Early Sinemurian

Wessex Basin

Frequent cyclicity between Type-II organic-rich mudstones and organic poor (mostly wood dominated Type-III) marls and micritic carbonate beds. These occasionally represent excellent source rock properties. This system is driven by cyclic variation in run-off that episodically leads to fresh water-induced stratification, subsequent anoxia and the proliferation of hydrogen rich organic-matter. In the Early Sinemurian, the source rock quality decreases and more wood is recorded. It seems that the basin receives more clastic material, likely as a consequence of sea-level lowering.

Cleveland Basin

Hettangian deposits are not accessibly exposed in the Cleveland Basin area. They are present in the foreshore of Redcar, but can not be accessed for further evaluation. Lower Sinemurian deposits of the Calcareous Shale Mb. are very shallow marine mudstones with carbonate (shell) beds that are the result of storm activity.

UK Southern North Sea and Netherlands

Based on log patterns we note a cyclicity between mudstone and limestone beds. Further offshore (e.g., Dutch Central Graben), this cyclicity is less apparent. In the southern part of the onshore NL (West Netherlands Basin), there is possibly organic matter enrichment in mudstone invervals (further studies needed), based on the gammalog signature.

Norwegian-Danish and Farsund Basin

Terrigeneous dominated mudstones (basal Fjerritslev Fm.) and near-shore sandstones (Gassum Fm.) are deposited in this area indicating very shallow marine to upper shoreface environments.

Viking Graben Area

Fluviodeltaic sandstones with coal layers are deposited as part of the Statfjord Group. These are derived predominantly from the uplifted Fennoscandian High. Elsewhere there is no substantial uplift of land-masses supplying coarse clastics.

Hettangian and Early Sinemurian

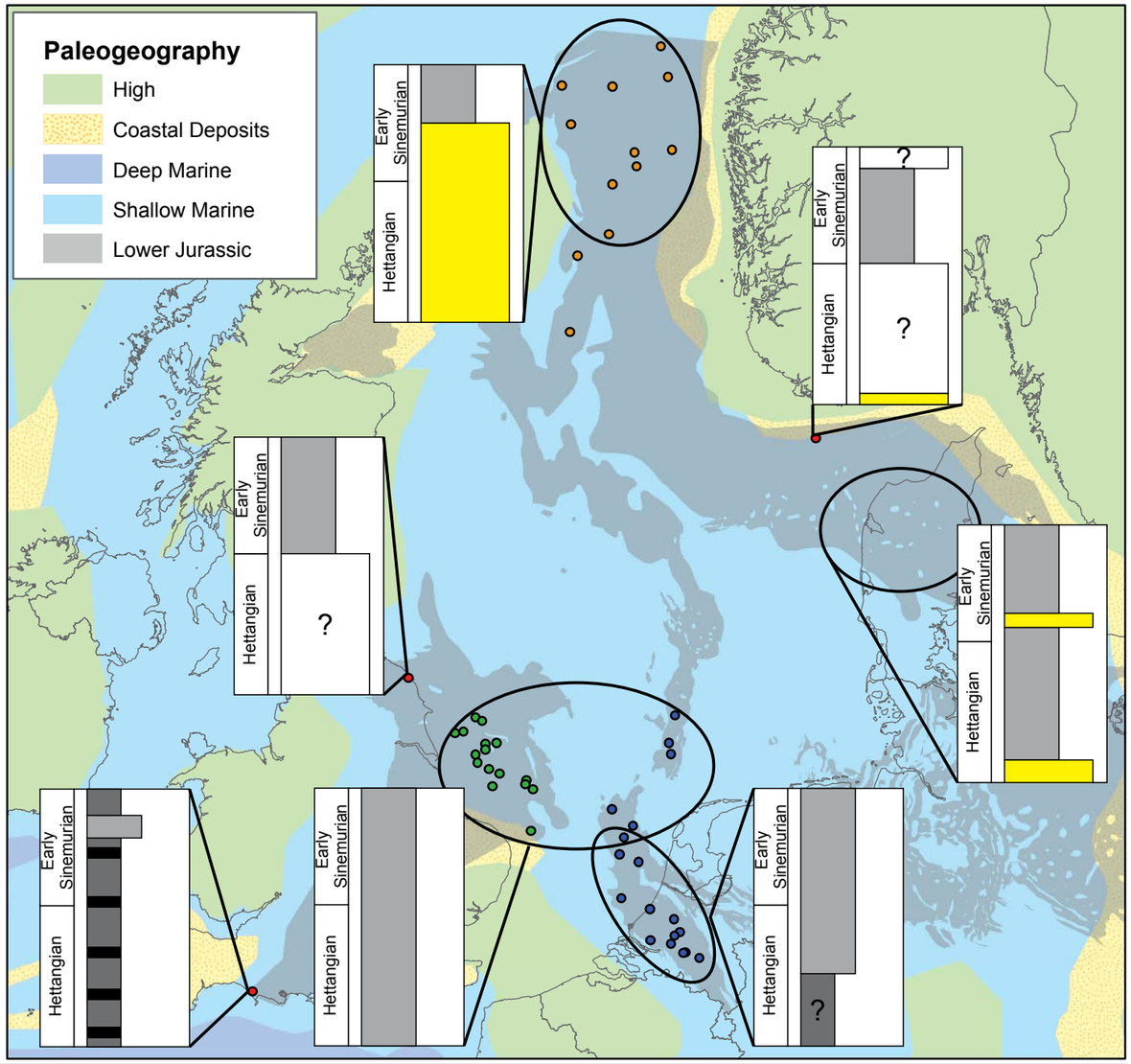

▲ **Figure 8.1: Sketch of the regional expression of the Hettangian to Lower Sinemurian sediments.** Black: organic rich mudstones, dark grey: dysoxic mudstones but no elevated TOC levels, light grey: mud- and fine siltstones, yellow: silt- and sandstones, white: no information or hiatus.

Summary

The Wessex Basin was the most distal, hemipelagic setting of the study area. Here, and arguably in parts of subsiding basins like the West Netherlands Basin, run-off driven source-rock, marl, limestone cyclicity is observed. Organic-matter in source-rock intervals is of marine and bacterial origin. It thus seems likely that the accummulations are the consequence of enhanced organic-matter production in the anoxic water-column. This system became active at the same time as the carbon isotope excursion that accompanies the Triassic-Jurassic boundary. The latter indicates enhanced CO_2-input and global warming.

In most of the Southern North Sea, shallow marine deposits with shell beds illustrate a general absence of coarse grained clastics. Despite the overall fine-grained nature, the depositional setting was not favourable for organic-matter accumulation, due to limited water depth and/or dilution.

In the Northern North Sea and Viking Graben area, deltaic depositional setting evidences major erosion from the Fennoscandian high(s). Organic matter is present in localized coal seams.

8.2 Late Sinemurian and Early Pliensbachian

Wessex Basin

Along the Dorset Coast, the Upper Sinemurian deposits predominantly comprise organic-lean claystones. The organic-matter that is present is of terrestrial origin, much akin to the organic-lean intervals of the Hettangian-Early Sinemurian.

The overlying Belemnite Marls Mb. comprises thin organic rich shales in the Lowermost Pliensbachian. These post-date the negative CIE across the Pliensbachian-Sinemurian boundary.

The depositional setting is still hemipelagic, receiving ample terrestrial material but without any coarser grained clastics. Bottom-water conditions were predominantly oxic.

Cleveland Basin

Bioturbated shales and marine mudstones with storm beds are deposited in the Late Sinemurian. Across the Sinemurian-Pliensbachian a transition to more distal and dysoxic settings of the Pyritous Shale Mb. took place. Substantial organic enrichment is not recorded. The dysoxic conditions pertain to the sediment-water interface and not to the actual water column. A productive anoxygenic ecosystem was not in place.

UK Southern North Sea and Netherlands

Based on logs and the Oldenzaal core, we conclude that in the Late Sinemurian, organic-lean mudstones with more consolidated carbonaceous intervals were deposited. In the Early Pliensbachian we note very uniform organic-lean mudstone deposition. We found no evidence for dysoxia in the Early Pliensbachian.

Norwegian-Danish and Farsund Basin

In the Norwegian-Danish Basin the Upper Sinemurian part of the Fjerritslev Fm. comprises rather uniform, terrestrial-dominated mudstones. Based on macrofaunal turnover the lowermost Pliensbachian is suggested to mark the effects of anoxic conditions locally.

Viking Graben Area

Upper Sinemurian to Lower Pliensbachian deposition is dominated by proximal marine bioturbated siltstones in the more distal Viking Graben(Amundsen Fm.) and sandstone (Johansen Fm.) on the Horda Platform to the east.

Late Sinemurian and Early Pliensbachian

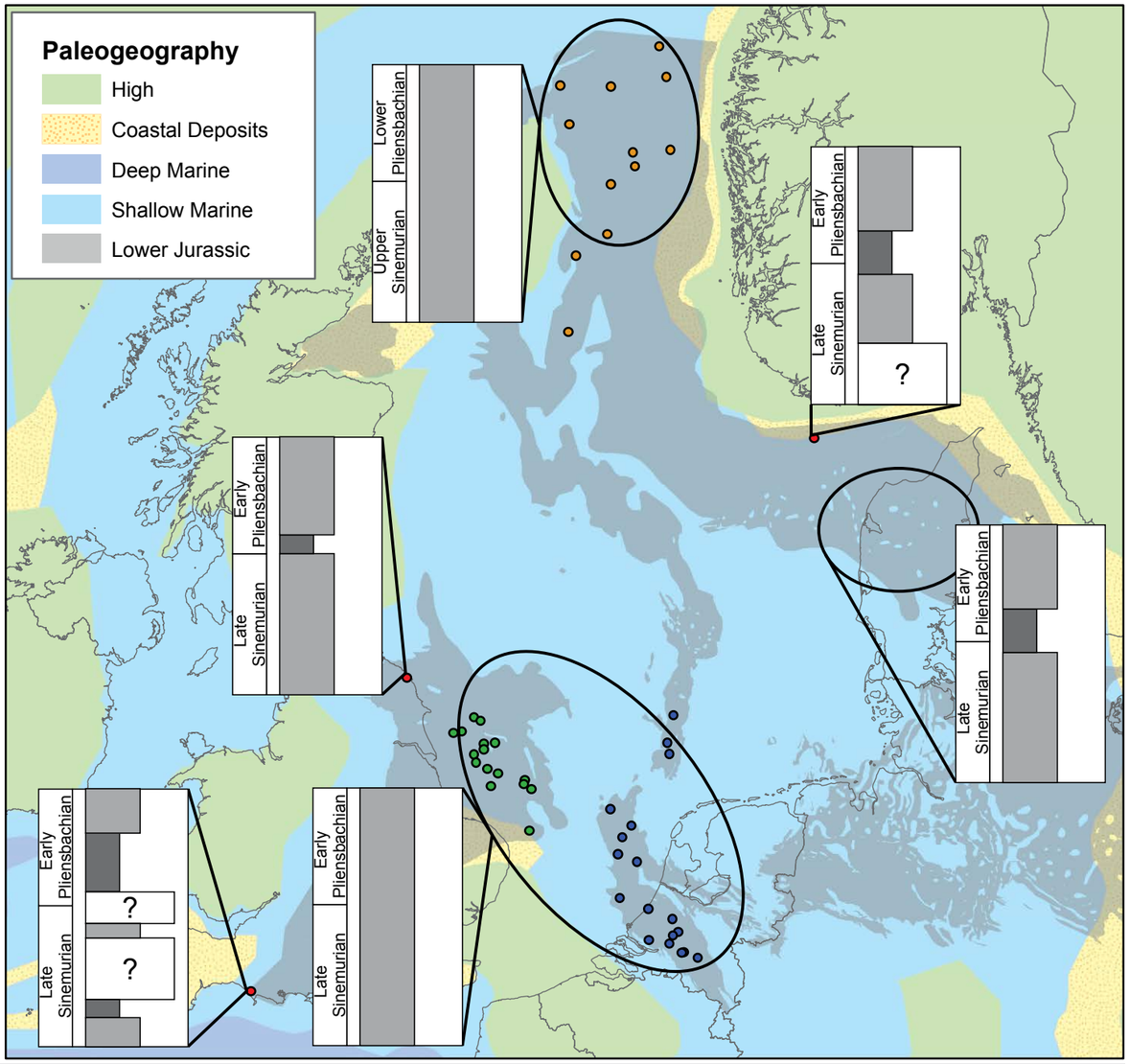

▲ Figure 8.2 Sketch of the regional expression of the Upper Sinemurian to Lower Pliensbachian sediments.
Dark grey: dysoxic mudstones but no elevated TOC levels, light grey: mud- and fine siltstones, yellow: silt- and sandstones, white: no information or hiatus.

Summary

The Late Sinemurian was a period of low relative sea level and relatively cool climate conditions. In most of the study area there is a predominance of fine-grained deposition. There is no evidence for pronounced oxygen depletion or organic enrichment in the Late Sinemurian.The Sinemurian-Pliensbachian boundary marks a change in this respect. This interval is marked by a carbon isotope excursion, a transgression and a transition to a warmer climate mode. At several localities, dysoxic conditions arise in a more distal settings.There is however no evidence for substantial organic-enrichment in the wells that we have investigated.

8.3 Late Pliensbachian

Wessex Basin
The Upper Pliensbachian corresponds to the condensed glauconitic sandstones of the Dyrham Fm. These and subsequent condensed sections probably result from sediment starvation with sediment accumulation occurring preferentially in more proximal settings.

Cleveland Basin
The Upper Sinemurian witnesses the most shallow and proximal depositional facies of the Lower Jurassic in the Cleveland with the Staithes Sandstone and Cleveland Ironstone Formations. The early Late Pliensbachian Staithes Sandstone Fm. is interpreted as shoreface sandstones, within the influence of wave action. The overlying late Late Pliensbachian Cleveland Ironstone Fm. is substantially more shallow and proximal with the deposition of oolitic ironstone and intercalated mudstones, interpreted to be indicative of a sediment-starved beach facies. Hence, albeit getting shallower the coarse clastic supply diminishes through the Late Pliensbachian.

UK Southern North Sea and Netherlands
In the lower part of the Upper Pliensbachian we have noted coarser silt to sandstone deposits. Logs show multiple coarsening upwards trends followed by a log-based decrease in grain-size. In the southern part of the Dutch onshore, we note a less clear coarsening signal. In analogy to the Cleveland Basin, we reconstruct a similar depositional history for this interval.

Norwegian-Danish and Farsund Basin
Organic-lean mudstones are consecutively becoming coarser finishing with shoreface sand deposition in the Latest Pliensbachian. There is no evidence for oxygen-depletion. Like in the Cleveland Basin, increased fresh-water influence is recorded up to the top of the Pliensbachian.

Viking Graben Area
Deposition in the area was fairly heterogenous, with proximal marine mudstones (Burton Fm.) intertwined with deltaic sandstones of the (Lower) Cook Fm. in areas under the influence of delta-lobe expansion from the east.

Summary
Overall the Upper Pliensbachian represents relatively shallow/proximal depositional settings ranging from deltaic and beach facies to shallow-marine mudstones. In the Southern North Sea area, the early Late Pliensbachian experienced a period of enhanced supply of coarse-grained clastics. This could be linked to a phase of enhanced erosion, possibly related to a phase of transient Mid-North Sea Thermal Doming. Climatic conditions were relatively cool, reaching the coldest phase of the Early Jurassic in the Margaritatus Zone.

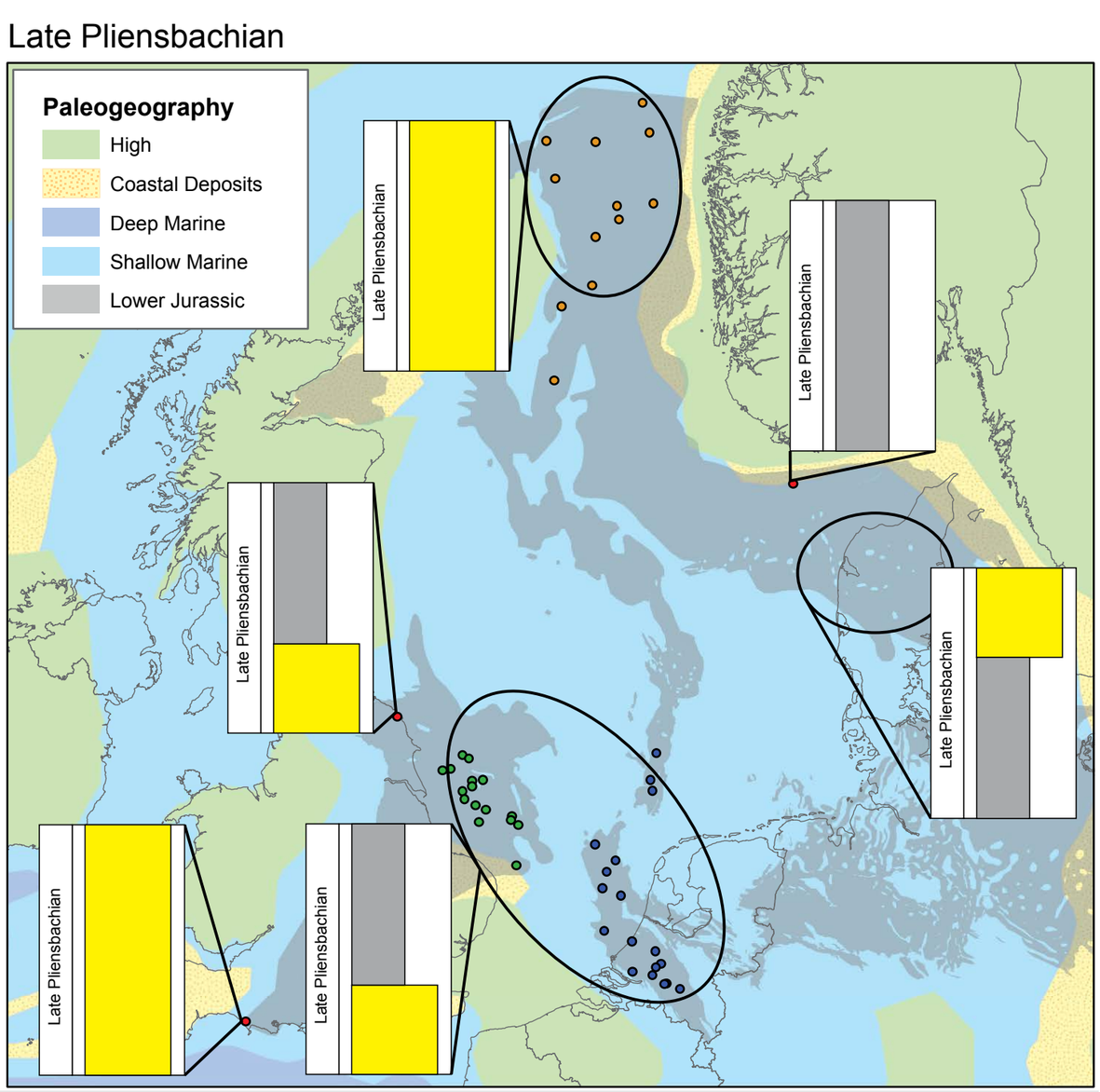

▲ **Figure 8.3 Sketch of the regional expression of the Upper Pliensbachian sediments.**
Light grey: mud- and fine siltstones, yellow: silt- and sandstones.

8.4 Toarcian

Wessex Basin
The Lower and most of the Upper Toarcian is contained in the condensed Beacon limestone bed. The Uppermost Toarcian corresponds to the lower shoreface sandstones of the Bridport Sandstone Fm. Hence, there was an overall absence of sediment supply through much of the Toarcian. A phase of hinterland uplift and increased sediment supply caused Late Toarcian sandstone deposition.

Cleveland Basin
The Grey Shale Mb. marks a substantial change compared to the underlying Cleveland Ironstone Fm. At the base of this unit the carbon isotope excursion of the Pliensbachian-Toarcian boundary is recorded. In this mudstone unit, organic-rich sulphur bands occur. The T-OAE is recorded in the Jet Rock Unit, with high organic-carbon content and conspicuous early diagenetic limestone concretions. The T-OAE expression is driven by enhanced run-off due to climatic warming and the installation of an anoxygenic microbial ecosystem under severe water-column stratification. The Lower Toarcian and lower Upper Toarcian successions remain predominantly fine-grained and somewhat elevated in TOC. However, the degree of stratification gradually diminishes, with an exception in the Bifrons Zone. TOC-content declines gradually to reach values of about 2% and anoxic conditions are recorded. The uppermost Toarcian marks a transition to silt- and eventually sandstones.

UK Southern North Sea
On the basis of log-patterns, mudstones seem the dominant lithology during the Toarcian. However, no distinct high Gammaray peaks are recorded, as known from the Dutch on- and offshore (see below). Possibly, the area was under the influence of more oxygenated Tethyan-derived water masses flowing across the landstrait that covers the modern-day British Island. The Upper Toarcian is typically eroded as a consequence of Aalenian uplift. In local graben structures, the remnants of shallow marine sheet sandstones are recorded (Phillips Mb.).

Netherlands
Organic rich shales with very organic-rich intervals were deposited during the T-OAE. Similar precursor beds like the Grey Shale Mb. in the Cleveland Basin are recorded. The thickest and most organic-prone deposits are encountered in the deeper basinal parts, such as the Central Graben area. Particularly noteworthy are the carbonate beds that are recorded in the Jet Rock in the Cleveland Basin. These are also recognized on logs in the Netherlands.The upper part of the Toarcian is sparsely penetrated, whenever encountered they represent organic poor to lean mudstones of the Lower Werkendam Mb.

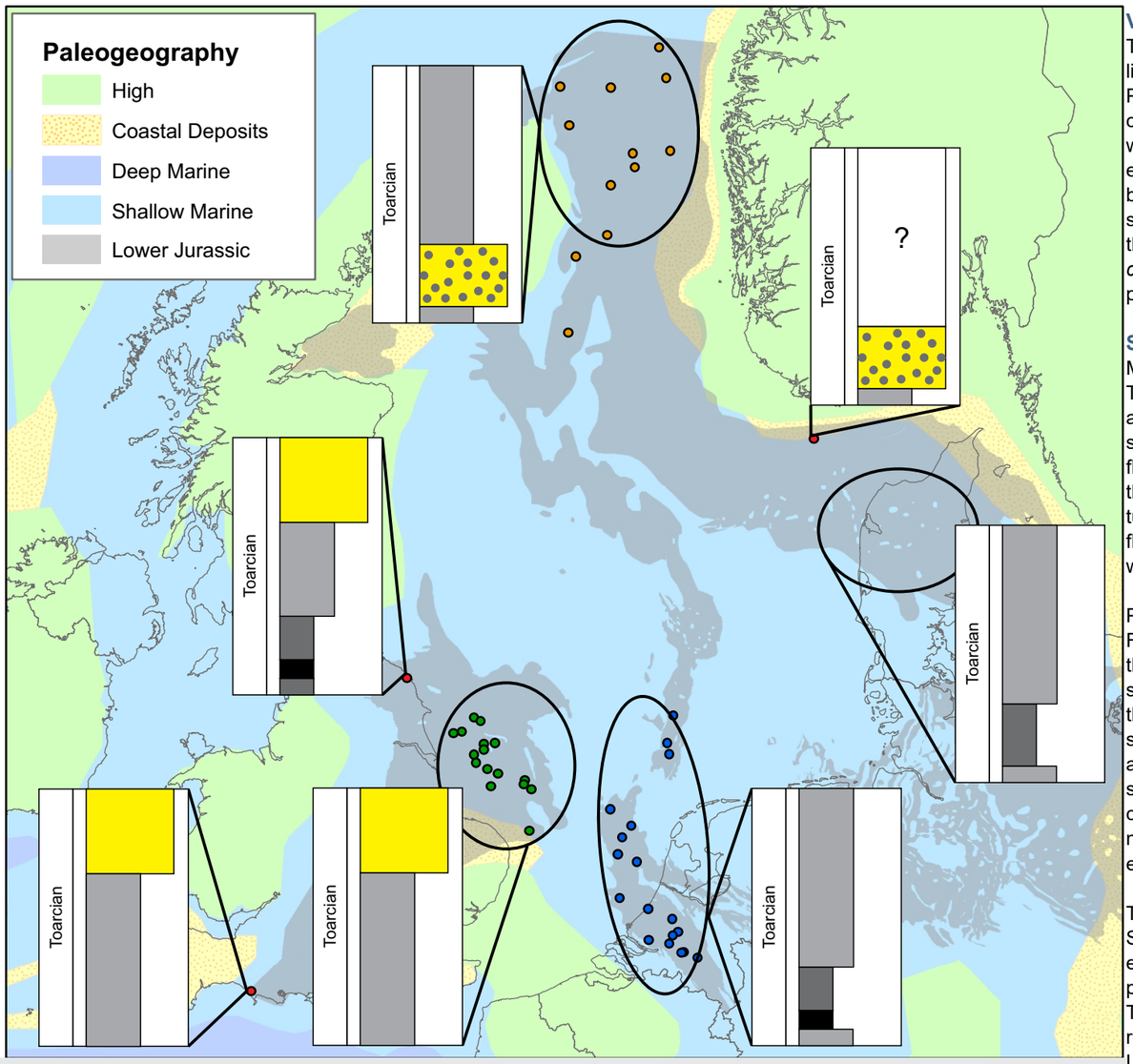

▲ Figure 8.4 Sketch of the regional expression of the Toarcian sediments.
Black: organic rich mudstones, T-OAE, dark grey: dysoxic mudstones but no elevated TOC levels, light grey: mud- and fine siltstones, yellow: silt- and sandstones, yellow with grey dots: sandstones containing organic material, white: no information or hiatus.

Norwegian-Danish Basin and Farsund Basin
In deeper parts of the basin, organic-rich Type-II marine shales are encountered, thus representing a similar T-OAE depositional mode as recorded in the UK and the Netherlands. However in general, TOC-enrichment is substantially less pronounced. This relates to shallower depositional setting and/or higher sedimentation rates. Upper Toarcian deposits are mainly marine mudstones with shoreface sandstones. In the Farsund Basin we have arguably recorded a very proximal fluviodeltaic sediment record across the T-OAE. The exact age-dating however remains somewhat elusive. If indeed the case, than the T-OAE corresponds to a run-off pulse, flooding the overbanks of the delta-system. Interestingly, the T-OAE then also represents a source-rock candidate due to the high abundance of the green alga *Botryococcus*.

Viking Graben Area
The deltaic Upper Cook Fm. contains the CIE of the T-OAE, likely in a transgressive systems tract of a delta system. Palynological patterns indicate a strongly stratified water column here as well. Albeit we have not encountered any wells in which the T-OAE is contained in a more shaly equivalent (Drake Fm.), organic matter accumulations might be encountered in a more distal setting. Interestingly, in some wells in the UK (211-block, East Shetland Platform), the Drake Formation contains very high GR values. These *could* correspond to the T-OAE. This can be tested by performing carbon isotope analyses on these wells.

Summary
Major sea-level rise characterizes the Earliest Toarcian. Two major CIEs, at the Pliensbachian-Toarcian-boundary and at the base of the Falciferum Zone are indicative of superimposed greenhouse warming and related high-order floodings. These perturbations also left a clear signal on the terrestrial vegetation records, that underwent major turnover. Perhaps as a consequence of Early Toarcian flooding, a biogeographic connection to the Arctic realm was established.

Particularly during the T-OAE (Exaratum Subzone of the Falciferum Zone), greenhouse warming led to altering the hydrological cycle causing widespread salinity-driven stratification and consequent water-column anoxia. Under these circumstances, areas with relatively low clastic supply were susceptible to the deposition of organic-rich and hydrogen-rich sediments. In areas with higher clastic supply, such as in the Upper Cook Fm., indicators for water-column anoxia are also recorded. Here however, this has not led to organic enrichment. Hence, in more ‘shaly’ facies equivalents, source-rock presence may be expected.

This ‘dysoxic’ mode is sustained through parts of the Southern North Sea Basin, and an additional ‘stagnation-event’ is recorded in the Bifrons Zone. However, perturbations as grave as the T-OAE are not recorded. The early Toarcian carbon cycle perturbations are possibly related to pulses of volcanic outgassing in the Karroo Farrar Large Igneous Province and associated feedbacks. This may explain why the event and its expression is so unique and non-repetitive.

The Late Toarcian general sea level fall and transition to coarser grained sediments marks the beginning of uplift of Central North Sea dome. In the Viking Graben area rift formation led to continuing subsidence and progressive deposition of finer grained sediments (Drake Fm.), until the Brent Group overstepped/incised. The latter is considered a consequence of uplift of the dome in the Bajocian.

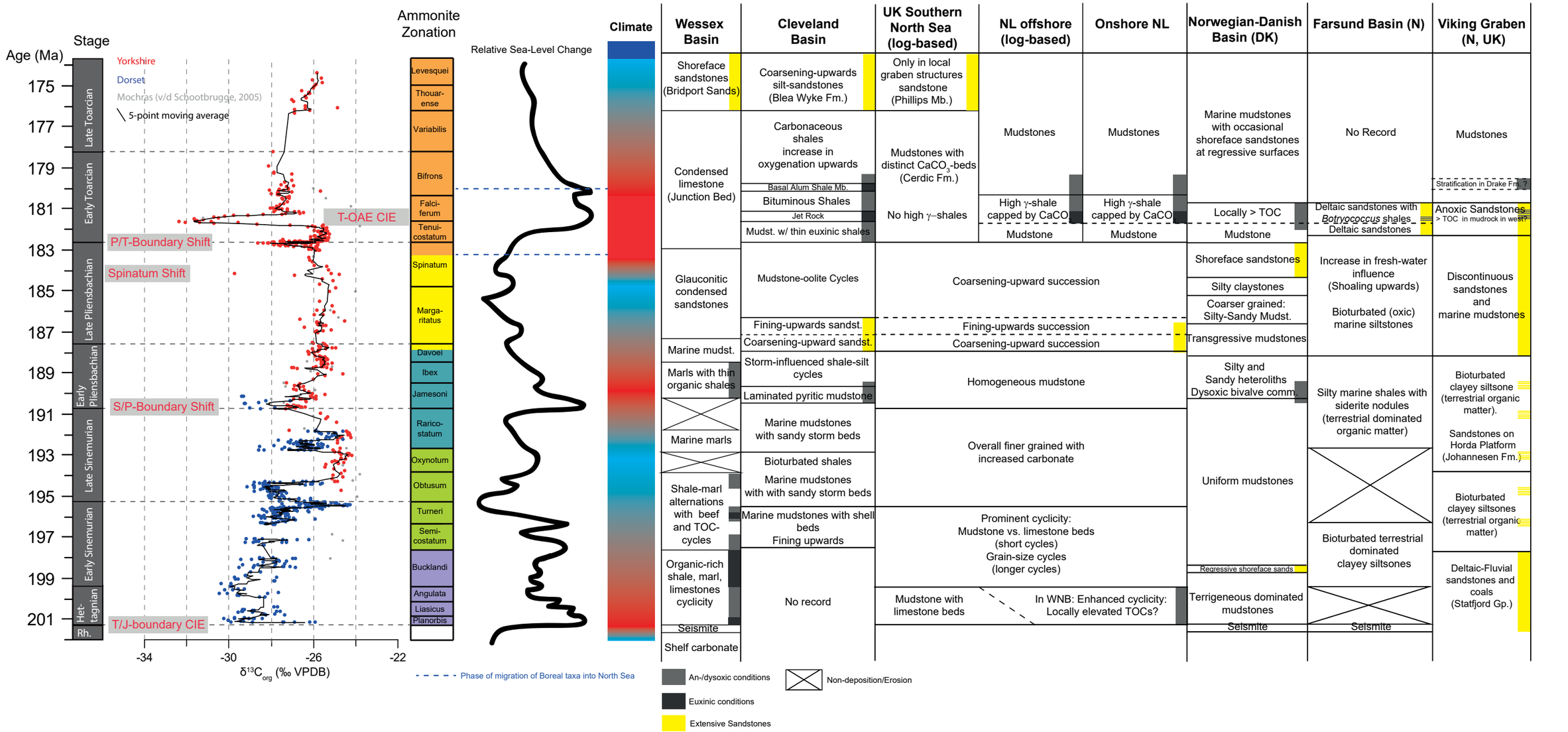

▲ **Figure 8.5 Summary of stratigraphic, sea-level and climatic patterns and description of regional environments.** The colored (grey, black and yellow) shading indicate phases of dys- and anoxia, euxinia (or strong anoxia) and the deposition of coarser grained clastics. Intervals that are not deposited in a certain area, are marked with a cross. The information is based on the present study and numerous publications that are cited elsewhere in this report. The information from Denmark is largely based on Petersen et al. (2008).

8.5 Main observations

1. During the Earliest Jurassic (Hettangian – Early Sinemurian) organic-rich strata were deposited in hemipelagic settings, with relatively low clastic supply. This follows upon the Triassic-Jurassic Boundary and its carbon cycle perturbation.

2. The Late Sinemurian contains no source rock potential. Climate was relatively cool.

3. The Early Pliensbachian marks dysoxic conditions at numerous localities. This follows upon the Sinemurian-Pliensbachian boundary CIE. No substantial organic matter enrichment was recorded in the studied section, but could be present in locally restricted (sub-)basins.

4. The Late Pliensbachian marks the lowest sea-level of the Lower Jurassic. Climate was relatively cool. In the Southern North Sea the early Late Pliensbachian is coarser-grained. This is related to relative sea-level fall and possibly initial thermal doming.

5. The Pliensbachian - Toarcian Boundary sets the stage for Early Toarcian deoxygenation. It contains a precursor Carbon Isotope Excursion (CIE) to the one widely known from the Toarcian Oceanic Anoxic Event (T-OAE). Biogeographic patterns indicate the establishment with the boreal realm just before the T-OAE.

6. The T-OAE culminates in run-off driven source-rock deposition, particularly in deeper, distal parts of the basins. In the Viking Graben area, the T-OAE corresponds to the Upper Cook Fm. sandstones. On the basis of log patterns, the T-OAE seems analogous to the Drake Fm. in a more shaly facies towards the western end of the Viking Graben area.

7. In most of the Southern North Sea area TOC remains elevated immediately after the T-OAE. No recurrence “events” of similar magnitude are recorded after the T-OAE.

8.6 Implications

1. The results reveal a remarkably close correspondence between carbon cycle pertrubations as revealed by isotope trends, climate, run-off, anoxia and organic-enrichment. Source-rock genesis is related to elevated anoxygenic primary productivity under anoxic water-column conditions.

2. Areas undergoing enhanced subsidence, and relatively low clastic supply are best suited for the accumulation of organic-rich deposits.

3. The Toarcian Oceanic Anoxic Event really stands out regionally and affects an array of depositional environments.

4. lowermost Lower Jurassic deposits (Hettangian - Early Sinemurian) are more widely distributed than those corresponding to the T-OAE, which are often eroded due to Thermal Doming and Aalenian sea-level fall. Since the lowermost Lower Jurassic is prone to be prolific in basinal parts, additional source-rock potential might be invoked.

5. The Late Pliensbachian, in addition to eustatic sea-level lowering marks a phase of widespread continental uplift, perhaps related to initial thermal doming.

09

References

9. REFERENCES

Ager, D.V., 1975. The Jurassic world ocean (with reference to the North Atlantic): J*urassic Northern North Sea Symposium, Stavanger*, 1–43.

Al-Arouri, K., Greenwood, P.F., Walter, M., 1999. A possible chlorophycean affinity of some Neoproterozoic acritarchs. *Organic Geochemistry* 30, 1323–1337.

Algeo, T.J., Maynard, J.B., 2004. Trace-element behaviour and redox facies in core shales of Upper Pennsylvanian Kansas-type cyclothems. *Chem. Geol.* 206, 289–318.

Algeo, T.J., 2004. Can marine anoxic events draw down the trace-element inventory of seawater? *Geology* 32, 1057–1060.

Algeo, T.J., Ignall, E., 2007. Sedimentary C_{org}:P ratios, paleocean ventilation, and Phanerozoic atmospheric pO_2. *Palaeogeography, Palaeoclimatology, Palaeoecology* 256, 130–155.

Algeo, T.J., Tribovillard, N., 2009. Environmental analysis of paleoceanographic systems based on molybdenum–uranium covariation. *Chemical Geology* 268, 211–225.

Anderson, R.F., Fleisher, M.Q., Lehuray, A.P., 1989. Concentration, oxidation-state, and particulate flux of uranium in the Black-Sea. *Geochim. Cosmochim. Acta* 53, 2215–2224.

Breit G.N., Wanty R.B., 1991. Vanadium accumulation in carbonaceous rocks: a review of geochemical controls during deposition and diagenesis. *Chem. Geol.* 91, 83–97.

Batten, D.J., 1974. Wealden palaeoecology from the distribution of plant fossils. *Proceedings of the Geologists' Association*, 85(4), 433–458.

Bessa, J.L., Hesselbo, S.P., 1997. Gamma-ray character and correlation of the Lower Lias, SW Britain. *Proceedings of the Geologists' Association*, 108(2), 113–129.

Bonis, N.R., Ruhl, M., Kürschner, W.M., 2010. Climate change driven black shale deposition during the end-Triassic in the western Tethys. *Palaeogeography, Palaeoclimatology, Palaeoecology*, 290(1), 151–159.

Bonis, N.R., Van Konijnenburg-Van Cittert, J.H.A., Kürschner, W.M., 2010. Changing CO_2 conditions during the end-Triassic inferred from stomatal frequency analysis on Lepidopteris ottonis (Goeppert) Schimper and Ginkgoites taeniatus (Braun) Harris. *Palaeogeography, Palaeoclimatology, Palaeoecology*, 295(1), 146–161.

Bottrell, S., Raiswell, R., 1989. Primary versus diagenetic origin of Blue Lias rhythms (Dorset, UK): evidence from sulphur geochemistry. *Terra Nova*, 1(5), 451–456.

Brenner, W., 1986. Bemerkungen zur Palynostratigraphie der Rhät-Lias-Grenze in SW-Deutschland (Palynostratigraphical Remarks on the Rhaetic-Liassic Boundary in SW-Germany). *Neues Jahrbuch für Geologie und Paläontologie-Abhandlungen*, 173(2), 131–166.

Brumsack, H.-J., Gieskes, J.M., 1983. Interstitial water trace metal chemistry of laminated sediments from the Gulf of California, Mexico. *Marine Chemistry* 14, 89–106.

Buchanan, J.G., 1998. The exploration history and controls on hydrocarbon prospectivity in the Wessex basins, southern England, UK. *Geological Society, London, Special Publications*, 133(1), 19–37.

Bujak, J.P., Williams, G.L., 1985. Mesozoic and Cenozoic dinoflagellates. *Plankton Stratigraphy. Cambridge University Press, Cambridge*, 847–965.

Chamock, M.A., Kristiansen, I.L., Ryseth, A., Fenton, J.P.G., 2001. Sequence stratigraphy of the lower jurassic dunlin group, northern North Sea. *Norwegian Petroleum Society Special Publications*, 10, 145–174.

Cobbold, P.R., Zanella, A., Rodrigues, N., Løseth, H., 2013. Bedding-parallel fibrous veins (beef and cone-in-cone): worldwide occurrence and possible significance in terms of fluid overpressure, hydrocarbon generation and mineralization. *Marine and Petroleum Geology* 43, 1–20.

Coward, M.P., Dewey, J., Hempton, M., Holroyd, J., 2003. Tectonic Evolution. *The Millennium Atlas: Petroleum Geology of the Central and Northern North Sea*, 17–33.

Courtinat, B., Malartre, F., & Giraud, F., 1998. Le Rhetien en region Lyonnaise: analyse palynologique. *Geol. Fr,* 1, 3-19.

Cox, B.M., Sumbler, M.G., Ivimey-Cook, H.C., 1999. A formational framework for the Lower Jurassic of England and Wales (onshore area). Keyworth, Nottingham, *British Geological Survey*, 1–25.

Davies, E.H., 1985. The miospore and dinoflagellate cyst oppel-zonation of the Lias of Portugal. *Palynology* 9, 105–132.

Dean, W.T., Donovan, D.T., Howarth, M.K., 1961. The Liassic ammonite zones and subzones of the north-west European Province. *Bulletin of the British Museum of National History* 4, 437–505.

Deconinck, J.F., Hesselbo, S.P., Debuisser, N., Averbuch, O., Baudin, F., Bessa, J., 2003. Environmental controls on clay mineralogy of an Early Jurassic mudrock (Blue Lias Formation, southern England). *International Journal of Earth Sciences* 92, 255–266.

Dera, G., Brigaud, B., Monna, F., Laffont, R., Pucéat, E., Deconinck, J.F., Pellenard, P., Joachimski, M.M., Durlet, C., 2011. Climatic ups and downs in a disturbed Jurassic world. *Geology*, 39(3), 215–218.

Dera, G., Donnadieu, Y., 2012. Modeling evidences for global warming, Arctic seawater freshening, and sluggish oceanic circulation during the Early Toarcian anoxic event. *Paleoceanography* 27(2), 1–15.

De Vains, G., 1988. Etude palynologique prèliminaire de l'Hettangien à l'Aalènien du Quercy (France). *Bulletin des Centres de Recherches Exploration–Production Elf-Aquitaine* 12, 451–469.

Doornenbal, J.C., Stevenson, A.G., 2010. Petroleum Geological Atlas of the Southern Permian Basin area. E*AGE Publications, Houten, NL* pp. 342.

Dreyer, T., Wiig, M., 1995. Reservoir architecture of the Cook Formation on the Gullfaks field based on sequence stratigraphic concepts. *In: Steel, R.J., Felt, V., Johannessen, E.P., Mathieu, C. (eds.), Sequence Stratigraphy of The Northwest European Margin. Norwegian Petroleum Society, Special Publication* 5, 109–142.

Dybkjær, K., 1991. Palynological zonation and palynofacies investigation of the Fjerritslev formation (Lower Jurassic—basal Middle Jurassic) in the danish subbasin. *DGU, Danmarks Geologiske Undersøgelse. Serie A* 30, 4–150.

Espitalié, J., Laporte, J.L., Madec, M., Marquis, F., Leplat, P., Paulet, J., Boutefeu, A., 1977. Methode rapide de characterisation des roches meres, de leur potential petrolier et de leur degre d'evolution. *Rev. Inst. Fr. Petr.* 32, 23–42.

Evans, D. (Ed.), 2003. The Millennium Atlas: Petroleum Geology of the Central and Northern North Sea *[a Project of the Geological Society of London, the Geological Survey of Denmark and Greenland and the Norwegian Petroleum Society]*.

Feist-Burkhardt, S., Wille, W., 1992. Jurassic palynology in southwest Germany–state of the art. *Cahiers de Micropaléontologie NS 7*, 141–156.

Fensome, R.A., Taylor, F.J.R., Norris, G., Sarjeant, W.A.S., Wharton, D.I., Williams, G.L., 1993. A classification of living and fossil dinoflagellates. *Sheridan Press,* Hanover, Pennsylvania, USA. pp. 351.

Folkestad, A., Veselovsky, Z., Roberts, P., 2012. Utilising borehole image logs to interpret delta to estuarine system: A case study of the subsurface Lower Jurassic Cook Formation in the Norwegian northern North Sea. *Marine and Petroleum Geology*, 29, 255–275.

French, K. L., Sepulveda, J., Trabucho-Alexandre, J., Gröcke, D. R., & Summons, R. E., 2014. Organic geochemistry of the early Toarcian oceanic anoxic event in Hawsker Bottoms, Yorkshire, England. *Earth and Planetary Science Letters*, *390*, 116-127.

Gage, M.S., Doré, A.G., 1986. A regional geological perspective of the Norwegian offshore exploration provinces. *In: Spencer, A.M., Campbell, C.J., Hanslien, S.H., Holter, E., Nelson, P.H.H., Nysæther, E., Ormaasen, E.G. (Eds.), Habitat of Hydrocarbons on the Norwegian Continental Shelf*, pp. 21-38. Graham and Trotman, London, UK.

Goldberg, T., Archer, C., Vance, D., Poulton, S.W., 2009, Mo isotope fractionation during adsorption to Fe (oxyhydr)oxides. *Geochimica et Cosmochimica Acta* 73, 6502-6516.

Gradstein, F. M., Ogg, J. G., Schmitz, M., & Ogg, G. (Eds.), 2012. *The geologic time scale 2012 2-volume set*. Elsevier, Amsterdam, NL.

Helz, G.R., Vorlicek, T.P., Kahn, M.D., 2004. Molybdenum scavenging by iron monosulfide. *Environmental Science & Technology* 38, 4263-4268.

Herngreen, W. (2005) Jurassic and Cretaceous sporomorphs of NW Europe: taxonomy, morphology ranges of marker species. *TNO Report* NITG 05-053-C.

Hesselbo, S. P., Gröcke, D. R., Jenkyns, H. C., Bjerrum, C. J., Farrimond, P., Bell, H. S. M., & Green, O. R., 2000. Massive dissociation of gas hydrate during a Jurassic oceanic anoxic event. *Nature* 406, 392-395.

Hesselbo, S. P., Robinson, S. A., Surlyk, F., & Piasecki, S., 2002. Terrestrial and marine extinction at the Triassic-Jurassic boundary synchronized with major carbon-cycle perturbation: A link to initiation of massive volcanism?. *Geology* 30, 251-254.

Hounslow, M. W., Posen, P. E., and Warrington, G., 2004. Magnetostratigraphy and biostratigraphy of the Upper Triassic and lowermost Jurassic succession, St. Audrie's Bay, UK. *Palaeogeography, Palaeoclimatology, Palaeoecology* 213, 331-358.

Husmo, T., Hamar, G. P., Høiland, O., Johannessen, E. P., Rømuld, A., Spencer, A. M., & Titterton, R., 2003. Lower and Middle Jurassic. *The Millennium Atlas: Petroleum Geology of the Central and Northern North Sea. Geological Society, London*, 129-155.

Hesselbo, S. P., 2008. Sequence stratigraphy and inferred relative sea-level change from the onshore British Jurassic. *Proceedings of the Geologists' Association*, *119*(1), 19-34.

Hesselbo, S. P., & Jenkyns, H. C., 1995. A comparison of the Hettangian to Bajocian successions of Dorset and Yorkshire. Field Geology of the British Jurassic. *Geological Society, London*, 105-150.

Hesselbo, S. P., Gröcke, D. R., Jenkyns, H. C., Bjerrum, C. J., Farrimond, P., Bell, H. S. M., & Green, O. R. 2000. Massive dissociation of gas hydrate during a Jurassic oceanic anoxic event. *Nature* 406, 392-395.

9. REFERENCES

Hesselbo, S. P., Robinson, S. A., Surlyk, F., & Piasecki, S., 2002. Terrestrial and marine extinction at the Triassic-Jurassic boundary synchronized with major carbon-cycle perturbation: A link to initiation of massive volcanism?. *Geology*, 30, 251-254.

Hesselbo, S. P., Jenkyns, H. C., Duarte, L. V., & Oliveira, L. C., 2007. Carbon-isotope record of the Early Jurassic (Toarcian) Oceanic Anoxic Event from fossil wood and marine carbonate (Lusitanian Basin, Portugal). *Earth and Planetary Science Letters* 253, 455-470.

Houben, A., 2015. Palynological indications for elevated microbial primary productivity during the Early Toarcian Anoxic Event: Implications for organic-carbon accumulation and the interpretation of $\delta^{13}C$-trends. In *2015 AGU Fall Meeting*. San Francisco, USA, AGU.

Hubbard, R. N., & Boulter, M. C., 2000.. Phytogeography and paleoecology in western Europe and eastern Greenland near the Triassic-Jurassic boundary. *Palaios* 15, 120-131.

Ivimey-Cook, H. C., & Powell, J. H., 1991.. Late Triassic and early Jurassic biostratigraphy of the Felixkirk Borehole, north Yorkshire. In *Proceedings of the Yorkshire Geological and Polytechnic Society* 48, 367-374.

Jaraula, C. M., Grice, K., Twitchett, R. J., Böttcher, M. E., LeMetayer, P., Dastidar, A. G., & Opazo, L. F., 2013. Elevated pCO_2 leading to Late Triassic extinction, persistent photic zone euxinia, and rising sea levels. *Geology* 41, 955-958.

Jenkyns, H. C.,1988. The early Toarcian (Jurassic) anoxic event; stratigraphic, sedimentary and geochemical evidence. *American Journal of Science* 288, 101-151.

Jenkyns, H. C., & Clayton, C. J., 1986. Black shales and carbon isotopes in pelagic sediments from the Tethyan Lower Jurassic. *Sedimentology* 33, 87-106.

Jenkyns, H. C., & Senior, J. R., 1991. Geological evidence for intra-Jurassic faulting in the Wessex Basin and its margins. *Journal of the Geological Society* 148, 245-260.

Jenkyns, H. C., & Weedon, G. P. (2013). Chemostratigraphy ($CaCO_3$, TOC, $\delta^{13}C_{org}$) of Sinemurian (Lower Jurassic) black shales from the Wessex Basin, Dorset and palaeoenvironmental implications. *Newsletters on Stratigraphy* 46, 1-21.

Jenkyns, H. C., Jones, C. E., Grocke, D. R., Hesselbo, S. P., & Parkinson, D. N., 2002. Chemostratigraphy of the Jurassic System: applications, limitations and implications for palaeoceanography. *Journal of the Geological Society* 159, 351-378.

Jenkyns, H. C., Jones, C. E., Grocke, D. R., Hesselbo, S. P., & Parkinson, D. N., 2002. Chemostratigraphy of the Jurassic System: applications, limitations and implications for palaeoceanography. *Journal of the Geological Society* 159, 351-378.

Kemp, D. B., Coe, A. L., Cohen, A. S., & Schwark, L., 2005. Astronomical pacing of methane release in the Early Jurassic period. *Nature* 437, 396-399.

Kent, P. E., 1980. Subsidence and uplift in East Yorkshire and Lincolnshire: a double inversion. *Proceedings of the Yorkshire Geological and Polytechnic Society* 42, 505-524.

Klinkhammer, G.P., Palmer, M.R., 1991. Uranium in the oceans— where it goes and why. *Geochim. Cosmochim. Acta* 55, 1799–1806.

Knight, K. B., Nomade, S., Renne, P. R., Marzoli, A., Bertrand, H., & Youbi, N., 2004. The Central Atlantic Magmatic Province at the Triassic–Jurassic boundary: paleomagnetic and $^{40}Ar/^{39}$ Ar evidence from Morocco for brief, episodic volcanism. *Earth and Planetary Science Letters* 228, 143-160.

Koppelhus, E.B. and Nielsen, L.H., 1994 Palynostratigraphy and palaeoenvironments of the Lower to Middle Jurassic Bagå Formation of Bornhorm, Denmark. *Palynology* 18, 139-194.

Korte, C., & Hesselbo, S. P., 2011. Shallow marine carbon and oxygen isotope and elemental records indicate icehouse-greenhouse cycles during the Early Jurassic. *Paleoceanography* 26.

Korte, C., Hesselbo, S. P., Jenkyns, H. C., Rickaby, R. E., & Spötl, C., 2009. Palaeoenvironmental significance of carbon-and oxygen-isotope stratigraphy of marine Triassic–Jurassic boundary sections in SW Britain. *Journal of the Geological Society* 166, 431-445.

Korte, C., Hesselbo, S. P., Ullmann, C. V., Dietl, G., Ruhl, M., Schweigert, G., & Thibault, N., 2015. Jurassic climate mode governed by ocean gateway. *Nature communications* 6.

Küspert, W., 1982. Environmental changes during oil shale deposition as deduced from stable isotope ratios. *Cyclic and Event Stratification* (pp. 482-501). Springer, Berlin.

Larsson, L. M., 2009. Palynostratigraphy of the Triassic–Jurassic transition in southern Sweden. *GFF* 131, 147-163.

Lash, G. G., & Blood, D., 2004. Geochemical and textural evidence for early (shallow) diagenetic growth of stratigraphically confined carbonate concretions, Upper Devonian Rhinestreet black shale, western New York. *Chemical Geology* 206, 407-424.

Lindström, S., Van de Schootbrugge, B., Dybkjær, K., Pedersen, G. K., Fiebig, J., Nielsen, L. H., & Richoz, S., 2012. No causal link between terrestrial ecosystem change and methane release during the end-Triassic mass extinction. *Geology* 40, 531-534.

Lindström, S., Pedersen, G. K., Van De Schootbrugge, B., Hansen, K. H., Kuhlmann, N., Thein and Weibel, R. 2015. Intense and widespread seismicity during the end-Triassic mass extinction due to emplacement of a large igneous province. *Geology* 43, 387-390.

Littler, K, Hesselbo, S. and Jenkyns, J., 2010. A carbon-isotope perturbation at the Pliensbachian–Toarcian boundary: Evidence from the Lias Group, NE England. *Geological Magazine* 147, 181-192.

Lott, G.K., Knox, R., 1994. Post-Triassic of the Southern North Sea. *In: Knox and Cordey, W.G. (Eds.): Lithostratigraphic nomenclature of the UK North Sea. British Geological Survey, Nottingham*.

Lund, J. J., 1977. Rhaetic to Lower Liassic palynology of the onshore south-eastern North Sea Basin. *CA Reitzels*.

Marjanac, T., Steel, R.J., 1997. Dunlin Group sequence stratigraphy in the northern North Sea, a model for Cook Sandstone deposition. *Bulletin of American Association of Petroleum Geologists* 81, 276-292.

März, C., Poulton, S.W., Beckmann, B., Küster, K., Wagner, T. & Kasten, S., 2008. Redox sensitivity of P cycling during marine black shale formation: Dynamics of sulfidic and anoxic, non-sulfidic bottom waters. *Geochimica Cosmochimica Acta* 72, 3703-3717.

McElwain, J. C., Beerling, D. J., & Woodward, F. I. (1999). Fossil plants and global warming at the Triassic-Jurassic boundary. *Science*, *285*(5432), 1386-1390.

Meister, C., Aberhan, M., Blau, J., Dommergues, J. L., Feist-Burkhardt, S., Hailwood, E. A., and Morton, N., 2006. The Global Boundary Stratotype Section and Point (GSSP) for the base of the Pliensbachian Stage (Lower Jurassic), Wine Haven, Yorkshire, UK. *Episodes* 29, 88-93.

Milsom, J., & Rawson, P. F., 1989. The Peak Trough–a major control on the geology of the North Yorkshire coast. *Geological Magazine* 126, 699-705.

Morbey, S. J., 1975. The palynostratigraphy of the Rhaetian stage, Upper Triassic in the Kendelbachgraben, Austria. *Palaeontographica Abteilung B*, 1-75.

Morbey, S. J., 1978. Late Triassic and Early Jurassic subsurface palynostratigraphy in northwestern Europe. *Palinologia* 1, 355-365.

Morbey, S. J., & Dunay, R. E., 1978. Early Jurassic to Late Triassic dinoflagellate cysts and miospores. Distribution of biostratigraphically diagnostic dinoflagellate cysts and miospores from the northwest European continental shelf and adjacent areas. *Continental Shelf Institute Publication* 100, 47-59.

Morford J.L., Emerson S., 1999. The geochemistry of redox sensitive trace metals in sediments. *Geochim. Cosmochim. Acta* 63, 1735–1750.

Morgenroth, P., 1970. Dinoflagellate cysts from the Lias Delta of Luehnde/Germany. *Neues Jahrbuch fuer Geologische und Palaeontologische Abhandlungen* 136345-359.

Nelskamp, S., Goldberg, S., Houben, S., Geel, K., Wasch, L., Verreussel, R. and Boxem T., 2015. Improved Sweet Spot idenfication and smart development using integrated reservoir characterisation (Phase 2). *Confidential TNO Report* 2015 R10740.

Nystuen, J. P., Kjemperud, A. V., Müller, R., Adestål, V., & Schomacker, E.R., 2014. Late Triassic to Early Jurassic climatic change, northern North Sea region. *From Depositional Systems to Sedimentary Successions on the Norwegian Continental Margin*, 59-99.

Odinsen, T., Reemst, P., Van Der Beek, P., Faleide, J. I., & Gabrielsen, R. H., 2000. Permo-Triassic and Jurassic extension in the northern North Sea: results from tectonostratigraphic forward modelling. *Geological Society, London, Special Publications* 167, 83-103.

Pacton, M., Gorin, G. E., & Vasconcelos, C., 2011. Amorphous organic matter—Experimental data on formation and the role of microbes. *Review of Palaeobotany and Palynology* 166, 253-267.

Page, K. N., 2003. The Lower Jurassic of Europe: its subdivision and correlation. *Geological Survey of Denmark and Greenland Bulletin* 1, 23-59.

Page, K.N., 2004. A sequence of biohorizons for the subboreal province Lower Toarcian in Northern Britain and their correlation with a submediterranean standard. *Rivista Italiana di Paleontologia e Stratigrafia* 110.

Pálfy, J., Demény, A., Haas, J., Hetényi, M., Orchard, M. J., & Veto, I., 2001. Carbon isotope anomaly and other geochemical changes at the Triassic-Jurassic boundary from a marine section in Hungary. *Geology* 29, 1047-1050.

Palliani, R. B., & Riding, J. B., 1997. Lower Toarcian palynostratigraphy of Pozzale, central Italy. *Palynology* 21, 91-103.

Palliani, R. B., & Riding, J. B., 2000. A palynological investigation of the Lower and lowermost Middle Jurassic strata (Sinemurian to Aalenian) from North Yorkshire, UK. In *Proceedings of the Yorkshire Geological and Polytechnic Society* 53, 1-16.

Palliani, R. B., & Riding, J. B. 2003. Biostratigraphy, provincialism and evolution of European Early Jurassic (Pliensbachian to Early Toarcian) dinoflagellate cysts. *Palynology 27*, 179-214.

Palliani, R. B., Mattioli, E., & Riding, J. B., 2002. The response of marine phytoplankton and sedimentary organic matter to the early Toarcian (Lower Jurassic) oceanic anoxic event in northern England. *Marine micropaleontology* 46, 223-245.

9. REFERENCES

Partington, M. A., P. Copestake, B. C. Mitchener, and J. R. Underhill, 1993. Biostratigraphic calibration of genetic stratigraphic sequences in the Jurassic-lowermost Cretaceous (Hettangian to Ryazanian) of the North Sea and adjacent areas. *In: J. R. Parker (Ed.) Petroleum geology of north-west Europe: Proceedings of the 4th conference.* Geological Society of London, 371–386.

Pedersen, G.K., 1986. Changes in the bivalve assemblage of an early Jurassic mudstone sequence (The Fjerritslev Formation in the Gassum-1 well, Denmark). *Palaeogeography, Palaeoclimatology, Palaeoecology* 53, 139–168.

Petersen, H., Nielsen, L., Bojesen-Koefoed, J. A., Mathiesen, A., Kristensen, L., & Dalhoff, F., 2008. Evaluation of the quality, thermal maturity and distribution of potential source rocks in the Danish part of the Norwegian–Danish Basin. *Geological Survey Of Denmark and Greenland Bulletin* 16.

Popp, B. N., Laws, E. A., Bidigare, R. R., Dore, J. E., Hanson, K. L., & Wakeham, S. G., 1998. Effect of phytoplankton cell geometry on carbon isotopic fractionation. *Geochimica et Cosmochimica Acta* 62, 69-77.

Prauss, M. L., 2007. Availability of reduced nitrogen chemospecies in photic-zone waters as the ultimate cause for fossil prasinophyte prosperity. *Palaios* 22, 489-499.

Price, G. D., 2010. Carbon-isotope stratigraphy and temperature change during the Early–Middle Jurassic (Toarcian–Aalenian), Raasay, Scotland, UK. *Palaeogeography, Palaeoclimatology, Palaeoecology* 285, 255-263.

Raiswell, R., 1971. The growth of Cambrian and Liassic concretions. *Sedimentology* 17, 147-171.

Richards, P.C., Lott, G.K., Johnson, H., Knox, R. and Riding, J.B., 1993. Jurassic of the Central and Northern North Sea. *In: Knox, R. and Cordey, W.G. (Eds.) Lithostratigraphic nomenclature of the UK North Sea. British Geological Survey,* Nottingham, UK.

Riding, J. B., 1984. A palynological investigation of Toarcian to early Aalenian strata from the Blea Wyke area, Ravenscar, North Yorkshire. *Proceedings of the Yorkshire Geological and Polytechnic Society*, 45, 109-122.

Riding, J. B., & Hubbard, R. N., 1999. Jurassic (Toarcian to Kimmeridgian) dinoflagellate cysts and paleoclimates. *Palynology* 23, 15-30.

Riding, J. B., & Thomas, J. E., 1992. Dinoflagellate cysts of the Jurassic System. *A stratigraphic index of dinoflagellate cysts* (pp. 7-97). Springer, Amsterdam.

Riding, J. B., Walton, W., & Shaw, D., 1991. Toarcian to Bathonian (Jurassic) palynology of the Inner Hebrides, northwest Scotland. *Palynology* 15, 115-179.

Riding, J. B., Leng, M. J., Kender, S., Hesselbo, S. P., & Feist-Burkhardt, S., 2013. Isotopic and palynological evidence for a new Early Jurassic environmental perturbation. *Palaeogeography, Palaeoclimatology, Palaeoecology* 374, 16-27.

Rosales, I., Quesada, S., & Robles, S., 2006. Geochemical arguments for identifying second order sea-level changes in hemipelagic carbonate ramp deposits. *Terra Nova* 18, 233-240.

Ruhl, M., & Kürschner, W. M., 2011. Multiple phases of carbon cycle disturbance from large igneous province formation at the Triassic-Jurassic transition. *Geology* 39, 431-434.

Ruhl, M., Bonis, N. R., Reichart, G. J., Damsté, J. S. S., & Kürschner, W. M. (2011). Atmospheric carbon injection linked to end-Triassic mass extinction. *Science 333*, 430-434.

Ruhl, M., Hesselbo, S. P., Hinnov, L., Jenkyns, H. C., Xu, W., Riding, J. B. and Leng, M. J., 2016. Astronomical constraints on the duration of the Early Jurassic Pliensbachian Stage and global climatic fluctuations. *Earth and Planetary Science Letters* 455, 149-165.

Ryseth, A., 2001. Sedimentology and palaeogeography of the statfjord formation (Rhaetian-Sinemurian), North Sea. *Norwegian Petroleum Society Special Publications* 10, 67-85.

Salem, N.-E., 2013. Geochemical characterisation of the Pliensbachian-Toarcian boundary during the onset of the Toarcian Oceanic Anoxic Event. North Yorkshire, UK. *Thesis School of Civil Engineering and Geosciences, Newcastle University*, UK, pp. 276.

Schenk, P. M., Thomas-Hall, S. R., Stephens, E., Marx, U. C., Mussgnug, J. H., Posten, C., ... & Hankamer, B. (2008). Second generation biofuels: high-efficiency microalgae for biodiesel production. *Bioenergy research*, *1*(1), 20-43.

Schulz, E., 1967. Sporenpaläontologische Untersuchungen rätoliassischer Schichten im Zentralteil des Germanischen Beckens. *Paläontologische Abhandlungen. Paläobotanik* B 2, 427–633.

Van de Schootbrugge, B., et al., 2005. Early Jurassic climate change and the radiation of organic-walled phytoplankton in the Tethys Ocean. *Paleobiology* 31, 73-97.

Van de Schootbrugge, B., Quan, T. M., Lindström, S., Püttmann, W., Heunisch, C., Pross, J. and Rosenthal, Y., 2009. Floral changes across the Triassic/Jurassic boundary linked to flood basalt volcanism. *Nature Geoscience* 2, 589-594.

Van de Schootbrugge, B., Bachan, A., Suan, G., Richoz, S., & Payne, J. L., 2013. Microbes, mud and methane: cause and consequence of recurrent Early Jurassic anoxia following the end-Triassic mass extinction. *Palaeontology* 56, 685-709.

Simms, M. J., 2004. British Lower Jurassic Stratigraphy (Vol. 30). *Joint Nature Conservation Committee - Habitas*.

Smelror, M., Jacobsen, T., Rokoengen, K., Bakke, S., Bo, R., Goll, R.M., Lippard, S.J., Mork, A., Rise, L., Vigran, J., Weiss, H.M., Arhus, N., 1989. Shallow Drilling in the Farsund Subbasin *Sintef Group Report*, Trondheim, Norway.

Smith, P. L., & Tipper, H. W. 1986. Plate tectonics and paleobiogeography: Early Jurassic (Pliensbachian) endemism and diversity. *Palaios*, 399-412.

Srivastava, S. K., 1987. Jurassic spore-pollen assemblages from Normandy (France) and Germany. *Geobios* 20, 5-79.

Steel, R. J., 1993. Triassic–Jurassic megasequence stratigraphy in the Northern North Sea: rift to post-rift evolution. *Geological Society, London, Petroleum Geology Conference series*, 4.

Storm, M., Hesselbo, S., Jenkyns, H., Leng, M., Xu, W. and Ruhl, M., 2016. A negative carbon-isotope excursion in the Upper Pliensbachian Margaritatus and Spinatum zone - New insight in carbon-cycle dynamics prior to the Toarcian OAE? S*EPM Research Conference Oceanic Anoxic Events - Austin, TX, USA*.

Suan, G., Schootbrugge, B., Adatte, T., Fiebig, J., & Oschmann, W., 2015. Calibrating the magnitude of the Toarcian carbon cycle perturbation. *Paleoceanography*, 30, 495-509.

Svensen, H., Planke, S., Chevallier, L., Malthe-Sørenssen, A., Corfu, F., & Jamtveit, B., 2007. Hydrothermal venting of greenhouse gases triggering Early Jurassic global warming. *Earth and Planetary Science Letters* 256, 554-566.

Tissot, B. P., and D. H. Welte, 1984, Petroleum formation and occurrence, 2d ed.: Berlin, *Springer Verlag*, 699 p.

Tribovillard, N., Algeo, T.J., Lyons, T.W., Riboulleau, A., 2006. Trace metals as paleoredox and paleoproductivity proxies: an update. *Chemical Geology* 232, 12-32.

Tribovillard, N., Algeo, T.J., Lyons, T.W., Riboulleau, A., 2012. Analysis of marine environmental conditions based on molybdenum–uranium covariation—applications to Mesozoic paleoceanography. *Chem. Geol.* 324–325, 46–58

Van Adrichem Boogaert, H.A. & Kouwe, W.F.P., 1993-1997. Middle and Lower Jurassic. *In: Stratigraphic Nomenclature of the Netherlands.*

Van Konijnenburg - Van Cittert, J. H., & Van der Burgh, J., 1996. Review of the Kimmeridgian flora of Sutherland, Scotland, with reference to the ecology and in situ pollen and spores. *Proceedings of the Geologists' Association* 107, 97-105.

Verreussel, R. *et al.*, 2008. Palynology of the Jurassic and Cretaceous sections from the Gullfaks Field. *Confidential TNO Report* 2008-U-R1026/C.

Vollset, J., & Doré, A. G. (Eds.), 1984. *A revised Triassic and Jurassic lithostratigraphic nomenclature for the Norwegian North Sea*. Oljedirektoratet, Norway.

Weedon, G. P. 1986. Hemipelagic shelf sedimentation and climatic cycles: the basal Jurassic (Blue Lias) of South Britain. *Earth and Planetary Science Letters* 76, 321-335.

Wall, D., 1965. Microplankton, pollen, and spores from the Lower Jurassic in Britain. *Micropaleontology*, 151-190.

Warrington, G., 1977. Palynological examination of Triassic (Keuper Marl and Rhaetic) deposits north-east and east of Bristol. *Proceedings of the Ussher Society* 4, 76-81.

Warrington, G., 1978. Palynological features of the late Triassic-early Jurassic sequence in west Somerset. *Proceedings of the Ussher Society* 4.

Warrington, G., 1983. Late Triassic and earliest Jurassic palynomorph assemblages from the Western English Channel and neighbouring areas. *Proceedings of the Ussher Society* 5, 473-476.

Warrington, G., 1984. The Triassic-Jurassic boundary in Britain. *Albertiana* 2, 17-18.

Weiss, M., 1989. Die Sporenfloren aus Rät und Jura Südwestdeutschlands und ihre Beziehungen zur Ammoniten-Stratigraphie. *Palaeontographica Abteilung B*, 1-168.

Wignall, P. B., 2001. Sedimentology of the Triassic-Jurassic boundary beds in Pinhay Bay (Devon, SW England). *Proceedings of the Geologists' Association* 112, 349-360.

Wignall, P. B., & Hallam, A., 1991. Biofacies, stratigraphic distribution and depositional models of British onshore Jurassic black shales. *Geological Society, London, Special Publications* 58, 291-309.

Wille, W., & Gocht, H.,1979. Dinoflagellaten aus dem Lias Südwestdeutschlands. *Neues Jahrbuch für Geologie und Paläontologie, Abhandlungen* 158, 221-258.

Woollam, R. & Riding, J.B., 1983. Dinoflagellate Cyst Zonation of the English Jurassic. Report of the Institute of Geological Sciences 83/2.

Xu, W., Ruhl, M., Hesselbo, S. P., Riding, J. B., & Jenkyns, H. C. (2016). Orbital pacing of the Early Jurassic carbon cycle, black shale formation and seabed methane seepage. *Sedimentology, in press*.

Young, G., & Bird, J., 1822. *A geological survey of the Yorkshire coast*. Printed at the Office of George Clark.

Young, T. P., Aggett, J. R., & Howard, A. S., 1990. The Cleveland Ironstone Formation. *Jurassic and Ordovician Ooidal Ironstones Conference*, 1-31.

Zakharov, V. A., Shurygin, B. N., Il'ina, V. I., & Nikitenko, B. L., 2006. Pliensbachian-Toarcian biotic turnover in north Siberia and the Arctic region. *Stratigraphy and Geological Correlation* 14, 399-417.

Zanella, E., & Coward, M. P., 2003. Structural framework. *The Millennium Atlas: Petroleum Geology of the Central and Northern North Sea*, *357*, 4.

Zheng, Y., Anderson, R.F., van Geen, A., Kuwabara, J., 2000. Authigenic molybdenum formation in marine sediments: A link to pore water sulphide in the Santa Barbara Basin. *Geochimica et Cosmochimica Acta* 64, 4165–4178.

Ziegler, P. A. 1990: Geological Atlas of Western and Central Europe. *2nd. Ed. Geol. Soc. Publ. House*, Bath, UK, 239 pp.

For more information and
questions, please contact:

Friso Veenstra
✉ friso.veenstra@tno.nl
✆ +31 (0) 88 866 53 55